“OVIDIUS” UNIVERSITY OF CONSTANTZA
UNIVERSITATEA „OVIDIUS” CONSTANȚA

“OVIDIUS” UNIVERSITY ANNALS CONSTANTZA

Year XIV– Issue 14
(2012)
Series: CIVIL ENGINEERING

ANALELE UNIVERSITĂȚII „OVIDIUS”CONSTANȚA

ANUL XIV – Nr 14
(2012)

Seria: CONSTRUCȚII
Ovidius University Press
2012

"OVIDIUS" UNIVERSITY ANNALS - CONSTANTZA
SERIES: CIVIL ENGINEERING
ANALELE UNIVERSITĂȚII „OVIDIUS" CONSTANȚA
SERIA: CONSTRUCȚII

EDITOR IN CHIEF:

Carmen MAFTEI, PhD, Eng., "OVIDIUS" University, Faculty of Civil Engineering,
124, Mamaia Blvd., 900527, RO., Constantza, Romania, phone +40-241-545093,
fax +40-241-612300 cemaftei@gmail.com

EXECUTIVE EDITOR:

Anca CONSTANTIN, PhD, Eng, University, Faculty of Civil Engineering,
124, Mamaia Blvd., 900527, RO., Constantza, phone +40-241-545093,
fax +40-241-612300 Romania, anca.constantin@ymail.com

EDITORIAL BOARD

DESK EDITORS
Gabriela BADEA, Cristina ŞERBAN, Diana ŢENEA, "OVIDIUS" University, Faculty of Civil Engineering, 124, Mamaia Blvd., 900527, RO., Constantza, Romania

Number of Copies: 100

PUBLISHED BY: OVIDIUS UNIVERSITY PRESS, 126, Mamaia Blvd., 900527, RO., Constantza, Romania, Phone/Fax +40-241606421, library@bcuovidius.ro

FREQUENCY: Yearly

COVERED BY: INDEX COPERNICUS, IC VALUES IN 2011 3.86
http://journals.indexcopernicus.com/karta.php?action=masterlist&id=5000

REMIT OF JOURNAL:
Journal can be free downloaded from the site: http://www.univ-ovidius.ro/revista-constructii/; the authors receive a copy of their paper.

ORDERING INFORMATION
The printed version of the journal may be obtained by ordering at the "OVIDIUS" University Press, or on exchange basis with similar Romanian or foreign institutions.
The price for a single volume is 40 euros plus postal charges.
126, Mamaia Blvd., 900527, RO., Constantza, Romania

For subscriptions and submission of papers, please use the e-mail address: serban.cristina@univ-ovidius.ro or costi_buta@yahoo.com or postal address 22B Unirii str., 900524 RO, Constantza, Romania

Instructions for authors can be found at: http://www.univ-ovidius.ro/revista-constructii/

ISSN 1584-5990

TABLE OF CONTENTS

ISSN-1584-5990

Section III. Hydraulics. Theory and Applications in Constructions

Section IV. Integrated Water Management

Section V. Surface and Groundwater Hydrology

Seismic Rehabilitation of the Assembly of Buildings Forming the National Theatre in Bucharest

Mircea Ieremia [1]

The assembly of buildings forming the National Theatre in Bucharest comprises four main parts/sections, as follows:

Section A – the Main Hall and the stage tower;

Section B – Annexes ;

Section C - Studio Hall;

Section D – Technical room and underground parking lot.

The buildings that compose The National Theatre of Bucharest assembly were designed between 1963 and 1968. There weren't significant degradations of the structural elements after the 1977 earthquake. On 17.08.1978, a fire burst in the Main Hall building and after that the theatre was totally rebuilt on the outside and partially on the inside. It had to disappear the reinforced concrete "hat" and the old edifice was totally covered with a carcass, which gives its actual shape. Following the State's directions in that period, in 1983, The Institute of Design "Carpati" elaborated a remodelation model of the Section A building – Main Hall – which changed the stress structure of the building. In this way the Main Hall's capacity was increased, by removing 4 of the 8 curved reinforced concrete walls, and it had been created a new façade that loads in a forbidden way the structural elements of the adjacent parking lot.

Proposed stages; problems that need to be solved:

Consolidation of the stress structure (façade structure, main hall structure), stage tower and parking lot structure;

Reshaping of the National Theatre building – section A, inspired from the London National Theatre – Barbican Hall building, as well as from theatres in Los Angeles and Copenhagen;

Consolidation of section B (including offices, green rooms, gyms, smaller auditoriums), which suffered the most significant damages from earthquakes;

Consolidation of section C – at present hosting the Musical Comedy Theatre (in the future it will host the Studio Hall of the National Theatre), which will be reshaped according to an Elizabethan-type variable geometry;

Three more auditoriums will be set up ;

The University Square will be reconfigured and several representative monuments will be added. Here are some examples:

"The Clowns' Cart" – a monumental sculpture displaying the main characters described by author Ion Luca Caragiale;

"The Crystal Monument", accompanied by an eternal flame, dedicated to the memory of 1989 heroes;

"Caragiale's Hat", meant to emphasize the National Theatre image according to the model used before 1983.

The erection of a National Dance Centre (now operating inside the National Theatre building);

Most building services from the National Theatre will be renewed; examples: the air conditioning system, the fire prevention system;

The number of seats in the auditoriums will be almost double, from 1720 at present to over 3100.

[1] Tehnical University of Civil Engineering Bucharest

ISSN-1584-5990

Hydroinformatics, an ICT solution for water-related problems

Ioana Popescu [1]

Hydroinformatics addresses the use of modern ICT to communicate on environment with particular interest on water related problems, presenting information on the actual state of the environment at specific user locations and possible associated health threats to all people. Information on environment is gathered in one place, where users can respond to what is presented. They can interact in a way they know from social networks and other interactive forums on internet. The focus of the presentation is on the EU FP7 project called *Lenvis*, which focused on the combined needs of government organisations and user groups. *Lenvis* takes into consideration recent developments in ICT such as use of GPS for localisation and internet on mobile devices. Internet has brought a wealth of information on any topic one could think of. However, it is the user who has to compile useful information from all sources available.

Lenvis makes a difference in that it aims to present location-based information on basically all environmental data in one portal. This web portal can be customised and parts of the website can be included in other applications. The *lenvis* information is based on monitoring of water, air and health data as well as online model outcomes in these three domains. Prototypes are built and practical tests are performed in case studies in the Netherlands, Portugal and Italy. Particular topics which are addressed in these case studies are: water pollution at recreational beaches and the associated health threats; smog alarms in urbanised areas and associated asthma warnings; water quality information and flooding threats in urban and rural areas and dedicated environmental and weather information for recreational users. The *lenvis* project run from October 2008 to December 2010, involved 10 EU organisations and was funded by the EC FP7 programme. During these years a team of professionals from universities, industries and governments cooperated closely and aimed to facilitate collaboration between different stakeholders, such as environmental protection agencies, health institutions and service providers, policy makers, citizens in general and environmental communities in Europe.

[1] UNESCO-IHE Institute for Water Education, Delft, the Netherlands

ISSN-1584-5990

SECTION I

COMPUTATIONAL METHODS IN WATER RESOURCES AND CIVIL ENGINEERING

Complex research on land use in relation to relief factor using GIS technology. Case study.

Biali Gabriela[1]

Abstract – **Knowing how to use the lands on a certain territory is very important and a current topic, consisting in the accumulation of precious information for various fields (hydrotechnical and hydroameliorative improvement, environment, cadastre, etc). The paper presents an analysis of the usage of the lands on a vast area, as well as the reports/relations that these have with various geographical factors through an optimal improvement of the territory.**

In order to develop such a complex study one has to have in mind the fact that the private property represents a restrictive factor which is not good for the precision of the obtained data, moreover, a solution would be a spatial database which can be processed in a GIS program. The software that was used in this paper is TNT Mips 7.3, with its help we can research a territory both under the aspect of the land's usage as well as according to its dynamics in relation with the geomorphic factors, an analysis that would be practically impossible without the GIS technique.

The paper will present products based GIS graphic data such as: The map of the use of the lands (product resulted after the ortophotoplan): the hypsometric map of the studied perimeter, informational layer of the altitudes; the map of the cliffs from the studied perimeter; informational layer of the declivity; the map of the exposition of the versants on the studied perimeters Based on these distributions can be executed criterial class: the balance of the categories of use of lands, the distribution of the classes of altitude within the category of use of the lands; the distribution of the classes of cliffs within the categories of use of the lands; the distribution of the exposition of the versants within the categories of usage of the lands

Keywords – **spatial database, GIS, relief, use of land.**

1. INTRODUCTION

The use of the lands represents a way of using a surface according to the natural conditions, the social-economic factors and according to the possibilities of developing the surfaces [1].

In the approach of the land's usage intervenes the notion of *landed fund,* where „lands of all kinds, no matter their destination, no matter the title on which basis they are owned or no matter the public or private domain from which they are a part of, constitute the landed fund of Romania" (article 1 from Law 18/1991, the Law of the Landed Fund) [8].

In the study of the usage of the lands we find a coded characterization made from the point of view of the destination of the land according to the purpose for which it is used. This is called *category of use of the land* .

For the development of such a complex study one has to have in mind that the private property represents a restrictive factor which is not desirable for the accuracy of the obtained data, therefore it would be a solution the

[1] Technical University "Ghe. Asachi" of Iasi , Bd. D. Mangeron nr.65, 700050, Iasi, Romania (gbiali@yahoo.com)

ISSN-1584-5990

space database which can be processed in a GIS program. The software that was used in this paper is called TNT Mips 7.3, which during this paper will show the profile of a study area from the point of view of the usage of the lands [2].

The reference points used in the development of the paper can be found in the general urban Plan which offers us access to a multitude of data which can be successfully processed in the approach of the paper, it can also provide us with the spatial database without which it would have been harder to obtain satisfactory data [7].

The modeling based on the geographic information systems was the main criteria in choosing the working instruments which stood at the base of the interpretation of the obtained results as well as at the base of the cartographic representations [6].

Because of the modern methods, the geographical information systems have represented the main instrument in processing the spatial database, in the interpretation of the results that were obtained and in their cartographic representation.

2. DESCRIPTION OF THE RESEARCH METHODOLOGY

The case study is developed on a surface of aprox. 7000 ha within the territory of Scobinți commune, Iasi county. The analysis was based on the modern methods of GIS technology, the TNT Mips 7.3 program, which on the base of some input data (plans, maps, etc.), have had as a result new geographical data (analytic maps, themes, profiles, diagrams, etc.), where we can find information about the categories of use of lands relief, soil, the dynamics of the localities, etc.

The pieces of information were based on the following sources:

- topographic-cadastral maps 1:5000;
- topographic maps 1:25000;
- maps of soils 1:10000;
- general urban plan and improvement plan of the peri-urban territory Hîrlău area (drawn pieces);
- ortophotoplans;
- vector data (geology, the limit of the relief units, Corine Land Cover 2000, the limits of the administrative – territorial units – according to ANCPI);
- raster data (STRM, Austrian maps from 1910 redesigned in stereo ‘70).

On the basis of the level curves obtained from the topographical-cadastre plans 1:5000, in a first phase were generated the numeric model of the land (DEM – Digital Elevation Model), after which there were obtained thematic models concerning the exposition, the cliff and hypsometry.

The ortophotoplans and the map of the soils were a support in the realization of some vector layers representing the categories of use of the lands, the types and subtypes of soil.

The drawn pieces within the general urban plan were georeferentiated through correspondence points with the ortophotoplanns, being a reference in the establishment of the inner-urban limits and to obtain the data concerning the types of existing roads in the territory.

On the basis of the vector polygons were calculated the surfaces of the basic units within the usage of the lands and their correlation with raster data concerning the hypsometry, the cliffs and the exposition of the versants.

Stages in the development of the maps of the lands with the help of the GIS technique

- Input data (ortophotoplans);
- Photointerpretation of the ortophotoplan;
- The vectorization of a polygon layer (the limits of the categories of usage);
- Supplying for each polygon an attribute which will show the category of usage;
- Choosing a set of colors in order to visually differentiate each category of usage;
- Adding the layer with the usage of the lands on a model within the GIS program;

- Presenting the final product.

The study of the usage of the lands was possible with the help of the ortophotoplans, scale 1: 5000 and with the help of the topographic-cadastre plans 1:5000, both were geodifferentiated having a 70 stereo projection, which allowed the development of an analysis concerning the surfaces occupied by each category of use and their localization within the administrative territory. For framing the categories of use were used cadastral classifications.

The map of the use of the lands was obtained through the digitalization of the limits of the categories of use, so that there were obtained polygons that allowed the automatic calculation of the surfaces and their perimeters.

Concerning the quality of the ortophotoplan's resolution, the pixel (the smallest measuring unit of the raster) occupies a perimeter of 2 m and a surface of 0,5 x 0,5 m (0,25 m^2), which lead to a detailed analysis. Nevertheless there were difficulties in establishing the categories of usage in the area of the incorporated area where the demarcation areas are very small and fragmented.

The total surface of Scobinți commune (according to ANCPI limit) is of 7148 ha, from which 6005,5 ha are occupied by agricultural surfaces and 1142,7 by the surfaces that are not agricultural (from the GIS analysis).

From the analysis of the map it can be seen that the studied area is dominated by the arable surfaces, which occupies 3682 ha, exceeding a little bit the percentage of 50% of the total surface. The explanations for this dominance of the arable surface are related with the physical-geographical position (the depression area occupies the biggest surface of the territory), the soils (present important characteristics which are favorable for plants), and with the tradition of the population concerning their administration of the resources of the landed fund.

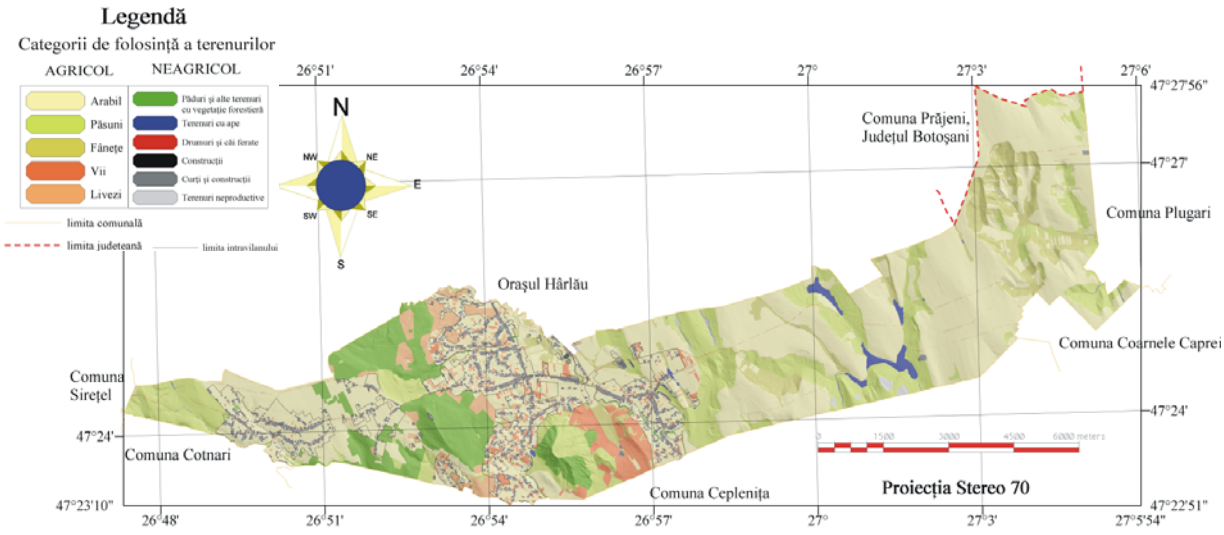

Fig. 1. The map of the use of the lands (product resulted after the ortophotoplan)

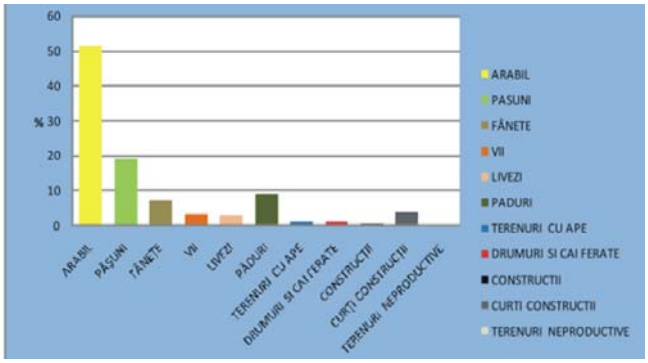

Fig.2. The balance of the categories of use of lands
(Processed data and data obtained with the help of the TNT mips7.3 program)

3. RESULTS OBTAINED AND DISCUSSION

The relief is an important component in establishing the categories of use of the lands, which may impose both restrictions as well as the favorability of placing these functions of altitude, cliff, exposition, etc.

Therefore, in the 2nd part of the paper is presented the relation between the relief of the area and the use of the lands. With the help of the software we could create the informational layers from the spatial database for altitude, cliff and exposition which will be presented as finished products.

In what the relations between the use of the lands and the relief are concerned, show the complexity of a geographic information system in what a complex analysis is concerned.

Within the numeric model of the land there were generated, with the help of a script language, classes of altitude, cliff and exposition. These layers may be brought individual and combined in the program, with one category of use (there can be generated more vector layers from one vector layer, marking in the menu with attributes the chosen polygons) being obtained text files data.

The GIS may be data generator (text files) for other programs like Excel, where there can be obtained graphs concerning the current situation of the land.

In order to obtain a report between the soils and the usage of the lands the situation is a little bit different, in the way in which we have to deal with two vector layers. At the development of the report there has to be a raster layer and a vector layer. The vector polygons of the layer with soils were converted in raster so that the text files were generated, text files that are meant to be important in Excel.

The altitude in Scobinți commune varies between 100 and 50 m, but the dominant one has values between 100 and 200 m, where the arable surfaces have the biggest variation.

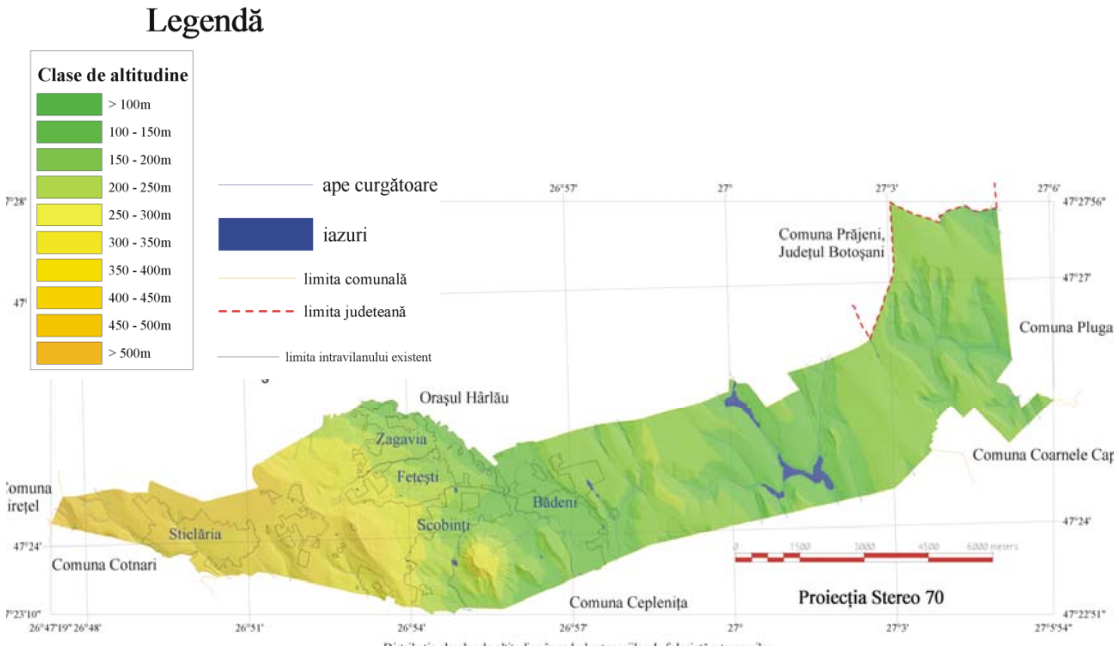

Fig. 3. The hypsometric map of the studied perimeter, informational layer of the altitudes

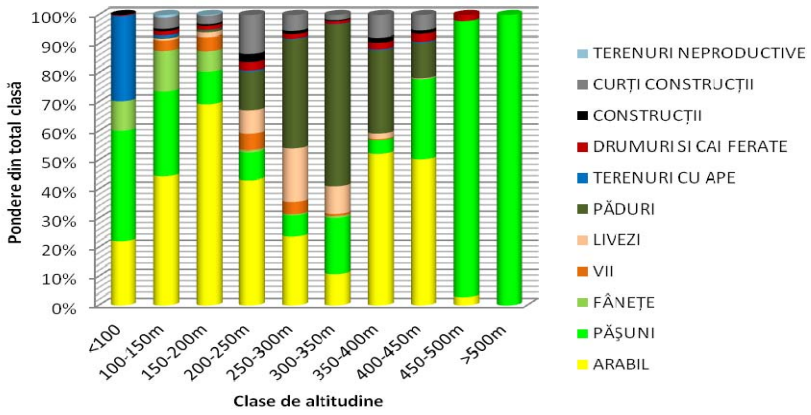

Fig. 4. The distribution of the classes of altitude within the category of use of the lands

The arable land has the biggest extension of the altitude level between 150 – 200 m, where it occupies a surface of 1770,2 ha, and on the level with an altitude between 100 and 150m, it has 1023,4 ha. At high altitudes the arable land occupies surfaces between 350 – 400 m, with 343 ha and between 400 -450 m with 229,7 ha (fig.4). The pastures occupy the biggest surface at altitudes between 100-150 m, having a surface of 671,4 ha, but this category of agricultural use dominates at altitudes of over 450 m, even if it occupies only 59,8 ha. The grass lands are found especially at altitudes between 100 – 150 m, where they occupy a surface of 323,6 ha and at 150 – 200 m the grass lands have 179,2 ha. The vineyards and the orchards are dominantly situated at 150 – 200 m (for vineyards – 124,7 ha) and 250 – 300 m (for orchards – 75,8 ha). The forests and other lands with forest vegetation occupy important surfaces starting from the level of 250 -300 m, having 154,8 ha, after which between 300-350 m are 172,6 ha and the biggest surface that is occupied is found between 350 – 400 m with 187,6 ha. In what the lands with waters are concerned, they are at altitudes under 100 m (55,2 ha), available especially for the hom of Bahlui river and ponds. At altitudes that are between 100-250 m are lands with constructions. The lands that are not productive occupy the largest part, 21 ha on the level of 100-150m.

The cliffs represent the cause of some geomorphologic processes and it considerably influences the way of using the lands.

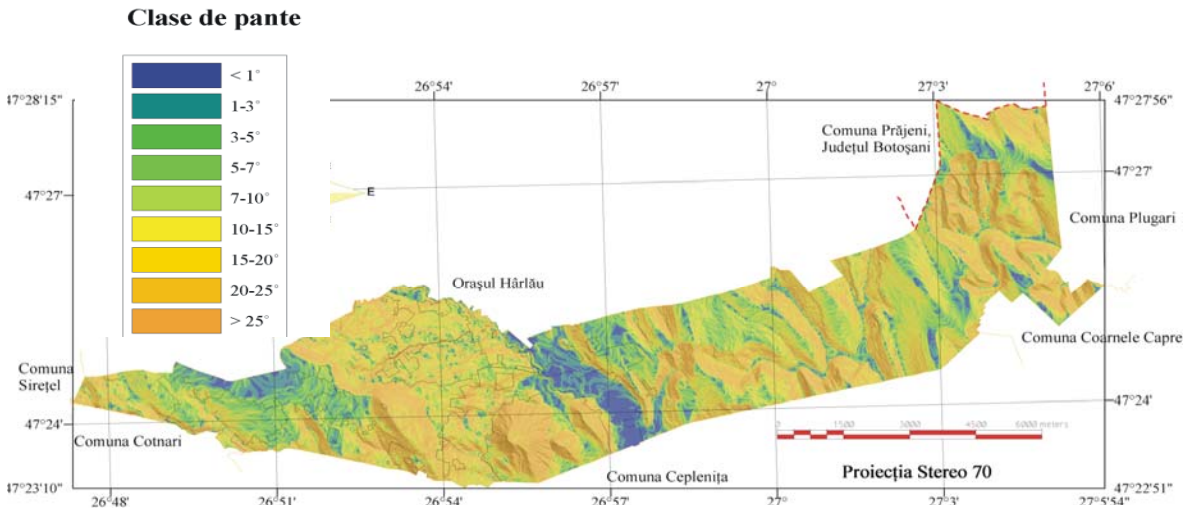

Fig. 5. The map of the cliffs from the studied perimeter; informational layer of the declivity

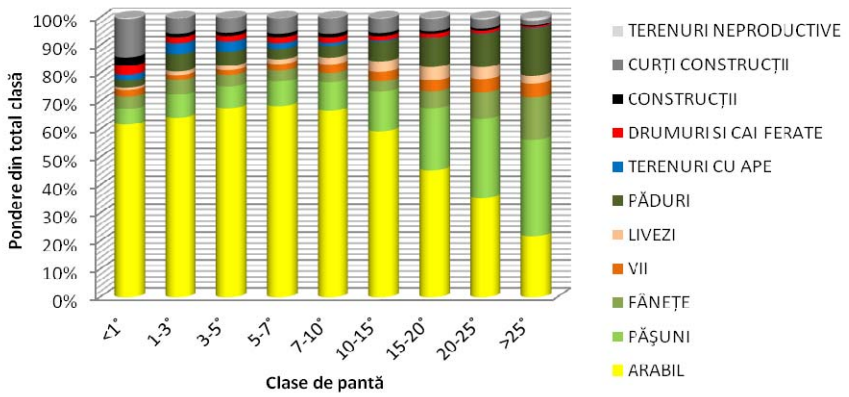

Fig.6. The distribution of the classes of cliffs within the categories of use of the lands

The arable surface is mainly quartered on lands with and inclination of 10-15˚, where they occupy 731,6 ha, but they are often found on cliffs with an inclination of 5-7˚. The dominance of the arable lands progressively drops in favor of pastures, where on the cliffs of over 25˚ have a surface of 513,3 ha.

The grass lands, as in the case of pastures, are found on cliffs that grow progressively, where they have very often values of over 25˚. The vineyards and the orchards can usually be found on versants with a bigger inclination. In what the vineyards are concerned, the cliffs of over 25˚ hold the biggest rate with a surface of 74,3 ha. In what the forests are concerned, we find again a dominance of values of over 25˚ with a surface of 252,7 ha. The lands with waters are quartered on very small classes, from 1-3˚ to 3-5˚. Within the categories of usage, the lands with constructions have the biggest rate on classes of cliffs of under 1˚; but their biggest extension is on values of 10-15˚. The lands that are not productive have the biggest difference of surface on cliffs of over 25˚.

The exposition plays an important role, especially in the case of agricultural surfaces, where different orientations of the versants are suitable for certain usages.

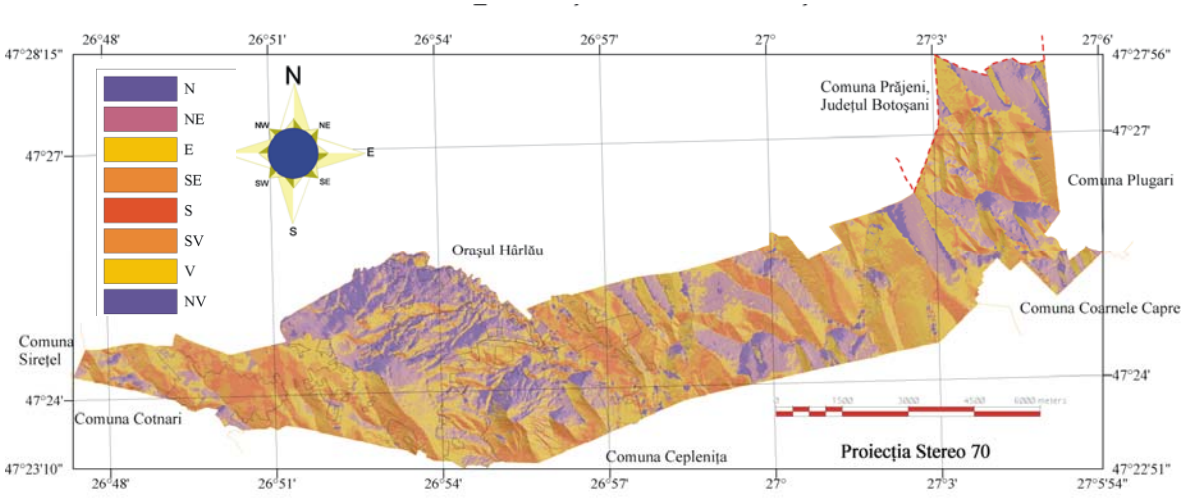

Fig. 7. The map of the exposition of the versants on the studied perimeters

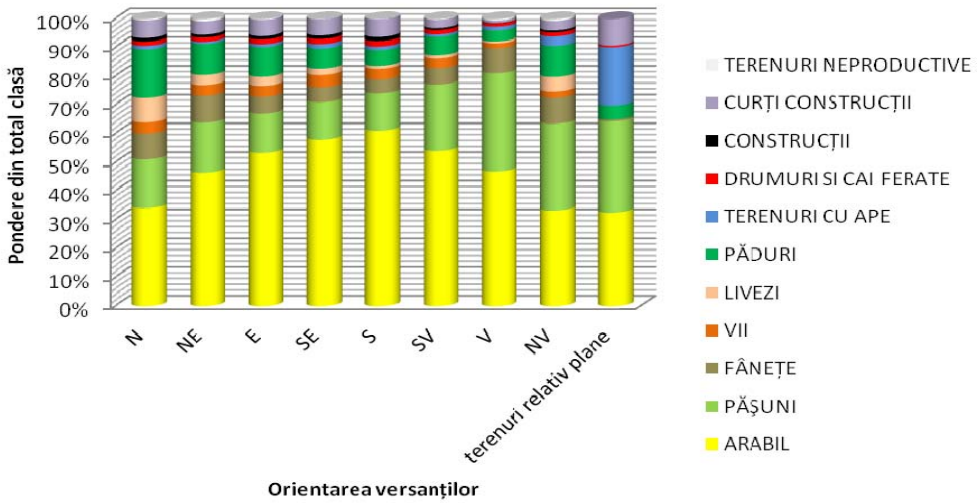

Fig.8. The distribution of the exposition of the versants within the categories of usage of the lands

Although the North-East and East orientation is dominated in what the surface is concerned for almost each use of land, the lands are distributed in a different way.

The balance of the arable surfaces within the land usage grows progressively from North to South, after which it drops; instead the fields have a greater extension of the W and NW versants.

Vineyards have an important proportion within the usages of the versants of SE, of 5%, and the orchards have an extension on the N and NW versants.

The forests that have a Northern orientation occupy 18% from the total of the use, but the biggest surface is occupied by the NE versants with 181, 2 ha.

The lands with waters and the lands with constructions occupy the biggest part of the total of usages on lands that are relatively leveled.

4. CONCLUSIONS

The way of using the lands reflects in a very good manner the directions and the conditions in which a certain territory developed until now, as well as their specific aspects.

The analysis, developed with the help of a GIS program, was established through information of quantity concerning the length, the surface and the relations between various thematic layers that have brought to light certain behaviours of space that are meaning to show certain spatial phenomenon that are more or less visible.

Scobinți commune is dominated by the categories of agricultural usage, especially arable surfaces which show an activity which is mainly oriented towards the primary sector. The agriculture which is done by the population is in general of subsistence on small surfaces that are meant to satisfy only the personal needs of the individual. These surfaces were and are today dominated by the cultivation of corn.

The vineyards and the orchards represent an important category for Scobinți commune within the development policies, thanks to the tradition and to the reputation which they earned in time.

The forest surfaces have a big extension in the West side of the territory, mounting opportunities of valuing the tourism in areas as the forest massif of Basaraba Hill.

The rural incorporated areas developed along Bahlui River, this fact being related with the presence of the phreatic waters near the surface, only Sticlăria village, which recently appeared, does not comply with this rule.

The studies concerning the usage of the lands and the improvement of the territory are necessary for knowing the actual status of a territory, where the public authorities may have new visions concerning the continuous development on a medium or long term.

In what the usage of GIS is concerned, it provides digital information about the real world from a certain territory identified according to its geographical position. The information may be related with the placement, connections between certain points in space, the topology of the network, different types of attributes.

In order to use GIS it is necessary to have hardware equipments, GIS programs, input data, analysis methods, specialists in the field.

The advantages of using GIS are various, having examples in the planning of the projects, which may contain many space components, being necessary certain thematic maps; when it comes to decisions when there are certain litigations related with territorial disputes, private properties, investigations, detailed analysis of the land, management of resources.

5. REFERENCES

[1] Bejan I. (2009) – *Studiu spațial privind utilizarea terenurilor în Republica Moldova*, Autoreferatul tezei de doctor în geografie, Chișinău

[2] Biali Gabriela, Popovici Nicolae (2003) - *Tehnici GIG în monitoringul degradării erozionale*, Editura "Gh. Asachi", Iași, ISBN 973-621-043-X.

[3] Cândea M., Cimpoieru I.,Bran F. (2006) – *Organizarea, amenajarea şi dezvoltarea durabilă a spațiului geografic*, Edit. Universitară, Bucureşti.

[4] Curea D. (2004) – *Studiu pedologic 1:10000 pe teritoriul administrativ al comunei Scobinți*, OJSPA, Iași.

[5] Minea I. (2009) – *Bazinul hidrografic Bahlui – studiu hidrologic*, Rezumatul tezei de doctorat, Universitatea "Al. I. Cuza", Iaşi.

[6] Popovici Nicolae, Biali Gabriela (2000) - *Sisteme Geoinformaționale*, Principii generale şi aplicații. Editura "Gh. Asachi", Iași, ISBN973-8050-43-X.

[7] *** – Planul Urbanistic general al comunei Scobinți, piese scrise şi desenate, 2005-2006.

[8] *** – Planul de amenajare a teritoriului zonal periurban Hârlău, piese scrise şi desenate, 2006.

[9] *** – http://www.ancpi.ro/pages/home.php

Behaviour of Seismic Resistant Eccentrically Braced Frames

Flavia S. Florea

Abstract – **This paper aims to observe the behaviour of eccentrically braced frames (EBF), both in terms of the provisions of the Romanian design seismic code P100-1:2006 and the American Seismic Provisions for Structural Buildings, and in terms of comparative numerical analysis for 4 of the widely used eccentric bracing systems. Numerical simulations consist in static and dynamic nonlinear analysis for a frame with a single span and 10 levels, eccentrically braced in four different systems. Results show main advantages and disadvantages of eccentrically bracing systems and their application in engineering practice.**

Keywords – **energy dissipation, nonlinear analysis, short link, plastic deformation**

1. INTRODUCTION

Eccentrically braced frames (EBF) have been defined as systems that merge the properties of the moment frames and the properties of concentrically braced frames. An eccentrically braced frame can provide structural rigidity similar to that of concentrically braced frame and links subjected to lateral loads deform inelastically, showing good energy dissipation capacity and high ductility, characteristics found in moment frames.

Hjelmstad and Popov use the ratio of link length (e) and frame length (L) to parameterize a continuous spectrum that ranges a moment resisting frame ($\frac{e}{L}=1$) to a concentrically braced frame ($\frac{e}{L}=0$). This ratio allows balancing of lateral stiffness of the frame and inelastic deformation requirements for the elements, and also indicates the contribution of stiffness brought by a bracing frame. It shows that for values of the ratio $\frac{e}{L}>0.5$, bracings effect is not significant, the stiffness considerably increases for a ratio lower than 0.5. We must still provide a sufficient length of the link to ensure ductility requirements of the framework elements subjected to extreme demands [1].

EBF resist to horizontal loads by axially loaded elements, but they are designed to exhibit first plastic deformations in links, provided to yield in bending moment and shear force according to their length.

Thus, the overall energy dissipation of EBF requires directing the hinges in links, while the connections and the other elements of the frame (structural elements outside links) are designed to remain in the elastic range. For a global behaviour without significant degradation of strength and stiffness to severe cyclic loading, in properly designed EBF only links will yield, except for base columns and braces from lower levels. It is sometimes hard to avoid the appearance of limited inelastic deformations in structural elements designed to

Manuscript received February 15, 2010.

F. S. Florea is with Technical University of Civil Engineering Bucharest, Lacul Tei Bvd., no. 122-124, 020396-Bucharest, Romania (corresponding author to provide phone: +40-073-311282; e-mail: florea.flavia@yahoo.com).

ISSN-1584-5990

behave in the elastic range. The overall performance of EBF will not be affected as long as the beam segments outside the link and diagonal braces have sufficient strength not to affect the deformation and strength provided by links during complete yielding.

Generally the design of a link beam is optimized by selecting a section with the minimum required shear capacity and the maximum available bending capacity. The most efficient link sections are usually the deepest sections with the minimum required shear area. The designer may customize the section properties by selecting both the web and flange sizes and detailing the link as a built up section [2].

Results of several experimental tests and numerical simulations have concluded that short links are able to withstand larger inelastic deformations and dissipate a greater amount of energy than those provided to yield due to bending moment. Even though moment resisting frames have a very good capacity in energy dissipation by bending moments in beams, plastic deformations in EBF's links are larger and more concentrated [1]. Short links dissipate more energy because of the specific plastic deformation distribution on a larger and more uniform surface, being able to withstand large inelastic deflections and remain effective for many cycling loads.

Many experimental and numerical studies have shown that plastic deformations in links from ground to upper levels decrease with increasing periods of the frame. As the largest plastic rotations of links are usually found at the first level, involving the risk of producing a story mechanism, Seismic Provisions for Structural Steel Buildings recommended a 10% increase of the minimum shear strength for the first stories links.

2. EXPERIMENT DESCRIPTION

Structural design

According to P100-1:2006, the design plastic values for bending moment and shear force for seismic links with I section are:

$$M_p = f_y b t_f (d - t_f) \tag{1}$$

$$V_p = (\frac{f_y}{\sqrt{3}}) t_w (d - t_f) \tag{2}$$

where: f_y - nominal yield strength of steel;

b, t_f, d, t_w - geometrical characteristics according to **Fig. 1**.

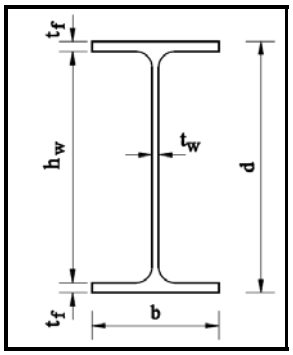

Fig. 1. Geometrical characteristics for I sections

Axial load in seismic links is neglected, if the ratio of design axial force N_{Ed} and plastic design axial load $N_{p,Rd}$ is less than 0.15. Thus, at both ends of the bar dissipative design efforts will be grater than the plastic capable efforts:

$$M_{Ed} \le M_p; V_{Ed} \le V_p \tag{3}$$

where: M_{Ed}, V_{Ed} - are the design action effects, respectively the design bending moment and design shear, at both ends of the link.

Resistance required to shear for the seismic links according to Seismic Provisions for Structural Buildings is limited to:

$$V_u \le \phi V_n \tag{4}$$

where: ϕ - strength coefficient;

$V_n = \min(V_p; \frac{2M_p}{e})$ - nominal shear yield strength;

$V_p = 0.6F_y A_w$ - nominal shear strength of an active link;

$A_w = (d_b - 2t_f)t_w$ - link web area;

Appropriate design of EBF should ensure that only the links will develop plastic deformations during a severe earthquake, while braces, columns and beam segments outside the link should be dimensioned in order to withstand the forces developed by the yielded and strain hardened links.

Designing demands of non-dissipative elements (columns, braces and beam segments outside the link) in EBF for the ULS according to P100-1:2006 are given in equations (5), (6), (7). The relationships provide

increasing the seismic forces with the increased limit material flow (γ_{ov}) and the multiplicative factor due to the design seismic action for the design of non-dissipative members (Ω).

$$N_{Ed} = N_{Ed,G} + 1.1\gamma_{ov}\Omega N_{Ed,E} \tag{5}$$

$$M_{Ed} = M_{Ed,G} + 1.1\gamma_{ov}\Omega M_{Ed,E} \tag{6}$$

$$V_{Ed} = V_{Ed,G} + 1.1\gamma_{ov}\Omega V_{Ed,E} \tag{7}$$

where:

N_{Ed}, M_{Ed}, V_{Ed} = design values of the of the axial force, shear force and bending moment;

$N_{Ed,G}, M_{Ed,G}, V_{Ed,G}$ = efforts in members not containing seismic links due to the nonseismic actions included in the combination of actions for the seismic design situation;

$N_{Ed,E}, M_{Ed,E}, V_{Ed,E}$ = efforts in members not containing seismic links due to design seismic action.

According to Seismic Provisions for structural Steel Buildings (2005), the nominal shear strength of the link, V_n, is increased by two factors: first by R_y to account for the possibility that the link material may have actual yield strength in excess of the specified minimum value and secondly, the resulting expected shear strength of the link, $R_y V_n$ is increased to account for strain hardening in the link.

For designing the diagonal brace, American Provisions have adopted a strength increase due to strain hardening only equal to 1.25, because R_y accounts for expected material strength in the link but not in the brace, and because of the use of resistance or safety factors when computing the strength of the brace.

For the design of the beam segment outside of the link, the Provisions permit calculation of the beam required strength based on link ultimate forces equal to only 1.1 times the link expected shear strength. Based on this approach, the required axial and flexural strength of the beam can be first computed as described above for the diagonal brace, assuming a strain hardening factor of 1.25. The resulting axial force and bending moment in the beam can then be reduced by a factor of 1.1/1.25 = 0.88.

A lower value for the resistance factor design used in beams reflected the observation that limiting yielding of the segment of beam outside the link can benefit the overall performance by reducing inelastic rotation requirement of the link [3].

For capacity design of the columns, Seismic Provisions permits reduction of the strain hardening factor to 1.1. This relaxation reflects the view that all links above the level of the column under consideration will not likely reach their maximum shear strength simultaneously.

Reduced overstrength factor in Romanian codes is counterbalanced by higher plastic shear resistance, so that the final value for maximum shear force estimated by the two codes have similar values. It is adopted a relatively conservative estimation of the maximum shear force [4]:

$$V_{\max} = 1.75V_y = (h - 2t_f)t_w \frac{f_y}{\sqrt{3}} \tag{8}$$

To highlight the behaviour of various systems for eccentrically braced structures we considered a steel frame with 9 stories of 3.0m height, and a 4.5m span. The structure is located in Bucharest, a seismic zone with design ground acceleration $a_g = 0.24g$, the upper limit of the period of the constant spectral acceleration branch $T_c = 1.6s$ and maximum dynamic amplification factor of horizontal ground acceleration of the structure $\beta_0 = 2.75$. The structure was designed according to seismic code P100-1:2006 and Eurocode 3: Design of steel structures. The eccentrically braces were designed in 4 different systems, as shown in **Fig. 2**: K frame, D frame, V frame, Y frame.

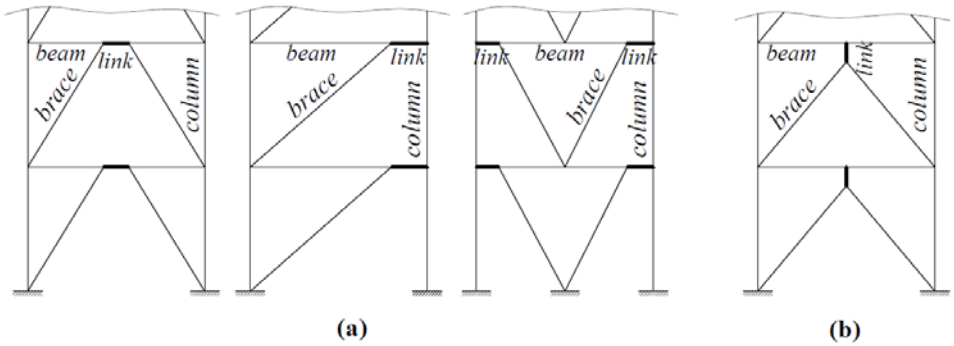

Fig. 2. (a) Horizontal links: K frame; D frame; V frame; **(b)** Vertical links (Y frame)

Columns have symmetric double T section (HEA), the beam segments outside the links have I section (IPE) and the braces have pipe section. Dissipative elements – seismic links will be made of S235 steel, and the items expected to behave within the elastic range will be made of S355 steel.

For all frames were considered at all levels short seismic links with 0.5m length. The links have I section (IPE) and were designed according to (5), (6), (7). The non-dissipative elementes were designed according to (8).

3. RESULTS AND SIGNIFICANCES

Linear analysis

The four EBC were designed so that they have very close eigenvalues. **Tabel 1** illustrates the values for the fundamental mode of vibration – period and frequency:

Table. 1. Eigenvalues for the fundamental mode of vibration

Mode 1	**K frame**	**D frame**	**V frame**	**Y frame**
Period - ***T***	0.862	0.905	0.894	0.902
Frequency - ***f***	1.159	1.105	1.119	1.108

For the K frame, the maximum bending moments in beam segments outside the links occurred at the ends of bars next to seismic links. Bending moments in columns were much lower compared with eccentric bracing systems in which links were attached to columns (D frame, V frame).

In D frame, axial forces in beams outside the link and the braces have the highest values of all studied systems. As it was expected, bending moments in columns have the highest values compared to the other system, due seismic link to column connection.

Because in V frames the beam segment outside the link carry together with the braces most of the gravitational loads from the floors, values for bending moments are greater than those from D and K frames.

The maximum shear forces in beam segments outside the links were located in Y frames.

Static nonlinear analysis results

The nonlinear behaviour of structural members was modeled using plastic hinges and acceptance criteria according to FEMA 356: hinges for columns are due to axial force-bending moment interaction, hinges for braces are due to axial force, hinges for beams are due to bending moment and hinges for short links are due to shear force.

For each eccentric bracing system a nonlinear static analysis was performed to illustrade the occurrence of successive plastic hinges and energy dissipation.

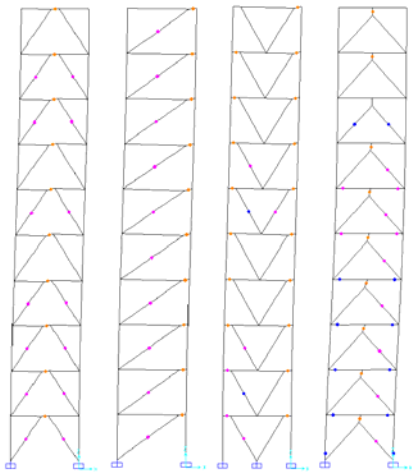

Fig. 3. Plastic hinges at the last step of the static nonlinear analysis

Fig. 3.shows that Y bracing system is the only one that developed plastic hinges in the columns and beam segments outside the link. Therefore we can say that bracing systems in "Y" have the most unstable hysteretic behaviour. This behaviour is explained by the fact that for these systems is very difficult to predict a global mechanism of failure after the yielding of seismic links [5]. On the other hand, Y frames are the only ones which can be used in seismic rehabilitation of the existing steel or reinforced concrete structures. They are also easy to replace after the occurrence of plastic deformations.

Because in the V frame the number of links is doubled, not all of the plastic deformations in links have grate values. The advantage from this point of view is that this brace system has the smallest number of plastic deformations in non-dissipative zones.

In the rest of the frames, almost all seismic links were subjected to plastic deformations, with a uniform distribution, and the other structural elements remained in the elastic range, except the occurrence of small post-yielding deflections in some braces, emphasizing a favourable global plastic mechanism for EBF in general.

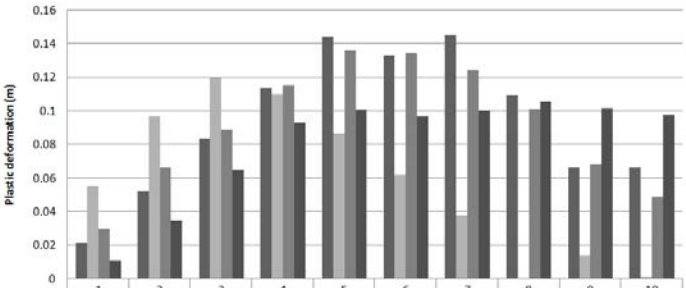

	1	2	3	4	5	6	7	8	9	10
K Frame	0.021684	0.052383	0.083942	0.113594	0.144048	0.133041	0.145537	0.109904	0.066766	0.066766
Y Frame	0.055652	0.097032	0.119896	0.110009	0.086855	0.06226	0.038119	0	0.014171	0.001476
D Frame	0.029903	0.066398	0.089133	0.115621	0.136192	0.13484	0.124243	0.101355	0.068198	0.048909
V Frame	0.011145	0.034873	0.064829	0.09298	0.10105	0.09685	0.100298	0.105648	0.102004	0.097674

Fig. 4. Maximum plastic deformations in seismic links per level

In **Fig. 4.** we compare the maximum values of the plastic deformations for the analysed frames on each level. Y bracing system has the most unpredictable behaviour. For first levels hinges have maximum values, and for the last levels, the smallest values. K and D frames have uniform plastic deformations in seismic links.

Dynamic nonlinear analysis

All the EBF systems were subjected to the base excitation taken from Vrancea 1977 earthquake – N-S component acceleration record. **Fig. 5.** reveals the greatest values of the peak horizontal displacement showing that although the four systems were designed to have close eigenvalues, their response to Vrancea excitation was different. The greatest peak displacements were obtained from the D frame, and K and V frames have almost similar behaviour.

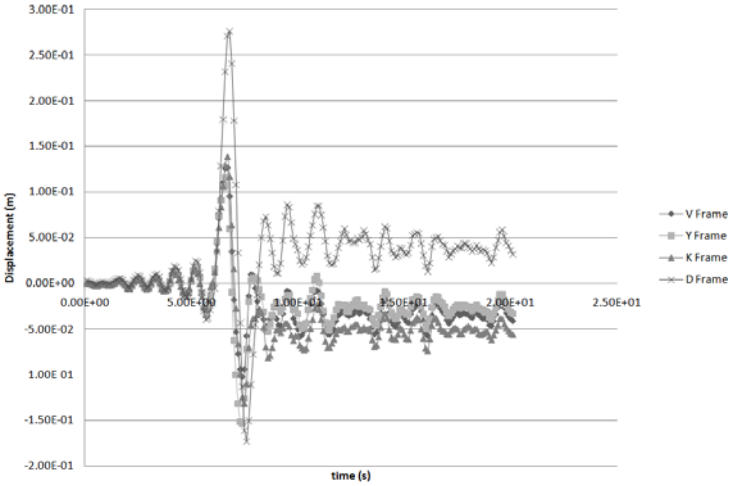

Fig. 5. Peak seismic displacement

4. CONCLUSIONS

In general EBF with short links demonstrated a good capacity of plastic deformation and of energy dissipation.

V frames, heaving more dissipative zones, had smaller values for plastic hinge deformations. From the same reason, the structural elements designed to remain in the elastic range, had de smallest and the fewest number of hinges.

The eccentrically bracing system "Y" showed the worst energy dissipation mechanism, despite the unique advantages of this system given by the fact that the seismic link is not included in the beam frame: it is easy to replace after he a strong earthquake and it can be used as a strengthening method for existing structures using short links as a displacement dependent damper dissipating energy through inelastic deformation of metal.

Bending moments in D frame's columns have the highest values compared to the other systems, due seismic link to column connection.

6. REFERENCES

[1] J.O. Malley, E.P. Popov, "Shear links in eccentrically braced frames," Journal of Structural Engineering, vol. 110(9), 1984, pp. 2275-2295.

[2] R. Becker, M. Ishler, "Seismic Design Practice for Eccentrically Braced Frames," Structural Steel Educational Council, Dec. 1996.

[3] T. Okazaki, "Seismic Performance of Link-to-Column Connections in Steel Eccentrically Braced Frames," Dissertation of the Requirements for the Degree of Doctor of Philosophy, The University of Texas at Austin, 2004.

[4] Stratan A., Dubina D. Bolted Links for Eccentrically Braced Steel Frames. Connections in Steel Structures V. Amsterdam. June 3-4, 2004.

[5] Kober H., Dima S. The Behavior of Eccentrically Braced Frames with Short Links. Recent Advances and New Trends in Structural Design – International Colloquium dedicated to the 70th Anniversary of Professor Victor Gioncu. Timisoara. May 7-8, 2004.

[6] P100-1/2006 - Cod de proiectare seismica – Partea I: Prevederi de proiectare pentru clădiri, August 2006.

[7] AISC (2005):Seismic Provision for Structural Steel Buildings, ANSI/AISC 341-05, American Institute of Steel Construction, Chicago, Illinois, 309 pp.

[8] AISC STANDARD: Specification for Structural Steel Buildings, American Institute of Steel Construction, Chicago, Illinois, Public Review Draft Dated December, 1, 2003.

[9] FEMA 356, Prestandard and Commentary for the Seismic Rehabilitation of Buildings.

Study On Overheated Concrete Behavior

C. D. Hâncu, M. Florea and M. Stănescu

Abstract – **To ensure the fire resistance safety of the studied building structure, 0 to 31.5 mm aggregate concrete (cubic specimens, with class C20/25) and concrete sand (samples supple, 4x4x16 cm, with class C16/20). The samples were submitted to fire. Resistance measurements were performed nondestructive.**

Keywords – **concrete, resistance, fire, nondestructive measurements.**

1. General

To ensure the fire resistance safety of the building structure several factors are very important:

- Time to reach maximum temperature combustion (burning up the stage regression);
- Maximum temperature can be achieved, depending on the combustible material and the existence of sufficient air (indoor or outdoor combustion);
- Knowledge of concrete behavior in repeated fires;
- Knowledge of fire fighters intervention effects on concrete at high temperatures.

2. Experimental Program

The materials under study were:

- Concrete with maximum aggregate grain 31.5 mm (cubic specimens, 10x10x10 cm) with class C20/25,
- Concrete sand (samples supple, 4x4x16 cm) with class C16/20.

The size of the specimen was chosen according to the size of the "burn" room available in the laboratory oven.

Tested concretes were made without additives. The maximum temperature that develops existing laboratory furnace is 1600°C. Therefore we tried simulating the effect of fire textiles, paper, wood, rubber and petroleum products on concrete (the material rather than the resistance structure as studied in problem [1]).

Fires were simulated over 1, 2 and 3 hours. We believe that the time intervals chosen are sufficiently relevant to possible fires. We have studied the fire behavior of concrete which suffered from previous fire. We

Manuscript received September 12, 2012.

C. D. Hâncu is with Ovidius University of Constanta, Bd. Mamaia nr. 124, 900356-Constanta, Romania (corresponding author to provide phone: +40-241-619040; fax: +40-241-618372; e-mail: dhancu@univ-ovidius.ro, danhancu@yahoo.com).

M. Florea is with Ovidius University of Constanta, Bd. Mamaia nr. 124, 900356-Constanta, Romania (corresponding author to provide phone: +40-241-619040; fax: +40-241-618372; e-mail: floream@univ-ovidius.ro).

M. Stănescu is with Ovidius University of Constanta, Bd. Mamaia nr. 124, 900356-Constanta, Romania (corresponding author to provide phone: +40-241-619040; fax: +40-241-618372; e-mail: mada_x_dobre@yahoo.com).

ISSN-1584-5990

have also experienced the effect of an attempt to extinguish the fire with large amounts of water (the specimens reaching the fire temperature were sprayed with large amounts of water).

Resistance measurements were performed nondestructive, with ultrasound Pundit - Elle device.

The work steps used were:

- Preparation of specimens: casting, hardening, marking,
- Separation of control samples,
- Determination of strength, non-destructive,
- Submission of samples lots to fire (1, 2, 3 hours at a certain temperature or 1 hour at different temperatures),
- Estimating mechanical resistance (nondestructive) after the fire and cooling temperature of 20°C (for at least about 24 hours),
- Processing the results,
- Conclusions, observations and recommendations.

3. RESULTS

Table 1 presents data characteristic of cubic specimens prior to submission to "fire".

Table. 1. Data characteristic of cubic specimens prior to submission to "fire".

Code		Witness tests			
		t (µs)	v (m/s)	ρ_a (kg/m^3)	Average porosity (%)
A	1	22,8	4386	2168	8,17
	7	22,5	4444	2153	
	8	22,8	4386	2139	
	10	22,6	4425	2147	
	11	22,8	4386	2130	
B	4	21,1	4739	2289	6,07
	12	21,5	4651	2145	
	16	22	4545	2095	
	18	21,7	4608	2167	
	20	21	4762	2162	
C	2	23,4	4274	2122	7,09
	3	23,4	4274	2139	
	6	24	4167	2100	
	9	23,3	4292	2121	
	17	23	4348	2121	
D	13	18,9	5291	2318	5,24
	14	18,4	5435	2280	
	19	18,2	5495	2308	
	23	18	5556	2230	
	24	18,9	5291	2310	

Obs. t – the time the ultrasound beam passed through the specimen (10-6 seconds),
v – the velocity of ultrasound in concrete,
ρ_a – the bulk density of concrete, open medium porosity of concrete.

We have no longer calculated the mechanical resistance as by determining ultrasound velocity in concrete because they are proportional to the velocity (higher velocity automatically shows higher strength class).

In Tables 2a and 2b we list the characteristic data cube after subjecting specimens to a "fire" or two "fire".

Table. 2a. Samples subjected to a "fire".

Code		Type of fire	t (µs)	v (m/s)	ρ_a (kg/m^3)	Average porosity (%)
A	1	1 hour – 933°C	82,8	1208	2117	-
	7	2 hours – 933°C	107,6	929	2095	10,74
	8	3 hours – 933°C	56,9	1757	2088	9,87
	10	1 hour – 1200°C	167	599	2068	x
	11	1 hour – 1467°C	280	357	2040	x
B	4	1 hour – 933°C	50,2	1992	2257	-
	12	2 hours – 933°C	86,5	1156	2082	10,47
	16	3 hours – 933°C	82,6	1211	2038	10,25
	18	1 hour – 1200°C	126	794	2095	10,74
	20	1 hour – 1467°C	310	323	2060	x
C	2	1 hour – 933°C	66,5	1503	2079	-
	3	2 hours – 933°C	114	877	2078	10,44
	6	3 hours – 933°C	59	1695	2054	10,18
	9	1 hour – 1200°C	172	581	2049	x
	17	1 hour – 1467°C	228	439	2035	x
D	13	1 hour – 933°C	45,4	2203	2288	-
	14	2 hours – 933°C	65	1538	2230	7,17
	19	3 hours – 933°C	57,2	1740	2260	6,73
	23	1 hour – 1200°C	138,2	724	2142	9,24
	24	1 hour – 1467°C	x	x	2190	x

Obs. x –the fire samples were too degraded to be able to make determinations.

Table. 2b. Samples subjected to two "fire" (2 x 1 hour at 933°C, 24 hours apart).

Code	The second fire	t (µs) **	v (m/s) **	ρ_a (kg/m^3)	Average porosity (%)
A 1	1 hour – 933 ^{0}C	37,4	2673	2107	10,35
B 4	1 hour – 933 ^{0}C	29	3448	2240	8,13
C 2	1 hour – 933 ^{0}C	34,5	2899	2072	10,52
D 13	1 hour – 933 ^{0}C	30,2	3311	2276	6,77

Obs. ** - the experimental technique has been reversed (saturation was done first, then porosity determination by oven drying, and finally, determination by means of ultrasound device; probably the drying was not complete) and the results are influenced to some extent.

Due to lack of space the experimental data on concrete sand are not presented.

4. CONCLUSIONS

For the study of 0 to 31.5 mm aggregate concrete (cubic specimens) attempts were made at:

- Various temperatures (933, 1200 and 1467°C),
- Different fire durations (1, 2 or 3 hours)
- One or two fires at a time that allowed cooling specimens at a temperature of about 20°C (about 24 hours).

Increasing the firing temperature has an obvious effect of degradation of the concrete structure. Resistance reductions to witness - specimens that have not suffered the fire - are 58 to 64.8% for 933 ^{0}C, 82.8 to 87% for 1200°C and 89.9 to 100% for 1467°C.

The fire duration had - from the witness - the effect of reducing the resistance by 58 to 72.5% in 1 hour, by 71.7 to 79.5% in 2 hours and by 59.9 to 75.1% at 3 hours of burning at 933°C. Unexpectedly, the resistance decreases are smaller for 3 hours than for 2 hours, probably due to the occurrence of partial melts in concrete (see photo – **Fig. 1**).

Fig. 1. Studied cubic specimens, 10x10x10 cm

The concrete class has influenced the fire resistance which means that higher class concrete have held up better (58.4% resistance loss to better concrete as appeared to 64.8% resistance loss to the weaker ones of those tested for 1 hour to 933°C; the situation applies to 2 hours but it is uncertain to 3 hours).

The degradation of concrete structural frame was highlighted by increasing the bulk density from 1.4 to 5.2% and by increasing open porosity up to 20.8 - 76.9%. This highlights the very significant decrease in durability of the concrete subjected to fire.

It is therefore necessary to assess the resistance of concrete structures subjected to strong or long lasting fire, before concluding that the building could be repaired or it should be demolished.

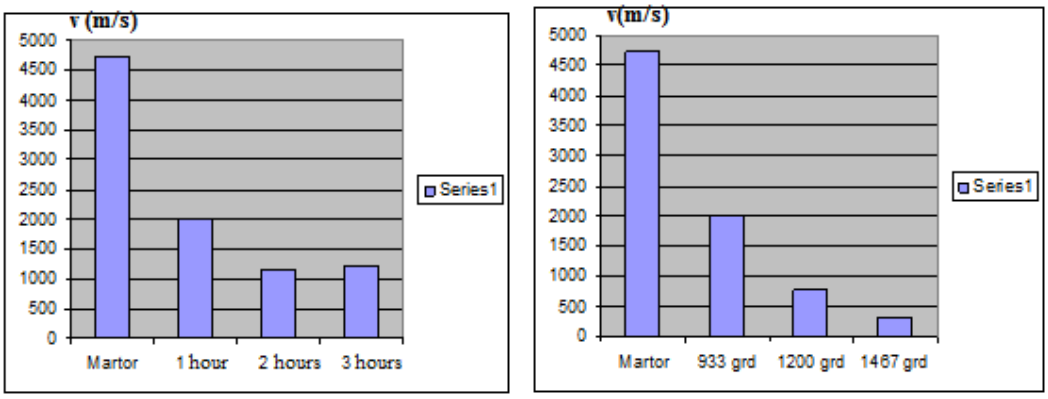

A – depending on the fire duration B – depending on the fire temperature

Fig.2 Resistance Loss

To analyze the behavior of the concrete sand (with aggregate 0-8 mm) attempts had to me made to:

- Different fire durations (1, 2 or 3 hours).
- Various firing temperatures (933 and 1600°C).
- One or two fires at a time that allowed cooling specimens at a temperature of about 20°C (72 hours).
- Simulating the fire-extinguishing action by spraying an abundant amount of water on the concrete reaching the combustion temperature.

Increasing the combustion duration from 1 hour to 2 hours led to a decrease of resistance between 33.9 to 77%. As in the case of 0 to 31.5 mm aggregate concrete a 3 hour fire had less damaging effect than a 2 hours fire (resistance increases from 41.8 to 51.7%; the likely reason would be the occurrence of partial melting in concrete mass).

Specimens showed residual dilatation (average) of 0.19 to 2.13% after a fire.

Combustion temperature of about 1600°C had devastating effects on mechanical resistance. The samples were so degraded that the porosity could not be determined and the mechanical resistance decreased severely (loss of 96.3 to 98.7%). The ultrasonic determination was made at 24 hours after firing.

Fig. 3 Sand concrete samples fired at 1600°C

The simulation of trying to extinguish the fire by spraying an abundant amount of water led to the complete destruction of the specimens in a few minutes.

It was also noted that some samples (A10, A11, B20, C9 and C17) had 24 hours of fire resistance that allowed measurements, but after a few days they were severely damaged by the disintegration. This suggests that the demolition of a fire risk building is very high even after a few days from the event.

It can be concluded that the fire extinguishing process of a concrete construction should be done in different methods: cooling the combustion zone, preventing air freshness, reducing the available amount of oxygen, introduction of fire inhibitors, reducing the combustion temperature of burning substances and/or removing the combustible from the combustion zone [5].

Subduing the concrete already exposed for 1 hour at 933°C to a second fire of 1 hour at 933°C showed resistance losses of 26.7 to 35.5% to weaker concrete and of 4.5 to 22% to higher class concrete (compared to the samples already exposed for 1 hour to 933°C).

In comparison with the control samples, the resistance losses were 43.1 to 53.7%. It is also observed in this case the better behavior of higher compressive strength class concrete.

It is also noted that two short fires (2 x 1 hour) degrade concrete less than a longer fires (2 hours). The fire fighting duration is essential for the viability of the resistance structure.

It is considered useful to make the resistance of high fire risk building structures of concrete with higher class strength than the one recommended in SR EN 206 to 1/2002. It is also believed that it would be useful to supplement Annex F of the above mentioned standard (appendix recommended minimum resistance classes according to the classes of exposure to various aggressive factors) with recommendations for the concrete used in high fire risk constructions.

Also, for the concrete used in high fire risk constructions, Portland cement and stabilizing ceramic or aluminous cement could be used; aggregates could be some of those recommended for concrete with refractory behavior.

Additional data can be found in [8].

6. REFERENCES

[1] SREN 1363 / 1,2,3 - 2001 - *Fire resistance tests*
[2] STAS 10903/79 - *Determination of thermal load in buildings*
[3] SR-ISO 8421/1 - 1987 – *Burning*
[4] Diaconu D., Burlacu L. - *Combustion Phenomena*, Reviews AICPS 1/2007, Bucharest
[5] *** *Command firefighters - General notions about burning and fire* - Course
[6] *** *Command firefighters - Fire Safety and Risk* - Course
[7] SR EN 206-1 / 2002 - *Concrete. Part 1: Specification, performance, production and conformity*
[8] Hâncu CD, M. Florea, M. Stanescu, Mardare G. - Study of concrete in fire behavior, 2/11/2011 Research Report, Research Centre of the Faculty of Civil Engineering in Constanta

Analysis of WWTP facilities using CFD methods

Ing. Michal Holubec, doc. Ing. Štefan Stanko, PhD., doc. RNDr Ivona Škultétyová, PhD., Ing. Ivana Mahríková, PhD., Ing. Kristína Galbová

***Abstract* – The paper will focus on CFD modeling (Computational fluid dynamics) of WWTP structures. The grit chamber and sedimentation/settlement tanks are the structures of mechanical treatment. Secondary sedimentation tank, settles the sludge after biological treatment. We can find various shapes of settlement tanks and many types of grit chambers at WWTPs. To achieve the effective operation concerning the proper technological processes and cost saving, we need to find the best solution for hydraulic conditions in these facilities. The CFD offers solutions without the need of building a physical model.**

***Keywords* – CFD, Settling tank, WWTP, Sedimentation**

1. INTRODUCTION

Computational Fluid Dynamics (CFD) as an interdisciplinary science forms a bridge between the fields of mathematics and physics and the engineering praxis through the fast evolving computer sciences. The basic notion is to simulate complex engineering problems through mathematical models solved by high performance computers. Coming from aerospace industries, it has gained a lot of ground in other branches as well and in the late 20th century, CFD was used in most industrial sectors. The main gains from this technology are, of course, the reduction of cost for most experiments and experimental design compared to physical modeling and lower time demand which results in faster production cycles in the industry and more effective research. (1) We can assume that CFD technologies will expand even further in the coming years, driven by the advancement of computer technologies which provide the means of calculating increasingly complex mathematical models in even less time.

A large part of the sanitary engineering field consists of wastewater transportation and treatment, which both offer a wide range of problems that could be solved more efficiently with the utilization of CFD technologies. For instance, the ongoing projects of sewer system constructions throughout Slovakia, reconstruction of old oversized waste water treatment plants in the bigger cities or the construction of new ones. There is a lot of waste water treatment plants (WWTP) in Slovakia which have problems with hydraulics in their technological processes, even after reconstruction.

Ing. Michal Holubec is with Slovak University of Technology in Bratislava; Radlinského 11, 81368, Bratislava, Slovakia; tel.: +421 2 5292 3275, e-mail: michal.holubec@stuba.sk.

doc. Ing. Štefan Stanko, PhD. is with Slovak University of Technology in Bratislava; Radlinského 11, 81368, Bratislava, Slovakia; e-mail: stefan.stanko@stuba.sk.

doc. RNDr Ivona Škultétyová, PhD. is with Slovak University of Technology in Bratislava; Radlinského 11, 81368, Bratislava, Slovakia; e-mail: ivona.skultetyova@stuba.sk.

Ing. Ivana Mahríková, PhD. is with Slovak University of Technology in Bratislava; Radlinského 11, 81368, Bratislava, Slovakia; e-mail: ivana.mahrikova@stuba.sk.

Ing. Kristína Galbová is with Slovak University of Technology in Bratislava; Radlinského 11, 81368, Bratislava, Slovakia; e-mail: ivana.mahrikova@stuba.sk.

ISSN-1584-5990

2. COMPUTATIONAL FLUID DYNAMICS

Simulating an engineering problem with the use of CFD systems consists of several parts. The basics are a topological model (geometry) representing the task, for instance a 3D model of a settling tank and of course the physical laws and values describing the flow and other phenomena in the space defined by this geometry. The three basic laws governing the hydrodynamics are the conservation of mass, energy and momentum. These laws are expressed by a set of partial differential equations known as the Navier-Stokes equations. The equations are an accurate representation of the motion of fluid substances they are, however, unsolvable in their analytical form. Therefore, we need to transform these equations into discretized systems of algebraic equations in order to solve them numerically. (2) Also, we need to define starting and boundary conditions, to ensure that there is only one valid solution to the problem. We combine these equations and the topological model into the mathematical model, which is then solved by the computer as a set of numerical equations. A diagram of the process can be seen on **Fig. 1**. Of course, the question of the results credibility of such virtual modeling is often raised.

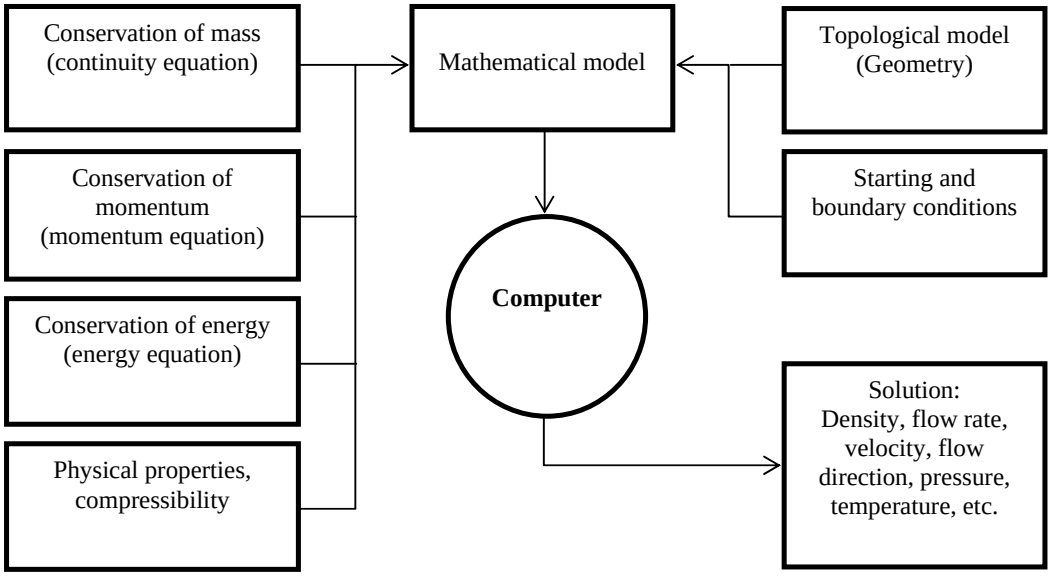

Fig. 1 Description of the process of a CFD simulation

Often the lack of accuracy is caused by inadequate calibration of the models and solution methods. To ensure proper results, various verification and validation methods are introduced to the process. The accuracy of the computational solution is investigated during the verification process, which tries to identify and quantify errors. These errors are mostly caused by the approximation of governing equations of the simulated physical phenomena. Validation process addresses the uncertainty and error margin of the conceptual and computational model. It can be achieved by comparing the simulated results to measurements on a physical model or a full scale representation of the simulated problem. This task of course, provides its own set of problems and complications and can by very costly, both in time and resources, depending on the type and scale of the simulated problem. The process of validation and verification requires the use of various experimental techniques from different scientific fields. The conceptual description of this process is illustrated in **Fig. 2**.

3. SEDIMENTATION TANKS

There are several incentives for the use of CFD technology in sanitary engineering. Treatment of waste water, more precisely, the simulation of fluid dynamics and settling processes in settling tanks (primary and secondary, even grit chambers) is one of the more interesting fields. The main reason is of course, economics. Civil engineering strives for optimization in every direction, to achieve the perfect balance between material quantities, effectiveness and cost. WWTPs in Slovakia offer a fairly large amount of space to improve in these regards. In terms of operational facilities, an overwhelming number of grit chambers and primary settling tanks are of rectangular construction. These tanks where designed using empiric calculations. This design approach is based on the Hazen's theory of ideal sediment basin with a factor to account for turbulence, which is widely accepted in engineering praxis. A schematic representation of Hazen's ideal basin can be seen in **Fig. 4**

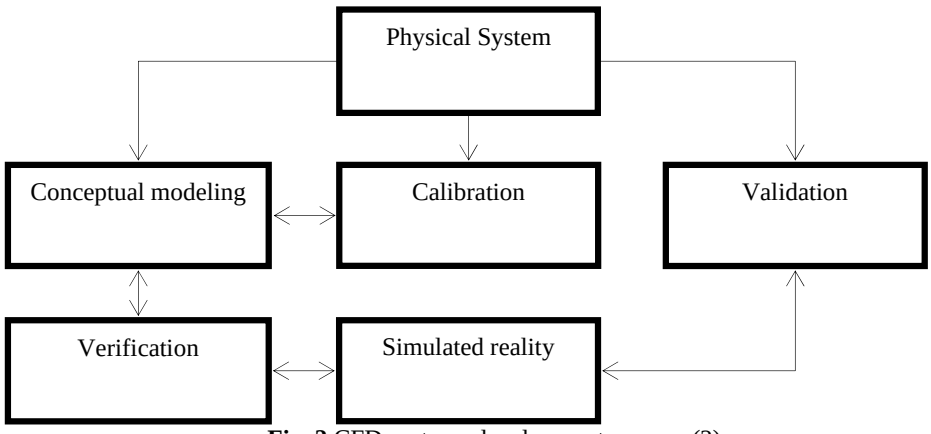

Fig. 2 CFD systems development process (2)

This method yields a reasonable approximation in most cases, however, it falls short when it comes to some important phenomena, mainly related to turbulence. In most cases, the flow pattern is far from the desired plug flow.(see **Fig. 3**)

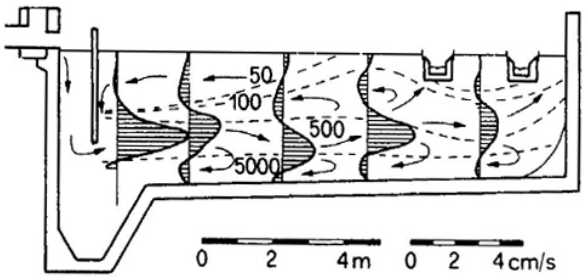

Fig. 3 Example of flow pattern in a settling tank, numbers equal solid s concentration in $mg.l^{-1}$(2)

The ideal sedimentation design is based on several assumptions:

- Homogenous particle distribution throughout the inlet zone
- Laminar flow in the settling zone

- Transformation to discharge flow occurs in the outlet zone
- Particles in the sludge zone no longer take part in the sedimentation process (no re-suspension)
- Discrete particles throughout the settling zone (Type I settling)

Non ideal flow behavior in the settling tank can by induced by one or more of these phenomena (2)(3):

- Short-circuit currents, when the active flow does not cover the available surface area of the tank
- Hindered settling of particles in the tank (Type III settling)
- Dead zones in the tank, mainly corners
- Density currents caused by suspended solids and temperature differentials
- Scour and re-suspension of deposited solids due to excessive velocity currents in near the sludge zone

Short-circuiting in a settling tank causes short hydraulic detention times, which has a negative impact on the sedimentation efficiency of the tank. The most common method used to mitigate this effect, is the design and installation of baffles and outlet weirs.

Density currents are caused by the difference in density of the influent water and the density of the relatively quiet fluid in the tank. This causes the influent to plunge to the bottom of the tank, which in turn, creates a secondary counter-current on the surface of the tank, as seen on **Fig. 5**. This has a negative effect on sedimentation in the tank because of the excessive speed near the sludge zone, which such a current can create, and re-suspend the deposited solids. (4) These currents can create a whole flow system in the tank, even with three or four layers of flow. Research has shown that this phenomenon can be mitigated and/or moderated, with the installation of a baffle before the inlet. It was indicated, that such a flow pattern could even be beneficial for the settling of solids, as the detention time in the layered flow (with varying directions) is very close to that of a uniform flow. (2)

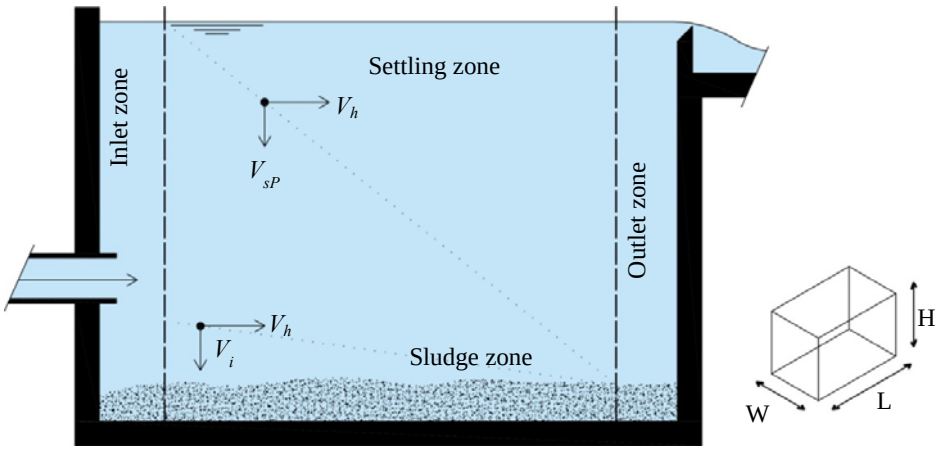

Fig. 4 Schematic view of an ideal sediment basin

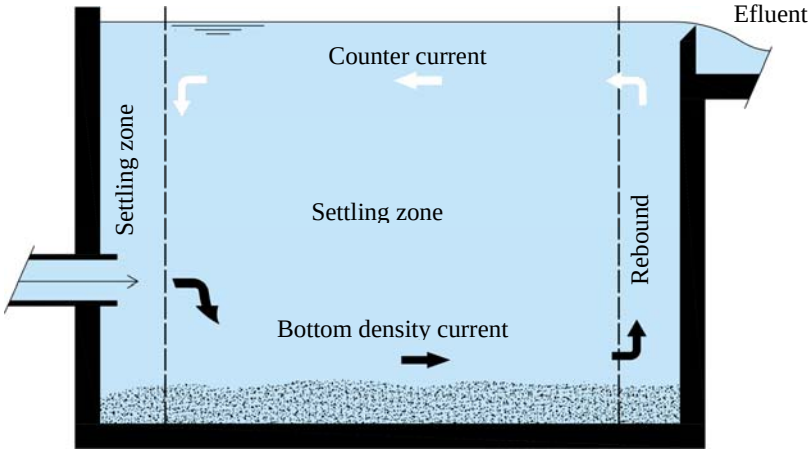

Fig. 5 Scheme of density flow

These factors can be, to a significant extend, simulated with the utilization of a CFD system, which enables a better approximation of the flow and sedimentation processes in settling tanks. Using a robust application like the ANSYS Fluent, methods can be put in place to account for turbulence based problems and solid particles behavior. To this end, not only the Navier-Stokes equations are needed, but also solid transport and turbulence needs to be modeled. The visualization of results then allows us to analyze the velocity, pressure fields and density and distribution of solid particles throughout the simulation domain. The visual imagery enables easy identification of most hydraulic problems in the flow field and provides means to quickly assess the impact of any optimization measures put in place, such as installation of baffles, modification of outlet weirs etc. (**Fig. 6**). Time and space conservation being the CFD technology's main advantages, allow for a more experimental approach to problem solving and optimization. We can tryout several modifications and adjustments to compare the outcomes and chose the best method in time, with which conventional methods cannot compete.

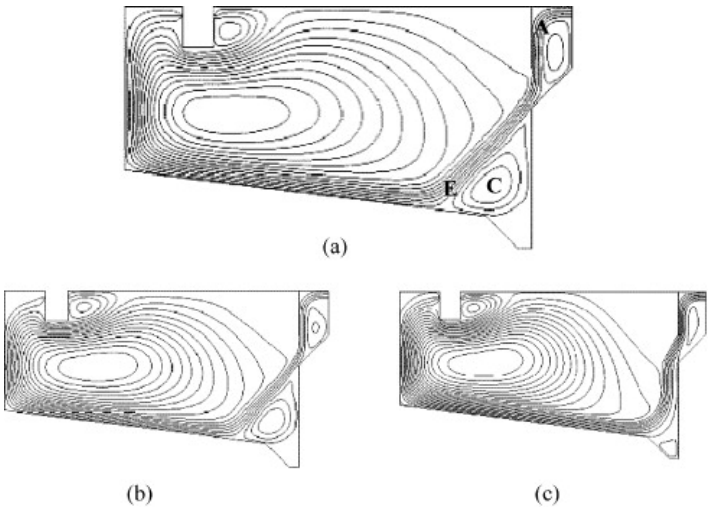

Fig. 6 Calculated streamlines for the standard and the modified sedimentation tank. (a) Standard tank, water, (b) standard tank, water + particles and (c) modified tank, water + particle(5)

4. CONCLUSIONS

This paper briefly describes problems that must be taken into account when simulating settling tanks with the use of CFD systems. As was showed above, the problematic of settling tanks simulation is more deep and complicated as the methods derived from the ideal sedimentation basin theory would suggest. This method, although applicable and applied in engineering praxis, leaves much room for improvement. CFD systems so far appear to be suitable tools to reach better efficiency of sedimentation tanks. However there are limits within this technology which require the development of strategies not only for the assembly of a mathematical itself but also for the process of simulation with the use of specific software. Compromises need to be made between the need of more precise approximation of a given problem and the time constraints, which are dictated not only by the scope of the problem and precision of the calculations needed, but also by accessible computational power. This makes the preparation phase of the model equally important as the quality and structure of the computational mesh has a significant impact on computing times. The process of simulation can also be divided into smaller tasks and the use various simplifications methods, for instance by making use of the symmetry of some settling tanks, and the use of 2D modeling instead of 3D where applicable. These methods help to speed up the whole process and free more time which allows the researcher to concentrate on the actual research and analysis of the results.

5. ACKNOWLEDGMENTS

6. REFERENCES

1. **Molnár, Vojtech.** *Počítačová dynamika tekutín: interdisciplinárny prístup s aplikáciami CFD.* Bratislava : Slovenská technická univerzita v Bratislave, 2011. ISBN 9788081060489.
2. **Ghawi, Ali Hadi.** *A numerical model of flow and settling in sedimentation tanks in potable water treatment plants.* Bratislava : STU Bratislava, Stavebná fakulta, 2008. 978-80-227-2964-2.
3. **Janssen, Robert H.** Analysis and design of sediment basins. *Eighth National Conference on Hydraulics in Water Engineering.* Gold Coast, AU : The Institution of Engineers, Australia, 2004.
4. **Rodi, Wolfgang.** *Turbulence models and their application in hydraulics, a state-of-the-art review.* Third edition. Rotterdam : A. A. Balkema, 1993. ISBN 90 5410 150 4.
5. **Athanasia M. Goula, Margaritis Kostoglou, Thodoris D. Karapantsios, Anastasios I. Zouboulis.** *A CFD methodology for the design of sedimentation tanks in potable water treatment: Case study: The influence of a feed flow control baffle*s. l. : Elsevier B.V., 2008, Zv. 140, s. 110-121.

Risk for Progressive Collapse of Seismically Designed RC Framed Structures: Long Side Column Case

Adrian G. Marchiş, Mircea D. Botez and Adrian M. Ioani

***Abstract* – The present study investigates the risk for progressive collapse of mid-rise RC framed buildings when subjected to damage case C_2, long side column removal, the most dangerous case for the structures under investigation as the previous study indicates. Four models are designed for three distinct seismic zones from Romania: high, moderate and low. The models located in moderate seismic areas are designed for two ductility classes: medium and high. The step-by-step linear static analysis procedure from GSA 2003 Guidelines is used to establish the potential for progressive collapse. The results show the beneficial influence of the seismic design on the progressive collapse resistance of buildings. In the same time, it was found that the GSA 2003 Guidelines cannot taking into account the positive effect brought by the seismic design when more ductile elements are provided in the structure.**

***Keywords* – GSA 2003 Guidelines, progressive collapse, RC framed building, seismic design.**

1. INTRODUCTION

Progressive collapse is a situation where local failure of a primary structural component leads to the collapse of adjoining members which, in turn, leads to additional collapse. Hence, the total damage is disproportionate to the original cause [1]. This phenomenon has been an important issue since the partial collapse of the Ronan Point Building, in England, 1968. The attack on the Murrah Federal Building in 1995 and terrorist attacks on September 11, 2001, started a second wave of attention on structural failure and better understanding of progressive collapse [2].

The design philosophy of structures subjected to abnormal loads is to prevent or to mitigate damage, not necessary to avoid the collapse initiation from a specific cause. The U.S Governmental Agency (GSA 2003) provides an independent methodology to assess the potential for progressive collapse of building based on the notional removal of load-bearing elements. Four "missing column" scenarios are specified: the loss of an exterior column located near the middle of the short side (case C_1), the loss of an exterior column located near the middle of the long side (case C_2), the loss of a corner column (case C_3) and the loss of an interior column (case C_4). In the linear static analysis the following load combination is considered:

$$\text{Load} = 2(\text{DL} + 0.25\text{LL}), \tag{1}$$

where DL and LL are dead and live loads. The factor of two takes into account the dynamic effect that occurs when the vertical support is instantaneously removed from the structure. The GSA acceptance criteria for the linear static analysis are based, in part, on the DCR (**D**emand-**C**apacity-**R**atios) concept adopted in FEMA 356 [3].

A. G. Marchi is with Technical University of Cluj-Napoca, Faculty of Civil Engineeering, Str. C. Daicoviciu, no. 15, 400020-Cluj-Napoca, Romania (e-mail: Adrian.Marchis@mecon.utcluj.ro).

M. D. Botez is with Technical University of Cluj-Napoca, Faculty of Civil Engineeering, Str. C. Daicoviciu, no. 15, 400020-Cluj-Napoca, Romania (e-mail: Mircea.Botez@mecon.utcluj.ro).

A. M. Ioani is with Technical University of Cluj-Napoca, Faculty of Civil Engineeering, Str. C. Daicoviciu, no. 15, 400020-Cluj-Napoca, Romania (e-mail: ioaniam@yahoo.com).

ISSN-1584-5990

$$DCR = Q_{UD} / Q_{CE} \quad (2)$$

Recent studies [4], [5], [6] demonstrated the beneficial effect of the seismic design: low potential for progressive collapse of mid-rise RC framed buildings located in high seismic areas unlike Bredean "to be published" [7] which shows that low-rise buildings are more vulnerable. In the same time, data from literature regarding the potential for progressive collapse of mid-rise structures located in low or moderate seismic zone are few [4], [5], and are missing if we refer to structures designed for the Romanian territory. Also, none of the previous investigations studied the consequences on progressive collapse behaviour of RC framed structures, located in moderate seismic zones, when different allowable options (medium or high ductility class) are considered in the seismic design. Therefore, such aspects were mainly investigated in a previous paper "submitted for publication" [8] but the progressive collapse analysis for mid-rise buildings are detailed only for the case C_4 of "missing column" scenario, a case rarely discussed in the technical literature. This paper refers to the damage case C_2 which seems to be the most dangerous case as the results indicated.

Therefore, a comparative investigation to assess the vulnerability to progressive collapse of four mid-rise buildings designed according to the provisions of the in use Romanian seismic design code P100/1-2006 [9] is presented. The first model is designed for a low seismic zone (Cluj-Napoca, a_g = 0.08g), two models are designed for a moderate seismic zone (Sibiu, a_g = 0.16g) according to the provisions of the medium ductility class (class M) and high ductility class (class H), and the fourth one is designed for a high seismic zone (Bucharest, a_g = 0.24g). For each model, the C_2 case of damage scenarios is investigated using the linear static step-by-step analysis procedure recommended by GSA (2003) Guidelines [1]. The distribution and magnitude of inelastic demands is determined and the progressive collapse potential of the models is evaluated.

2. STRUCTURAL CHARACTERISTICS

The 13-story buildings have the same 3D configuration, as illustrated in Fig. 1. The structures consist of five 6.0 m bays in the longitudinal direction (y-y) and two 6.0 m bays in the transverse direction (x-x), and have a story height of 2.75 m, except the first two floors where the story height is 3.6 m. The thickness of the slab is 150 mm.

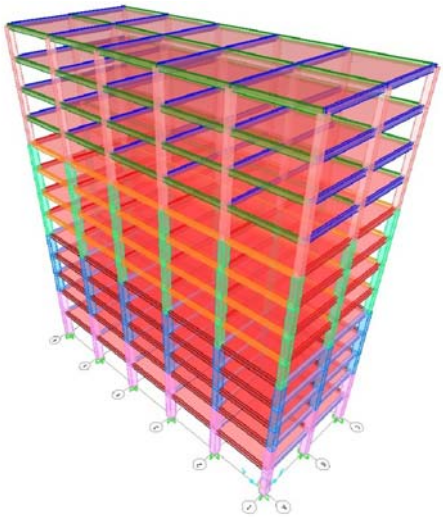

Fig. 1. Structural model

The design of structure is made according to the provisions of the active Romanian seismic code P100-1/2006 [9], provisions that are similar to those specified by SR EN 1998-1/NA: 2008 [10]. The Special Combination and the Fundamental Combinations of loads, taken into account in design is D+0.4L+E,

respectively 1.35D+1.5L+1.05W or 1.35D+1.5W=1.05U, where D is the dead load (self-weight plus a supplementary dead load of 2.0 kN/m^2), L is live load (2.4 kN/m^2), E is the earthquake effect and W is the wind action (for a wind speed of 30m/s).

The seismic design is made for each structure in association with the seismic zone where the building is located. Hence, for the Cluj-Napoca structure, where the design value of the peak ground acceleration is a_g = 0.08g (low seismic zone), the Romanian code P100-1/2006 [9] as well as Eurocode 8 (SR EN 1998-1/NA: 2008) [10] specify that currently, the design should be made according to the provisions of medium ductility class (M), using the behaviour factor q = 4.725. For structures located in Sibiu, the design value of the peak ground acceleration is a_g = 0.16g (moderate seismic zone), and both seismic codes accept that design may be done according to the medium (M) or high (H) ductility class. In order to observe the differences in behaviour, the models located in a moderate seismic zone are designed corresponding to each ductility class provisions (M, respectively H). The following structure is located in Bucharest, a high seismic zone where the peak ground acceleration is a_g = 0.24g; the codes specifies that the design shall be done according to the provisions of ductility class H (high ductility class), using the behaviour factor q = 6.25. Based on the same code (P100/1-2006 [9]) provisions, the compressive strength class of the concrete is C25/30, and the steel for the longitudinal and transverse reinforcement is S500 type.

The structures are modelled as 3D linear elastic models (Fig. 1) using the FEA computer program SAP 2000. The complete design is made following the provisions of the in use Romanian seismic code P100/1-2006 [9] and the design code for concrete structures SR EN 1992-1-1:2004 [11].

3. PROGRESSIVE COLLAPSE ANALYSIS OF THE STRUCTURAL MODELS

Following the GSA (2003) Guidelines [1], demands (Q_{UD}) in structural components (beams) are compared to their expected un-factored capacities (Q_{CE}), as shown in equation (2). The DCR values for flexure and for shear are determined at column faces. The progressive collapse analysis is performed for the damage analysis case C_2 (long side column removal), the most dangerous case for the buildings under investigation.

A. Model designed for low seismic zone

The first 3D model representing a 13-story RC framed structure is located in a low seismic zone (Cluj-Napoca, Romania), and is seismically designed, as the current code P100/1-2006 [9] specifies, for the medium ductility class (M). For the damage case C_2 (long side column removal), the step-by-step procedure for conducting the linear static analysis is:

Iteration 1 – Step 1: The exterior column located near the middle of the long side is removed. The model is loaded according to equation (1);

Iteration 1 – Step 2: DCR values for flexure and for shear are determined. In the longitudinal direction (y-y), the DCR values range from 1.19 to 2.34 and in the transverse direction (x-x) from 0.22 to 1.16. Large inelastic demands (DCR > 2.0) appear at beams ends at the majority of stories of the longitudinal frame. A plane failure mechanism of three hinges type is formed for the longitudinal (y-y) frame. Due to the interconnection with the transverse (x-x) frame which behaves elastically (DCR < 1.0) the 3D model will stand and a spatial mechanism will not occur;

Iteration 1 – Step 3: In the beam sections were DCR values for flexure exceed the allowable value of 2.0, plastic hinges are inserted;

Iteration 1 – Step 4: Bending moments equal to the expected flexural strength of the sections are applied at each inserted hinge;

Iteration 2: The analysis is re-run from Step 1 through 4 and new DCR values are calculated. After the moment redistribution, more beam section from the longitudinal (y-y) frame have DCR values higher than 2.0. In these sections, a new plastic hinges should be inserted;

Iteration 3: The analysis is re-run, and the final DCR values are displayed in Fig. 2.

After this iteration all DCR values for flexure are below 2.0 and thus the GSA acceptance criteria are fulfilled. For the longitudinal frame, all beam end sections behave inelastic and thus a plane failure mechanism

of three hinges type is expected to occur only for the longitudinal (y-y) frame. Due to the interconnection with the transverse (x-x) frame which behaves elastically (DCR < 1.0) at its upper part, the 3D model will stand and a spatial mechanism will not occur. In the same time, the DCR values for shear are below the allowable value (1.0). Consequently, in this case, there is a low potential for progressive collapse.

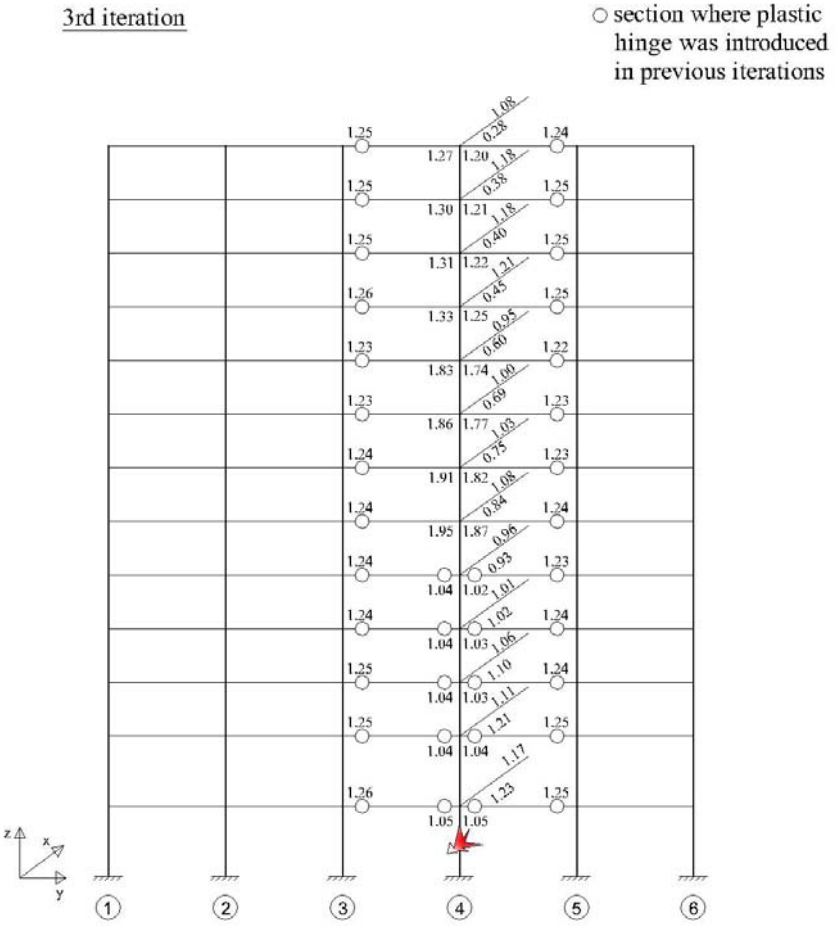

Fig. 2. DCR values for flexure in the damage case C_2 - Cluj model designed for medium ductility class

B. Models designed for moderate seismic zone

The structure located in Sibiu, a zone with moderate seismic risk (a_g = 0.16g), is designed both for medium (M) and high (H) ductility class. The influence of the design option (M or H) on the vulnerability to progressive collapse is investigated.

B1. Model designed for medium ductility class

The structural model designed for medium ductility class, option alternatively accepted by the seismic codes (P100-1/2006 [9], SR EN 1998-1/NA: 2008 [10]), is subjected to the damage case C_2 (long side column removal). The step-by-step linear static analysis procedure stops after the forth iteration (Fig. 3) when all DCR values meet the GSA acceptance criteria (DCR ≤ 2.0).

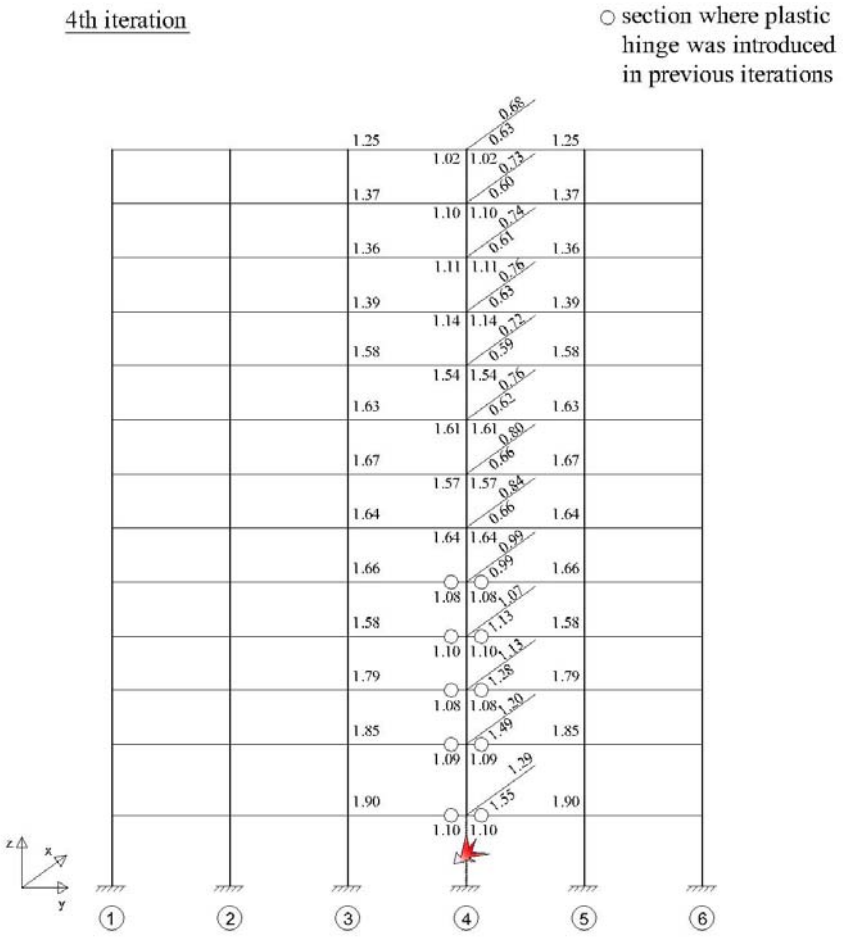

Fig. 3. DCR values for flexure in the damage case C_2 - Sibiu model designed for medium ductility class

A plane failure mechanism of three hinges type is expected to occur for the longitudinal (y-y) frame because all beam end sections have an inelastic behaviour. Due to the interconnection with the transverse (x-x) frame which behaves partially elastically (DCR < 1.0), the 3D model will stand and a spatial mechanism will not occur. Also, the DCR values for shear are below the allowable value (1.0) and consequently, the model has a low potential for progressive collapse.

B2. Model designed for high ductility class

When the 13-story is designed for high ductility class, option recommended by the seismic codes, the results indicate a different diagnosis regarding the potential for progressive collapse unlike the structure designed for medium ductility class. The analysis stops after the forth iteration when all beam end sections behave inelastic and thus a spatial mechanism of three hinges type is expected to occur for the 3D model. Consequently, the building would have a high potential for progressive collapse. This aspect is new in literature and would indicate a probable higher sensibility to progressive collapse of high ductility (H) model with respect to models designed in the medium ductility class (M). The result can be explained: GSA acceptance criteria take into consideration an elastic behaviour of the structure when a load increase factor of 2.0 is applied to static vertical loads (equation 1), and consider only the strength capacity of the section (not its increased ductility) in the evaluation of DCR values (equation 2). Consequently, a member designed for the high ductility class, having a

smaller strength capacity (but an increased ductility), will generates higher DCR values compared to a member designed in the medium ductility class. The result is not validated by nonlinear analyses and cannot be accepted in practice as a final conclusion. In the author's opinion, to account for the inherent inelastic and ductile behaviour of RC frames designed for M and H ductility class, a different load increase factor (LIF) smaller than 2.0 would be more suitable; similar suggestion has been made in other works [12], [13], and the calibration of LIF is in progress in our works.

C. Model designed for high seismic zone

The last 3D model is designed for Bucharest, a zone with high seismic risk, where the design value of the peak ground acceleration is $a_g = 0.24g$. As the current codes P100/1-2006 [9] and SR EN 1998-1/NA: 2008 [10] specify, the buildings located in these areas can be designed only for high ductility class (H). DCR values are determined for the damage structure (C_2 case). Due to the fact that all DCR values for flexure meet the GSA acceptance criteria (DCR $\leq$ 2.0), no further iterations are required. The DCR values range from 0.44 to 0.90 for the longitudinal (y-y) frame and from 0.3 to 0.81 for the transverse (x-x) frame and consequently, the structural members behaves elastically. In addition, the DCR values for shear are below the allowable value (1.0) specified by the GSA (2003) Guidelines [1]. Therefore, there is no risk for progressive collapse when mid-rise buildings are designed for high seismic zones where $a_g \geq 0.24g$.

4. PROGRESSIVE COLLAPSE SAFETY MAP

The damage case C_2 (long side column removal) seems to be the most dangerous case for these models as the previous study "submitted for publication" [8] indicate and thus only investigating this damage case, a general conclusion regarding the potential for progressive collapse can be drawn. Therefore, a suggestive graphic representation of the risk for progressive collapse of mid-rise RC framed structures located in different seismic zones (a_g = 0.08g, 016g and 0.24g) of the Romanian territory is displayed in Fig. 4. This progressive collapse safety map provides new and useful information for structural engineers and will be completed by future researches for other seismic zones (a_g = 0.12g, 0.20g, etc.) and by the existing analyses for low-rise buildings from the study "to be published" [7]. A similar safety map is presented in the previous study "submitted for publication" [8] for the mid-rise structures subjected to damage case C_4 (interior column removal).

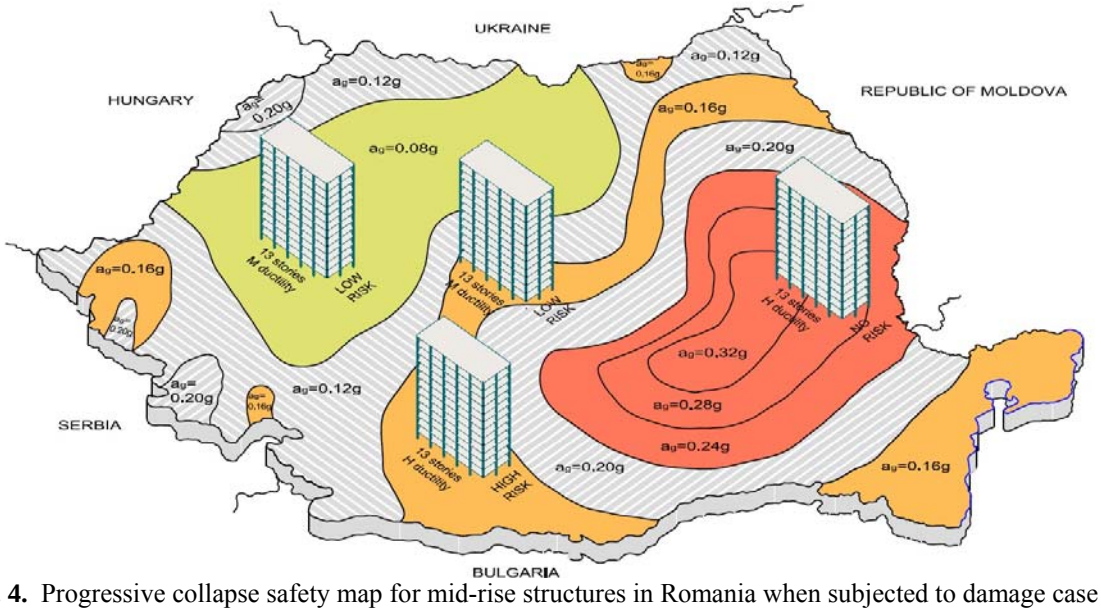

Fig. 4. Progressive collapse safety map for mid-rise structures in Romania when subjected to damage case C_2

5. CONCLUSIONS

This paper investigates the risk for progressive collapse of mid-rise buildings located in different seismic areas from Romania using the provisions of the GSA (2003) Guidelines [1]. Four 3D models representing the 13-story RC framed structure have been designed and detailed according to the active codes P100/1-2006 [9] and SR EN 1992-1-1:2004 [11] for three seismic zones (high, moderate and low); the building located in a moderate seismic area has been designed for two ductility classes (medium and high). The models are subjected to the damage case C_2 (long side column removal) which seems to be the most dangerous case and thus, the final conclusion regarding the risk level for progressive collapse can be given only by investigating this damage case.

For the model located in a high seismic zone (a_g = 0.24g), there is no risk for progressive collapse. The building response elastically when subjected to "missing column" scenario (DCR < 1.0). The models located in moderate and low seismic zone (a_g = 0.16g, 0.08g) and designed for medium ductility class have a low potential for progressive collapse. But the seismic codes P1001/-2006 [9] and SR EN 1998-1/NA: 2008 [10] recommend, as an alternative option, the design for high ductility class for the buildings located in moderate seismic zones. Consequently, for this model, a high potential for progressive collapse is obtained. This is due to the fact that the linear static procedure from GSA (2003) Guidelines [1] cannot take into account the positive effect brought by the seismic design when more ductile elements (not necessary more strength) are provided in the structure. For this reason, structures designed in the high ductility class seem to be more vulnerable to progressive collapse than the similar structures designed for a medium ductility class, a conclusion not validated by nonlinear analyses or by practice. To correct this aspect, an improved expression to determine the magnitude of DCR is proposed in the previous paper "submitted for publication" [8]:

$$DCR = \frac{Q_{UD}}{Q_{CE}} = \frac{Q_{UD}}{q_{pc}} \cdot \frac{1}{Q_{CE}} \tag{3}$$

In the last equation, a new parameter q_{pc} is introduced, representing the behaviour factor used in the progressive collapse analyses. This parameter estimates the beneficial influence of the ductility class of the structural members. The calibration of the parameter q_{pc} is in progress.

In the same time, the influence of the seismicity area on the vulnerability to progressive collapse of mid-rise buildings is investigated. As in the previous study "submitted for publication" [8], the general opinion of structural engineers that the seismic design and detailing has a beneficial influence on the progressive collapse resistance of reinforced concrete structures is confirmed:

- This influence is strong for structures designed for high seismic zones. The analysed structures behave elastically when subjected to damage case C_2 and do not have a risk for progressive collapse; this is a consequence of the fact that the Special Combination of loads where the earthquake effect E intervenes (D + 0.4L + E), determine the magnitude of internal forces and moment used in design and detailing of structural members.
- The beneficial influence of seismicity is reduced for mid-rise structures located in low or moderate seismic zones. These structures are more vulnerable to progressive collapse (low and high potential) and this is due to the fact that the Fundamental Combination of loads (where the earthquake effect E is not considered) determine the design and detailing of structural members; this finding shows that the positive effect of seismic design exists, but it must be prudently considered for structures located in moderate seismic zones.

6. ACKNOWLEDGMENTS

This paper was supported by the project "Improvement of the doctoral studies quality in engineering science for development of the knowledge based society-QDOC" contract no. POSDRU/107/1.5/S/78534, project co-funded by the European Social Fund through the Sectorial Operational Program Human Resources 2007-2013.

7. REFERENCES

[1] GSA 2003, *Progressive Collapse Analysis and Design Guideline for New Federal Office Buildings and Major Modernisation Projects*. 2003, General Service Administration, Washington, USA.
[2] Sasani M. and Kropelnicki J., *Progressive collapse analysis of an RC structure*. 2007, The Structural Design of Tall and Special Buildings, Vol. 17, pp. 757-771.
[3] FEMA 356, *Prestandard and Commentary for the Seismic Rehabilitation of Buildings*. 2000, Federal Emergency Management Agency, Washington, USA.
[4] Baldridge S.M. and Humay, F.K., *Preventing Progressive Collapse in Concrete Buildings*. 2003, Concrete International No.11, Vol. 25, pp.73-79.
[5] Bilow N.D. and Kamara, M., *U. S. General Services Administration Progressive Collapse Guidelines Applied to Moment – Resisting Frame Building*. 2004, ASCE Structures Congress.
[6] Ioani A.M., Cucu H.L. and Mircea C., *Seismic Design vs. Progressive Collapse: A Reinforced Concrete Framed Structure Case Study*. 2007, Forth International Structural Engineering and Construction Conference, Melbourne, Australia.
[7] Bredean L., Botez M., Ioani A.M., "Progressive Collapse Risk and Robustness of Low-Rise Reinforced Concrete Buildings", 2012, Eleventh International Conference on Computational Structures Technology, to be published.
[8] Marchis A., Mircea B., Ioani A., "Vulnerability to Progressive Collapse of Seismically Designed Reinforced Concrete Framed Structures in Romania", 2012, Fifteenth World Conference on Earthquake Engineering, submitted for publication.
[9] P100-1/2006, *Seismic design code – Part I: Design Rules for Buildings*. 2006, MTCT, Bucharest, Romania.
[10] SR EN 1998 -1/NA, *Eurocode 8: Design of Structures for Earthquake Resistance – Part 1: General Rules, Seismic Actions and Rules for Buildings*. 2008, ASRO, Bucharest, Romania.
[11] SR EN 1992-1-1, *Eurocode 2: Design of Concrete Structures - Part 1-1: General Rules and Rules for Buildings*, 2004, ASRO, Bucharest, Romania.
[12] Kim H., Progressive collapse behaviour of reinforced concrete structures with deficient details, 2006, The University of Texas, Austin, Texas, USA.
[13] Tsai M.H., *Investigation of progressive collapse resistance and inelastic response for an earthquake-resistant RC building subjected to column failure*. 2008, Journal of Engineering Structures, Vol. 30, pp. 3619-3628.

Analysis of the sea-land interface variability on the Romanian littoral, based on the Remote Sensing and GIS techniques applications

Razvan Mateescu , Alina Spinu, Ichinur Omer

Abstract The relative importance of the shoreline is linked to its significance on the coastal socio-economical activities development and extension of Coastal/marine Protected Areas. Consequently, its delineation, jointly with specific areas of different types of usage and utilities, including the delineation of the public and private space areas, and the setbacks extensions as specific measures of the coastal management, it had become crucial, in the context of the growing anthropogenous pressures on the coastal space.

The present paper focuses on the outcome of the implementation of GIS and Remote Sensing methods for a series of specific coastal management activities, includingcoastal protection and delineation criteria in relation with the coastal geomorphologic processes and its driving forces.

***Keywords* – shoreline variability, GIS, Remote sensing, vulnerable areas, ICZM, coastal delineation.**

1. INTRODUCTION

The Romanian Black Sea littoral, stretching over 250 km, includes several geomorphologic areas grouped in two shore sectors: northern sector of the Danube Delta area, consisting of alluvial sediments with dunes, extensive lowlands, marshes and lagoons, where the highest dimension has about 3m high in the case of dunes, and southern sector, a higher zone that consists mainly of ground cliffs interrupted by short beaches in front of the old marine lagoons.

Under the influence of the marine factors the shoreline is moving, advancing and receding in relation with local or regional specifics. Using the results of the coastal measurements, it can follow the development of the coast from one year to the next, but also, based on the spatial analysis of historical maps, remote sensing images and aerial orto-rectified images it can make a reasonable prediction for the coastline development in coming years and specify the vulnerable that need protection measures.

Even the patterns of the Romanian coastal processes (accretion and erosion) are now well known, the modern techniques of analysis on a synoptic scale, such as GIS and remote sensing, had become essential tools to achieve this goal. A number of problems have been identified which need to be addressed urgently, so as to protect the coast against erosion in order to achieve its sustainable management. Among these, some problems are of fundamental importance: Coastal erosion monitoring and elaboration of the database system, support for the necessary measure to rehabilitate and protect the coast against erosion for a good evaluation of the shore

This work was supported in part by the by the strategic grant POSDRU/89/1.5/S/58852, Project ”Postdoctoral program for researcher formation in the field of sciences” and POSDRU/88/1.5/S/61150, Project “Doctoral Studies in the field of life and earth sciences”, co-financed by the European Social Found within the Sectorial Operational Program Human Resources Development 2007 – 2013.

F. A. and S. B. Author is with the National Institute for Marine Research and Development, Mamaia 300, Constanta 900581, Romania (e-mail: razvan_doru@yahoo.com, alina_daiana_ct@yahoo.com).

T. C. Author is with Ovidius University of Constanta, Bd. Mamaia nr. 124, 900356-Constanta, Romania (e-mail: icky@univ-ovidius.ro).

ISSN-1584-5990

state, respectively the efficiency of the coastal protection and the required ICZM solutions extended on the Romanian littoral.

Recent developments in coastal processes studies have constantly been keeping up with the accelerated development of the new technologies of Remote sensing and GIS, together with the growth involved resources, proportional to specific socio-economical needs of the coastal zone, but especially due to the challenge of the processes complexity insufficient knowledge, determined by the great variability of the conditions characterizing the marine and coastal zone, as well as the multitude of interaction levels to be found here, [1].

Taking into account its impact on the entire Black Sea basin, of this summarized techniques to approach the coastal problematic, the GIS and remote sensing techniques are emphasized as the most advanced tools to support data management, analysis and modeling, together with the possibility of reaching an advised and operational intervention.

2. DESCRIPTION OF THE EXPERIMENT

In our attempt to examine coastal morphological changes on long and medium term we approached the available historical maps and satellite images at different resolutions, together with GPS measurements afferent to the current shoreline monitoring data, in order to namely record the shoreline variability in the GIS environment. The additional spatial data, mainly from open or remunerated sources: NASA, ESA, USGS, ANCPI, GEOSPATIAL Portal and the Ministry of the Environment Portal, as well NIMRD monitoring and surveillance coastal erosion data, it were used for the shoreline changes validation and analysis, and also coastal delineations [7].

Thus, the morphological analysis of the shoreline changes was conducted by comparing historical maps, satellite imagery, and aerial-photograms from different periods of time. The process involved two steps: moving images in the same coordinate system based on benchmarks identified in images and historical topographic maps, ortho-rectified plans or measured directly in the field (GPS) and classifying the images in two classes using the spectral intervals method with specialized software (ERDAS, ArcGIS) or by manual digitalizing, [2].

The method of analysis for the shoreline variability in the last decades includes shoreline extraction from the recorded remote sensing images, and detection algorithm provided by ERDAS Imagine software, based on the arithmetic difference between a ”new” image and a ”old” imagine. The difference between pixels values was realized with the function “*Change detection*” *(Interpreter/Utilities)* which produces the operation, automatic for each pixel: the examination of spectral bands give the possibility to consider the difference of reflectance for sand and water, and in end result, shoreline extraction.

The graphical representation obtained based on raster data was analyzed in an application of ArcGIS 10, considering historical maps, topographic measurements, GPS, aerial photos etc. The ArcGIS spatial analysis techniques were developed on shoreline recordings/representations (GPS data, digitization data) in a plane model, referenced configuration, which allowed the assessment of the geomorphologic dynamics of coastal areas; the results were considering the following spatial data available:

- Hydrographic map of DHM / Captain Commander Cătuneanu, 1898, 1: 250000;
- Topo-hydrographic map of the State Committee for Water - Water Management General Directorate (1962), 1:25,000, 1942 coordinate system, Black Sea MWL system, Sulina;
- Topo-hydrographic maps, (1951, 1993, 2007) - Maritime Hydrographic Directorate at different scales (1:750.000 - 1:10.000);
- Topographic maps (DTM 1975) - scale 1:25.000, 1:50.000.

The photograms and aerial photographs (1980-1985, scale 1:45.000 - 1:1.500), the Landsat, SPOT, ASTER, ERS and, for some sectors, IKONOS satellite imagery, generally from open source and only rarely with a fee (especially for the ortho-rectified plans purchased in various projects within NIMRD) have been used and processed/vectorized in order to detect the changes in various medium and short time scales, with the view to obtaining a sufficiently large data collection for the assessment of the variability of the shoreline.

The Landsat images were thus downloaded for free via FTP using the GLOVIS (*Global Visualization Viewer*) search engine, made available by USGS, through the *Earth Resources Observation and Science Department* (EROS).

Landsat 5 images were downloaded (TM) and Landsat 7 (ETM +) on the 181/29 frame, from 2000 until 2005, in June, July or August, to be as homogeneous as possible in terms of phenomenology.

SPOT 2007 and ASTER 2003 images, as well as the 2004/2008 ortho-rectified maps, located in the cost effective field, were vectorized accordingly in order to obtain an image of the shoreline at a certain time.

The spatial analysis of the data collection provided the visual interpretation and manual or automatic vectorization of the shoreline characteristics at different time scale, it were realized through ArcGIS extensions for spatial analysis and QC procedures.

3. RESULTS AND RELEVANT IMPLICATIONS OF THE EXPERIMENT

A map is the end outcome of our undertaking, in which we compared the shorelines obtained by differentiated processing during multiple time horizons with highlighted areas that have been undergoing morphological changes which were conspicuous in the range studied - more than 40 years. The historical maps, redesigned in Stereo70 and subsequently vectorized were used to evaluate the shoreline withdrawals, corresponding to surfaces that have undergone significant changes during this period, thus highlighting different periods of shoreline evolution.

The qualitative analysis of these vector maps emphasizes some important aspects concerning the sedimentation / erosion processes in specific sectors, especially in the Northern unit - the accumulation shoreline of the Danube Delta. Also, on medium and short term, natural factors that influence coastal dynamics include two main categories: meteorological (wind by sand dissipation from emersion beach and wave and marine currents forming, temporally sea level increases) and hydrological (waves and currents – the main factors for shore dynamics, the oscillations of sea level).

The most dynamic shoreline changes are observed close to secondary delta of the Danube River, within Musura bay. After the extension of protection dykes from Sulina channel, sedimentation processes intensified mainly because silt transport on Chilia arm was blocked by dikes. The present tendency is to warping the bay and in the future to transform into a lagoon by closing with a sand spit. The appearance of the island in from of Musura bay involves problems regarding border with Ukraine, which was until now on Musura arm. The border should be redefined according with actual geomorphologic changes.

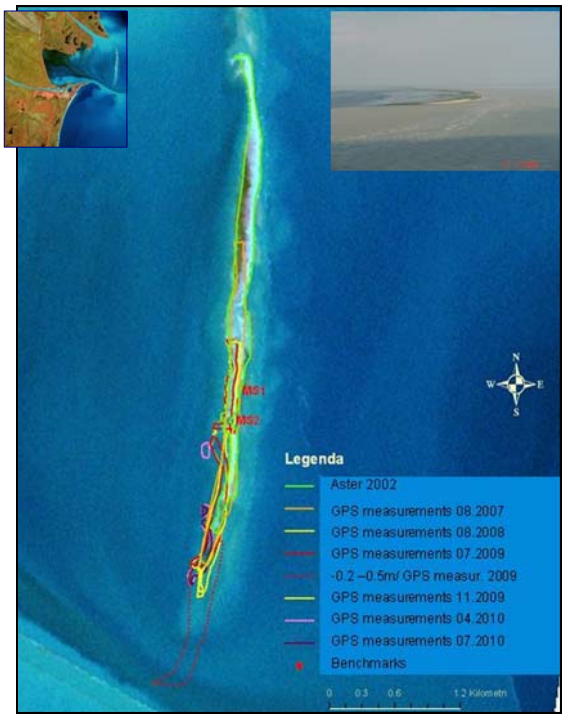

Fig. 1 Musura sand spit: Shoreline dynamics showed by GPS measurements and satelitar data. The present development of the sand spit is related to the southward sediment drift blockage, by the Sulina channel jetties, and also to sea-level, Danube hydrological regime and the local refraction and diffraction phenomena.

For this sector, the correlation of the sedimentations processes with the Danube's hydrological event and dredging works was difficult to make because of the lack of data and the transboundary context.

Other, highly dynamic sector is, in the last decades Sahalin island was moved to west with ~ 750 m, the length increased with 3,8 km and the width with 200 m. Increasing rate calculated for period between 1975-1990 is 167 m/an. After 1990, the processes changed into erosion until 2000. In 2006 eroded and accretion areas are relative balanced, **fig. 2** and **fig. 3**.

GPS measurements campaigns from 2008, 2009 and 2010 showed an elongation and curvature of the island/peninsula to south-west [3]. It has been found the existence of a very thin sand belt in extension of the island, unstable during the storms. Sahalin area was until 1990 an accretion area, but after this year the predominant process was erosion, with different rate by sectors. If, in 1990 the area of peninsula was 670 ha, in 1996 the area decreased at 620 ha and at 450 ha in 2000. Conform with this dates erosion rate of sand surface between 1990 and 1996 was 8,3 ha/year. In the time interval1996 and 200 erosion rate increased to 42,5 ha/year, and also within period of 2000 and 2006 it was observed a stagnation of erosion rate, reaching to a relative balance between eroded and accretion areas, [4].

Fig. 2 – Shoreline evolution in Sahalin area, 2007-2010 (GPS measurements, SPOT image)

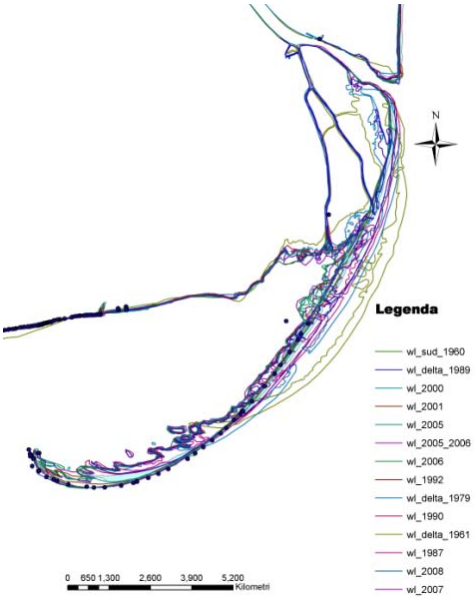

Fig. 3 – Shoreline evolution in Sahalin area, 1960-2008 (LANDSAT, historical maps, SPOT image)

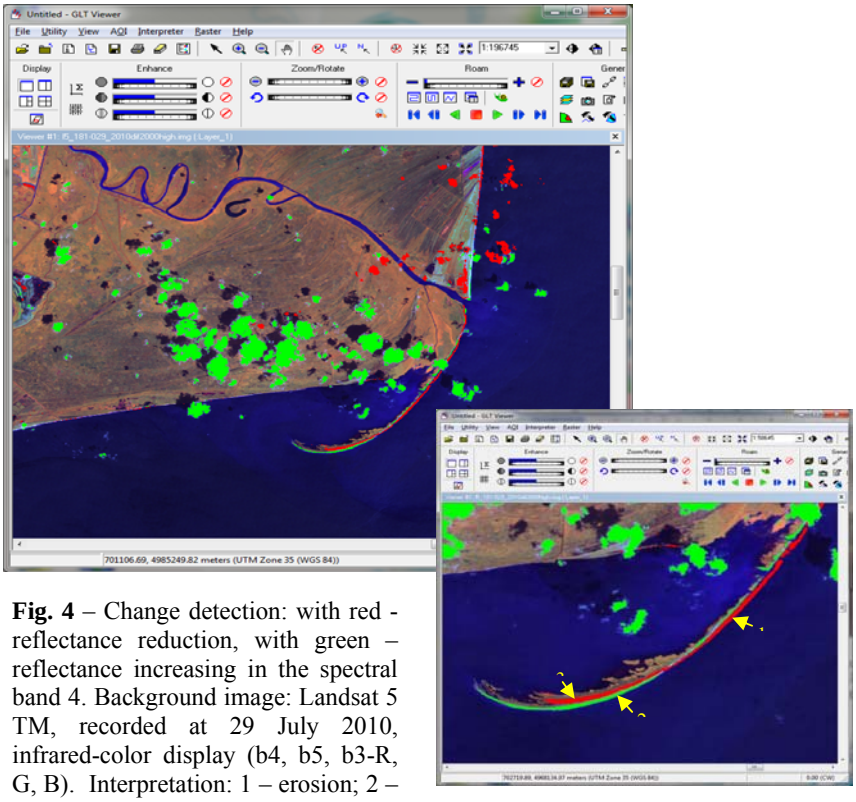

Fig. 4 – Change detection: with red - reflectance reduction, with green – reflectance increasing in the spectral band 4. Background image: Landsat 5 TM, recorded at 29 July 2010, infrared-color display (b4, b5, b3-R, G, B). Interpretation: 1 – erosion; 2 – shoreline extension (sand spit); 3 –

Another application of the GIS and remote sensing techniques was developed in the context of build shore, southern Romanian shore, where there are important differences between the erosion process and beach flooding at different hydrological events, like winter storms. But the shoreline retreat is related to the both processes.

The coastal zone's ecological and physical conditions are not optimal for the ecological integration of shoreline variability, and it is crucial to consider the ecosystem based practices for the management of the Romanian Black Sea Coastal Zone (BSCZ). The new setbacks limits, and its consequents resettlement, it have an important role in the coastal protection and management, but it may create a further population/investment pressure in the Romanian BSCZ.

The average rate of the beach erosion was calculated based on the cross-shore profile analysis afferent to landmarks system of different shore sectors, as well based on the last four decades historic maps and measurements, showing an interval of variation from -6m/yr at Navodari to +1.5m/yr at Eforie Nord, but the shore were shown a generally erosion rate of 1,2m/yr in more than 80% of its length.

The estimation of beach erosion due to forecast sea level rise was considerate on a time interval of the next 10 years, [8] (ECOH/JICA Study, 2005) –

Table 1.

Sub-sector	Annual rate of the beach erosion at a rate of sea level increasing of 2,2 mm/yr, in meter/yr.
Năvodari- Mamaia	0,18
Constanţa	0,18
Eforie Nord – Sud	0,15
Costineşti	0,08
Olimp-Venus	0,08
Saturn – Mangalia	0,13
2 Mai - Vama Veche	0,12

For southern unit, the touristic littoral, once the calculus for the shoreline retreat was made based on several composed analysis and certain coastal response models included in CEDAS4.0, the rest of the driving factors had a relative subjectivity (indicators of coastal vulnerability: environmental carrying capacity, existence of different MPAs, traditional tourist resorts, etc), and it can be considerate within calculus on cross-sections trends, by multiplying the rate of retreat with certain coefficient/factor on different sub-sectors.

The delineation of the public space thus limits itself at the beach front within the coastal zone, respectively the delineation of the safe set-backs limits. It is based on the consideration of the forecast worst-case scenario of the coastal evolution/vulnerability, including the delineation of a baseline of the reference for a ten years acceptable coastal behavior.

Delineation of the sea-land interface, as a seaward limit of the public sector delineation and setback limits, from which the set-backs are gradually extended for different uses/facilities, is determinate by three chosen components:

- Shoreline changes (p), including historical shoreline on maps, aerial photoplans and geomorphologic parameters of the beach cross-shore profiles;
- Dune line changes at storms event, or vertical changes on the beach cross-shore profiles at different seasons and hydrological events(f);
- Shoreline forecasted changes due to sea-level rise in the next 10 years (n).

Limit of the sea-land interface = (p) + (f) + (n)

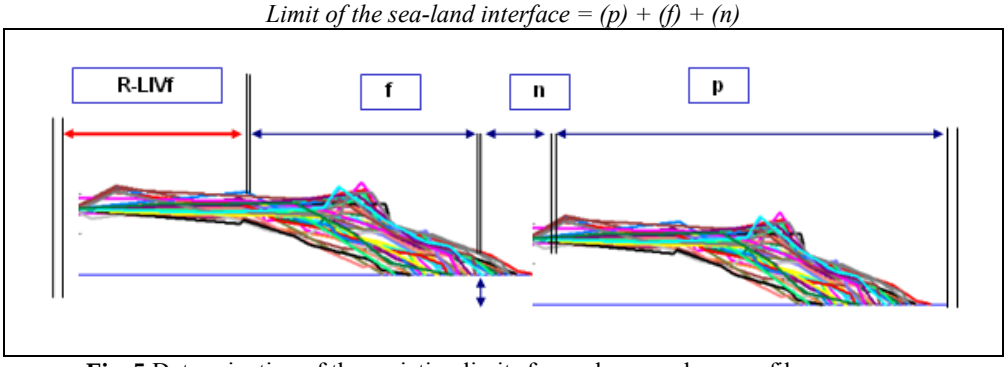

Fig. 5 Determination of the variation limits for each cross-shore profile
(Measuring section afferent to landmarks network)

Calculation for each beach area, shore sub-sector was made in tabular mode and drew on certain classes of extension according to the vulnerability or specificity of the sub-sectors. The extension of the forecasted

shoreline and delineation line, in case of non-intervention, it was made in ArcGIS 10, for all beach sectors using the chosen criteria.

Fig. 6. a, b, c and d. Mamaia Bay delineation

4. CONCLUSIONS

The modern methods of GIS &RS used for change detections, it provides necessary grounding for a precise analysis and decision support in the case of anthropogenous impact evaluation and in the case of the risk mitigation projects approaches, extended in several vulnerable areas. Extraction of class vector forms permits its import in GIS environment and usage of certain methods and procedures of vector processing and spatial analysis using ArcGIS software.

Major changes in Danube discharges regime were induced the change coastal sediment transport regime drive by marine and coastal currents and waves, and in consequence were induced rapid erosion/deposition processes nearshore. Diminishing of brackish water habitats surfaces, due to closing of the Musura Bay and its gradual transforming in a fresh water dominated lagoon, together with significant changes of Sacalin Island/peninsula can have important consequences over afferent fauna/species.

In general, the effects of hydrological and meteorological factors, especially of storms, it is not limited only to the natural shore. They are extended to areas governed by anthropogenous factor, were the impacts of winter storms are more visible and consequences become more dramatic on short terms, due to strong wind/waves magnitude, or its durations [5], [6].

The methods used in present study emphasized the general characteristic of shore response, which together with the followed numerical modeling works; it will make possible the correct understanding of the phenomena at different space and time scales.

Due to the shoreline variability and present accelerated geomorphologic changes, it can be summarized that it is necessary to exceed present lacks toward a dynamic understanding of the connected impacts processes in new climatic conditions, and a real ecosystem base management of the Romanian coastal zone.

5. ACKNOWLEDGMENTS

This work was partly supported by the strategic grant POSDRU/89/1.5/S/58852, Project ”Postdoctoral program for researcher formation in the field of sciences” and POSDRU/88/1.5/S/61150, Project “Doctoral Studies in the field of life and earth sciences”, co-financed by the European Social Found within the Sectorial Operational Program Human Resources Development 2007 – 2013.

6. REFERENCES

[1] Scally R., 2006 – GIS for Environmental Management. Environmental Systems Research Institute (ESRI) Press, Redlands, California;
[2] Carvalho, A., Fitzpatrick,K. [online] *Streamlining Coastal Monitoring Programs with GIS in Martin County, Florida,* http://gis.esri.com/library/userconf/proc03/p0603.pdf;
[3] Constantinescu, Ş. [online] *III. Litoralul românesc în documente cartografice. Perioada modernă şi contemporană,*http://earth.unibuc.ro/articole/iii-litoralul-romanesc-in-documente-cartografice-perioada-moderna-i-contemporana;
[4] Grigoraş I., Constantinescu A. (1994)– GIS în sprijinul managementului în Rezervația Biosferei Deltei Dunării, Analele INCDDD Tulcea;
[5] Ielenicz, M., Visan, Gh., (2003), *Morphology of the Romanian Black Sea shoreline*. Comunicari de geografie, vol. 7. Ed Universitatii din Bucuresti;
[6] Vespremeanu, E., (2004), *Geografia Marii Negre*, Editura Universitatii din Bucuresti;
[7]*** *GIS, Spatial Analysis and Modeling*. ESRI Press, Redlands, California, 2005;
[8] ECOH/JICA Masterplan for protection, 2005.

Changes in Seismic Design Codes from the Perspective of Progressive Collapse Vulnerability of RC Structures

Teodora S. Moldovan, Lucian A. Bredean, and Adrian M. Ioani

Abstract – **The paper estimates the influence of Romanian seismic design codes changes on the progressive collapse resistance of a typical mid-rise RC framed structure located in a high seismic area (Bucharest). The progressive collapse potential is assessed following the linear static procedure recommended by the GSA (2003) Guidelines. Three distinct models representing a 13-storey RC framed structure are designed according to the seismic design codes in use in 1992, 2006 and 2008, and detailed considering the provisions of concrete structures design codes STAS 10107/0-90 and Eurocode 2. The research results show that a mid-rise structure located in an area with a_g = 0.24g does not experience risk for progressive collapse when is subjected to different "missing column" scenarios. The last 20 years of changes in the seismic design codes lead to improvements on the progressive collapse resistance of RC framed buildings.**

Keywords – **GSA (2003) Guidelines, progressive collapse, RC framed structures, seismic codes**

1. INTRODUCTION

Progressive collapse is a chain reaction of failures that propagates throughout a portion of structure disproportionate to the original local failure [4]. The main causes that lead to progressive collapse of buildings are: explosions, impact by vehicles, human errors, wind gusts, floods and major earthquakes.

The U. S. General Services Administration and the Unified Facilities Criteria provide Guidelines (GSA 2003 [1], DoD 2005 [2] and DoD 2009 [3]) that propose procedures to evaluate the progressive collapse resistance of structures. The GSA (2003) Guidelines [1] define a detailed methodology to assess the potential to progressive collapse of buildings, based on a linear static analysis and different "missing column" scenarios.

In their works, Baldridge and Humay [4], Bilow and Kamara [5] assessed the progressive collapse potential of mid-rise RC framed structures seismically designed for areas of moderate or high seismic risk. Recently, Botez, Bredean, and Ioani [6] studied the progressive collapse vulnerability of RC framed structures taking into account the influence of the number of stories. Ioani and Cucu [8], [9] examined the effects of the two former Romanian codes P100-92 [10] and P100-1/2006 [13] on the progressive collapse resistance of RC framed structures; only one damage case (short side column) was investigated. The authors, in a previous paper [17], following the GSA (2003) Guidelines [1], presented the influence of the active seismic design code EC-8 [16] in the assessment of progressive collapse potential of RC framed structures, when all four damage cases are considered. In this paper only the results for the damage case C_2 (long side exterior column removal) of "missing column" scenarios are presented.

In accordance with the need for research in this area, the objective of this study is to assess the progressive

Manuscript received June 25, 2012. This work was supported in part by the Romanian Government under Grant PNII IDEI No. 193/2008.

T. S. Moldovan is with Technical University of Cluj-Napoca, Faculty of Civil Engineering, Str. C. Daicoviciu, no. 15, 400020-Cluj-Napoca, Romania (e-mail: Teodora.Moldovan@mecon.utcluj.ro).

L. A. Bredean is with Technical University of Cluj-Napoca, Faculty of Civil Engineering, Str. C. Daicoviciu, no. 15, 400020-Cluj-Napoca, Romania (e-mail: Lucian.Bredean@mecon.utcluj.ro).

A. M. Ioani is with Technical University of Cluj-Napoca, Faculty of Civil Engineering, Str. C. Daicoviciu, no. 15, 400020-Cluj-Napoca, Romania (e-mail: ioaniam@yahoo.com).

ISSN-1584-5990

collapse potential of three distinct models representing a 13-storey RC building, designed and detailed according to Romanian seismic codes in use, in 1992, 2006 and nowadays. In the analyses of structures all four damage cases defined in GSA (2003) Guidelines [1] are considered. The paper estimates the influence of the changes in Romanian seismic design codes on the progressive collapse resistance of a typical RC framed structure located in a high seismic area (Bucharest).

2. BUILDING CHARACTERISTICS

The study was conducted on a typical 13-storey RC framed building, designed according to three distinct Romanian seismic codes in use in the last 20 years. The structure consists of five 6.0 m bays in the longitudinal direction and two 6.0 m bays in the transverse direction. The story height is 2.75 m, except the first two floors which are 3.6 m in height. The thickness of the slab is 150 mm. Based on this structure, three distinct models were developed. The model, represented in **Fig. 1**, was generated in the FEA computer software Autodesk Robot 2010; the dimensions of the structural components are presented in **Table 1**.

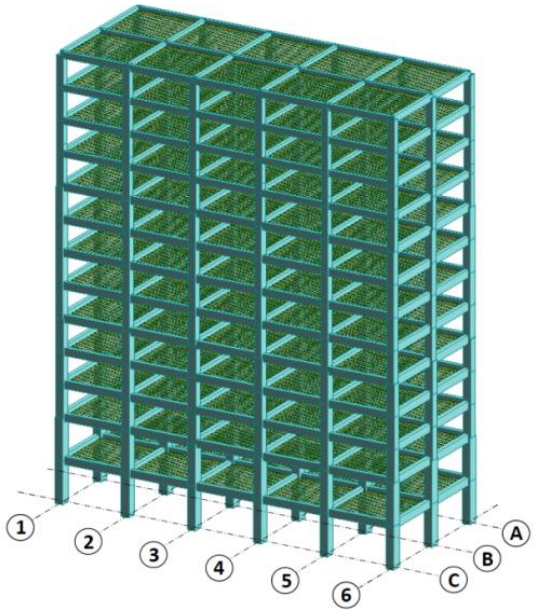

Fig. 1. Model of structure

Table. 1. Dimension of the structural elements [mm].

Story	Columns	Beams	
		Longitudinal direction	Transversal direction
1, 2	700x900	350x650	350x700
3, 4, 5	700x750	350x650	350x700
6, 7, 8, 9	600x750	300x650	300x700
10, 11, 12 13	600x600	300x550	300x600

3. SEISMICALLY DESIGNED MODELS

A. Model P100-92

The structure was designed according to the provisions of the seismic design code P100-92 [10]. In design

at the Ultimate Limit State, the Special Combination of loads according to the Romanian Standard STAS 10101/0A-77 [11] is: DL + 0.4LL + E, where DL is dead load (composed by self-weight and an additional dead load of 2.00 kN/m^2), LL is live load, which is 2.4 kN/m^2, and E is the earthquake effect.

The seismic analysis is performed for Bucharest (zone C on the Romanian seismic map with k_s = PGA/g = 0.2). The magnitude of total equivalent seismic force S_r is:

$$S_r^{P100-92} = \alpha \cdot k_s \cdot \beta_r \cdot \psi \cdot \varepsilon_r \cdot G = 0.095G \quad (1)$$

where: α is the importance factor of the structure depending on the importance class (for building of importance class II, α has the value 1.2); k_s is the seismic coefficient; β_r is the coefficient of dynamic amplification and has the value 2.5); Ψ is a reduction coefficient of the seismic action, it has the value 0.2); ε_r is the coefficient of equivalence between real system and a SDF system corresponding to the mode "r" of vibration and G is the weight of the structure: G = 49531 kN.

The structural response of the model is determined by a 3D linear static analysis performed in the FEA computer software Autodesk Robot. The material properties are given in **Table 2**. Reinforcement is made following the provisions of the standard for concrete structures STAS 10107/0-90 [12]. The modal response spectrum analysis provides the following values for the fundamental periods: T_1 = 1.23 s and T_2 = 1.22 s.

Table. 2. Strengths of materials for the model P100-92 [MPa].

Material		**Seismic design**	**Progressive collapse analysis**	
		Design values*	**Characteristic un-factored values**	**With 1.25 factor**
Concrete Bc 20		R_c= 12.5	R_{ck}= 16.6	20.75
		R_t= 0.95	R_{tk}= 1.43	1.78
Steel	PC 52	R_a = 300	R_{ak}= 345	431
	OB 37	R_a = 210	R_{ak}= 255	318

*R_c (R_t) – design value for the compressive (tensile) strength of concrete; R_a – design value for the yield strength of steel reinforcement.

B. Model P100-1/2006

The structure was designed according to the provisions of the former seismic code P100-1/2006 [13] and detailed according to EC-2 [14] – standard which had replaced the national standard for RC structures STAS 10107/0-90 [12]. According to CR 1-1-3-2005 [15], the snow load for Bucharest has a new value: S = 1.28 KN/m^2. In the seismic code P100-1/2006 [13], the expression for the seismic base shear force F_b is:

$$F_b^{P100-2006} = \gamma_1 \cdot S_d(T_1) \cdot m \cdot \lambda = 0.09996G \quad (2)$$

where: γ_1 is the importance factor of the structure depending on the importance class (for buildings of importance class II, γ_1 has the value 1.2); m is the total mass of the building above the foundation; λ is the correction factor which takes into account the contribution of the fundamental mode of vibration (the building has more than two stories and if $T_1 < T_C$, then λ = 0.85). T_1 is the fundamental period of building vibration and $S_d(T_1)$ is the ordinate of the design spectrum ($S_d(T) = a_g \cdot \frac{\beta(T)}{q}$). The new Romanian seismic map [13] considers that the ground of Bucharest is characterized by: a_g= 0.24g, T_B = 0.16 s, T_C = 1.6 s and $\beta(T) = \beta_0$ = 2.75. The parameter a_g is the design ground acceleration and q is the behavior factor ($q = 5 \cdot \frac{\alpha_{11}}{\alpha_1}$, for multi-story and multi-bay frames $\frac{\alpha_{11}}{\alpha_1}$ = 1.35, result that q has the value 6.75). Structures located in seismic regions with a_g > 0.16g should be designed according to the requirements of the high ductility class (DCH).

The magnitude of the base shear force calculated with the seismic design code P100-1/2006 [13] increases by 5.2% with respect to the total equivalent seismic force calculated with the design code P100-92 [10]. The seismic design code P100-1/2006 [13] places the RC structures located in seismic areas with a_g > 0.16g in a high

ductility class, and provides specific provisions for this class. The material properties are given in **Table 3**. Reinforcement of the beams and columns is made considering the provisions of the design code for concrete structures EC-2 [14] and the additional measures required by the design of elements in the high ductility class. From the modal response spectrum analysis of the model result the following fundamentals periods: T_1=1.15 s and T_2=1.13 s. The fundamental periods are decreasing with respect to the model P100-92 because the modulus of elasticity E for concrete is different: for concrete class Bc 20 it has the value 27 000 MPa and for concrete class C25/30 it has the value 31 000 MPa.

Table. 3. Strengths of materials for the model P100-2006 [MPa].

Material	**Seismic design**	**Progressive collapse analysis**	
	Design values*	**Characteristic un-factored values**	**With 1.25 factor**
Concrete C25/30	f_{cd} = 16.67	f_{ck} = 25	31.25
	f_{ctd} = 1.20	$f_{ctk0.05}$ = 1.80	2.25
Steel S500	f_{yd} = 435	f_{yk} = 500	625

*f_{cd}(f_{ctd}) – design value for the compressive (tensile) strength of concrete; f_{yd} – design value for the yield strength of steel reinforcement.

C. Model EC-8

A similar analysis was conducted considering the structure seismically designed according to the provisions of the present seismic design code EC-8 [16] and detailed according to the design code for concrete structures EC-2 [14]. The seismic design code EC-8 [16] provides the following equation for the seismic base shear force F_b:

$$F_b^{EC-8} = S_d(T_1) \cdot m \cdot \lambda = 0.155G \quad (3)$$

where: m and λ have the same values as in the model P100-1/2006. A difference appears in the expression of the design spectrum $S_d(T_1)$: $S_d(T_1) = a_{gR} \cdot S \cdot \frac{2.75}{q}$. The values for parameters that define the elastic response spectrum for Bucharest (zone z_3) are: a_{gR}= 0.24g, T_B = 0.16 s, T_C = 1.6 s and S = 1 (S is the sol factor); a_{gR} is the peak value of the reference ground acceleration on type A ground. The behavior factor $q = q_0 \cdot k_w = 4.5 \cdot \frac{\alpha_{11}}{\alpha_1} \cdot 1 = 5.85$, q_0 is the basic value of the behavior factor, k_w is the factor reflecting the prevailing failure mode in structural systems with walls, k_w = 1 and $\frac{\alpha_{11}}{\alpha_1}$ = 1.3 for multi-story RC framed structures.

The magnitude of the base shear force calculated with the seismic code EC-8 [16] increases by 21% with respect to the total equivalent seismic force calculated with the design code P100-92 [10], and by 15% with respect to the seismic force calculated with the design code P100-1/2006 [13]. The reinforcement of the structural elements is made considering the provisions of the design code for concrete structures EC-2 [14] and also, considering the additional measures required by the design of elements in the high ductility class from the seismic design code EC-8 [16]. The materials properties are the same as in the model P100-2006.

4. PROGRESSIVE COLLAPSE OF DAMAGED MODELS

The GSA (2003) Guidelines [1] provide a detailed methodology for minimizing the potential for progressive collapse in the design of new buildings and for assessing the vulnerability to progressive collapse of existing buildings. For structures of 10 stories or less, with relatively simple layouts, GSA (2003) Guidelines [1] recommend the *Alternative Path Method* based on a linear elastic analysis. In the static analysis, the vertical combination of loads applied downward to the structure is: $\text{Load} = 2(\text{DL} + 0.25\text{LL})$. The progressive collapse potential is assessed considering the following "missing column" scenarios: the instantaneous loss of column at the first story located at or near the middle of the short side of the building – case C_1, at or near the middle of the

long side – case C_2, at the corner of the building – case C_3 and an interior column – case C_4. Following the linear static analysis, a **D**emand-**C**apacity **R**atio (DCR) is calculated for each structural element:

$$DCR = \frac{Q_{UD}}{Q_{CE}} \quad (4)$$

where: Q_{UD} is the acting force determined in component or connection (moment, axial force, shear and possible combined forces) and Q_{CE} is the expected ultimate un-factored capacity of the component or connection, which results from the seismic analysis. The structural elements and connections that have DCR values greater than 2.0 are considered to be severely damaged or collapsed. If all the DCR values are less than or equal to 1.0, then the structure is expected to behave elastically when a vertical support is removed.

The progressive collapse analysis has been performed for all those four cases C_1, C_2, C_3 and C_4, and this paper presents the numerical results only for the case C_2 – long side exterior column removal. After the removal of the exterior column, the bending moment and shear force diagrams on the damaged structure under gravity loads, for the exterior longitudinal frame CL_A are represented in **Fig. 2.a** and **Fig. 2.b**.

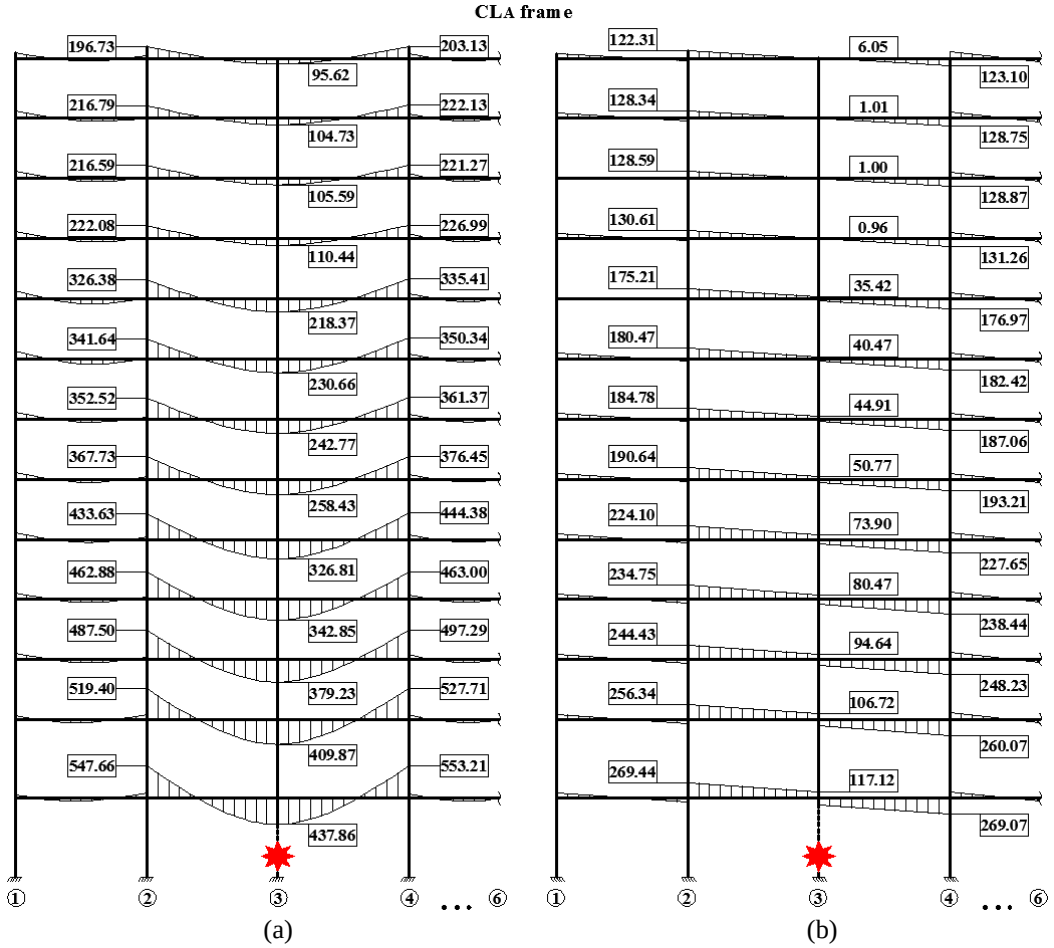

Fig. 2. Damaged structure – longitudinal frame CL_A: a) bending moments [kNm]; b) shear forces [kN]

A. Damaged model P100-92

Demands in beams Q_{UD} are assessed and compared to the expected ultimate un-factored beam capacities Q_{CE}. For the damaged model P100-92, the DCR values for significant beam sections at the lower part of interior

transverse frame CT_3 are represented in **Fig. 3**, and for the longitudinal frame CL_A in **Fig. 4**.

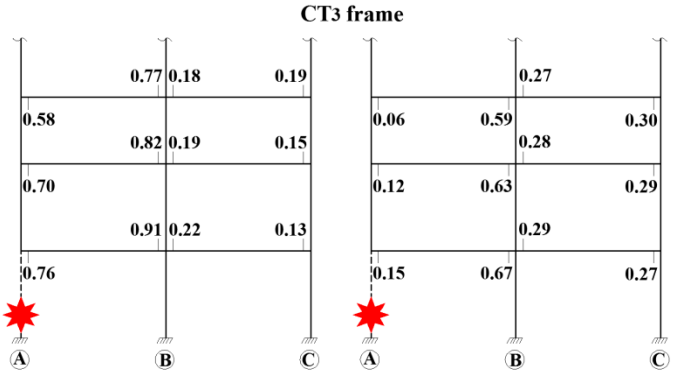

(a) (b)

Fig. 3. DCR values for damaged model P100-92 - transverse frame CT_3: a) for flexure; b) for shear

At the transverse frame CT_3 all the DCR values for flexure are below the allowable limit (2.00); the maximum DCR value is 0.91 at the first floor beam. The DCR values for shear, represented in **Fig. 3b**, are also well below the allowable limit (1.00), the maximum value being 0.67. As at the transverse frame CT_3, in the case of longitudinal frame CL_A, all the DCR values are also below 1.00. For flexure, the maximum DCR value is 0.93 at the first floor beam, and for shear, the maximum DCR value is 0.56 in the same section. Finally, the model P100-92 behaves elastically and consequently, there is no risk for progressive collapse. All four damage scenarios (C_1 to C_4) lead to a similar conclusion.

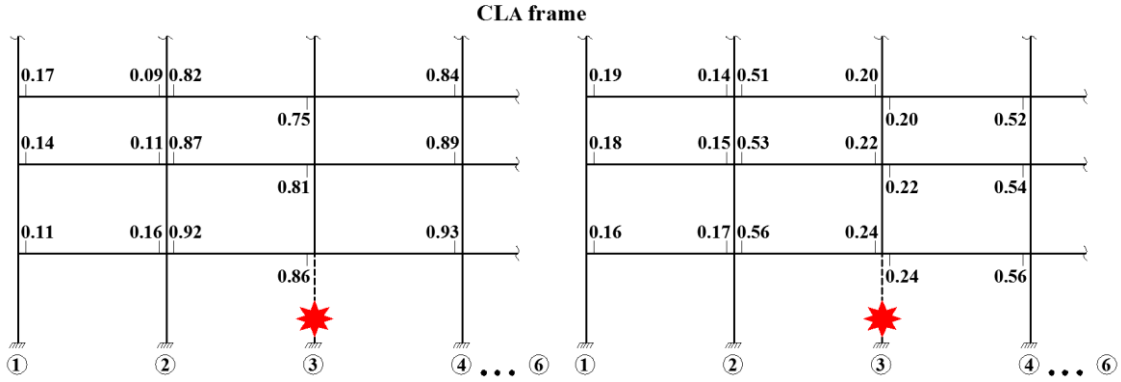

(a) (b)

Fig. 4. DCR values for damaged model P100-92 - longitudinal frame CL_A: a) for flexure; b) for shear

B. Damaged model P100-2006

The structure designed according to the provisions of the seismic design code P100-1/2006 [13] is subjected to progressive collapse and result the following maximum DCR values for flexure: 1.10 at the transverse frame CT_3 and 0.88 at the longitudinal frame CL_A. The maximum DCR values for shear are: 0.77 for the transverse frame CT_3 and 0.75 for the longitudinal frame CL_A. Therefore, the progressive collapse is not expected to occur when an exterior column near to the middle of the long side is suddenly removed. All the four damage scenarios confirm this conclusion.

Compared to the structure design according to the codes P100-92 [10] and STAS 10107/0-90 [12], the model P100-1/2006 has an increase in terms of DCR values for flexure from 0.93 to 1.10, because the material properties have been changed, as shown in **Table 2** and **Table 3**. The maximum DCR values for shear are

increased from 0.67 to 0.77, due to the decrease of the expected ultimate un-factored capacity Q_{CE}, calculated according to the provisions of the present code EC-2 [14]. The model P100-2006 has an improved shear reinforcement (Φ10/130 mm of S500 steel type) compared to the model P100-92 (Φ8/140 mm of OB37 steel type), but the ultimate un-factored shear capacity of the beam is significantly lower ($V_{Rd}^{P100-2006}$ = 451.30 kN compared to $V_{Rd}^{P100-92}$ = 522.25 kN). This unexpected change in shear DCR values has been explained by Ioani and Cucu in their paper [8].

C. Damaged model EC-8

After the removal of the exterior column near to the middle of the long side, the damaged structure designed according to the provisions of the present seismic design code EC-8 [16] has the following maximum DCR values for flexure: 0.77 at the 10th floor beam on the longitudinal frame CL_A, and 0.82 at the first floor beam on the transverse frame CT_3. The maximum DCR values for the longitudinal frame CL_A is 0.65, and for the transverse frame CT_3 is 0.72. If all the DCR values are below 1.00, the structure designed according to the present codes remains in the elastic stage when a long side exterior column of the building is suddenly removed.

When the structure is designed according to the present seismic design code the internal forces greater (with approximately 15%) than those obtained when the structure is designed according to the former seismic design code P100-1/2006 [13]. This fact leads to an increase of the expected un-factored capacities of structural members Q_{CE} and consequently the DCR values decrease compared with the damaged model P100-2006.

5. CONCLUSIONS

The present study investigates the vulnerability to progressive collapse of a typical mid-rise (13-storey) structure located in a high seismic area (Bucharest). In the last 20 years, the Romanian seismic design codes were changed three times: in 1992, 2006 and 2008. A RC framed structure is designed according to each of the three seismic codes. Some important parameters that intervene in the seismic analysis have been changed: concrete class (from Bc 20 to C25/30), type and quality of steel (from PC52 to S500), ground acceleration of the location a_g (from 0.20g to 0.24g), the provisions regarding the allowed minimum ductility class of structural elements as well as the magnitude of the behavior factor q (from 6.75 to 5.85).

The progressive collapse potential is assessed following the static linear elastic procedure specified by GSA (2003) Guidelines. A typical mid-rise RC framed structure located in a high seismic area (Bucharest), designed and detailed according to the seismic codes P100-92 [10], P100-1/2006 [13] or EC-8 [16], does not experience risk for progressive collapse when is subjected to different missing column damage scenarios. In the damage case C_2 (long side exterior column removal), the DCR values for flexure and for shear are below the allowable values (2.00 for flexure and 1.00 for shear). Therefore, the models satisfy the acceptance criteria defined by GSA (2003) Guidelines [1] and the progressive collapse is not expected to occur. Excepting very few beam sections where low inelastic demands are identified ($1.00 \leq DCR \leq 1.10$), the structures practically behaved elastically (DCR < 1.00).

The evolution of the Romanian seismic design codes has an important influence on the level of equivalent static seismic forces. Compared to the seismic design code P100-92 [10], the more recent codes P100-1/2006 [13] and EC-8 [16] lead to an increase of the seismic design force of 5.2%, respectively 21%. As a direct consequence, the expected flexural capacity of beams will also be increased, and the magnitude of demand-capacity ratio (DCR) decreases. The structure designed and detailed according to the active codes EC-8 [16] and EC-2 [14] represent the safest model against the progressive collapse. Thus, an important finding of this study, of great importance for structural engineers, is that the changes in the Romanian seismic codes brings an improvement in terms of progressive collapse resistance of RC structures, and confirm the implicit benefits on progressive collapse resistance when the modern European design codes are used in design of concrete structures.

A similar analysis is conducted considering that the structure is located in a seismic area with a_g = 0.20g, being the lower limit of a high seismic zone. In this case, the DCR values are higher than the structure located in

an area with a_g = 0.24g, but are still below allowable values, which means that the progressive collapse is not expected to occur. In conclusion a 13-storey structure design and detailed according to the present codes for at least a seismic area with $a_g \geq 0.20g$ has a low potential to progressive collapse when an exterior column near to the middle of the long side is suddenly removed.

6. ACKNOWLEDGMENTS

The writers gratefully acknowledge the support from Romanian National Authority for Scientific Research (ANCS and CNSIS-Grant PNII IDEI No. 193/2008) for this study.

7. REFERENCES

[1] GSA 2003, *Progressive collapse analysis and design guidelines for new federal office building and major modernization projects*. 2003, General Service Administration, Washington, DC.
[2] DoD 2005, *Design of buildings to resist progressive collapse.* 2005, Unified Facility Criteria, UFC 4-023-03, Washington, DC.
[3] DoD 2009, *Design of buildings to resist progressive collapse.* 2005, Unified Facility Criteria, UFC 4-023-03, Washington, DC.
[4] Baldridge S. M. and Humay F. K., *Preventing Progressive Collapse in Concrete Buildings.* 2003, Concrete International No. 11, Vol. 25, pp. 73-79.
[5] Bilow N. D. and Kamara M., *U. S. General Services Administration Progressive Collapse Guidelines Applied to Moment – Resisting Frame Building*. 2004, ASCE Structures Congress, Nashville, Tennessee.
[6] Botez M., Bredean L. and Ioani A., *Inelastic demands of RC Structures: Corner Column Case in the Progressive Collapse Analysis*. 2012, Proceedings of the 4th International Conference in Civil Engineering – Science and Practice GNP 2012, pp. 853-860, Montenegro, Zabljak.
[7] Ioani A. M., Cucu H. L. and Mircea C., *Seismic design vs. Progressive Collapse: A Reinforced Concrete Framed Structure Case Study.* 2007, Proceedings of ISEC-4, Melbourne, Australia.
[8] Ioani A. M. and Cucu H. L., *Improving resistance to progressive collapse of concrete structures through seismic design (P100-92, P100-1/2006).* 2010, Computational Civil Engineering 2010, Iasi, Romania.
[9] Ioani A. M. and Cucu H. L., *Resistance to progressive collapse of RC structures: principles, methods and designed models.* 2010, Computational Civil Engineering 2010, Iasi, Romania.
[10] P100-92, *Seismic design code for buildings*. 1992, Ministry of Public Works of Romania, Bucharest. (in Romanian)
[11] STAS 10101/0A-77, *Actions upon structures. Classification and combination of actions for non-individual and industrial structures.* 1977, Romanian Standard Institute (IRS), Bucharest. (in Romanian)
[12] STAS 10107/0-90, *Design and detailing of concrete, reinforced concrete and prestressed concrete structural members.* 1990, Romanian Standard Institute (IRS), Bucharest. (in Romanian)
[13] P100-1/2006, *Seismic Design Code – Part I: Design rules for buildings.* 2006, MTCT, Bucharest. (in Romanian)
[14] SR EN 1992-1-1:2004, *Eurocode 2: Design of concrete structures – Part 1-1: General rules and rules for buildings*. 2004, ASRO, Bucharest. (in Romanian)
[15] CR1-1-3-2005, *Design code. Evaluation of the snow action on buildings.* 2005, MTCT, Bucharest. (in Romanian)
[16] SR EN 1998-1-1:2004/NA:2008, *Eurocode 8: Design of structures for seismic resistance – Part 1: General rules, seismic actions and rules for buildings*. 2008, ASRO, Bucharest. (in Romanian)
[17] Moldovan T. S., Bredean L. and Ioani A. M., "Earthquake and Progressive Collapse Resistance based on the Evolution of Romanian Seismic Design Codes". 2012, Fifteen World Conference on Earthquake Engineering, submitted for publication.

Application of additional linear viscous dampers solution for a 6-storey steel structure

Loredana Elena Roşu and Cătălin Constantin Roşu

***Abstract* – During the last years, there were used increasingly more passive devices for seismic energy dissipation, both for new buildings and for the strengthening of existing ones. The use of these devices has also begun in our country and the tendency is for their application to a large extent. In this article are analyzed variants of structural response reduction by adding supplemental linear viscous dampers. It is considered a regular steel structure with 6 levels in three variants of conformation: moment resisting frames structure, structure with linear viscous dampers and dual frames structure with concentrically braced frames and moment resisting frames. The performance of the solutions are compared, the comparative terms being values of the structural response: peak displacement, absolute acceleration and base shear force, vibration period and the steel quantity, obtained by nonlinear dynamic analysis. WS represents welded section (Malta cross shape).**

***Keywords* – supplemental damping, peak displacement, viscous damper, seismic response.**

1. INTRODUCTION

Although the constructed background in Romania includes a reduced number of multi-storey steel structures compared with the number of concrete and masonry structures, most of them being built in recent years, on international level was noted a good behaviour for these type of structures in case of a major earthquake. Although they have suffered damages, due to their capacity to dissipate a part of seismic energy, their behaviour has been better than other types of structural systems. By introducing additional energy dissipation devices one aims to increase structural damping.

Fluid viscous energy dissipation devices are included in the category of passive devices because they do not need an additional source of energy to get into work. Viscous dampers have been used successfully to increase damping ratio for structures where the use of other types of devices was difficult or was not enought. Fluid viscous dampers works on the principle of fluid flow through orifices. A viscous damper force depends on the relative velocity between the two ends of the damper. The force-velocity relation depends in particular on the fluid characteristics and has the general formula [2]:

$$F_{disip} = c \times v^{\alpha} \ , \tag{1}$$

July 15, 2012

Loredana Elena Roşu is PhD Student, Metallic Structures Department, Technical University of Civil Engineering, Faculty of Civil Engineering, 124 Lacul Tei Av., District 2, 020396, Bucharest, Romania (phone: 0733022163; fax: +40-21-3271371; e-mail: dana_rrosu@yahoo.com).

Cătălin Constantin Roşu is Civil Engineer, Vilared S.R.L., 231A 13 Septembrie Av., District 5, Bucharest, Romania (e-mail: rosucatalin@gmail.com).

ISSN-1584-5990

Where: F_{disip} – is the damper force; c – is the damping constant for the device (it depends on the physical and geometrical characteristics of the device and it has a direct proportional influence on the area of the hysteretic curve); ν - is the relative velocity between the two ends of device and α is the velocity exponent (damping exponent) for the device, with values between 0.01-2.0.

The hysteretic curve for a linear viscous damper (α=1) is an ellipse.

The analyzed structure was designed and dimensioned according to norm P100-1/2006 – „Standard for seismic design of residential, social, cultural, agricultural and industrial buildings", for Bucharest area.

The analyzed variants of structural systems are:

A. Moment resisting frames structural system
B. Structural system with viscous dampers
C. Concentrically braced frames structural system.

For this analysis, the software design used was SAP2000.

2. DESCRIPTION OF ANALYZED STRUCTURAL SYSTEM VARIANTS

2.1. Variant A – moment resisting frames structural system

In A variant (Fig.1.(a);(b)) energy dissipation is made entirely by steel yield in dissipative zones (beam ends and column bases).

The structure has three spans and three bays of 6.00m and 6 levels, each of 3.80m high. The steel used is S355JR which has the yield strenght f_y=355 N/mm^2. Structural system was designed considering two load hypothesis :

Variant A.0. – the gravitational and wind loads;

Variants A.1.0, A.1.1 – considering the seismic load;

The variant A.0. structure is dimensioned considering actions of fundamental load cases (gravitational loads and wind loads), without taking into account the seismic load. In A.1.0 variant, based on the structure designed in A.0 variant, the structure was calculated considering actions of load cases that contain seismic load, in wich case resistance and deformability requirements have not been achieved. In order for these requirements to be accomplished, the increase of elements sections was necessary and A.1.1. variant structure was derived. The structure analysis considering load cases that contain seismic load was performed using the equivalent static seismic forces method. For A.1.1 variant, nonlinear dynamic analysis was performed using Vrancea 1977, N-S, INCERC, Bucharest, recorded accelerogram, scaled by a factor of 1.2. According to seismic zoning maps (P100-1-2006) for structure location a corresponding peak ground acceleration has the value equal tu 0.24g, with a control period (Tc) of response spectrum equal to 1.6s, considering a seismic action with the medium return period of 100 years (used in P100-1-2006 for structural design to Ultimate Limit State). Dynamic amplification factor is, according to P100-1-2006 standard, βo=2.75, for the period TB-TC.

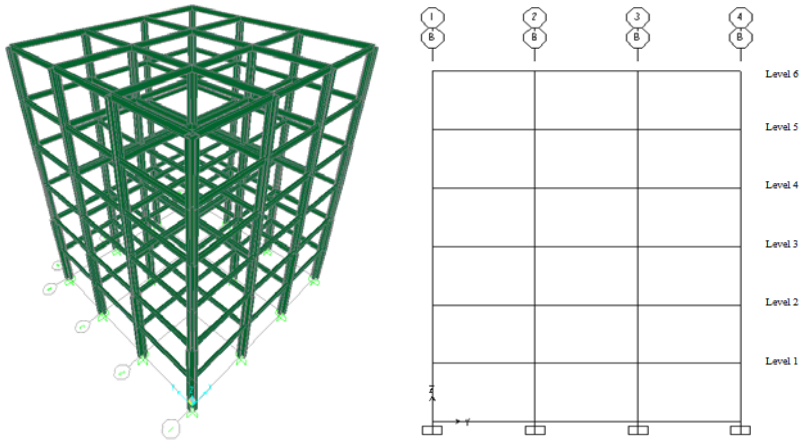

(a) (b)

Fig.1. (a)Axonometric view moment resisting frames structural system; (b)Central moment resisting frame.

Section shapes used for structural elements are: columns – Malta cross shape made of HEA profiles type and WS (WS represents welded section - Malta cross shape), main beams – double – T section (IPE profile). Floors are made from reinforced concrete slabs and are considered infinitely rigid in their plans. In the analysis model slabs are considered by the loads they are transmitting to structure nodes. Structural elements sections are presented in Table 1.

Table. 1. Elements sections for structures A.0, A.1.0,A.1.1,B.0,B.1,B.2,B.3,B.4,C.0,C.1.

Structural system variant	Level	Elements sections			Description
		Beam	Column	Brace	
A.0, A.1.0, B.0	1-2	IPE400	WS275x8-260x14	-	A.0-Moment resisting frames structural system designed by fundamental load cases; A.1.0-Structure from A.0 with seismic load cases; B.0-Structure from A.0 with seismic load cases and viscous dampers.
	3-4	IPE400	WS235x8-220x12	-	
	5-6	IPE360	WS235x8-220x12	-	
C.0	1-2	IPE400	WS275x8-260x14	CHS193.7*8	C.0-Structure from A.0 with seismic load cases and concentrically braces.
	3-4	IPE400	WS235x8-220x12	CHS168.3*8	
	5-6	IPE360	WS235x8-220x12	CHS139.7*8	
A.1.1.	1-2	IPE450	2HEB650	-	Moment resisting frames structural system designed by fundamental and seismic load cases.
	3-4	IPE400	2HEA500	-	
	5-6	IPE400	2HEA400	-	
B.1, B.2, B.3, B.4	1-2	IPE400	2HEA500		Moment resisting frames structural systems with additional viscous dampers designed by fundamental and seismic load cases.
	3-4	IPE360	2HEA340		
	5-6	IPE360	WS300x8-280x14		
C.1.	1-2	IPE400	2HEA500	CHS193.7*8	Structural system with concentrically braces designed by fundamental and seismic load cases.
	3-4	IPE400	2HEA340	CHS168.3*8	
	5-6	IPE360	WS260x8-240x12	CHS139.7*8	

The first two vibration modes are of translations with a participation mass factor higher than 75%. Thus: $T_{1.A.1}$= 2.05s., $T_{1.A.2}$=1.42 s.

2.2. Variant B – structural system with viscous dampers

In B variant (Fig. 2(a)) the energy dissipation is done both by steel yield (natural damping) and by viscous dampers (additional viscous damping). They transform seismic energy into heat that is released into the atmosphere.

In B.0 variant, based on the structural system dimensioned in A.0 variant, viscous dampers were added and the structure was analyzed considering seismic load. Because, as noted, the resistance and deformability conditions have not been achieved, the structure was conformed and dimensioned again so that they cand be complied by introducing viscous dampers. There have been considered several options for dampers placing in order to obtain a more effective positioning. Dampers location in a frame was made throughout the entire height of the structure, as follows:

B.0. şi B.1. Structural system with viscous dampers - placed in the central spans of each transversal frame and in the central bays of each longitudinal frame, a total of 48 dampers (Fig.2(b), Fig.3(a));

B.2. Structural system with viscous dampers - placed in the marginal spans of each transversal frame and in the marginal bays of each longitudinal frame, a total of 96 dampers (Fig.2(c), Fig.3(b));

B.3. Structural system with viscous dampers - placed in the central spans and central bays of marginal transversal frames and marginal longitudinal frames, a total of 24 dampers (Fig.2(b), Fig.3(c));

B.4. Structural system with viscous dampers - placed in the marginal spans and marginal bays of marginal transversal frames and marginal longitudinal frames, a total of 48 dampers (Fig. 2 (c), Fig.3(d));

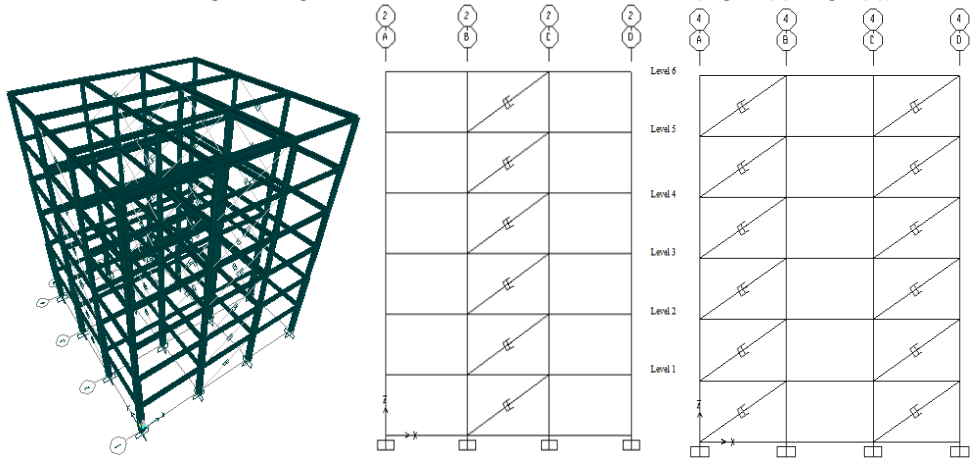

(a) (b) (c)

Fig.2. (a) Axonometric view structural system with viscous dampers; (b) Structural frame with viscous dampers located in the central span; (c) Structural frame with viscous dampers located in the marginal spans.

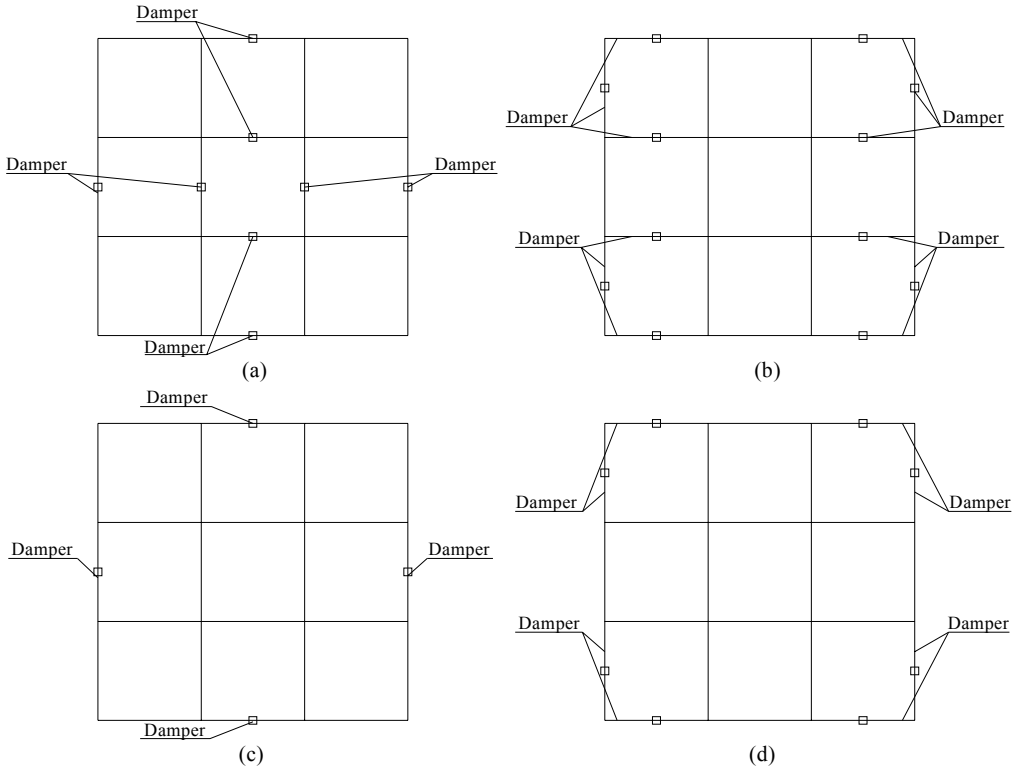

Fig.3. (a), (b), (c), (d) – Dampers allocation types into the structure

Structural elements of the building are calculated using a seismic force corresponding to a damping ratio of 25% from wich 3% represents the natural damping ratio. In this case the base shear force it was affected by the factor η (ecuation 2) [3]. Structural elements sections are presented in Table 1.

$$\eta = \sqrt{\frac{10}{e + \xi_{eq}}} \tag{2}$$

The damping constant *c* of viscous dampers will be calculated from the condition for the equivalent damping ratio (ξ_{eq}), due to the action of the supplemental viscous dampers, to be equal with 22% of the critical damping ratio. In order to determine viscous dampers characteristics, one will use the methodology described in FEMA 356 [2].

$$\xi_{eq} = \frac{E_D}{4\pi E_S} \tag{3}$$

The above relation results from equalising the energy dissipated in one complete oscillation cycle by the actual structure to the energy dissipated by an equivalent viscous system. E_D is the energy dissipated by the

devices in an oscillation cycle and is calculated as the sum of work done by each device in that cycle using relation (4). E_S is the maximum potential energy of deformation calculated with relation (5) [2].

$$E_D = \sum_j (W_j) = \sum \frac{2\pi^2}{T} c_j \delta_{rj}^2 \tag{4}$$

Where: T – is the fundamental mode period for the analyzed direction; c_j – is the damping constant of linear viscous damper „j"; δ_{rj} – is the relative displacement between the ends of device „j".

$$E_S = \frac{1}{2} \sum (F_i \delta_i) \tag{5}$$

Where: F_i – is the inertia force at floor level „i"; m_i – is the structural mass at level „i"; a_i – is the acceleration at floor level „i".

Damping constants of devices c_j are calculated by the equation (6) where c_0 is a reference value and k_j are coefficients chosen by the designer [2]. In this specific case, all k_j coefficients are assigned to value 1 ($k_j = 1$).

$$c_i = c_0 k_i \tag{6}$$

By replacing relations (4) and (5) in equation (3) one can obtain an equation (7) to calculate damping constant of viscous damper:

$$c = \frac{\xi_{eq} 4\pi \frac{1}{2} \sum_i (F_i \delta_i)}{\frac{2\pi^2}{T} \sum_j \delta_{rj}^2} \tag{7}$$

As a condition for dimensioning the structure with dampers (B2 variant), additionally it was required to check the strength and deformability elements (relative level displacements) to service limit state and to ultimate limit state. Structural systems with viscous dampers for the analyzed variants had an elastic behaviour.

2.3. Variant C - concentrically braced frames structural system

In C variant (Fig.4 (a); (b)) energy dissipation is entirely made by steel yield in dissipative zones (tensioned braces, beam ends from the moment resisting frames and column bases). Structural elements sections are presented in Table 1.

The first two vibration modes are of translations with a participation mass factor higher than 72%. Thus: $T_{1.C}$= 0.73s.

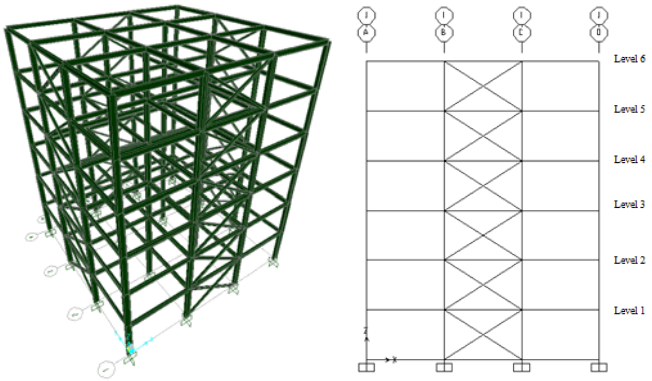

(a) (b)

Fig.4. (a) Axonometric view concentrically braced frames structural system; (b) Concentrically braced frame.

3. ANALYSIS RESULTS AND OBSERVATIONS

The nonlinear dynamic analysis results are summarized in table 2 and they are presented as the structural response values, the steel consumption values resulted for each conformation variant and the damping constant values of viscous dampers.

One can note that the base structure A.0, exclusively dimensioned to load cases that do not contain seismic action do not meet the resistance and deformability conditions for load cases that contain seismic load, as follows:

- A.0.1 variant (structure from base variant A.0) – deformations exceeding by 211% and resistance exceeding by 248% (for columns)
- B.0 variant (structure from base variant A.0 with dampers) – deformations exceeding by 73% and resistance exceeding by 107% (for columns)
- C.0 variant (structure from base variant A.0 with centric braces) – deformations are verified and resistance exceeding by 84% (for columns)

In B.0 variant (structure from base variant A.0 with 48 viscous dampers), one can observe that dampers added as energy dissipation devices, are capable to support the majority of the seismic action so that the deformability requirements to be almost achieved. However, the obtained structure can not support the efforts on which the structural elements are subjected to, especially the structures columns (moment and axial force), due to seismic action. The structure no longer satisfy the resistance requirements.

In B.1 variant (structural system with 48 viscous dampers) one can observe that for a decrease in the vibration period of the structure there is an increase of the damping constant of the devices. In order to provide an additional stiffness for the structure, dampers must develop a higher force. One can also notice that the structure level masses have increased in B1 variant compared to B0 variant (structure from base variant A.0 with dampers) and therefore the damping constant (wich depends on the structure level mass) of the devices increased.

Instead, if the dampers number increases, the corresponding damping constant decreases, but the structural response values changed to a minor degree. In B2 variant (structural system with 96 viscous dampers) one can observe that even though the dampers number has doubled, damping constant value has not decreased by half, and one may conclude that a smaller number of dampers can be more efficient from an economical perspective, even if they have a higher damping constant value. If it is analyzed instead the B3 variant (structural system with 24 viscous dampers) compared to B1 variant (structural system with 48 viscous dampers) of dampers location,

one can observe that the dampers constant is directly proportional to dampers number from wich one can conclude that this type of allocation is more favorable to dissipate seismic energy.

Table. 2. Comparative table of structural response values

Structural system	Response parameters				Steel quantity (Kg)	Damper coeficient c (KNs/m)
	Maximum peak displacement (mm)	Absolute max. peak accel. (m/s^2)	Base shear force (KN)	Fundamental vibration period (s)		
A.0- Moment resisting frames structural system designed by fundamental load cases	-	-	-	2.09	95700	-
A.1.0-A.0 Structure with seismic load cases	0.644	6.22	4469	2.09	95700	-
B.0-A.0 Structure with seismic load cases and 48 additional viscous dampers	0.475	4.81	4047	2.09	95700	913
C.0-A.0 Structure with seismic load cases and concentrically braces	0.157	6.91	5818	0.9	95700	-
A.1.1- Moment resisting frames structural system designed by fundamental and seismic load cases.	0.431	8.44	8149	1.25	179200	-
B.1-Moment resisting frames structural systems with 48 additional viscous dampers designed by fundamental and seismic load cases.	0.374	6.46	6309	1.49	130200	1143
B.2- Moment resisting frames structural systems with 96 additional viscous dampers designed by fundamental and seismic load cases.	0.340	5.99	6068	1.49	130200	762
B.3- Moment resisting frames structural systems with 24 additional viscous dampers designed by fundamental and seismic load cases.	0.374	6.48	6340	1.49	130200	2286
B.4- Moment resisting frames structural systems with 48 additional viscous dampers designed by fundamental and seismic	0.377	6.51	6333	1.49	130200	1143

load cases.						
C.1-Structural system with concentrically braced frames designed by fundamental and seismic load cases.	0.096	6.33	6180	0.73	140400	-

A change in the value of the damping constant of devices can be achieved if structures level masses will change, wich means a change in the additional viscous damping level.

4. CONCLUSIONS

Viscous dampers are used as *additional* energy dissipation devices, dissipation throught inelatic incursions of some structural elements (natural damping), even though with a lower rate from the total damping ratio of the structure, being indispensable in case of an earthquake. These dampers bring an additional damping to the structure being very usefull when it is required to decrease displacements due to seismic or wind action, and also adds a certain rigidity for structure (see table 2).

One can observe that for a moment resisting frames structure with viscous dampers it seems to be efficient a regular allocation of dampers into the structure (in symmetrical spans and bays in both directions). Also, in order to be more economicaly efective the number of dampers should be kept as low as possible.

For a chosen level of damping ratio, structural response parameters change to a minor degree depending on the number of dampers (table 2). They have similar performances and the only value that varies significantly is the damping constant of viscous devices. After the introduction of dampers into the structure, for the analysed cases, the structure has an elastic behaviour for all dampers allocation variants.

The reduction of efforts due to an additional damping provided by dampers leads to the reduction of structural elements sections and therefore to the reduction of steel consumption. The steel quantity decreases with 43% in B.1. variant (structural system with viscous dampers) compared to A.1 variant (moment resisting frame structure) and with 8% compared to C.1 variant (concentrically braced frames structure).

Under these circumstances, still, an open issue it is the achievement, based on further research of devices as economical effective as possible in order to be used as a solution for seismic response reduction in the current designing procces.

It appears of interest realisation of further theoretical researches on the behaviour of structural systems with concentrally braces to wich viscous dampers to be placed in different allocation types (the replacement of some braces with viscous dampers).

6. REFERENCES

[1] Vezeanu G., and Bețea Șt., *Soluții alternative pentru structuri din oțel cu contravântuiri centrice*. 2009, Conferința națională de Inginerie Seismică (CNIS), Proceeding, vol. II, pag. 1-2,5-6.

[2] FEMA 356. *Prestandard and Commentary for the Seismic Rehabilitation of Building*. 2000, Federal Emergency Management Agency, p.5.1-5.54, p.9.1-9.33.

[3] P100-1-2006, *Normativ pentru proiectarea antiseismică a constructiilor de locuințe, social culturale, agrozootehnice si industriale*, 2006, Cap.3, Cap.4, p.4.2-4.15, Cap.6, p.6.1-6.10, p.6.16-6.20, Anexa A, p.5, Anexa D.

[4] Eurocode 8: Design of structures for earthquake resitance - *Part 1: General rules, seismic actions and rules for buildings,* 2004, Cap.3, p.3.1-3.2, Cap.4, p.4.1-4.4, Cap.6, p.6.1-6.10.
[5] Dalban C., Dima S., Chesaru E., Serbescu C., *Construcţii cu structură metalică*, 1997, Editura Didactică şi Pedagogică, Bucureşti.

The evaluation of the effect of damping on a structure of reinforced concrete frames P+4

Ţepeş Onea Florin

Abstract – **This paper intends, in the first instance, to compare the response of reinforced concrete frame structures subjected to seismic action obtained by two methods of calculation: the use of equivalent static seismic forces and the use of integration in time, considering the same seismic area.**
In the second phase we intends to determine the influence of viscos damping. Comparative analysis will be made through methods accepted by the existing normatives (P100/2006).

Keywords **– concrete, finite elements, seismic forces**

1. THE FOUNDATION OF THE METHOD OF ANALYSIS

In order to determine the stress within the structure including the mesh nodes a discretisation with 8-node quadrilateral elements, was used with quadratic interpolation functions.

The quadrilateral element was chosen instead of the "beam" element because:
- it leads to a state of tension throughout the structure
-the discretization does not involve special problems in the case of modern programes
-the finite-elements were used in the plain stress , with their thickness implied.
-there is the advantage of further analysis in which the reinforcement effect, will be introduced advantage, that does not exist in the case of th "Beam elements".
-linear quadrilateral elements were not used because the main disadvantage of the linear elements and therefore of linear izoparametric is the lack of accuracy in reproducing the bending phenomenon .

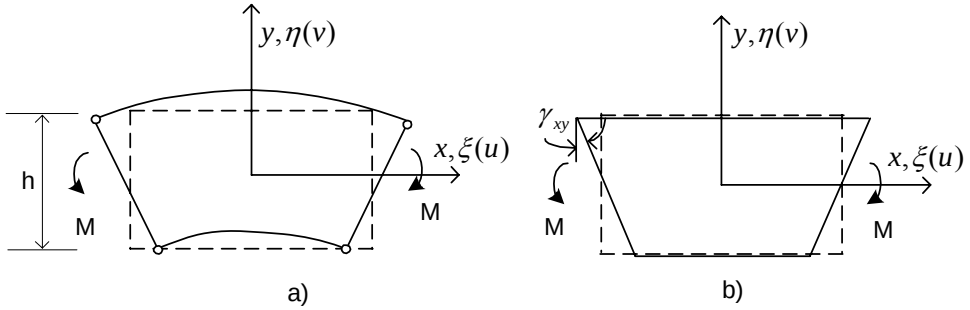

Author is with Ovidius University of Constanta, Bd. Mamaia nr. 124, 900356-Constanta, Romania (corresponding author to provide phone: +40-241-619040; fax: +40-241-618372; e-mail: tflorin@univ-ovidius.ro).

ISSN-1584-5990

Fig. 1 The condition of deformation of an element subjected to pure bending: a) produced physical b) reproduced by linear quadrilateral element

The specific strain γ_{xy} produced in the element and actually void makes that some strain energy is stored in "parasitical" stress τ , the element becomes too stiff in bending.

In the case of quadrilateral membrane, izoparametric, parabolic (8 nodes/16 nodal degrees of freedom the functions element of the of geometry are parabolic with the expression: $\xi, \eta \in [-1,1]$

$$x = \alpha_1 + \alpha_2\xi + \alpha_3\eta + \alpha_4\xi\eta + \alpha_5\xi^2 + \alpha_6\eta^2 + \alpha_7\xi^2\eta + \alpha_8\xi\eta^2$$

$$y = \alpha_9 + \alpha_{10}\xi + \alpha_{11}\eta + \alpha_{12}\xi\eta + \alpha_{13}\xi^2 + \alpha_{14}\eta^2 + \alpha_{15}\xi^2\eta + \alpha_{16}\xi\eta^2$$

In the case of the izoparametric element the shape functions for geometry being also used to describe the description of the field displacements.

These degrees of freedom can provide to the finite element the possibility to represent a constant bending moment. Tests show that using incompatible quadrilateralelements leads to solutions converging monotonously.

In conclusion it is notable that incompatible quadrilateral elements do not introduce errors in the structural response as compared with elements the “Beam” elements. A comparison of response was made too in the case of equivalent static seismic forces between a discretization with quadrilateral mesh type elements with 8 nodes.

The results in terms of displacements are similar between the two types of analysis (Fig. 2), which means that the bending with quadrilateral elements with 8 nodes is correctly modelled.

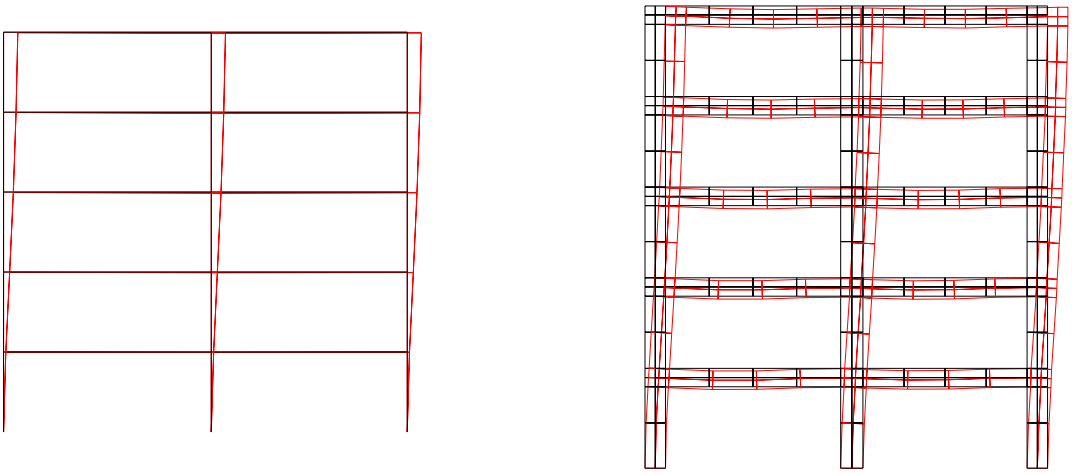

Fig.2 a) deformed shape discretization of mesh elements Dy Beam max = 0.6E-2m b) deformed shape discretization 8-node izoparametric elements Dymax = 0.5E-2m

The calculation using the equivalent static seismic forces is easy because it needs an effort of calculation reduced, the necessary information for obtaining seismic forces are easy to obtain and not least of all most programmes with which the design companies operate do not allow integrations in time.

In the case of the integration in time an accelerogram is required recorded in the respective area and scaled to an appropriate value from P100/2006. The calculation step length is chosen small enough (0.02s) in order to obtain a good numerical accuracy and to avoid numerical instability.

It is considered that for a sufficiently accurate calculation at least 20 time steps in a period of time $2\pi / \omega_{\max}$. $\omega_{\max}$ must exist. This represents the greatest pulsation that is important in the dynamic response as follows: $\Delta t \le \frac{1}{20}\frac{2\pi}{\omega_{\max}} = \frac{0.3}{\omega_{\max}}$

The matrix [C] is selected after the Rayleigh model, the scaling parameters being evaluated depending on the fractions of critical damping. One of the major advantages of the direct numerical integration method consists in its application withot difficulties on the nonlinear dynamic analysis of structures. Another advantage of the integration in time is represented by the fact that the equation of motion is the most apropiate way to approximate the real phenomenon.

2. THE STRUCTURAL RESPONSE ANALYSIS FRAMEWORK USING THE TIME INTEGRATION

Comparative studies were realized on the same discretization (element with 8 nodes) applying seismic forces in two ways: a) the corresponding equivalent static seismic forces for seismic zones 0.16g b) using integration in time while using an accelerogram scaled to 0.16g having a duration of 16s and with 800 time steps with dt = 0.02s.

We used the resilience modulus appropriate to the C20/25 concrete.

The comparative results in terms of displacements and unitary efforts are presented in Table 1.

Table 1

Analysis type	Dy max	σ_x (daN/cm^2)	σ_y (daN/cm^2)
Equivalent static seismic forces	0.458E-2	-60.23 +60.82	-53.68 +17.37
Integration time (quadratic element 8 knots) accelerogram duration 16s	0.887E-2	-97.03 +96.79 At end rulers first level	-94.26 +51.96 Based on pillars

The results obtained in the first case study show a underevaluation of displacements and efforts in the case of using equivalent static seismic forces instead of the integration time. The diferences, in the displacements case, are almost double.

In the case of unitary efforts the differences between the two assessment methods of the seismic response are 61.6%.

The stretching efforts are irrelevant because in the stretched zone the concrete works cracked, and the stretching efforts are taken by the reinforcement.

The time integration analysis can be considered as a baseline study since it represents close mathematical formulation which is the closest to reality.

3. EVALUATING THE DAMPING

If the notions of mass and stiffness are relatively easy to wield, given their static nature, the concept of depreciation is difficult to deal with. This is because depreciation out of static problem has been treated superficially in standardized structural dynamic analysis because of the difficulty of getting adequate information for all problems of interest. From the experience gained by researchers until now, it appears as certain the following fact: damping plays an important role in determining the response of a structure required by dynamic action, an uncertainty of the order of 20-30% in assessing the response falsify the damping rate by 15 -40%.

The damping is a phenomenon that causes dissipation of energy in a mechanical system in motion. This dissipation of energy is achieved by: feedback in the field, losses in the environment, energy losses in absorber with which the system can be equipped, internal damping due to inelastic behavior of materials.

The energy returned to the land transformed patially into heat due to internal damping land and partly in waves that are transmitted over long distances.

Regarding the internal damping materials, elements or structures in general, the problem is quite delicate.

In this study only viscous damping was considered not hysteretic damping (material nonlinearity).

The analytical determination of the engineering structures damping is not reliable engineering structures. The fraction of critical damping for different types of structures and two levels of application are shown in Table 2.

It is noted the fact,that most seismic design standards do not recognize damping variation by the type of material and the level of the efforts in the structure, in all cases a fraction of critical damping of 5% being specified.

Table 2

Stress level	Type structure	ξ %
Efforts within 0.5 of yield strong concrete structures	Reinforced concret structure (cracks limited)	2-3
	Significant cracks in concret cracks	3-5
Efforts yield close to concrete structures	Concret structure	7-10

Last run (table 3) was performed using a 5% damping. The accelerogram of 16s was kept and nodal masses were introduced in order that the damping matrix can be calculated using the Rayleigh model.The damping matrix has the form $[C] = \alpha[M] + \beta[K]$

Table 3

Analysis type	Dy max	σ_x (daN/cm^2)	σ_y (daN/cm^2)
Integration time (quadratic element 8 knots) accelerogram duration 16s + 5% damping	0.64E-2	-175.0 +161.0 (At end rulers first level)	-112.01 +147.6 (Based on pillars)

4. CONCLUSIONS

The calculation model using the quadratic element with 8 nodes provides a good solution in terms of obtaining displacements and stress.

There is an understatement of displacements and stress when using equivalent static seismic forces comparatively with the integration in time.

In case of unitary stress differences between the two assessment methods of the seismic response are of 61.6%.In the last method of analysis, in which the depreciation was taken into account, major changes are in terms of unitary stress. Thus the maximum tension σ_x does not occur in step 322 but in step 539.

There is also an increase in terms of state power from 96daN/cm2 to 175 daN/cm2.So if the area of concrete is large and work cracked , the efforts are taken to the reinforcement. For the compressed zones of concrete the stress values are high.

6. REFERENCES

[1] M. Jeremiah, Elasticity, *Plasticiy, Nonlinearity*, Ed Printech, New York (1998), Romania
[2] M. Jeremiah C. Trăistaru, S.Gînju, *Influence of viscous damping in nonlinear dynamic analysis of a multi-storey steel structure*, ICMS 2000, University Politehnique Timişoara
[3] D.Stematiu, *Calculation of hydraulic structures by finite element method*, Technical Publishing House Bucharest, 1988

SECTION II

CIVIL WATER ENGINEERING

Landfill Water Management

Michal Holubec, Kristína Galbová, Ivona Škultétyová, Štefan Stanko, Ivana Mahríková

Abstract – **Protection of groundwater quality is a primary performance goal for all waste containment systems, including final cover systems. The potential adverse impact to groundwater quality results from the release of leachate generated in landfills or other waste disposal units such as surface impoundments. The rate of leachate generation (and potential impact on groundwater) can be minimized by keeping liquids out of a landfill or contaminated source area of a remediation site. As a result, the function of minimizing percolation becomes a key performance criterion for a final cover system.**
Landfills are a potential threat to the surrounding environment during their design or technical error throughout their operation in terms of leachate. Leachate represents water that gets into the landfill body by rainwater and in the contact with waste it gains harmful properties. Percolation through the landfill body is improperly designed or implemented sealing, drainage system of landfills, its closure and reclamation, as well as in the case of accidents, these buildings can result in contamination of the ground as well as the groundwater.
The control of leachate quantity and quality is the basis for long-term landfill operation with minimized emissions and also for leachate treatment.

Keywords: **waste water, leachate, groundwater quality**

1. INTRODUCTION

Of all unit processes conducted at a solid waste landfill, leachate management is one of the most critical to overall site environmental integrity. Proper leachate management is essential to avoid surface and ground water contamination and is one of the principal elements of a landfill management program that remains when the site closes.

Refuse contains decomposable matter, as well as the nutrients and organisms that promote decomposition. The limiting factor controlling the amount of decomposition taking place in municipal solid waste is usually the availability of moisture. The decomposition of solid wastes in an MSW landfill is a complex

24th July 2012. The Research Grant VEGA 1/1079/12 held by the Department of Sanitary Engineering Faculty of Civil Engineering, Slovak University of Technology Bratislava has supported this paper

Michal Holubec is with Slovak University of Technology Bratislava, Civil Engineering Faculty, Department of Sanitary & Environmental Engineering, Radlinského 11, 813 68 Bratislava, Slovak Republic michal.holubec@stuba.sk

Kristína Galbova is with, Slovak University of Technology Bratislava, Civil Engineering Faculty, Department of Sanitary & Environmental Engineering, Radlinského 11, 813 68 Bratislava, Slovak Republic kristina.gggalbova@stuba.sk

Ivona Škultétyová, PhD. is with Slovak University of Technology in Bratislava; Radlinského 11, 81368, Bratislava, Slovakia; e-mail: ivona.skultetyova@stuba.sk.

Štefan Stanko, PhD. is with Slovak University of Technology in Bratislava; Radlinského 11, 81368, Bratislava, Slovakia; e-mail: stefan.stanko@stuba.sk.

Ivana Mahríková, PhD. is with Slovak University of Technology in Bratislava; Radlinského 11, 81368, Bratislava, Slovakia; e-mail: ivana.mahrikova@stuba.sk.

ISSN-1584-5990

process. It may be characterized according to the physical, chemical, and biological processes that interact simultaneously to bring about the overall decomposition. The by-products of all these mechanisms are chemically laden leachate and landfill gas.

Predicting the amount of leachate is a critical design parameter when designing a landfill. The amount of generated leachate will impact operating costs for leachate collection and treatment.

2. THE LEACHATE

With every landfill, the engineers have to decide for the most qualified, ideal cover lining system. Hereby, the main targets are to reduce the leakage through the capping into the waste body (and indirectly the pollutant emission of the total landfill) and to design an appropriate system with respect to the location specific conditions. The leakage is part of the complex water processes which occur in the cover lining system. The processes depend especially on the climate (precipitation, temperature) and on the cover lining system itself (e.g. vegetation, soils used). A good aid to examine these processes and to compare different cover lining systems is the use of water balance models (programmes). In addition, these programmes support the optimization, the comparison of the hydrological efficiency of different cover lining components (e.g. restoration and drainage layer) and the specific risk estimation [1].

Leachate is liquid that penetrated deposited waste and emitted from landfills or remain detained in a landfill [2].

Leachate is a liquid that has passed through or emerged from the waste in a landfill. It contains soluble, suspended, or miscible materials removed from such waste. When designing leachate collection and treatment facilities one has to consider the concentrations and variability of leachate with regard to its many constituents. Leachate generation rates depend on the amount of liquid originally contained in the waste (primary leachate) and the quantity of precipitation that enters the landfill through the cover or falls directly on the waste (secondary leachate). Under normal conditions, leachate is found at the bottom of the landfill and moves through the underlying strata. Although, some lateral movement may also occur, depending on the characteristics of the surrounding material, leachate percolates through the underlying strata and many of its chemical and biological constituents will be removed by filtering and absorptive action of the material composing the strata. In general, the extent of this action depends on the characteristics of the soil. The exact volume of the produced leachate cannot be easily estimated as it depends on groundwater infiltration and waste composition. The hydrometeorological conditions in the area of the landfill and its surroundings are of high importance as they affect the hydrogeological status of the area, leachate production and subsequently the risk of contamination [3].

3. MODEL FLOW OF LEACHATE

In recent decades several water flow models for landfills have been developed. However, their application was almost exclusively limited to laboratory experiments. Comprehensive simulations of leachate flow and its generation rate using data from full scale landfills are very rare [4]- [5].

Computing leachate production in sanitary landfills is necessary for selecting management methods, design treatment systems and assess environmental impact. Several methods for computing leachate quantity are currently available in the literature. A serious drawback for most of the existing methods is the lack of detailed input data and the complexity of the computations. A simpler approach, described in Tchobanoglous et al., is based on a water balance, which takes into account water infiltration, water from solid waste, water consumed for biogas production, and water vapours escaping with biogas emission. Leachate production occurs when the remaining water in the cell exceeds field capacity of the buried waste.

Factors influencing leachate generation and indirectly the potential for detrimental water resources impacts at a landfill are:
1. Climate;
2. Site topography;
3. Final landfill covers material;
4. Vegetative cover;
5. Site phasing and Operating procedures;
6. Type of waste materials in the fill.

The amount of leachate generated from landfills over long time periods (e.g. years) can be predicted quite well using available water balance models (e.g. HELP [6]).

Their quantity is influenced by the intensity of rainfall, the surface runoff, evaporation and the ability to accumulate the landfill body water [2]. They calculate leachate discharge equal to the difference between precipitation and the sum of actual evapotranspiration, runoff, and water storage within the waste body, whereby the later one is determined on the concept of field capacity (no water flow until the soil or waste reaches certain water content). However, the variation of the leachate discharge rate over time is much more difficult to describe, since it requires an understanding of the water flow processes inside the landfill [7].

Despite the need for obtaining information on the quantity of leachate from the landfill, they have so far not been sufficiently addressed. Process water balance for the landfill is more complex than the water balance of natural origin, because in addition to natural conditions affect the quantity water and bio-chemical processes inside a landfill [7]. Informative Annex A - STN 83 810 Landfilling, waste leachate from landfills describes the calculation of the amount of landfill leachate. It states that quantity leachate can be determined by water balance of landfill, which is generally expressed as follows:

$$Q = Z – P – V + W \pm U + R \quad (1)$$

where:
Q - is the quantity of leachate collected for landfill sealing system;
Z - rainfall;
P - surface runoff;
V - evaporation;
W - moisture content of the waste deposited;
U - water consumed by or underlying the on-going march of the landfill;
R - retention capacity of landfill.

Getting quality input data is determined by several factors: the complexity of relationships in a landfill, the availability of necessary information, financial capabilities and etc.. To balance modelling of existing landfills is appropriate equation to calculate the quantities of leachate (1) modified [8].

The water balance method serves as a useful engineering tool in conducting environmental assessments of proposed or existing sanitary landfill sites, specifically in regards to leachate generation.

Process water balance for the landfill is more complex than the water balance of natural origin, because in addition to natural conditions affect the quantity water and bio-chemical processes inside a landfill. The water balance equation shown in Fig. 1., estimates the amount of water which will percolate through the landfill cover.

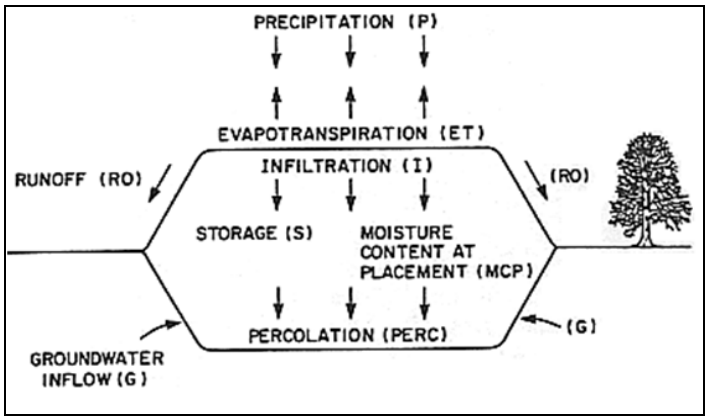

Fig. 1. The water balance equation

The amount of leachate generated from landfills over long time periods (e.g. years) can be predicted quite well using available water balance models.
Their quantity is influenced by:

- the intensity of rainfall,
- the surface runoff,
- evaporation,
- and the ability to accumulate the landfill body water.

To estimate the water balance of surface covers or liner systems under the climate of a specific location simulation models are suitable provided tools, as they are sufficiently validated and critically applied by the user (Berger, 2003). The most famous and widespread model for the prediction of leachate production is the computer model HELP first reported by Schroeder et al. [1984] and developed further to Visual HELP (Schroeder et al., 1994). The HELP-model is a distributed water balance model. The water input to the landfill is calculated by solving the water balance equation for the surface. The landfill is divided into several subsystems and the water movement through the landfill is calculated by a routine procedure using Darcy's law [9].

Hydrologic evaluation of landfill performance (Visual HELP) computer program is a quasi-two-dimensional hydrologic model of water movement across, into, through and out of landfills. Model use - simple tool for evaluating the performance of alternative landfill design. The program was developed to conduct water balance analyses of landfills, cover systems, and solid waste disposal facilities.

The primary purpose of the model is to assist in the comparison of design alternatives as judged by their water balances. The model is sufficiently sophisticated to consider all of the principal design parameters including vegetation, soil types, geosynthetic materials, initial moisture conditions, thicknesses, slopes, and drain spacing as well as climate effects [10].

Model requirements for climatic data on a local or regional scale are crucial for correct water balance estimations. To get the climatic data in an appropriate time and spatial scale may be difficult and is therefore a potential source for uncertainty in the calculations. Moreover, to verify the estimated surface runoff at a landfill site, and to obtain reliable data on the collected leachate generation in the field may be difficult. The input of soil/waste properties is essential for calculation of leachate production. In particular, the choice of hydraulic conductivity is of major importance for the outcome of the simulations, and the input data must be obtained under relevant and reliable conditions.

Table 1. Input data requirements and output options

Input / Output	Parameters
Climate data requirements	evapotranspiration
	precipitation
	temperature
Soil data requirements	porosity
	field capacity
	wilting point
	Initial moisture content
	saturated hydraulic conductivity
Design criteria requirements	slope angle
	slope length
	Layer thickness
Output options	runoff
	evapotranspiration
	drainage
	leachate collection
	liner leakage

The HELP-model exemplifies the use of a distributed water balance model. In Table 1., typical data requirements (input) and output options for a leachate production model are compiled [9].

The HELP model and water balance method need the calibration of measured data of generated leachate quantities from the landfill. After obtaining the measured and estimated amount of leachate it is useful to make a statistical analysis of the results of the methods, used to compare and evaluate the degree of relationship between the results of methods. The measured and estimated quantities of leachate have to be compared in the light of the used methods, metrological conditions, and site preparation and operation aspects of landfill. Statistical analysis of the results of the used methods is a helpful tool to compare and evaluate the degree of relationship between the results of the two methods.

4. CONCLUSIONS

Recognizing the importance of percolation in the environmental assessment of a potential leachate problem at a land disposal site, this paper describes leachate generation and discusses a methodology to estimate the leachate quantity. Simulation models and programmes are tools and calculation assistance to process complex and complicated systems and procedures. The modelling is based on complex (exact) physical equations and dependencies. The conversion is normally carried out by numerical approaches of the finite element or finite difference method. Consequently, the handling of the programmes is complicated, i.e. one needs high computing power, and the simulation duration is relatively long. Practical-oriented models are used to simulate technical sceneries and various concepts. They contain relatively simple arithmetic approaches. Therefore, they are user-friendly and fast. The water balance depends on such complex procedures. Therefore, a vast number of water balance models and programmes were widely developed.

For a complete understanding of the processes, the target is to develop a model which can simulate the water movement in the total landfill.

5. ACKNOWLEDGMENTS

The Research Grant VEGA 1/1079/12 and Vega 1/1143/11 held by the Department of Sanitary Engineering Faculty of Civil Engineering, Slovak University of Technology Bratislava has supported this paper.

6. REFERENCES

[1] Rainer M. Zeh, Karl J. Witt, *Water Balance Models and Programmes- Comparisons and Calculation Results*. Bauhaus-University Weimar - Professorship of Foundation Engineering, Weimar, Germany.
[2] Derco, J., Mencáková, A., Almásiová B., *Utilization of Ozone for Treatment of Landfill Leachate*, Chemické listy – ISSN 1213-7103 – Vol. 103, č. 7 (2009), s. 581 – 588.
[3] Shao-gang Dong, Zhong-hua Tang, Bai-wei Liu, *Numerical modeling of the environment impact of landfill leachate leakage on groundwater quality-A field application*, 2009 International Conference on Environmental Science and Information Application Technology, pp. 565-568.
[4] García de Cortázar, A.L., Tejero Monzón, I., *Application of simulation models to the diagnosis ofMSWlandfills: an example*, 2007, Waste Management 27 (5), pp. 691–703.
[5] Lobo, A., Muñoz, J., Sánchez, M.M., Tejero, I., *Comparative analysis of three hydrological landfill models through a practical application (MODUELO 2, HELP and MODUELO 1*, Christensen, C.A.S. (Ed.), Proceedings of the Ninth International Landfill Symposium, Sardinia 2003. CISA, Cagliari, Italy.
[6] Škultétyová, I., *Water source protection from landfills leachate*, WMHE 2009.Vol.I., Eleventh International Symposium on Water Management and Hydralic Engineering. Ohrid, Macedonia, 1.-5.9, Skopje, University Ss.Cyril and Methodius, 2009. – ISBN 978-9989-2469-6-8. pp. 523-532.
[7] Pelikán, V., *Ochrana podzemních vod. Vyd. Praha*, SNTL 1983, pp. 324.
[8] Mikita, S., Horvát, O., *Využitie bilančného hydrologického modelovania pri štúdiu režimu kontaminačných prejavov zo skládok údolného typu*, Podzemná voda 2008 - ISSN 1335-1052, XIV, 2/2008, pp. 185-190.
[9] Wahlström, M. - Laine-Ylijoki, J. - Hjelmar, O., Bendz, D. & Rosqvist, H., *Models for impact evaluation on landfill – Aspects for appropriate modeling*, Nordic Innovation Centre, 2006. ISSN 0283-7234, pp. 43.
[10] Schroeder, P.R., Morgan, J.M., Walski, T.M., Gibson, A.C., *The hydrologic evaluation of landfill performance (HELP) model*, volume I, user's guide for version 1. Technical Resource Document EPA/530-SW-84-009, 1984, US Environmental Protection Agency, Cincinnati.

Ovidius University Annals Series: Civil Engineering, Issue14, October 2012

Accessibility of water in heritage buildings materials

Bucur Dan Pericleanu, Mihaela Drăgoi

***Abstract* – Accessibility of water itself is one of the processes causing damage to the building material by transporting soluble salts in water composition. In a sufficient quantity of water they dissolve and become soluble; otherwise, they crystallize in solid forms. On the other hand, crystallized salts can store molecules of water which, depending on the temperature, can be eliminated by changing the volume. Accessibility of water on the bricks characteristic to heritage buildings can be determined by combining different measurements such as porosity, water absorption under low pressure and water absorption by capillarity.**

***Keywords* – Absorption, accessibility of water, bricks, heritage buildings, porosity.**

1. INTRODUCTION

Water action with different origins and shapes acting on construction elements is the origin of most degradations in heritage buildings. The presence of water is not considered a disease itself, although it can be considered as such. Water from different sources causes the degradation of a masonry making the walls vulnerable to its action. First of all, the exterior coatings are affected, next is the mortar and the brick element which may lead to a loss of structural strength. Heritage buildings can be affected by humidity in different areas, by different factors, such as vapor diffusion, hygroscopic humidity, water condensation, rainfalls, surface water, infiltration water with diluted salts and soil humidity.

Water accessibility in the structure of a material refers mainly to the absorption of water by capillarity, usually due to material porosity. Porous materials are almost invariably permeable and water under the many forms it can penetrate the pores of the material and enter its structure through them. Due to the porosity of bricks characteristic to heritage buildings, water is absorbed spontaneously by capillary forces and once absorbed it migrates freely under the same forces action. Porosity is a fundamental property of brick which can influence its durability. Many processes of alteration bring an increase in porosity and so the water accessibility inside the material has more important values. Another important test to measure the water accessibility is by water absorption under low pressure. This test is important to characterize the intact material and, by means of comparison, to assess the superficial modifications of alterations that modify the water absorption at surface level. Water mainly penetrates into materials by absorption and most damages are related with the presence of water. The objective was to apply these tests on the buildings materials in order to assess water accessibility on bricks from heritage buildings at a certain time in order to be able to characterize them. Our primary interest is to determine water accessibility in bricks characteristic to heritage buildings like „Saints Apostels Petru and Pavel" Cathedral in Constanta.

2. EXPERIMENT DESCRIPTION

The tests to determine accessibility of water have been conducted on 10 unaltered samples, taken from the heritage building structure. The samples do not need to have a regular form but if it's possible it is preferred that they do and also to have almost the same dimensions, usually prisms of 4 cm or 5 cm section and a length of 12

B. D. Pericleani is with Ovidius University of Constanta, Faculty of Civil Engineeering, Bd. Mamaia, no. 124, 900356-Constanta, Romania (phone: +40-241-619040; fax: +40-241-618372; e-mail: pericleanu_dan@yahoo.com).

M. Drăgoi is with Ovidius University of Constanta, Faculty of Civil Engineeering, . Mamaia, no. 124, 900356-Constanta, Romania (e-mail: dragoi.mihaela@gmail.com).

ISSN-1584-5990

cm or 15 cm, because they offer a better homogeneity between the samples, especially in terms of degree of alteration, but their volume must be at least 25 cm^3. The samples to be tested have to be as homogeneous as possible, so they were taken from the same area of the monument and were cut in a way that one face of the cube is the same face as the one previously exposed on site.

The samples were dried till constant mass in a ventilated oven (60 ± 5)ºC according to RILEM laboratories recommendations [3] and then cooled to the ambient temperature in a dry environment. Constant mass M_1 (g) is reached when the difference between two successive weighing at a 24 hours interval is not greater than 0.1% of the samples mass, determined with an accuracy of 0.1%. After systematic weighing we concluded that the constant mass M_1 (g) was reached after 72 hours, and this is the time that we considered as the reference time for drying the samples for the tests.

Table. 1. Constant dry mass determination

Samples	**Samples mass (g), at different intervals:**				**Constant dry mass of the sample after 72 hours:**
	24ore	**48ore**	**72ore**	**96ore**	**$M_{1\,(g)}$**
1	1557,1	1546,8	1542,4	1542,4	1542,4
2	1584,5	1573,2	1567,8	1567,8	1567,8
3	1560,8	1550,7	1546,7	1546,7	1546,7
4	1563,5	1553,9	1549,1	1549,1	1549,1
5	1572,2	1561,4	1557,9	1557,9	1557,9
6	1559,6	1548,5	1543,1	1543,1	1543,1
7	1568,4	1556,9	1552,8	1552,8	1552,8
8	1565,1	1554,1	1549,2	1549,2	1549,2
9	1571,5	1561,3	1555,9	1555,9	1555,9
10	1578,4	1566,7	1563,2	1563,2	1563,2

After reaching dry constant mass, the samples were placed in a vacuum vessel. The pressure in the vessel was decreased gradually to 2.667 Pa (20 mm Hg). This pressure is maintained constant for 24 hours to remove the air contained in the pores of the samples. After 24 hours the vessel is slowly filled with water at 15 – 20 ºC, so that the samples will be completely immersed in water in more than 15 minutes. The vacuum is maintained during this process and for 24 hours after.

Fig. 1. Equipment used during the porosity test

After this, the samples are left under water for another 24 hours at atmospheric pressure and then they are weighted by hydrostatic weight M_2. The sample is then wiped with a damp cloth and is weighted again in the opened air (M_3). To make this measurement we have to use an instrument with an accuracy of 0.1%.

Table. 2. Determination of masses M_1, M_2, M_3..

Samples	Dried mass M_1 (g)	Hydrostatic mass M_2 (g)	Open air mass M_3 (g)	Porosity (%)
1	1542,4	949,9	1857,9	34,75
2	1567,8	974,3	1884,3	34,78
3	1546,7	955,2	1863,9	34,91
4	1549,1	956,4	1862,4	34,58
5	1557,9	965,1	1874,1	34,79
6	1543,1	950,9	1858,5	34,75
7	1552,8	962,3	1872,3	35,11
8	1549,2	954,7	1861,6	34,45
9	1555,9	963,9	1871,1	34,74
10	1563,2	970,1	1877,0	34,60

Accessibility of water within materials depends also on their ability to absorb water under low pressure. When a column of water is applied on a porous material it penetrates the material. The amount of water absorbed after a defined period of time is a characteristic of that material. This test is used to measure the quantity of water absorbed by a porous material under low pressure after a certain period of time. Measuring the absorption of water under low pressure is useful in experimental laboratory works and in situ:

- to characterize the intact material and in comparison to assess the changes or alterations which modify the absorption of water at the material surface level;
- to analyze the effectiveness of the treatments by impregnation or of the treatments that alters the permeability of the surface (waterproofing, water repellent products, etc);
- to characterize the effects of the climatic actions on the material surface;
- to determine the depth of the water repellent treatments.

The equipment is very simple and it exists in two forms, depending on the position of the surface to be tested, vertical or horizontal. The instrument used for this test is a cylindrical tube that has a lower end section of 5.7 cm^2 which is applied to the material. The vertical tube is graduated from 4 cm^3 in the bottom part till 0 cm^3 in the upper part and each area is divided into units of 0.1 cm^3.

Fig. 2. Karsten tube characteristics

On the lower section of the tube mastic is applied to ensure the tightness connection between the tube and the surface material and then by pressing the tube onto the surface tested the tube is fixed. By the upper part of the tube water is poured until it reaches the graduation 0 cm^3 and then you start registering the amount of water

absorbed by the sample at different time intervals. Readings will be made directly on the scale of the tube at different time intervals characteristic to the type of the tested material: 2, 3, 5, 10, 15, 30 and 60 minutes.

Table. 3. Determination of water absorption under low pressure

Time (min)	Amount of water absorbed (cm^3) on each sample									
	1	**2**	**3**	**4**	**5**	**6**	**7**	**8**	**9**	**10**
2	0,175	0,210	0,300	0,325	0,250	0,380	0,190	0,190	0,355	0,190
3	0,450	0,515	0,710	0,750	0,625	0,760	0,425	0,480	0,680	0,475
5	0,675	0,865	1,075	1,075	0,975	1,570	0,550	0,795	1,025	0,660
10	1,150	1,590	1,800	1,700	1,650	1,650	1,200	1,520	1,855	1,240
15	1,575	2,350	2,450	2,225	2,300	2,510	1,525	2,380	2,435	1,600
30	2,125	3,220	3,275	2,950	3,200	3,220	2,790	3,190	3,260	2,240
45	2,750	3,640	3,850	3,410	3,800	3,755	3,240	3,675	3,635	3,210
60	3,450			3,700			3,625	3,755		3,620

Another test used to reveal the accessibility of water in bricks is absorption of water by capillarity. To reduce the absorption by the four lateral surfaces the test is performed in a saturated atmosphere obtained by using a cap to cover the tray used for this test. On the bottom of a tray two glass rods were fixed. On the samples is marked a 2 mm line in the bottom part that represents the water level on the sample. The tray is filled with water until the water level reaches the marked line and during the test the water cannot go beneath this level (if it's necessary to complete the amount of water it can be done during the test).

A timer has to be used to monitor the time. The samples are placed in the water so that no air bubbles enter the bottom of the samples. The tray is covered with a plastic cap so that the experiment is not influenced by any heat source that will facilitate the evaporation of the water. The water level is measured on each of the four sides of the samples at certain intervals of time. The samples are removed from the tray at due time, wiped with a damp cloth and weighted and then the water level is measured on all four lateral sides. In the first 30 minutes the samples are weighted more often, at short intervals of time, after this initial period the samples will be weighted every 1 hour till 6h and then each 24h. We must observe with great care when the water level reaches the high rate and weight them often and carefully to determine the experimental capillarity coefficient.

3. RESULTS AND SIGNIFICANCES

Porosity accessible to water is expressed as a percentage of bulk volume and it is calculated using the following formula:

$\frac{M_3 - M_1}{M_3 - M_2} \cdot 100$ [%] where:

M_1 – mass of the dried sample;
M_2 – mass of the saturated sample with water under vacuum, weighted in water;
M_3 – mass of the saturated sample with water under vacuum, weighted in the air.

Table. 4. Determination of porosity for each sample tested

	Samples									
	1	**2**	**3**	**4**	**5**	**6**	**7**	**8**	**9**	**10**
Porosity (%)	34,75	34,78	34,91	34,58	34,79	34,75	35,11	34,45	34,74	34,60

The results can be expressed in an absorption graph Fig. 3. in which on the vertical axis is the volume of water absorbed by the material in cm^3 and on the horizontal axis the time, in minutes. The amount of water absorbed

by each sample M_i on unit surface area at the end of the time interval t_i is calculated with the following expression:

$$M_i = \frac{m_i - M_1}{S}$$

where:
m_i – the mass of the sample at the end of a time interval t_i [g];
M_1 – mass of the dried sample at the beginning of the test [g];
S – the surface of the sample in contact with the water [cm^2].

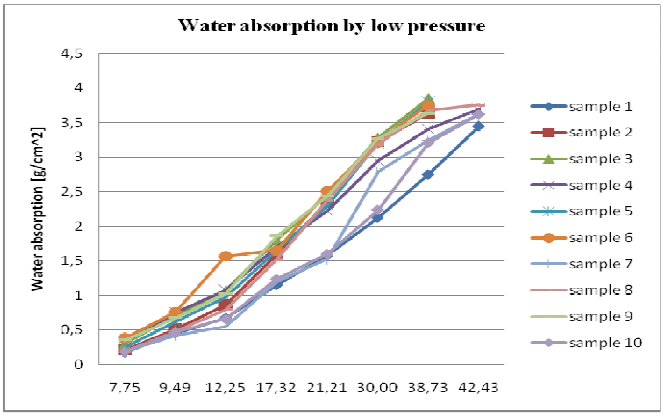

Fig. 3. Water absorption by low pressure results

With the results registered we can constitute the capillarity absorption curve that expresses the amount of water absorbed per unit area according to the square root of the time. This curve shows in general an initial linear portion and then tends asymptotically to a maximum amount absorbed. The capillarity absorption coefficient corresponds to the slope of the initial section and can be expressed in $[g \cdot cm^{-2} \cdot s^{-0.5}]$.

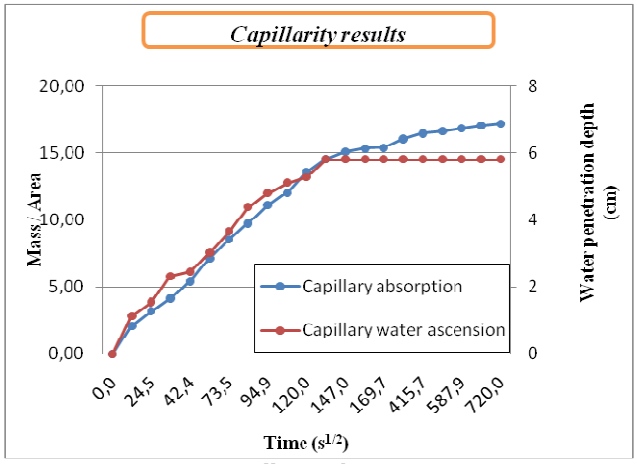

Fig. 4. Capillarity absorption

4. CONCLUSIONS

During the research were conducted laboratory tests to characterize the material specific to the resistance structure of the cathedral in Constanta in terms of water accessibility because water is one of the most important factors that can lead to deterioration of the monument.

The porosity tests showed an average of 34.75%. The value obtained is quite high but very close to that of the existing masonry mortar which leads to a behavior of the masonry as a homogeneous material, susceptible to penetrate easily into the material.

The capacity of a material to absorb water inside its structure was also assessed by water absorption at low pressure. This test simulates what happens with a film of water entering the material forced by wind pressure or capillarity suction. Test results show that half the samples have absorbed 4 cm^3 of water in about 50 minutes and the other half in a little bit over one hour. So we can say that the material has a pretty good capacity to absorb water at low pressure in a relatively short time comparable with the time needed for a mortar to absorb the same amount of water and this is why it's surface will have to be very well protected.

Water absorption coefficient by capillarity is experimentally determined and has a value of 0.110 $kg \cdot m^{-2} \cdot s^{-0.5}$. The values presented in Fig. 4. are average values. Water absorption by capillarity is an important element for the characterization of an unsaturated porous medium in which the water and air coexist. It is found that the dimension of the pores makes a significant difference. Water ascension in the material analyzed is performed in two phases – in the first phase is faster and this can be seen in the data recorded during the tests when the water enters the free pores and then, in a second phase, water will dislodge the existing air from the pores and the increasing of the mass will be slower, so that the constant mass of the sample saturated with water is reached in 144 hours.

In the future we want to continue our research upon the materials characteristic to this monument and extend the research also on the mortar. One of the final main objectives of this study consists in recommending interventions measures that will not affect the internal structure of these materials – surface treatments – and that will help protect them from water actions. Because the monument that is considered has an important heritage value, the study aims to propose an maintenance plan which will contain also the repeating of these tests after certain intervals of time in order to assess the accessibility of water during time and to verify the durability of the treatments applied in order to be able to act in time if deficiencies are encountered.

5. ACKNOWLEDGMENTS

The authors would like to thank professors: Fernando Branco, João Gomes Ferreira, Ana Paula Pinto and Grãmescu Ana Maria.

6. REFERENCES

[1] L. Binda, T. Squarcina, R.P.J. van Hees, "*Determination of moisture content in masonry materials: calibration of some direct methods*", Proceedings 8th International Congress on Deterioration and Conservation of Stone, Berlin, 1996, pag 423 – 435;

[2] NEN 2778, "*Moisture control in buildings. Determination methods*", Netherlands Standard, Nederlands Normalisatie Institut, Delft, 1991;

[3] RILEM, Test no. II.4,"*Water absorption under low pressure (pipe method)*", Paris, 1987.

Ovidius University Annals Series: Civil Engineering, Issue14, October 2012

Water – a key factor in heritage buildings chromatics

Bucur Dan Pericleanu, Mihaela Drăgoi

Abstract – **In south – east of Romania, the annual days with precipitation totals in general between 40 – 70 days per year. This leads to the idea that 40 – 70 days annually the heritage buildings are in a state of nonstructural degradation. Water coming from rainfall is contributing to the nonstructural degradation of heritage buildings by affecting the visual appearance, by modifying the chromatics of the exterior constitutive materials. The study is trying to show how water, in different percentages, is a key factor in chromatic changing of heritage buildings, affecting their color saturation and hue.**

Keywords – **Brick, chrome, heritage buildings, water.**

1. INTRODUCTION

Heritage buildings in Romania are defined as immovable property of the Romanian state, situated in the country or abroad, significant for the national and international history, culture and civilization. The protection of these buildings is represented by all scientific measures designed to ensure the identification, research, inventory, classification, tracking and putting them into value.

Is a well known fact that water, especially the one that is coming from rainfall, leads to a nonstructural and also a structural degradation in heritage buildings. One of the most common nonstructural degradation caused by water is the degradation of the visual and chromatic aspect of these monuments. Rainfall water, in contact with the constituent materials of the buildings, leads to their exterior chromatic change, usually by closing their original color.

Normally, in Romania, the precipitations are moderate and fall with amounts of water ranging from 400 l / year in Danube Delta to 1400 l / year in the mountains area. The average annual rainfall throughout the country is 637 l / year. Despite the fact that Dobrogea usually has the lowest amounts of precipitations during the year, at Letea rainfall station in 1926 fell 600 l / m^2. A statistic shows that the maximum annual number of days with precipitation totals from 100 – 140 in mountains areas, from 60 – 100 in hilly areas and from 40 – 70 in the plain areas. Normally, the largest amounts of precipitation in Romania fall in May and June, when the atmospheric circulation and weather conditions allow rapid development of the vertical cloud formations. According to the National Institute of Statistics, between 1901 – 2001, the average rainfall in June has exceeded 70 l / m^2 in several areas of the country and reached 140,1 l / m^2 in the mountains area (Omu). Most precipitations fall in Romania from December to June. In the very rainy years, the maximum number of rainy days per month totals between 14 – 30 days in the mountains areas, from 15 – 25 in the hilly areas and 14 – 20 in the plain areas, which means that in the mountains, were registered periods when it rained for a month almost every day. In this study we aim to demonstrate how the water leads to changes in initial chromatic of bricks characteristic to heritage buildings and produces a characteristic nonstructural degradation regarding the visual aspect, if they are used at the façade.

The color of a brick is influenced by the chemical content of minerals of the constituent material, by the combustion temperature and furnace atmosphere. For example, the pink brick has a higher content of iron, the white one and the yellow one has a higher content of lime. As temperature increase in the furnace, most bricks

B. D. Pericleani is with Ovidius University of Constanta, Faculty of Civil Engineeering, Bd. Mamaia, no. 124, 900356-Constanta, Romania (phone: +40-241-619040; fax: +40-241-618372; e-mail: pericleanu_dan@yahoo.com).

M. Drăgoi is with Ovidius University of Constanta, Faculty of Civil Engineeering, . Mamaia, no. 124, 900356-Constanta, Romania (e-mail: dragoi.mihaela@gmail.com).

ISSN-1584-5990

burn in shades of red (light red to dark red), purple and even brown. Calcium silicate bricks have a wider range of shades and colors, depending on the colorants used. Sometimes a specific color or shade of the brick may reflect their origin, such as London bricks or the specific one called "The white brick of Cambridgeshire".

2. EXPERIMENT DESCRIPTION

The bricks samples for this study were from Dobrogea area, from the „Saints Apostels Petru and Pavel" Cathedral in Constanta, where a total of six samples were taken and the tests were conducted only on the faces exposed in situ. The chromatic characterization of the bricks is made in a quantitative manner by using a spectro-colorimeter. The equipment and principles of methodology adopted in this study are based on the ISO standard - ISO 11664-4:2008 – which specifies the method of calculating the coordinates of the CIE 1976 L*a*b* color space including correlations of lightness, chrome and hue. It includes two methods for calculating Euclidean distances in this space to represent the perceived magnitude of color differences. ISO 11664-4:2008 is applicable to tristimulus values calculated using color-matching functions of the CIE 1931 standard colorimetric system or the CIE 1964 standard colorimetric system. ISO 11664-4:2008 may be used for the specification of color stimuli perceived as belonging to a reflecting or transmitting object, where a three-dimensional space more uniform than tristimulus space is required. It does not apply to color stimuli perceived as belonging to an area that appears to be emitting light as a primary light source, or that appears to be specularly reflecting such light. ISO 11664-4:2008 does apply to self-luminous displays, like cathode ray tubes, if they are being used to simulate reflecting or transmitting objects and if the stimuli are appropriately normalized. The methods established in this standard are designed for monochromatic surfaces, so it was necessary to adapt, especially in terms of area reserved for measuring the number of readings taken at each determination.

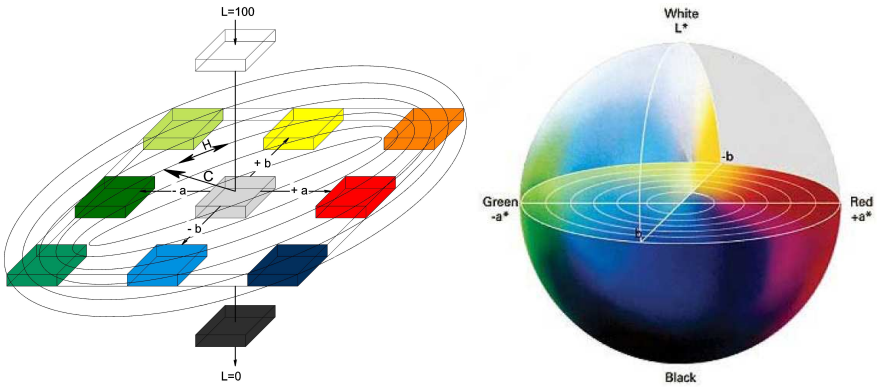

Fig. 1. CIELAB System

The color determination was achieved using the chromaticity coordinates of the reference color system CIE 1931, in the uniform chromatic space CIE 1976. The color was determined using CIELAB system determining the chromatic coordinates L^*, a^* and b^*. In this system, the color stimulation is represented in a three-dimensional space in which the vertical axis 0-Z coordinate measures the lightness L ranging from 0 which signifies the darkness and 100 which signifies the lightness, the variations of the colors are obtained in X-Y plane. Thus, in the X-Y plane are represented the coordinates: coordinate a – that measures the position on the green – red axis and the coordinate b – that measures the variations on the blue – yellow axis. In quantifying the color we used a colorimeter with a light source that emits radiation in the spectrum used and a spectrophotometer to analyze and measures the light reflected from the surface tested. We used a CANGGUA NG WSD-3A Tristimulus colorimeter model with a measuring window of 2 cm diameter and the ability to automatically store data and processing results.

Fig. 2. Equipment used during the test

Selection of the light used to quantify the color of an object must be in accordance with the type of the light the object will be observed. Light source used was set at D65 brightness because it represents better the sunlight and the values were obtained using a standard observer, positioned at 10 degrees from a horizontal plane. The samples used are not homogeneous from the color point of view and because of this a number of readings were made on different parts of the same surface by which we could determine the color of the surface, using an average of the readings.

Although average values cannot illustrate the chromatic aspects of a heterogeneous material surface, these values allow an evaluation and a rapid comparison between two different surfaces. Therefore, color evaluation of a surface material is done by measuring the color coordinates L^*, a^* and b^* of the CIELAB system and complementary to the chromatic values it can be determined:

- color saturation or chrome – C_{ab}, that represents the resultant of the color components coordinates a^* and b^*;

$$C_{ab} = \sqrt{a^2 + b^2} \tag{1}$$

- the hue angle – H_{ab} that can take values between 0^0 and 360^0;

$$H_{ab} = arctg(b/a) \tag{2}$$

It can also determine the color differences of the analyzed samples towards a color taking as a reference color.

- color difference ΔE_{ab} represents the geometrical distance between the corresponding points with the coordinates L_1, a_1, b_1 and respectively L_2, a_2, b_2 corresponding to analyzed sample 1 and reference sample 2.

$$\Delta E_{ab} = \sqrt{\left[(\Delta L)^2 + (\Delta a)^2 + (\Delta b)^2\right]} \tag{3}$$

- total color difference ΔE_{ab} it can be decomposed into components that highlights the difference in lightness, the difference of chrome and the hue difference.

$$\Delta E_{ab} = \sqrt{\left[(\Delta L)^2 + (\Delta C_{ab})^2 + (\Delta H_{ab})^2\right]} \tag{4}$$

In the first phase, the coordinates of the colors L^*, a^*, b^* were determined on three samples, previously dried until constant mass in an ventilated oven. On each sample were selected three positions and in each position a minimum of two readings were made. These samples were considered the reference samples during the study.

Table. 1. Color coordinates determination

Sample	Mass	Area	Readings	L*	a*	b*
brick C1	578,00g	pos 1	1	59,49	14,09	24,69
			2	59,49	14,02	24,70
			3	59,48	13,79	24,17
		pos 2	1	59,53	13,73	24,13
			2	59,53	14,33	24,14
		pos 3	1	59,60	14,18	23,44
			2	59,60	14,04	23,50
brick C2	665,30g	pos 1	1	56,13	15,87	27,12
			2	56,14	15,81	27,15
			3	56,12	15,79	27,09
		pos 2	1	55,89	16,24	28,12
			2	55,89	16,16	28,14
		pos 3	1	56,13	16,00	28,09
			2	56,13	15,98	28,11
brick C3	605,24g	pos 1	1	57,36	15,12	26,09
			2	57,38	15,23	26,07
		pos 2	1	57,27	15,01	26,21
			2	57,27	15,11	26,24
		pos 3	1	57,29	15,21	25,43
			2	57,30	15,32	25,48

After testing the reference samples it was possible to determine also the maximum percentage of water that can be absorbed by these samples. From the six samples taken, three of them were used for the porosity test during which we could determine the dried mass of the sample, the saturated mass of the sample by hydrostatic weighing and at atmospheric pressure. The average of the results was used to determine the average percentage of water that can exist in these samples.

On the three previous dried tested samples it was applied by brushing a quantity of water that equals 10% of the average percentage of water and then it was determined again the color coordinates L^*, a^* and b^*.

Table. 2. Determination of color coordinates and saturation for the samples with 10% water content

Sample	Mass	Area	Readings	L*	a*	b*
brick C1$^{10\%}$	589,79g	pos 1	1	49,27	23,59	27,85
			2	49,27	23,40	28,85
			3	49,29	23,26	28,22
		pos 2	1	49,27	23,49	27,72
			2	49,33	23,25	28,10
		pos 3	1	47,88	24,31	28,66
			2	47,94	24,16	28,62
brick C2$^{10\%}$	678,87g	pos 1	1	45,45	25,25	28,67
			2	45,53	25,18	28,31
			3	45,57	25,2	28,29
		pos 2	1	44,32	25,28	28,7
			2	44,27	25,34	27,66

		pos 3	1	44,60	25,51	28,53
			2	44,52	25,49	27,47
brick C3$^{10\%}$	617,59g	pos 1	1	44,42	24,12	27,96
			2	44,44	24,18	28,04
		pos 2	1	44,45	24,18	28,03
			2	45,05	23,88	27,53
		pos 3	1	44,41	24,17	28,07
			2	44,46	24,16	28,14

Using the same samples, also by brushing it was applied a quantity of water that equals 20% of the average percentage of water and we determined the color coordinates L^*, a^*, b^* again.

Table. 3. Determination of color coordinates and saturation for the samples with 20% water content

Sample	Mass	Area	Readings	L*	a*	b*
brick C1$^{20\%}$	692,47g	pos 1	1	44,16	24,77	28,87
			2	44,07	24,83	28,21
		pos 2	1	44,52	24,06	28,52
			2	44,49	24,13	28,49
		pos 3	1	45,34	24,75	28,49
			2	44,34	24,82	27,53
brick C2$^{20\%}$	665,30g	pos 1	1	42,60	25,63	28,67
			2	42,61	25,58	28,84
		pos 2	1	41,68	25,93	28,71
			2	41,75	25,91	28,61
		pos 3	1	43,04	25,83	28,11
			2	43,08	25,66	28,26
brick C3$^{20\%}$	629,94g	pos 1	1	45,81	25,17	29,20
			2	45,81	25,22	29,28
		pos 2	1	41,27	26,02	29,94
			2	41,28	26,93	29,01
		pos 3	1	44,34	26,67	29,52
			2	44,34	26,64	29,60

3. RESULTS AND SIGNIFICANCES

From the readings made resulted the color saturation, hue angle and chrome difference presented in the table below, the differences between these characteristics being represented in the graph Fig. 3.

Table. 4. Color coordinates determination and saturation for the samples with 20% water content

Sample	C_{ab}*	H_{ab}*	ΔE_{ab}*
brick C1	27,89	1,04	
brick C2	31,96	1,04	
brick C3	30,03	1,04	
brick C1$^{10\%}$	36,86	0,87	14,93
brick C2$^{10\%}$	37,92	0,84	14,97
brick C3$^{10\%}$	36,92	0,86	15,72
brick C1$^{20\%}$	37,51	0,85	18,85
brick C2$^{20\%}$	38,44	0,83	16,77

brick C3$^{20\%}$	39,33	0,84	17,73

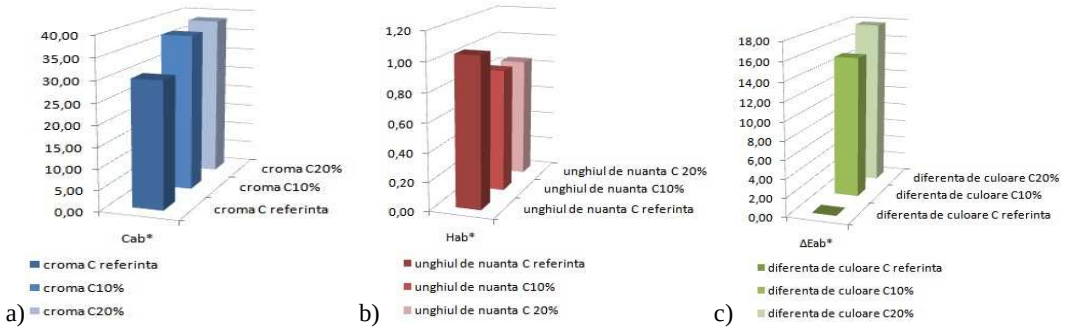

a) b) c)

Fig. 3. a) lightness difference, b) hue angle difference, c) chrome difference.

a) b) c)

Fig. 4. a) chromatic of the dried sample, b) chromatic of the sample with 10% water, c) chromatic of the sample with 20% water.

4. CONCLUSIONS

The number of mediations conducted depends on the surface that needs to be characterized and its color homogeneity, but also on the objectives that the mediation has. From the readings made, we can conclude that the samples used don't have a homogeneous color, but we could characterize the color of the material using an average of the readings. Although the average values cannot illustrate the chromatic aspects of a material with a heterogeneous surface, they do allow an evaluation and a rapid comparison between two different surfaces. Considering the weather statistics we can say that the water coming from rainfall has the tendency to degrade in a nonstructural way the brick façade of the heritage buildings, by changing the initial chromatics.

5. ACKNOWLEDGMENTS

The authors would like to thank professors: Fernando Branco, João Gomes Ferreira, Ana Paula Pinto and Grãmescu Ana Maria.

6. REFERENCES

[1] *Evaluation of performance of surface treatments for the conservation of historic brick masonry – Protection and conservation of the European cultural heritage*, Research report no. 7, ISSN 1018-5593, Office for official Publications of the European Communities,1998
[2] Costa, Jose Manuel Aguiar Portela da, Cor e cidade istorica: estudos cromáticos e conservação do patrimonio, Porto 2002, ISBN 972-9483-47-7
[3] http://meteoplus.antena3.ro/meteo-stiri/studiu-
[4] http://www.cs.ubbcluj.ro/~per/C9%20Pi/Prel_Img%20C9.pdf

The effect of mooring lines on vessels oscillation period

Mirela Popa, Radu George Joavină

***Abstract* – A harbor is a sheltered part of a body of water deep enough to provide anchorage and refuge for ships and a place where commercial or other activities can develop. Is of great importance for the moored vessels to evaluate the oscillation period - depending on vessel displacement, number, type and position of the mooring lines. The resonance between the natural oscillation of the vessel in cargo or bunkering operations and the waves, stationary or not, with unexpected and high surge displacement, can lead to pollution or even greater accidents if chemical or LPG – LNG operations are involved.**

The purpose of the present paper is to evaluate the changes in surge natural oscillations period of moored vessels for different scenarios.

***Keywords* – line tension, mooring lines, length lines, natural surge period, ship mass**

1. INTRODUCTION ABOUT MOORING VESSELS

Ships respond to external actions with motions of tri axial translations and spins.

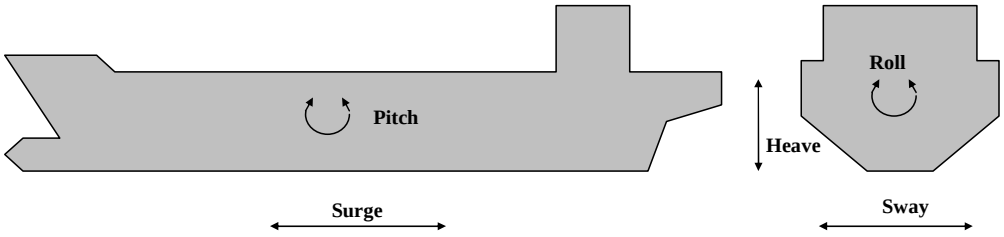

Fig 1 Definition of vessel motions

Safety admissible values of translations and spins depend on ship's type and characteristics (equipment type etc). For example, recommended gas tankers surge is about 2m, sway 2m, heave 1m, yaw, roll and pitch 2^o; for oil tankers, surge is about 3m, sway 3m, heave 1m, yaw, roll and pitch 2^o; for bulk carriers with crane equipment surge is about 2m, sway 1m, heave 1m, yaw 2^o, roll 2^o and pitch 2^o and for the same vessels with conveyor belt loading equipment surge is about 5m, sway 2,5m, heave 1m, yaw 3^o, roll 2^o and pitch 2^o [2].

The mooring purpose is to hold a ship safely alongside a berth, dock or other ship for operations such as loading and discharging, maintenance and repairs, salvage or lay up (ships in an inactive status).

Manuscript received July 27, 2012.

Phd eng. Mirela Popa is with Ovidius University of Constanta, Bd. Mamaia nr. 124, 900356-Constanta, Romania (corresponding author to e-mail: mpopa@univ-ovidius.ro).

Phd eng. Radu George Joavină is with Seatrans, Bergen, Norwey; as Ch. Off. (e-mail: raduj68@yahoo.com).

ISSN-1584-5990

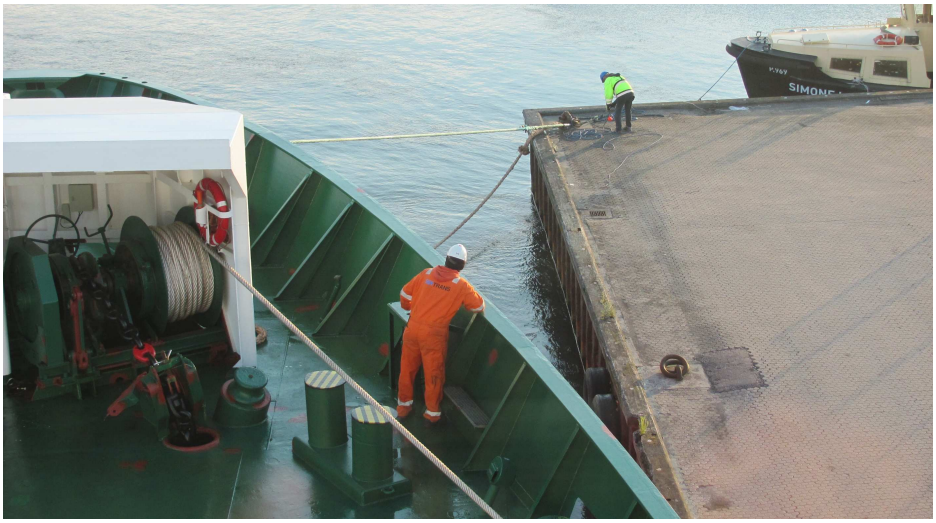

Fig. 2 Mooring operations in Kobenhavn port

The most used mooring pattern is presented in Fig. 3.

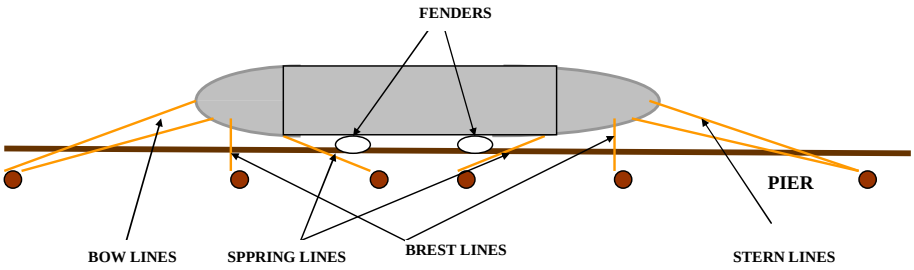

Fig. 3 Mooring pattern

Anyway, this is not the only one. There are many mooring configurations, depending on the berth and ships size, shape, equipment and requirements. For example in some of New Zeeland harbours, for space economy reasons, the position of springs is changed with the one of the stern and bow lines.

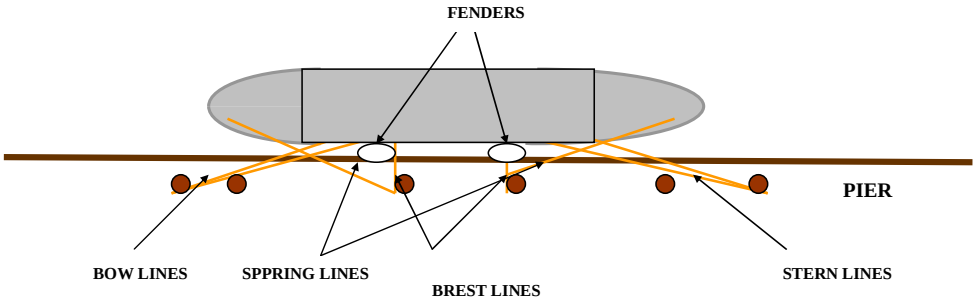

Fig. 4 Modified mooring pattern

Environmental forces acting on the ship produce the mooring load.

a. Diffraction at a harbor entrance. The main process affecting wave conditions in small harbors is wave diffraction in the two main types: wave diffraction past the breakwater head (for one long breakwater) and wave diffraction through a relatively small harbor entrance between breakwaters.

The wave orientations and heights are significantly altered when waves propagate past the end of a breakwater, the wave crests spreading into the shadow zone of the breakwater.

b. Harbor oscillations are initiated by forcing through the harbor entrance and are long-period standing wave oscillations with typical periods between 30 sec and 10 min [5], with vertical motions generally small, but with horizontal motions that can be large. The basin size, shape, and depth determine the waves parameters. The phenomenon, referred as surging or seiching, can induce harbor resonance when the period coincides with a natural resonant period of the harbor.

The design-mooring load is derived from an algorithm that sums the combined forces of wind and current loads acting in the direction that produces the highest possible force against the ship structure pushing the ship in the direction away from the pier. The design-mooring load remains constant throughout the life of the ship.

For dynamical point of view a vessel moored is modeled as an oscillating single dynamic degree of freedom linear system with longitudinal movement - surge. The natural period of surge movement is an internal characteristic of the vessel, giving information regarding the amplification of the ship's response in resonance with an oscillatory phenomenon. The natural period is dependent on stiffness at the surge movement of the oscillating system formed by the ship rope-line connected to the jetty. Evaluation of the stiffness permits the horizontal displacement calculation, depending on the mooring load component on the same direction.

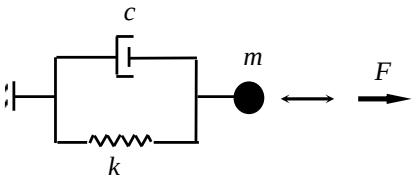

Fig. 5 Single freedom degree dynamic system

2. NATURAL SURGE PERIOD CALCULATION

As per each single dynamic degree of freedom mechanical system, angular frequency in absence of the dumping (which can be neglected in this particular case) is defined as:

$$\omega = \sqrt{\frac{k}{m}} \tag{1}$$

and the time interval required for a complete free oscillation, named natural period is:

$$T = \frac{2\pi}{\omega} = 2\pi\sqrt{\frac{m}{k}} \tag{2}$$

m - is the virtual mass of the vessel (ship's displacement + 15% due to the inertial effects of the water moved by her)

k - the effective elastic constant deduced only from the stiffness of stretched lines (k_n), [5]:

$$k = \sum_n k_n \sin(\theta_n)\cos(\varphi_n) \tag{3}$$

θ_n – horizontal angle between the line direction and the perpendicular on the vessel hull;

φ_n - vertical angle between the line direction and the perpendicular on the vessel deck;

k_n - individual stiffness of the stretched line defined as the ratio between the axial stress of the line and elongation (in numerical simulations realized with the CEDAS the axial stress was considered to be equal to the traction in bollard, estimated in compliance with the recommendations from the literature, according to the vessel displacement).

The elastic behavior of the line is very complex. A fiber line initially loaded to around 50% or more of mean breaking load will not return to its original length when unloaded. Under cyclic loading, force deformation relation will take a stable hysteretic loop with the relatively predictable elastic properties. Therefore Young's modulus cannot be accurately defined. For example, "nylon line exhibits stiffer behavior under cyclic loading, and greater elongation at a given load when wet than dry. The dynamic load elongation behavior of nylon line is dependent upon the initial tension and its magnitude in relation to the line's ultimate strength" [2]. Usually, the producers provide experimental curves, where the specific deformation, expressed as a percentage, is given according to the load (expressed as percentage from the capable axial stress).

Based on these considerations in CEDAS software rope elongation is evaluated as $\Delta l = \varepsilon \cdot l$ and percent elongation is obtained from charts provided by manufacturers, according percents of axial loading [5].

Assuming a linear behavior, given that the elongation is defined $\Delta l = \frac{N_n l}{EA}$, it follows that rope stiffness can be expressed according to its intrinsic characteristics, length and axial stiffness $k_n = \frac{EA}{l}$

3. CASE STUDY

Behavior of three different types of vessels of different size was studied: a chemical tanker Trans Emerald, a gas carrier Trans Catalonia and a OBO vessel Banastar.

Table 1

	Ship	Stern line	Spring line	Bow line	GRT (tone)
A	Trans Emerald	2×30m	2×30m	2×30m	5815
A1			2×35m		
B	Trans Catalonia	3×40m	2×40m	3×40m	13005
C	Banastar	4×60m	4×40m	4×60m	38889

The module „Surging of a moored vessel" implemented in CEDAS software was used.

As input, line tension, ship mass, percent elongation, breaking strength, distance between deck and dock, angle of line to perpendicular breast line, line length and number of the lines are required.

The following cases of natural surge period dependence were studied:

a) draft variation during the loading operations for ships A and B (2 respective 3m), for constant values of line tension 250kN and percent elongation 8.7% (ships with auto-mooring system)

Table 2

	Ship A			Ship B		
D draft%	D draft m	Ship's weight (t)	T surge (s)	D draft (m)	Ship's weight (t)	T surge (s)
0%	Fully loaded ship 0	8650	37.78	0	19715	57.17
20%	-0.4	8083	36.53	0.6	18373	55.19
40%	-0.8	7516	35.24	1.2	17031	53.16
60%	-1.2	6949	33.90	1.8	15689	51.05
80%	-1.6	6382	32.50	2.4	14347	48.84
100%	Ship in ballast -2	5815	31.04	3	13005	46.54

In the next step was considered that if the line tension varies with ship displacement. the elongation should also change. In the linear elastic behavior of the line, elongation is determined according to axial load and tensille stiffness

$$\varepsilon = \frac{\Delta l}{l} \qquad \Delta l = \frac{Nl}{EA} \rightarrow \varepsilon = \frac{N}{EA} \tag{4}$$

The value of tensile stiffness for line of the ship A is EA=2045 kN, and for the ships B and C is EA=4090kN. The results for these case studies are summarized in Tab. 3 and plotted in Fig. 6

Table 3

	D draft%	0%	20%	40%	60%	80%	100%
Ship A	Ship's weight (t)	8650	8083	7516	6949	6382	5815
	Traction in bollard (kN)	273	262	250	239	227	216
	Elongation (%) for EA=2045 kN	13.3	12.8	12.2	11.7	11.1	10.6
	T surge A (s)	44.7	43.3	41.7	40.2	38.5	36.8
Ship B	Ship's weight (t)	19715	18373	17031	15689	14347	13005
	Traction in bollard (kN)	591.45	551.19	510.93	470.67	430.41	390.15
	Elongation (%) for EA=4090 kN	14.5	13.5	12.5	11.5	10.5	9.5
	T surge B (s)	47.9	46.3	44.57	42.77	40.9	38.91
Ship C	Ship's weight (t)	72562	65827	59093	52358	45624	38889
	Traction in bollard (kN)	890	863	836	809	771	726
	Elongation (%) for EA=4090kN	21.8	21.1	20.4	19.8	18.9	17.8
	T surge C (s)	84.72	80.63	76.35	72.03	67.34	62.25

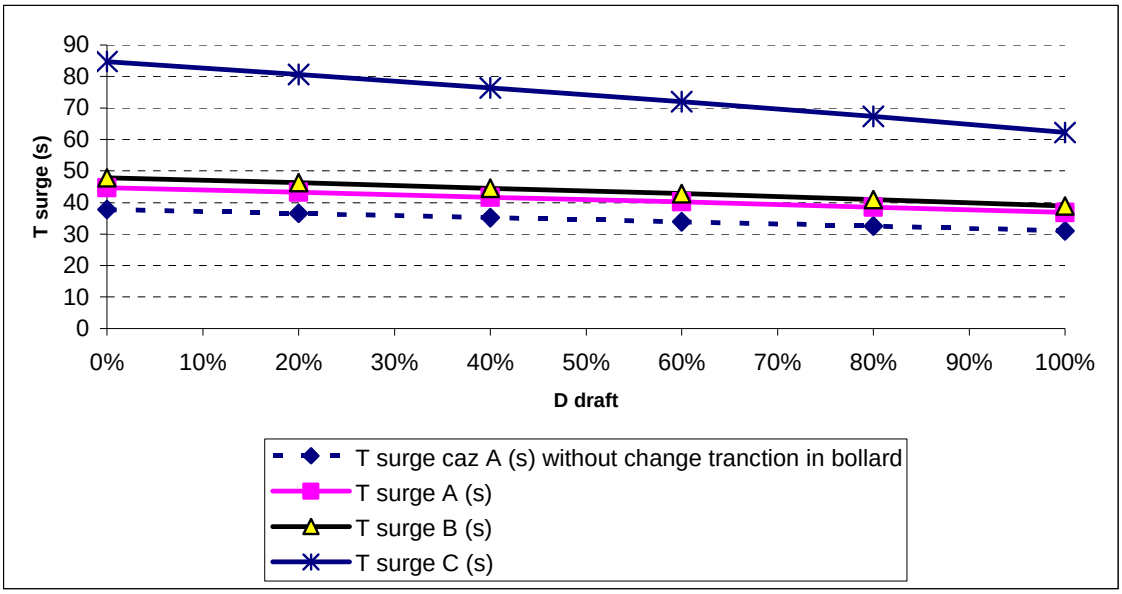

Fig. 6

It is observed a negative variation of 18 -18.5% (corresponding for loaded ship and respectively ballast ship) in the value of the surge period for vessels with auto-mooring system and also higher and quicker variation (showed in the graphic angle) reported to the draft variation of the ship's C surge period – 36% - in comparison with A and B ships– 21.4% respective 22.8%

b) evaluation of the natural surge period behaviour in case of the line breaking. Full loaded and ballast condition were studied for ship A and ship C.

Table 4

		T surge (s) in case of one broken line	T surge (s) for normal mooring
Ship A loaded	broken bow line	48.86	44.7
	broken stern line	48.88	
	broken spring line	49.17	
Ship A ballast	broken bow line	40.27	36.8
	broken stern line	40.31	
	broken spring line	40.55	
Ship C loaded	broken bow line	87.83	84.72
	broken stern line	87.83	
	broken spring line	89.83	
Ship C ballast	broken bow line	64.53	62.25
	broken stern line	64.54	
	broken spring line	66.00	

There are small diferences between lines and spring breaking for the ship A (9.3-10%), as long as for ship C (Panamax size) the diference is noticeble (3.6-6%). Also a breaking line on vessel C has less effect on T- but this

is normal as long as the number of ropes is different, coresponding with the ship's size. The variation is almost the same for loaded and ballast conditions.

c) increase of the length of one of the ship's bow **line** for ship A for loaded and ballast state and the variation of the bow line and spring line for ship A in ballast condition.
Increased values of natural surge period have been reported to the value obtained for the line lengths of Tab. 1

Table 5

Length increasing of one bow line	Length variation [%]	Ballast ship		Loaded ship	
		T surge (s) increasing lenght BOW	Increasing T surge	T surge (s) increasing lenght BOW	Increasing Tsurge
31	3.33%	37.05	0.68%	44.9	0.45%
32	6.67%	37.23	1.17%	45.16	1.03%
33	10.00%	37.4	1.63%	45.37	1.50%
34	13.33%	37.5	1.90%	45.58	1.97%
35	16.67%	37.7	2.45%	45.77	2.39%
36	20.00%	37.9	2.99%	45.96	2.82%
39	30.00%	38.3	4.08%	46.47	3.96%
40	33.33%	38.4	4.35%	46.63	4.32%
45	50.00%	39.0	5.98%	47.34	5.91%
60	100.00%	40.2	9.24%	48.85	9.28%

The variation of T increase slowly up to aprox 9% on double length of the line. Even if T surge is increasing from ballast state to loaded state with 21 - 22%, the modification with the line length is almost the same for both scenarios. Also length variation of the line influence T a little more then spring length variation.

Table 6

Length increasing of line (%)	Ship A ballast increasing BOW line		Ship A1 ballast increasing BOW line		Ship A1 ballast increasing SPRING line	
	T surge (s) modified	Increasing T surge	T surge (s) modified	Increasing T surge	T surge (s) modified	Increasing T surge
3.33%	37.05	0.68%	37.94	0.56%	37.92	0.32%
6.67%	37.23	1.17%	38.14	1.09%	38.10	0.79%
10.00%	37.4	1.63%	38.33	1.59%	38.28	1.27%
13.33%	37.5	1.90%	38.51	2.07%	38.45	1.72%
16.67%	37.7	2.45%	38.68	2.52%	38.54	1.96%
20.00%	37.9	2.99%	38.85	2.97%	38.75	2.51%
30.00%	38.3	4.08%	39.31	4.19%	39.17	3.62%
33.33%	38.4	4.35%	39.45	4.56%	39.30	3.97%
50.00%	39	5.98%	40.08	6.23%	39.87	5.48%
100.00%	40.2	9.24%	41.44	9.83%	41.08	8.68%

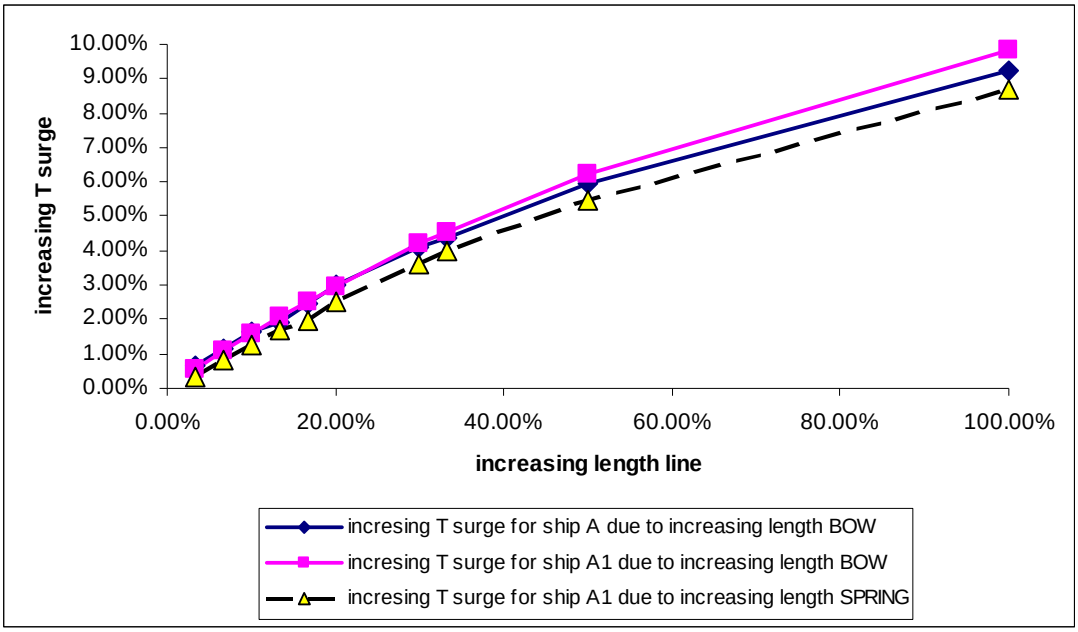

Fig. 7

d) **modification of the horizontal angle** between the line direction and the perpendicular on the vessel hull. Changing of the angle was studied for both spring and bow line was compared with the values given by the common situation (bow and stern orientation of 70^{o} and spring orientation of 85^{o}) and also with the situation when one line (bow or spring) is acting like breast.

Table 7

horizontal angle between the line direction and the ship's longitudinal axis	Ship A1 ballast -modified horizontal angle for BOW line			Ship A1 ballast -modified horizontal angle for SPRING line		
	T surge (s)	Changes of T surge – reference value = 90 deg	Changes of T surge – reference value for original line's orientation	T surge (s)	Changes of T surge – reference value = 90 deg	Changes of T surge – reference value for original line's orientation
90	37.07		-1.07%	37.45		-0.05%
110, 70	**37.47**	1.08%	0.00%	37.81	0.96%	0.91%
130, 60	38.72	4.45%	3.34%	38.98	4.09%	4.03%
150, 30	40.9	10.33%	9.15%	40.78	8.89%	8.83%
170, 10	44.15	19.10%	17.83%	43.51	16.18%	16.12%

As the Table 7 shows, the % changes in surge period values are double then in the case of line length modification. It leads to the conclusion that this is the most efficient way to change the moored ship period.

4. CONCLUSIONS

If resonant characteristic periods of moored vessels fall into the same range of periods as harbor oscillations, dangerous mooring conditions can be created.

Ships in ballast are sensitive on waves with lower periods then loaded ships where surge period increases.

Also small ships surge period is lower that bigger ones.

Generally, distance between bollards is 15-25m. It can be seen that the angle variation induces a higher difference in surge period. Obvious, the changing in one line position on a different bollard will also cumulate the effect of length variation.

When resonant oscillations appear in the harbor basin, the authors recommend the changing of lines position as long as spring lines should be always in tension and more difficult to change. Also the effect of changing the lines is slightly better that for springs.

In the unfortunate case of broken line not only the reconnecting of a new line should be taken into account but also the changing of the bollard where this new line is fastened.

Knowing of the surge period of the vessel toghether with the evaluation of harbor oscillations allow the crew to take a optimal decision regarding the mooring.

Fastening a line one bollard more forward or more aft can make the difference between a safe berthing or the unpleasant situation of broken mooring lines, delays of loading and discharging operations or even damage of port facilities or of the vessel.

REFERENCES

[1]. Bruun, P.- "Port Engineering", vol. 1, Gulf Publishing Comp., 1993
[2]. John Gaythwaite - Design Of Marine Facilities For The Berthing, Mooring, And Repair Of Vessels, ASCE Press, 2end edition
[3]. Ciortan R. –„Construcţii hidrotehnice portuare", Ed. Agir, Bucureşti, 2009
[4]. Berescu S. – "Caracteristici constructive dinamice ale acvatoriului Constanta", PHD thesis sustained in the Technical University of Cluj Napoca, Faculty of Civil Engineering
[5]. *** - EM 1110- 2-1100 Part II, 2002, Chapter 7 "Harbor hydrodinamics"
[6]. *** - EM 1110-2-1613 31 May 2006 Hydraulic Design of Deep-Draft Navigation Projects,
[7]. *** - S9086-TW-STM-010/CH-582R2 Naval Ships' Technical Manual Chapter 582 „Mooring and towing"
[8]. *** - Guidelines and Recommendations for the Safe Mooring of Large Ships at Piers and Sea Islands , Oil Companies International Marine Forum (OCIMF) Islands.

Issues related to the Adapting of Variable Operating Regime Pumping Plants by the use of Variable Speed Drives

Daniel Toma

***Abstract* – This paper describes some issues related to the opportunities for upgrading and modernizing a boost pumping station ("hydrophore") that is serving a district with high-rise apartment blocks. A topic of the discussion is focused on the implementation of variable speed pumps, by ensuring a control system based on static frequency converters. The final goals of such systems is to provide a continous correlation between the consumers' variable demands and the pumping's efficiency.**

***Keywords* – boost pump, power consumption efficiency, static frequency converters, variable speed**

1. INTRODUCTION

The pumps that operate on pressurized water networks (transport, distribution) are important power consumers. Hence, there is need to adapt their operating regime to the actual variable water demand (the consumers' water need). Thus, if the annual average costs are decreased to a minimum, the global efficiency of the water service will be increased. Considering this, in many cases there is need to modernize the boost pumps by means of which high-rise apartment blocks are supplied with water. In order to optimize the efficiency of pumps there is need to take measures on two directions:

- upgrading the pumping plants – that is, implementing adequate measures in order to soundly correlate the pumping capacities and the functional characteristics with the new demands of consumers;
- modernizing the equipment – this means the need to reach those technical performances that are comparable to those reached at a worldwide scale (especially in reference to power consumption).

During the last two decades, in order to ensure a correlation to the consumers' needs, the use of variable speed pump motors became frequent. Such variable speed is provided by means of static frequency converters (rated for adequate powers). This control system can be efficient only if the subsequent power savings (obtained on a normed time of pump operating) will cover at least the costs of such pump driving systems. The method for adapting the pump's operation regime to the consumers' demand (by a discontinous operating regime of one pump or by variable speed motor) has to be established on basis of the „global average efficiency" factor and also by taking into account the specific power consumption.

Manuscript received June 29, 2012.

Daniel Toma is with "Gheorghe Asachi" Technical University of Iasi, Faculty of Hydrotechnical Engineering, Geodesy and Environmental Engineering, 65 Prof. dr. docent Dimitrie Mangeron Street, 700050, Iasi, Romania (corresponding author to provide tel-fax office: +40232 270804, mobile phone: +40721 811373; e-mail: daniel_10hid@yahoo.com).

ISSN-1584-5990

2. THEORETICAL ASPECTS

Within the pumping systems that are fitted on water networks such a regulation can be obtained by varying the speed of the pump's rotor [1]. In order to achieve this there is need to adopt adjustable electric drives, that is variable speed controls for asynchronous motors. This is provided by static frequency converters.

When the pump rotor's speed is varying the pump's load characteristic $(H\sim Q)_P$, will change. Therefore the total pumping head may match exactly to the water network's characteristic $(H\sim Q)_R$.

When the pump's speed is decreasing the pump's characteristic will be modified in compliance to the transposition laws. The next elements will be obtained in plan *(Q,H)* (see **Fig. 1.**) [2]:

- a family of parallel load curves, of which ordinates get lower when sped gets lower. The load curves can be analytically expressed by a parabolic function (1):

$$H = A_0 n^2 + A_1 nQ + A_2 Q^2 \tag{1}$$

- an efficiency isolines network, representing parabola arcs that pass through origin, and on which are located the operating regimes obtained with the same efficiency, at different speeds. These iso-lines have a quadratic form (2):

$$H = k_{\eta x} Q^2 \tag{2}$$

where $k_{\eta x}$ is a parameter determined by values (Q_x, H_x) which are typical for a regime that, on a load curve corresponding to speed n_x, is achieved at indicated efficiency η_x:

$$k_{\eta x} = \frac{H_x}{Q_x^2} = \frac{H_o}{Q_o^2} \tag{3}$$

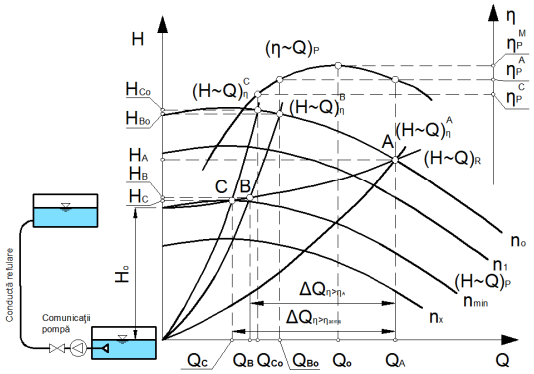

Fig. 1. Adapting a pump to variable working regimes using variable speed drives

In order to provide a normal working condition to the pump, the minimum flow that this pump can provide is Q_C (see **Fig. 1.**). The total pumping head H_C under which a Q_C is to be supplied is corresponding to the network characteristic $(H\sim Q)_R$. The pump's efficiency, in such an operating regime, corresponds to the $k_{\eta C}$ parameter iso-line, this being given by equation (4):

$$k_{\eta C} = \frac{H_C}{Q_C^2} \tag{4}$$

The value $k_{\eta C}$ is computed on the efficiency characteristic $(\eta \sim Q)_P$:

$$\eta_P = R_0 + R_1 Q + R_2 Q^2 \tag{5}$$

That corresponds to a flow Q_{Co}, provided by normal speed n_o within the similar working regime – located on the same iso-line, at the intersection of this one with the load characteristic $(H \sim Q)_P$ at n_o.

Taking into account the issues described above, the values that are defining the operational regime for the system made by pump and network are resulting as a solution of system (6) that includes the equations (1) and (2) with $k_{\eta x} = k_{\eta C}$ from (4):

$$\begin{cases} H_{Co} = A_0 n_o^2 + A_1 n_o Q_{Co} + A_2 Q_{Co}^2 \\ H_{Co} = k_{\eta C} Q_{Co}^2 \end{cases} \tag{6}$$

The resulting flow is given by (7):

$$Q_{Co} = \frac{-A_1 n_o + \sqrt{(-A_1 n_o)^2 - 4A_0 n_o^2 \left(A_2 - \frac{H_C}{Q_C^2}\right)}}{2\left(A_2 - \frac{H_C}{Q_C^2}\right)} \tag{7}$$

which will correspond to the efficiency resulted from (8):

$$\eta_P^C = \eta_P^{Co} = R_0 + R_1 Q_{Co} + R_2 Q_{Co}^2 \tag{8}$$

A frequently used solution for adapting pumps to variable network needs is to provide a discontinous operation of pumps and, in the same time, by compensating flows by using a tank fitted with a compressed air cushion („hydrophore"). In order to maintain the load H (in the network's origin) within the limits of the domain into which the pre-set distribution quality is ensured, when efficiency is high, and also to compensate (when pumps work intermittently) the gap between their delivered flows and the newtork demanded flow, the hydrophore has to allow the creation of a water serviceable volume V_u.

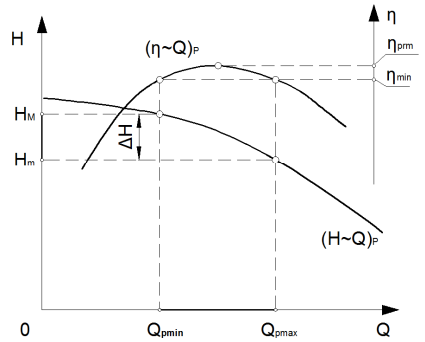

Fig. 2. Hydrophore: pump operating domain with an eff. close to max. eff. η_{prm}

Such volume must be between the minimum level (corresponding to the pressure needed for maintaining the minim load demanded by the network, H_m) and a maximum level which is accepted on basis of power consumption points of view, which ensures, within the network's origin, the maximum load considered the upper limit for the recommended operating domain ($H_M = H_m + \Delta H$) (see **Fig. 2.**) [3].

The serviceable volume V_u is determined from a condition that says that, in comparison to the pump's average flow Q_{pm} (at discontinous operating on the recommended (H_m , H_M)):

$$Q_{pm} = \frac{2}{3}\frac{Q(H_m)^2 + Q(H_m)Q(H_M) + Q(H_M)^2}{Q(H_m) + Q(H_M)} \tag{9}$$

the duration of filling cycle T_c, between two consecutive pump start-ups must be at least equal with a minimum admissible time T_e, imposed by the parameters of the electric driving system:

$$V_u \geq \frac{Q_{pm}T_c}{4} \quad , \quad T_c \geq T_e \tag{10}$$

If the hydrophore's functioning is assimilated to an iso-thermal process, the minimum air volume (needed at maximum pressure) results from:

$$V_a^m = V_u \frac{H_m + 10}{\Delta H} \tag{11}$$

thus:

$$V_H = V_o + V_u\left(1 + \frac{H_m + 10}{\Delta H}\right) \tag{12}$$

The reliability of a system adopted for pumps' variable regimes can be objectively assessed by defining the pumping's specific power consumption, for a period that has to be significant for the user, respectively by evaluating the pumping plant's global efficiency - within that period of time [4]. The plant's average global efficiency can be computed by dividing the hydraulic energy E_H supplied within the period of time ΔT, considered for the study, to the electric enery that is effectively consumed for pumping, in the same period, E_E:

$$\eta_{IP}^{fih} = E_H / E_E \tag{13}$$

The effective hydraulic energy E_H can be fairly estimated via the energy that is supplied by the plant in order to ensure the effective flow distributed by the served network Q_R, for the load [within reference section (O)] that corresponds to the optimal functioning of served system ($H_R = H_o = H_{Hm}$ - the minimum static load that is accepted by consumers). Within a period of time ΔT, the respective energy results from the equation (14):

$$E_H = 9{,}81 Q_R H_R \Delta T \tag{14}$$

If we represent the energy consumption involved in the water pumping, inside the studied installation, for the volume unit of distributed water, the energy specific consumption e_s is expressed in kWh/m^3 and is

determined by taking into account the energy consumed during the reference period and of the water volume distributed in the same period:

$$e_s = \frac{E_E}{W} = \frac{E_H}{\eta_{IP}^{fih} W} \quad , \qquad W = 3600 Q_R \Delta T \tag{15}$$

In the case of a variable speed pump the global average efficiency of the system made by the converter, the motor and the pump itself is conditioned by the efficiencies of each component (in various operating regimes):

$$\eta_{IP}^{t\,\mathrm{var}} = \eta_{csf} \eta_m \eta_P \tag{16}$$

where η_{csf} is the efficiency of the frequency converter, with values within the range between 0,90 and 0,96 [5].

3. CASE STUDY: THE „CODRESCU" PUMPING STATION (HYDROPHORE)

3.1. THE PUMPING STATION'S CURRENT CHARACTERISTICS AND THE RATING REGIME FOR THE UPGADING OF THE PUMPING STATION

This pumping station is located in „Punctul Termic Codrescu" (district heating distribution station) and ensures drinking water supply towards a city district made of high-rise apartment blocks (Groundfloor+10), by re-pumping water drawn from the Iasi City municipal network.

The current facility includes 1+1 LOTRU 100b pumps, featuring the next parameters: n = 3000 rpm, Q = 84 m^3/h, H = 45 mWC, η_P = 70,5 % and P = 18,5 kW. The pumps are drawing water from the City's network and the water is delivered towards the district network. The district pressure is maintained by means of a 2 m^3 hydrophore. The operating schedule is as it follows:

- between 05.00h and 22.00h operation ensured by hydrophore, with one pump controlled by means of a by-pass. The absorbed power is P_{AP} = 16,1 kW, the energy consumption is E = 274 kWh/zi, and the daily volume of pumped water reaches W = 250 m^3/day;
- between 22.00h and 05.00h, the facility works on the network (by-pass being fully opened), at a pressure of p = 2,2...3,0 bar.

According to these parameters, for a normal operation in the interval H_m = 40 m - H_M = 55 m, this meaning a ΔH = 15 m, the hydrophore's effective volume has to be at least: $V_u = Q_p T_c/4$ = 1,725 m^3, the total necessary volume becoming: $V_H = V_o$ + 6,9 m^3, therefore: $V_H \approx$ 10 m^3. If a minimum protection volume $V_o \approx 0{,}2 V_u$ is accepted for the given presure conditions, the hydrophore's effective volume (compensation volume) is not exceeding V_u = 0,25.0,8.V_H =0,2V_H. Thus, in the case of the existing hydrophore, that has V_H = 2 m^3, the result will be V_u = 0,4 m^3, volume that is fitted for the use of a discontinously operated pump at an average flow: $Q_p \leq 4V_u/T_c$, and therefore $Q_P \leq$ 0,0053 m^3/s (19,2 m^3/h). When the existing hydrophore is operated, 80 % of the pumped flow is re-circulated through the bypass main, the network's requested head (H = 45 m) being provided by a global efficiency of: η_{IP} = 0,275.$W.H/E$ = 11,2 %, i.e. with a specific power consumption five times greater than the normal one.

In compliance to existing data, the „Codrescu" water PS is supplying 840 persons. In order to design the upgrading works for the Codrescu drinking water PS it is assumed that the specific flow for the household consumption is q_o = 165 l/person.day [6]. The minimum pressure provided by contract at the PS inlet p_{min}=1,5 bar. During normal operation the PS inlet pressure is p = 2,2...3,0 bar, and on delivery the pressure must reach p_{sp} = 5,5...6,0 bar. Using SR 1343-1/2006, the maximum hourly flow is Q_{omax} = 16,2 m^3/h (4,5 l/s) and the pumping station exceptional head is $H_{exc} = 10{,}2(p_{sp} - p_{min}) \approx 40$ m.

3.2. MATHEMATICAL MODELLING AND CALCULATION ALGORYTHM FOR VARIABLE SPEED PUMPS THAT WORK ON A NETWORK WITH GIVEN CHARACTERISTICS

The basic data are the network's static head H_{RM}, the hydrophore's static head H_h and the hydraulic resistence modulus, network-hydrophore M_{rH} = 0,0871 s^2/m^5. The pump's catalog specification are:

- motor: power N_{mo} = 4,0 kW, nominal speed n_o = 2840 rpm, efficiency η_{mo} = 0,863;
- LOWARA 15SV04 pump: nominal flow Q_o = 0,0047 m^3/s, nominal head H_o = 45 m, efficiency η_{po} = 0,72.

The parameters of the pump's head and efficiency analtytic characteristics are:
A_{s0o} = 52,34; A_{s1o} = 3,17; A_{s2o} = -1,00;
A_{r0o} = 17,77; A_{r1o} = 24,22; A_{r2o} = -2,70;
The network's characteristic is given by:

$$HI(H_h, H_{RM}, Q) = H_h - H_{RM} + M_{rH} Q^2 \quad \text{(m)} \tag{17}$$

The pump's head characteristic can be analytically expressed by a parabolic type function:

$$H(n,Q) = A_{s0o}\left(\frac{n}{n_o}\right)^2 + A_{s1o}\frac{n}{n_o}Q + A_{s2o}Q^2 \quad \text{(m)} \tag{18}$$

and the pump's efficiency characteristic at nominal speed n_o is defined with:

$$R_p(Q) = A_{r0o} + A_{r1o}Q + A_{r2o}Q^2 \quad (\%) \tag{19}$$

The quadratic forms of efficiency isolines (2) are matching the efficiencies: R = 60, 65, 70, 72 %, and the parameters k_{r1} and k_{r2} can be obtained by applying the equations (3):

$$\begin{cases} k_{r1} = \dfrac{H_{r1}(R)}{Q_{r1}(R)^2} \\ k_{r2} = \dfrac{H_{r2}(R)}{Q_{r2}(R)^2} \end{cases} \tag{20}$$

where:

$$\begin{cases} Q_{r1}(R) = \dfrac{-A_{r1o} - \sqrt{A_{r1o}^2 - 4A_{r2o}(A_{r0o} - R)}}{2A_{r2o}} \\ Q_{r2}(R) = \dfrac{-A_{r1o} + \sqrt{A_{r1o}^2 - 4A_{r2o}(A_{r0o} - R)}}{2A_{r2o}} \end{cases} \quad \text{(l/s)} \tag{21}$$

to which, on the head characteristic at nominal speed, the next heads will correspond:

$$\begin{cases} H_{r1}(R) = A_{s0o} + A_{s1o}Q_{r1}(R) + A_{s2o}Q_{r1}(R)^2 \\ H_{r2}(R) = A_{s0o} + A_{s1o}Q_{r2}(R) + A_{s2o}Q_{r2}(R)^2 \end{cases} \quad \text{(m)} \tag{22}$$

In case of variable speed pump the pumped flow will be:

$$Q_i(H_{RM},H_h,n)=\frac{A_{s1o}\frac{n}{n_o}+\sqrt{A_{s1o}^2\left(\frac{n}{n_o}\right)^2+4(M_{rH}-A_{s2o})\left[A_{s0o}\left(\frac{n}{n_o}\right)^2+H_{RM}-H_h\right]}}{2(M_{rH}-A_{s2o})} \quad \text{(l/s)} \tag{23}$$

the head being:

$$H_i(H_{RM},H_h,n)=A_{s0o}\left(\frac{n}{n_o}\right)^2+A_{s1o}\frac{n}{n_o}Q_i(H_{RM},H_h,n)+A_{s2o}Q_i(H_{RM},H_h,n)^2 \quad \text{(m)} \tag{24}$$

The parameter that is a characteristic of the efficiency isoline η is given by:

$$k_R(H_{RM},H_h,n)=\frac{H_i(H_{RM},H_h,n)}{Q_i(H_{RM},H_h,n)^2} \tag{25}$$

The reference flow is defined with:

$$Q_R(H_{RM},H_h,n)=\frac{A_{s1o}+\sqrt{A_{s1o}^2-4[A_{s2o}-k_R(H_{RM},H_h,n)]A_{s0o}}}{2[k_R(H_{RM},H_h,n)-A_{s2o}]} \quad \text{(l/s)} \tag{26}$$

and the pump efficiency that coresponds to the isoline of parameter k_R is:

$$R_i(H_{RM},H_h,n)=A_{r0o}+A_{r1o}Q_R(H_{RM},H_h,n)+A_{r2o}Q_R(H_{RM},H_h,n)^2 \quad \text{(\%)} \tag{27}$$

The pump's absorbed power is defined by the next equation:

$$N_{ip}(H_{RM},H_h,n)=9{,}81\frac{H_i(H_{RM},H_h,n)Q_i(H_{RM},H_h,n)}{R_i(H_{RM},H_h,n)} \quad \text{(kW)} \tag{28}$$

The specific unitary energy consumption, used for evaluating the pump's efficiency (in terms of economy and power consumption), is given by:

$$E_{su}(H_{RM},H_h,n)=\frac{10^3 N_{ip}(H_{RM},H_h,n)}{3600\eta_{mo}Q_i(H_{RM},H_h,n)H_i(H_{RM},H_h,n)} \quad \text{(Wh/m}^3\text{/m)} \tag{29}$$

4. RESULTS AND SIGNIFICANCES

If calculation algorythm is applied into Mathcad software, the next results have been obtained:
- the graph for the operating regimes of pump-network system, at variable speed (see **Fig. 3.**);
- the variation of flow, power and specific unitary energy consumption at various speeds (see **Fig. 4.**);
- the variation of head and efficiency at various speeds (see **Fig. 5.**).

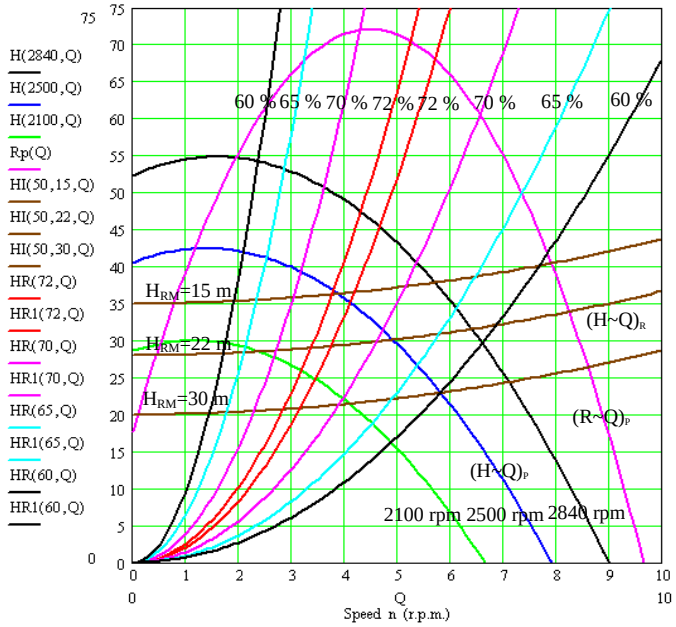

Fig. 3. Adapting a pump to variable working regimes
in the case of pumping on a network with given characteristics

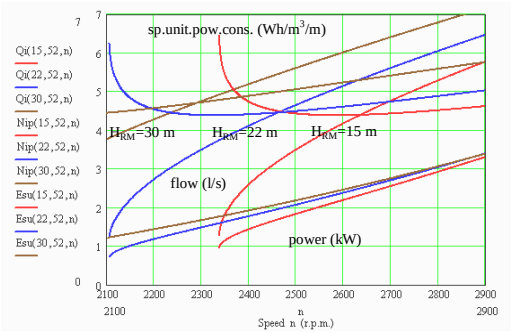

Fig. 4. Variation of flow, power and
specific unitary power consumption at variable speed

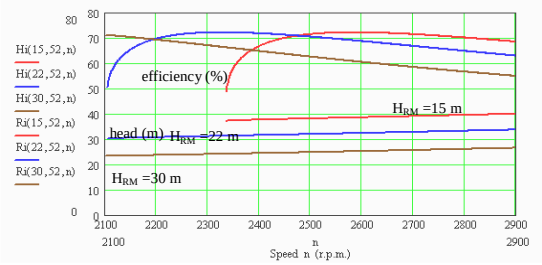

Fig. 5. Variation of head and efficiency
at variable speed

The need to ensure the flow demanded by consumers below a head of 40…55 m, leads to the fact that the efficiency of a variable speed pump will decrease when the pumped flow decreases below the respective heads (see **Fig. 4.-5.**).

Efficiencies superior to 50 % can be provided for flows that exceed 1,80 l/s (see **Fig. 3.**), flows that are dominant during the current operation of the network. Taking into account the fact that the frequency static converter's efficiency reaches values of 0,90 – 0,96, and the motor's efficiency is 0,85, it is obvious that if such technology is adopted for a pumping plant, its global efficiency would be much higher than in the case of the existing situation.

5. CONCLUSIONS

There ar many cases when there is need to modernize and upgrade pumping plants within water supply systems, in order to provide a sound correlation bewteen the pumps capacities and the actual demand of consumers. In the case of the „Codrescu" pumping station the existing equipment features is worn-out (expired technological life) and, hence, its characteristics do not longer fit the current pumping needs. An upgrading of this pumping station would mean the full replacement of pumps with new ones, pumps able to ensure for the network all optimal operational conditions, both in terms of economy and power consumptions, due to the best technologies available today.

Considering that the cost of variable speed drives for alternative current motors has decreased during the last decade, it can be stated that an upgrading of the „Codrescu" PS by adopting variable speed pumps is now strongly recommended. In fact, with only moderate expenditure significant positive economic outcomes can be obtained, this meaning technological parameters much superior to the current ones.

6. REFERENCES

[1] Ionel I., *Acționarea electrică a turbomaşinilor*, Ed. Tehnică, Bucureşti, 1980
[2] Alexandrescu O., *Stații de pompare*, Editura "Gh. Asachi", Iaşi, 2003
[3] Alexandrescu O., *Rolul hidroforului în adaptarea la regimuri variabile a instalațiilor de pompare şi caracteristicile sale funcționale*, CTS IC-EE, AIIR - UTI, Iaşi,1994.
[4] Alexandrescu O., *Randamentul global al adaptării instalațiilor de pompare la regimuri variabile prin folosirea hidroforului*, CTS IC-EE, AIIR - UTI, Iaşi, 1995.
[5] Poiată T., *Optimizarea structurii şi regimurilor de funcționare a subsistemelor energetice industriale*, Teză de doctorat, Iaşi, 1997
[6] SR 1343-1/2006, *Alimentări cu apă. Determinarea cantităților de apă potabilă pentru localități urbane şi rurale*, Asociația de standardizare din România (ASRO)

Monitoring and Controlling of Process Parameters in the Chirita Pumping Station, facility included in the Iasi City Water System

Daniel Toma

***Abstract* – This paper is describing the techniques of monitoring and controlling the process parameters in the Chirita pumping station, facility belonging to the Iasi City water systems. The implementation of such systems has been carried in the context of a global upgrading of the plant and brought multiple benefits: decreasing of power consumption of the three pumping plants, possibility of pro-active maintenance, performing of analysis and technical diagnosis, strict scheduling of operating periods outside the power grid's load curve peak periods.**

***Keywords* – monitoring and control, process parameters, pumping station, static frequency converters**

1. INTRODUCTION

The pumping stations are main items within water systems that supply the large urban communities, being operated in numerous sectors: source water catchment, water conveying (when terrain's configuration is not suitable for gravity flowing), in water plants (in all process stages such as sludge draining from clarifiers, filter backwashing) and, finally, for providing the normal supply pressure inside water networks [1].

According to the US Energy Department the water electric pumps in America are consuming around 25 % of the entire power amount that is produced [2]. According to Almeida, the situation is nearly the same in the European Union, where 22 % of power consumption appears in water pumps. (see **Fig. 1)** [3].

Manuscript received June 30, 2012.

Daniel Toma is with "Gheorghe Asachi" Technical University of Iasi, Faculty of Hydrotechnical Engineering, Geodesy and Environmental Engineering, 65 Prof. dr. docent Dimitrie Mangeron Street, 700050, Iasi, Romania (corresponding author to provide tel-fax office: +40232 270804, mobile phone: +40721 811373; e-mail: daniel_10hid@yahoo.com).

ISSN-1584-5990

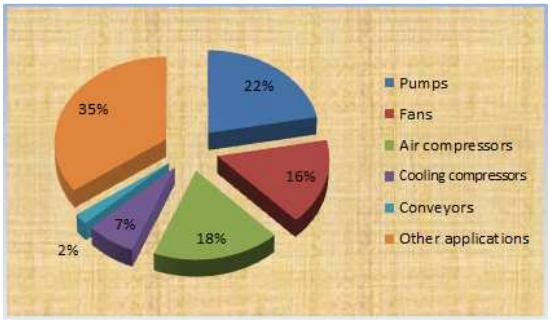

Fig. 1. EU: Estimated distribution of power consumption

Drawing a parallel, we see that in Romania, in the 80s, the electric pumps were consuming approximately the same 25% of the electricity used at national scale [4].

Given this and the important value of the equipment, there is need for a strict monitoring and control of all operational parameters related to water pumps (including those referring to power consumption).

2. GENERAL CONSIDERATIONS

The pumping stations monitoring and control systems are hierarchical management structures, divided on four levels, applied to the technological system itself [5]:

- field level: the automated plant;
- automatic local level controls, achieved with PLCs (Programmable Logic Controller);
- local control room level: average capacity PC, interfaced to PLCs, the main role being of process GUI interface;
- central control room level: high capacity PC interconnected to all local control room and other technical systems, provides the supervision and the correlation of the entire pumping system.

A proper running of a pumping station is in fact based on processing the information related to:

- the plant's status:
  - voltage presence / absence;
  - presence / absence of water on suction;
  - pump unit on / off;
  - open / closed valve;
  - any improper operating regimes;
  - defective insulation of electrical equipment (motor overheating, over / under voltages, overcurrents, imbalances between phases, incorrect phase sequences, current absence of one or more phases, grid frequency, power factor);
  - idle regime (heavy startups, jammed motors);
  - pump de-priming.
- water level in suction tank;
- water level in discharge tank;
- pressure on the pump discharge pipe and / or, where appropriate - the pressure on pumps' suction pipe;
- pumped flow;
- the volume of water pumped;
- power consumption;

and the controls for pumps startup/shutdown or valves the opening / closing.

3. DESCRIPTION OF CHIRITA PUMPING STATION

The Chirita water plant complex is located in the eastern-southeastern part of Iasi, on Iasi-Tutora road, nearby the Dancu village.

The Tutora-Iasi main supply pipeline system is a link between the Tutora pumping facility, the Chirita reservoir, the Chirita water plant and the Sorogari water plant. The main supply system pipeline has been gradually completed, in accordance with the development of the City's water supply City. It currently consists of 5 pipes with different diameters [6]:

- two pipes (I - II DN 600 and II DN 1000/900) that are feeding the Sorogari WP via the "I. Creanga" pumping station;
- two pipes (III - DN 1000 and IV - DN 1200) that supply the Chirita water plant & pump and also the Chirita reservoir (via pipes of the same diameter);
- the pipe V (DN 1200) supplies with cooling water the Holboca CET (power and heating plant), and the Chirita reservoir via the DN 1000 section that continues up to the connection with the 3rd pipe derivation towards the lake.

The Chirita pumping station called SP1 Chirita, was constructed for pumping clarified water from the Chirita lake, towards the Iasi City's industrial water network and, via the "I. Creanga" pumping station, towards the Sorogari water plant, respectively to re-pump water from the Tutora-Iasi pipeline system towards the same water plant. In order to achieve this the Chirita PS was equipped with 5 different types of pumps (1 CERNA unit, 1 SIRET unit, 1 12-NDS unit, 1 14-NDS unit and 3 18NDS units). The pumping station that delivers treated water towards the city's distribution network was named Chirita SP2. This PS was located beneath the filter rooms, in a confined space, with no adequate lifting gear, fact that was hindering the maintenance and repair processes. The station was equipped with three 14 NDS pumps and one 12 NDS pump [6].

All pumps were worn-out (technological life expired) and hence it was very hard to keep them in a proper operational state. Due to the fact that the consumers' water needs were decreasing the pumps were operating in conditions totally different from the designed ones. Thus the rehabilitation and modernization of the Chirita PS has been proposed.

Figure 2 shows a general layout of the complex after its upgrading [7].

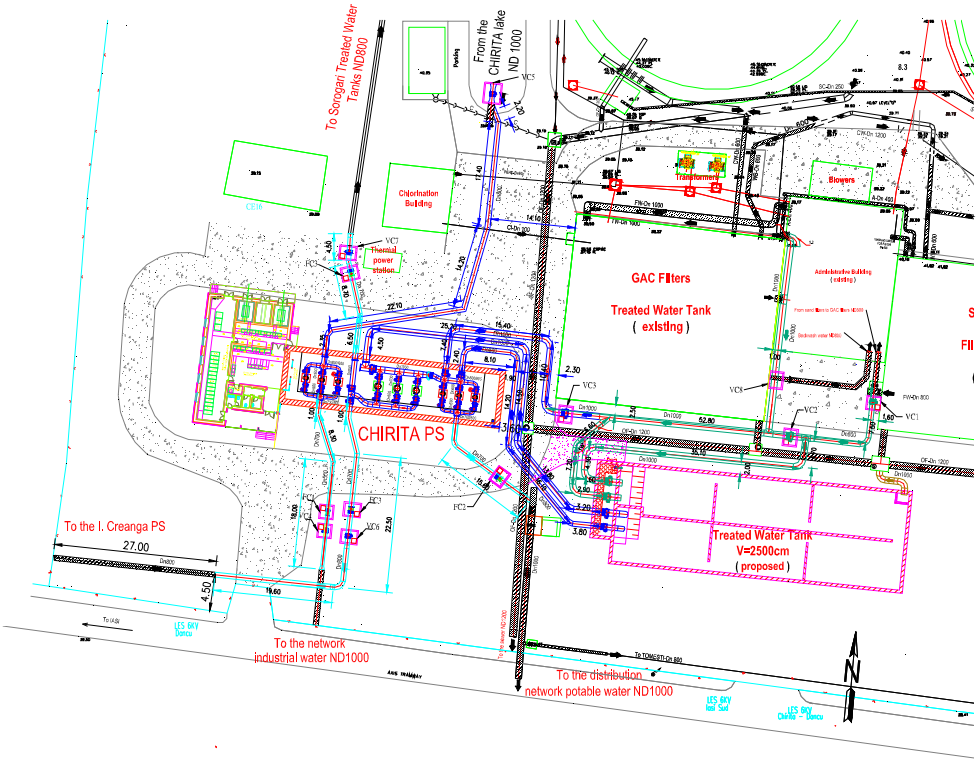

According to the new designs the treatment of water drawn from River Prut is fully achieved within the recently modernized Chirita water plant. Water is pumped by three pumping groups named in compliance to the zone towards which water is supplied, as it follows [7]:

- the CITY pumping group delivers drinking water from the filter station towards the city network. Pumping takes place during the 6 hours of peak consumer water demand (06:00 ÷ 08:00 and 17:00 ÷ 21:00). The group includes (2+1) WILO ASPV 250C–185/4–R4–C1–EO–FC-ACH pumps, coupled in parallel, featuring the following operational parameters: Q = 300 l/s and H = 48 mWC. The pumps have unitary powers of 185 kW, and are supplied at voltages of 0,4 kV;

- the SOROGARI pumping group delivers drinking water towards the Sorogari water tanks facility during the 18 hours outside peak consumption period (08:00 ÷ 17:00 and 21:00 ÷ 06:00). This group includes (2+1) WILO ASPV 300DS – 450/4 – 6kV – C1 – EO – ACH pumps, coupled in parallel, having Q = 450 l/s and H = 78 mWC. Each pump has a power of 450 kW, supply voltage 6 kV. These pumps deliver water towards the Sorogari tanks by two routes: directly (normal operating scheme) or via the „I. Creanga" repumping station (reserve scheme);

- the 3rd pumping group is named INDUSTRY group an is conveying the water from the Chirita Lake towards the City's industrial zone. Includes (2+1) WILO ASPV 250B – 110/4 – T4 – C1 – EO – FC – ACH, pumps, coupled in parallel, with Q = 250 l/s and H = 30 mWC. Each pump has a power of 110 kW, and supply voltage of 0,4 kV.

Figure 3 shows the layout of Chirita PS.

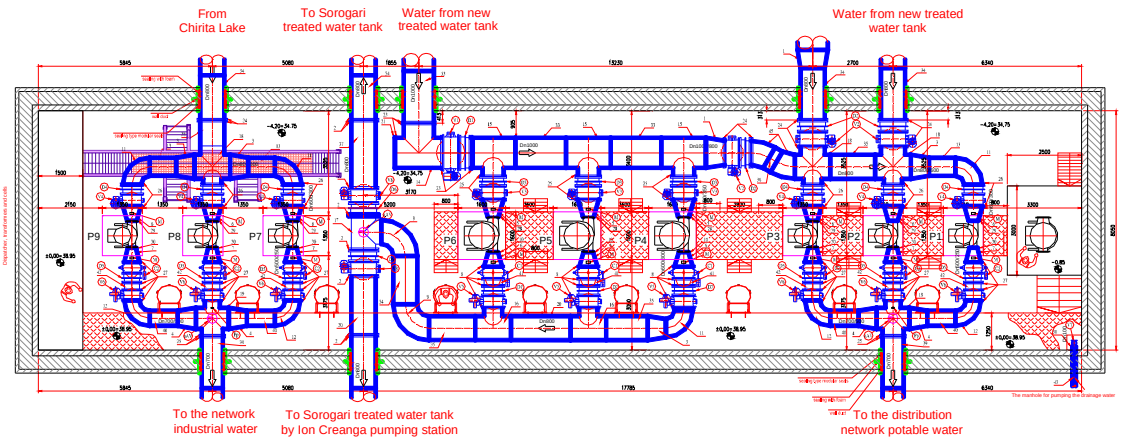

Fig. 3. Layout of Chirita PS

4. CHIRITA PUMPING STATION: THE MONITORING AND CONTROL SYSTEM

At the Chirita pumping station the plant for which a monitoring and controlling system is implemented includes the following items: pumps, actuated valves, electric equipment (switches and protection devices), measuring devices (flowmeters, pressure gauges) and all the devices needed for measuring electrical parameters (voltage, current, power factor, active energy, reactive energy).

The automation systems that have been designed for the Chirita pumping station are PLC based systems, that rely on industrial microcontrollers. These devices have logical autonomy, operational flexibility in use and the feature of serial standardized communication capability, being superior to any other automation solutions based on other devices.

All acquisition and control equipment are integrated through a communication system, by a SCADA program (Supervisory Control and Data Acquisition), installed on a workstation that is located in the central control room. The program, through its transmission-reception protocol is able to verify the accuracy of conveyed data and ensures the integrity of information transmitted inside the network. It works under Windows operating environment and is "user friendly" being accessible to anyone who is familiar to personal PCs.

The SCADA application consists mainly of three modules:

• server: parameters management, alarms, data bases, reports;

• client: user interface;

• communication: acquisition of the PLC parameters.

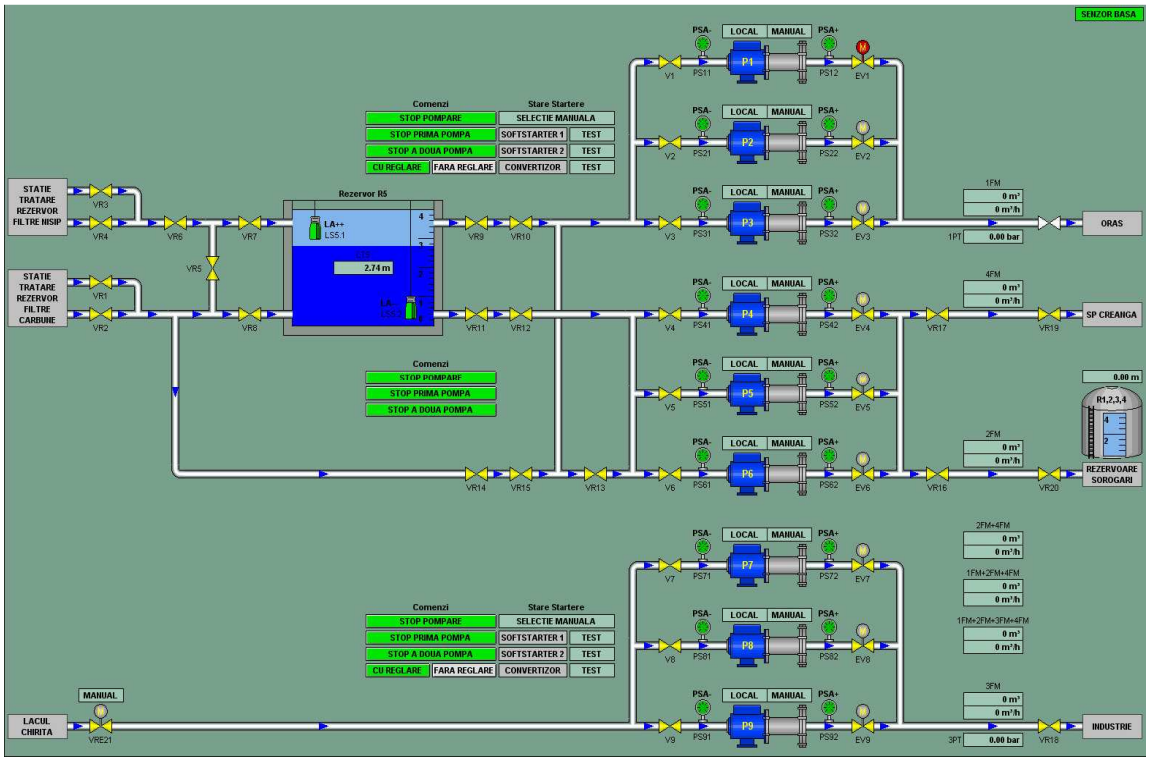

Fig. 4. The Chirita pumping station: Functional diagram

In **Fig. 4** we can see the pumping station's functional diagram. The diagram shows the pumping groups, the distribution valves, the intermediate tank, the output parameters, flows, pressures and the Sorogari tanks [7].

The distribution valves are monitored by their position.

For the R5, 2500 m^3 tank, are shown the water levels inside the tank (with a level sensor) and the status of "no water" and "overflow" sensors.

The CITY pumping group is composed of pumps P1, P2 and P3 which draw water from the R5 intermediate tank reservoir or directly in the WWTP's tanks, depending on the configuration of distribution valves. On the group's outlets pressures and flows are measured. The pumps are driven by two ATS48 soft starters and an ATV61 frequency converter that is switchable on all three pumps. The role of this group is to

maintain a constant discharge pressure and works with one or two pumps, adjustable or not, depending on operator settings within the Magelis terminal.

The SOROGARI pumping group consists of P4, P5 and P6 pumps which suck water from the R5 water tank or directly from WWTP tanks depending on the configuration of distribution valves. The group has two outlets: one towards the Sorogari tanks, and another towards „I. Creanga" pumping station (backup). On each of them flow is measured. The function of this group is to maintain a pre-set level in the Sorogari tanks and works with two pumps on duty and one backup pump. During normal operation this pumping group SOROGARI delivers water as long as a water storage reserve exists in these tanks and if operator has set this on the Magelis screen. Levels within the four 5,000 cubic meters tanks at Sorogari are continuously surveyed and their levels are transmitted towards the Chirita pumping station. Depending on the Start and Stop levels, set by operator, on the Magelis screen, the pumps within this group will start and will stop.

The INDUSTRY pumping group consists of pumps P7, P8 and P9 that draw water from Chirita lake. On the group outlets pressure and flow are measured. As for the CITY group, two pumps are operated by two ATS48 soft starters and one ATV61 frequency converter switchable on all three pumps. The task of this group is to maintain a constant pressure on discharge and works with one or two pumps, in adjustable mode or not, depending on the operator settings from the Magelis screen.

Each of the nine pump is fitted on suction connection with a manual valve and a low pressure switch and, on discharge connection, with an actuated valve and a high pressure switch. For all pumping groups, one of the three pumps is in reserve. Nevertheless the configuration allows each of the three pumps to become a backup pump, in order to even the run times for all pumps.

For the CITY and INDUSTRY pumping groups the main discharge manifold will be fitted with a pressure transducer. The normal operating mode implies that operator is setting the discharge pressure (on the Magelis screen), that is, with a frequency converter. In case that the frequency converter is defective, until the malfunction is solved, the operator can handle the pumping group only by means of softstarters.

For Şorogari tank water level is displayed.

The working modes allowed by the PLC are:

- manual mode:
  . local command, from the low / medium voltage control panel;
  . remote command for changing the status of an execution item, launched from keyboard;
- automatic mode:
  . in normal operation (optimal pumping regime);
  . under emergency/failure situations, *n* restarts launched - programmable for each type of failure, switching to backup mode in case of failure and creation of a defect evolution history in order to have a proper diagnosis of it.

In Chirita PS the main functions performed by the monitoring and control system are:

1) Pump operating status

The three pumping groups are shown on a physical map that enables users to quickly and intuitively locate them. On the map, along with the pump's name or number, its operational status is also marked (on, off or malfunction). From the central control room operator can start and stop the available pumps or may request additional information on the electric, energy or process parameters. Requested parameters can be obtained by investigating a historical database or can be taken at a certain time from a local measuring point, through successive acquisition orders.

2) The status of the supply grid

In order to record the voltage differences between daytime and night regimes, between weekdays and holidays or the imbalance due to a disproportionate load imbalance of phases with monophase consumers the system takes over, displays and stores the main parameters of power grid, as it follows:

- grid frequency;
- voltages on each phase;
- voltage imbalance between phases.

The voltage or frequency fluctuations in the grid and also the phase imbalance lead to changings of motors' operating characteristics, this meaning overheating of coils' insulations and afterwards, their destruction. The recording of voltage fluctuations as a document is eventually, in most of the cases, a solid proof in the case of litigations that occur between consumer and the power company.

3) Electrical parameters of motor pumps

Along with the power grid parameters, the monitoring system allows the survey of all motors' electrical status parameters, namely:

- currents on each phase;
- current imbalance between phases;
- phase shifts between current and voltage on each phase;
- the motor's insulation electrical resistance (measured using a 500 VDC source).

Together with the list of messages provided by the protection system, the electrical parameter values may indicate the causes that have generated an abnormal functioning of the motor or pump. Under-currents may indicate that the motor is idling, a poor coupling, damage of motor rotor, or lack of water (maybe a closed valve). The current imbalance between phases may result from damages in the motor windings, decreasing of electrical insulation resistance or a disrupting of supply grid.

An overload can be generated by too much load (may a valve opened above the maximum allowed limit), bearing failure, the decrease of insulation resistance or an excessive weight of the pumped fluid. A decrease of insulation resistance can be determined by a defective supply cable, by the improper mounting of motor, by a winding insulation failure (by impact or strain) or by water entering through sealing elements. All this information help to develop a comprehensive preventive and corrective maintenance program, necessary to maintain the pumps within normal functional parameters.

4) Pumps' energy parameters

Most of the costs needed for the procurement, the maintenance and the operation of a pumping plant over its average life span are in fact the amounts spent on power supply. Therefore it is crucial to calculate and, where possible, to optimize all energy consumptions. The monitoring system allows for each pumping group an assessment of energy consumption. The system displays and stores the next factors:

- active power;
- reactive power;
- apparent power;
- power factor;
- active energy;
- reactive energy.

Information obtained are underlying the efficiency analysis phases and the defining of the optimal method for operating the pumping groups.

5) The pumps' process parameters

Depending on the transducers installed on discharge pipes the monitoring system provides information that can be used in order to detect the status of pumps, valves or closing elements. Thus the next items may be surveyed:

- the pressure inside the discharge manifold;
- the pumped flow (MAGFLO electromagnetic flowmeters, comprising a MAG 1100 or 3100 sensor and a 5000 or 6000 type converter).

The suction and discharge pipes of each pump are fitted with pressure gauges that allow the verification of operation within the range of optimal parameters (in compliance to the pressure limits shown in the pump's characteristic graphs).

6) Available water resources

In order to check whether the water needs can be satisfied, the monitoring system provides information about the status of resources, consumption and available pumping capacity, namely:

- pump status (available / failure);
- pumped water flow;
- water levels from within the R5 intermediate tank and the Sorogari tank (measured by level sensors).

Data can be related for an optimal management of resources, with minimum power expenditure.

7) The pumps' efficiency and exploitation rate

In order to reduce power costs an optimal pumping schedule is developed for each pumping group. This is performed on basis of several factors: pump efficiency, consumers demand, storage capacity and the power tariffs. For this, the monitoring system provides the user data in reference to the next items:

- pump efficiency (ratio between pumped flow and consumed active energy);
- exploitation rate for each pump (total running hours);
- level in tanks;
- total flow of pumped water;
- hourly tariffs.

From this information an optimization plan for consumption can be drafted. Hence, the storage capacity is scheduled to be ensured during the periods with minimum power tariffs.

8) Type of detected failures and their time of occurrence

Some of the malfunctions that may occur are: failure of softstarters or frequency converters, excessive pressures on each pump's suction or discharge line, exceeding of tanks' overflow levels, excessive motor winding temperatures, flooding of the pumping station etc. Malfunctions are recorded in a separate database (as tables or histograms).

Therefore the operator may easily learn about the number of malfunctions that occur within a certain period of time, their frequency of occurrence or the time required for remediation. Also the operator can find if the solving of a malfunction means the removal of the effects or causes that have generated it.

5. CONCLUSIONS

The main benefits of implementing a monitoring and control system are:

- optimization of pump operating in terms of energy factors, ensured by the continuous monitoring of all instantaneous values of pumped water and power consumption;
- preventive maintenance, ensured by a follow-up of all hydraulic and electrical values, thus reducing all costs associated to maintenance and repair;
- technical analyzes and diagnoses;
- programming of operating periods for the pumping groups, outside the periods of peak power load curves, thus ensuring significant power savings.

6. ACKNOWLEDGMENTS

This paper was based on results of contract no. 1278P/2003, additional work at project "Upgrading of the Chirita water treatment plant – Iasi City", the Polytech Center for Research, Design and Engineering, "Gh Asachi" Technical University of Iasi and was funded by RAJAC Iasi. Moreover, the results of the work will be part of the author's thesis for a doctor's degree.

7. REFERENCES

[1] Dobre A.S., *Construc□ii edilitare*, Conspress, Bucure□ti, ISBN 973-7797-82-5, 2006.
[2] U.S. Department of Energy, *United States Industrial Motor Systems Market Opportunities Assessment*, U.S. Department of Energy, Washington D.C., USA, 1998.
[3] A.T. de Almeida, P. Fonseca, H. Falkner and P. Bertoldi, "Market Transformation of Energy-Efficient Technologies in the EU," *EnergyPolicy*, Vol. 31, Iss. 6, May 2003, pp. 563–575.
[4] Ionel I., *Acționarea electrică a turbomașinilor*, Editura Tehnică, București, 1980.
[5] Alexandrescu O., *Sta□ii de pompare*, Editura "Gh. Asachi", Ia□i, 2003.
[6] xxx *Lucrări adiționale la proiectul "Modernizarea stației de tratare a apei Chirița – municipiul Ia□i"*, Studiu de Fezabilitate, Contract 1278P/2003, Universitatea Tehnică "Gh. Asachi" Iași, Centrul de Cercetare, Proiectare și Transfer Tehnologic "Polytech", Colectivul Ingineria Sistemelor Hidraulice, Iași, 2003.
[7] xxx *Reabilitarea sta□iei de pompare Chiri□a Ia□i*, proiect tehnic, 2010.

SECTION III

HYDRAULICS. THEORY AND APPLICATIONS IN CONSTRUCTIONS

Ovidius University Annals Series: Civil Engineering, Issue14, October 2012

FILTRATION GEOMETRIC MODELS

Josif Bartha, Nicolae Marcoie, Aron Gabor Molnar, Lucian Alexandru Luca, Daniel Toacă, Daniel Toma

***Abstract* – This paper describes two geometric models that have been developed in order to achieve the problem related to the post–Darcy filtration through rigid permeable medium: the thin tubes fascicle model and the equivalent homogenous solid spheres model.**

The measuring of energy losses that occur along the thickness of macroscopic material bed pack helps to determine the motion's microscopic parameters and the microscopic geometric characteristics of permeable material.

***Keywords* – Filtration, microscopic sizes, geometric model**

1. INTRODUCTION

The dissipation of fluid's energy by flowing through permeable mediums is significantly important in various engineering domains. As regards filtration study several flowing models have been developed, as it follows:

- phenomenological models [2, 8, 9];
- geometric models (flowing in tubes) [6, 9, 12, 14, 15]
- statistic models [8,16]
- analytic models for the solving of Navier-Stokes equations [2, 3, 7, 11, 12]
- models for flowing around solid models.

The goals of such studies is to define the flowing parameters. All models include unknown parameters that are to be experimentally determined. Most of experiments are measuring, at a macroscopic scale, the pressure decreasing, depending on the velocity of the fluid that flows through various permeable materials of known thickness.

The filtration scheme, as described by Darcy, expresses the velocity as if the fluid circulates within the entire space which is occupied by the permeable material and the voids (**Fig. 1.)**

Manuscript received June 25, 2012.

Josif Bartha is with "Gheorghe Asachi" Technical University of Iasi, Faculty of Hydrotechnical Engineering, Geodesy and Environmental Engineering, 65 Prof. dr. docent Dimitrie Mangeron Street, 700050, Iasi, Romania (corresponding author to provide phone: +40232 270804; e-mail: i_bartha@yahoo.com).

Nicolae Marcoie is with "Gheorghe Asachi" Technical University of Iasi, Faculty of Hydrotechnical Engineering, Geodesy and Environmental Engineering, 65 Prof. dr. docent Dimitrie Mangeron Street, 700050, Iasi, Romania (e-mail: nmarcoie@yahoo.com).

Aron Gabor Molnar PhD Student is with "Gheorghe Asachi" Technical University of Iasi, Faculty of Hydrotechnical Engineering, Geodesy and Environmental Engineering, 65 Prof. dr. docent Dimitrie Mangeron Street, 700050, Iasi, Romania (e-mail: agmolnar@yahoo.com).

Lucian Alexandru Luca PhD Studentis with "Gheorghe Asachi" Technical University of Iasi, Faculty of Hydrotechnical Engineering, Geodesy and Environmental Engineering, 65 Prof. dr. docent Dimitrie Mangeron Street, 700050, Iasi, Romania (e-mail: proing@rdslinc.ro).

Daniel Toacă is with "Gheorghe Asachi" Technical University of Iasi, Faculty of Hydrotechnical Engineering, Geodesy and Environmental Engineering, 65 Prof. dr. docent Dimitrie Mangeron Street, 700050, Iasi, Romania (e-mail: daniel.toaca@yahoo.com).

Daniel Toma is with "Gheorghe Asachi" Technical University of Iasi, Faculty of Hydrotechnical Engineering, Geodesy and Environmental Engineering, 65 Prof. dr. docent Dimitrie Mangeron Street, 700050, Iasi, Romania (e-mail: daniel_10hid@yahoo.com).

ISSN-1584-5990

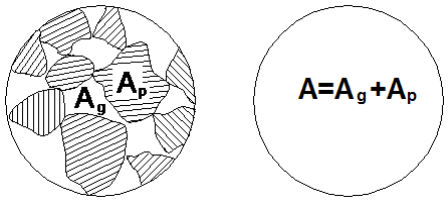

Fig. 1. Filtration scheme, according to Darcy

2. THE GENERAL EQUATIONS OF FILTRATION

The iso-thermal motion of uncompressible fluids within rigid porous media is governed by the Navier-Stokes equations and the mass conservation laws [10].

$$\frac{\partial V}{\partial t}+(V\cdot\nabla)V=-\frac{1}{\rho}\text{grad}\ p+\nu\cdot\nabla^2V+g+\frac{1}{\rho}F \tag{1}$$

$$\nabla V=0 \tag{2}$$

where: $X=[x,y,z]^T$ is the positioning; and t – time.

$$V=(x,t)=[V_x(x,t),V_Y(y,t),V_z(z,t)]^T \tag{3}$$

is the velocity, $p(x, t)$ – pressure, ρ - density, g – gravitational acceleration, μ - dynamic viscosity coefficient and $\nu=\mu/\rho$ - kinematic viscosity coefficient.

Equation (1) describes the temporal changing of velocity field under the effect of inertia, pressure, viscous, gravity forces, and other forces that might be implied in motion (in gravitational field $F = 0$).

Equations (1) and (2), together with the contour and the initial conditions, are forming four non-linear partial differential equations, with four unknowns $V(x, t)$ and $p(x, t)$.

Non-dimensional parameters:

- Reynolds number

$$Re=\frac{V_0L_0}{\nu} \tag{4}$$

- Froude number

$$Fr=\frac{V_0^2}{L_0g} \tag{5}$$

(with a dimension "$_0$" subscript, within the motion scale) are the relative measure of viscous, inertial and gravitational forces. These values can be highlighted in equations (1) and (2) by introducing the non-dimensional values.

$$\overline{V} = V / V_0;\ \overline{x} = x / L_0;\ \overline{t} = t \cdot V_0 / L_0;\ \overline{p} = p / \rho \cdot V_0^2 \tag{6}$$

Thus obtaining:

$$\frac{\partial V}{\partial t} + (V \cdot \nabla)V = -\frac{1}{\rho}\text{grad}\, p + \frac{1}{Re}\nabla^2 V + \frac{1}{Fr} \tag{7}$$

$$\nabla V = 0 \tag{8}$$

The decreasing of *Re* number involves an increasing of effects of viscous forces. By the other hand the increasing of number *Fr* means an increasing of the influence of gravitational forces on motion.

Usually, the flowing within porous media takes place under a difference of pressure along the macroscopic given length $\Delta p / L$, L being the length's macroscopic scale and corresponds to the thickness of the porous material. The analysis of the Navier-Stokes equation, which governs the motion of an uncompressible fluid within the voids of the permeable (granular) material, is defining the scale of velocities:

$$V = \frac{d_p^2}{\mu} \cdot \frac{\Delta p}{L} \tag{9}$$

Where d_p is the measure of solid particles, respectively of voids between them, and is the microscopic scale of lengths.

The microscopic (local) Reynolds factor is defined as it follows:

$$Re_{dp} = \frac{\rho V d_p}{\mu} = \frac{\Delta p d_p^2 \rho}{L\mu^2} \tag{10}$$

The pressure gradient is directly depending of this number (respectively the geometric parameters of the porous medium).

The Darcy law derives from the Navier-Stokes equations for numbers $Re_{dp} < 1$:

$$V = \left(\frac{k_p}{\mu}\right)(\nabla p - \rho g) \tag{11}$$

where k_p is the permeability (L^2).

The inertial correction of filtration (for $Re_{dp} > 1$), within the theory of permeable medium, is a cubic relation of filtration velocity [1,5].

$$-\frac{dp}{dx} = \frac{\mu}{k_p} \cdot V + \frac{\mathsf{H}}{\mu}\rho^2 V^3 \tag{12}$$

where H is the low inertia factor.

For the high inertia domain Forchheimer has proposed the equation [1]:

$$-\frac{dp}{dx} = \frac{\mu}{k_{Fh}} V + \beta \rho V^2 \tag{13}$$

where k_{Fh} is the permeability according to Forchheimer and β - the inertial resistance coefficient.

The deviations of pressure gradient from Darcy law, first noticed by Forchheimer, and afterwards widely debated, have lead to a zoning of velocity on the following domains:

- the Darcy domain – $Re_{dp} = (0; 1)$;
- the weak inertia domain $Re_{dp} = (1; 4{,}3)$;

- the Forchheimer domain (strong inertia) Re_{dp} =(4,3; 180);
- the transition domain, towards turbulence Re_{dp} = (180; 900);
- the turbulent domain Re_{dp} = (900; 10000).

3. GEOMETRIC MODEL OF FILTRATION

For a Darcy type permanent filtration, the simplified scheme solves certain theoretical and practical problems at a macroscopic scale, operating at an apparent velocity V_0.

The filtration at a microscopic scale (non-permanent filtration) needs the use of fluid's actual velocity within inter-spaces, and sometimes even its distribution.

Geometric models are representing the real porous medium (**Fig. 2**) as fascicles of tortuous thin tubes, having the same diameter, or as uniform spherical particles, positioned in various positions.

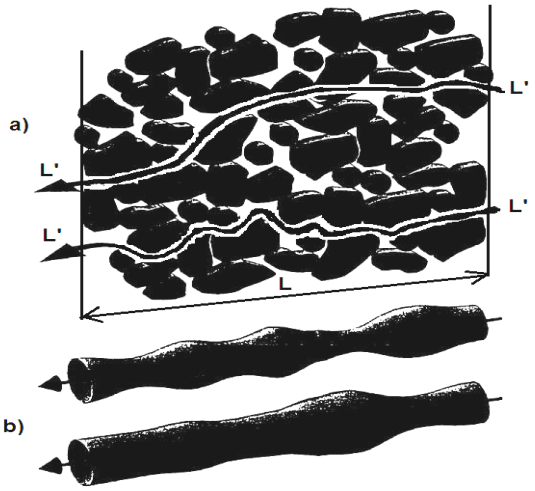

Fig. 2. Flowing through a solid material made of particles (a) and non-uniform tubes (b)

The nowadays technique is using permeable materials of uniform or random geometry in the next applications: various filters (gas, liquid), heat exchangers, porous burners, catalysers (**Fig. 3a**), porous chemical reactors.

3.1. THE THIN TUBES FILTRATION MODELS [6]

It is assumed that the random permeable material, featuring an effective porosity n (see **Fig. 2a**) made of a fascicle of tortuous tubes with a diameter d and a length L', and having contact with the liquid on a surface A (**Fig. 3b**).

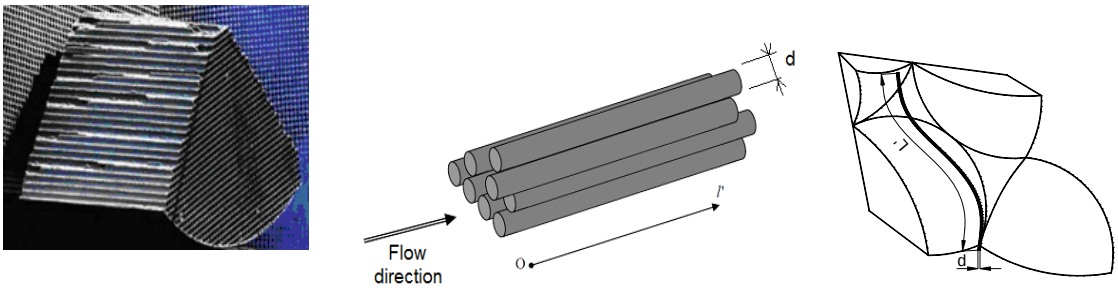

a) b) c)

Fig. 3. Thin tubes filtration model

The filtering column has a total volume W, a diameter D and an apparent thickness (length) L.

The trajectory of streams L' is greater than the thickness of the column made of permeable material L, these having a curved shape between solid particles (according to **Fig. 3c**) and, hence, tortuosity τ can be defined:

$$\tau = L'/L \tag{14}$$

If the pores' volume is made equal to the tubes' volume and if the contact area of particles with liquid is made equal to the fictive tube's area, the diameter d of fictive tubes can be defined, as it follows:

$$d = \frac{4V \cdot n}{A} = \frac{4n}{A_d(1-n)} \tag{15}$$

Where n is effective porosity, and A_d is the specific dynamic area (the ratio between contact area of solid particles with liquid and the solid's volume). The static specific area A_s can be defined as the ratio between the solid particle's area and its volume (for spheres $A_s=6/d$).

The model's geometric characteristics d and τ (featured by the model at micro scale level), are resulting from direct measurements of pressure gradient $\Delta p / L$, of porosity n and of apparent filtration velocity V_0 on an infiltrometer (at macro scale).

The relation between the apparent and the real velocity is:

$$V = \frac{V_0 \cdot \tau}{n} \tag{16}$$

The energy losses at filtration that takes place through the model's material features two components:

- The first term, related to the viscous friction, for which the Poisenille relation is accepted

$$\frac{(\Delta p)^3}{L'} = \frac{32\mu}{d^2}\nu \tag{17}$$

with $\lambda = 64 / Re_{dp}$

- The second term is related to the inertial losses in tubes featuring a roughness equal to the diameter, $k_e=d$.

According to Nikuradze:

$$\frac{1}{\sqrt{\lambda_t}} = 2\lg\frac{3{,}7d}{k_e} \tag{18}$$

and the result being $\lambda_t = 0{,}7743$.

For the global energy losses the Weisbach relation can be accepted:

$$\frac{\Delta p}{\gamma} = \lambda \frac{L'}{d} \frac{V^2}{2g} = \left(\frac{64}{Re} + \lambda_t \right) \frac{L'}{d} \frac{V^2}{2g} \tag{19}$$

which, after replacements, will lead to the form:

$$\frac{\Delta p}{L \cdot V_0} = MV_0 + N \tag{20}$$

with,

$$M = 0{,}0968 \frac{\rho \tau^3 (1-n) A_d}{n^3} \tag{21}$$

and

$$N = \frac{2\mu \tau^2 (1-n)^2 A_d^2}{n^3} \tag{22}$$

The statistic processing of pressure gradient measurements as a function of apparent velocity with the form (20) allows for the computing of parameters τ and A_d. If A_d, the specific dynamic area is known, the equation (15) will give the fictive tubes' diameter d.

3.2. MODEL OF FILTRATION THROUGH PERMEABLE MATERIAL MADE OF HOMOGENOUS SPHERES

For this study it is assumed that the random permeable material, having a porosity n (**Fig. 2a**) is made of homogenous spheres, each with a diameter d_p (**Fig. 4**).

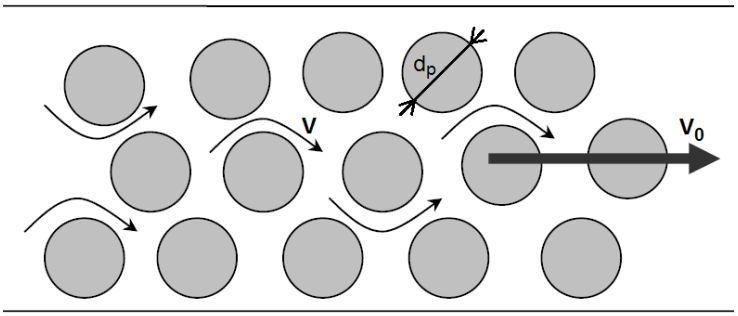

Fig. 4. Model for a permeable medium made of equivalent homogenous spheres

If the equality between the real filtering medium's porosity and the model is to be observed, this will imply the need to assume a certain positioning of the fictive spheres.

According to Schlichter the porosity is:

$$n = 1 - \frac{\pi}{6(1-\cos\delta)\sqrt{1+2\cos\delta}} \tag{23}$$

Where δ is the rhombohedron angle, this factor having the following limit-values:

- maximum for $\delta = 90^0$, cubic positioning, n= 0,4764
- minimum for $\delta = 60^0$, rhombohedral positioning, n= 0,2595.

This fictive material made of homogenous spheres implies a mutual punctual contact. Therefore $A_d = A_s$ and the average geometric tortuosity.

$$\tau = \frac{1+\cos\delta}{\sin\delta\sqrt{1+2\cos\delta}} \tag{24}$$

with values between $\tau = 1{,}02.....1{,}22$.

For the real permeable material the dynamic specific area can be sometimes lesser than the static specific area ($A_d / A_s \le 1$).

If for energy losses the same mechanism is accepted as for 3.1, the equations (17…20), where *d* is the solid particle's diameter we shall have the next result:

$$M = \frac{\lambda_t \rho \tau^3}{2dn^2} \tag{25}$$

$$N = \frac{32\mu\tau^2}{nd^2} \tag{26}$$

With factors *M* and *N* computed from the statistic processing of pressure gradient measurements, as a function of apparent velocity V_0 (at macroscopic scale) and porosity *n*, the result will be the next:

$$\tau = \left[\frac{128\mu \cdot n \cdot M^2}{\lambda^2 \rho^2 N}\right]^{1/4} \tag{27}$$

and

$$d = \left[\frac{32\mu\tau^2}{n \cdot N}\right]^{1/2} \tag{28}$$

For the calculations, there is need to observe the equality between the real porosity and the model's porosity, hence the result being the positioning of model's spheres. Afterwards, the macroscopic hydraulic gradient is to be measured as a function of the apparent velocity V_0. This, combined with equations (27) and (28), will lead to the diameter of the equivalent spheres *d* and also the tortuosity τ .

The tortuosity values within equations (24) and (27) may differ because for the real permeable material $A_d / A_s \le 1$, for the model $A_d / A_s = 1$, and the average length of the particles' trajectories may differ from the average geometric length within equation (24).

4. CONCLUSIONS

This paper describes two geometric models that have been developed in relation to the post–Darcy filtration: the *thin tubes fascicle model* and the *equivalent homogenous solid spheres model*. By means of measurements of the hydraulic gradient as a function of apparent velocity (at macroscopic scale) certain microscopic filtration hydraulic and geometric factors are computed (this being the diameter, the tortuosity, the real velocity, Re_{dp}). If all these parameters are known the filtration study will become closer to reality

(permanent and non-permanent filtration). The calculation of filtration parameters is sensitive to the next factors: the considered porosity *n* and the microscopic diameter *d*.

5. REFERENCES

[1] Forchheimer, P., 1914 *Hydraulic*, Leipzig und Berlin Druck und Verlang von B.G.Teubner.
[2] Barabasi, A.-L. and Stanley, H.E. 1995, *Fractal concepts in surface growth*, Cambridge University Press.
[3] Batrouni, G.G. and Hansen, A.1998, "*Fracture in three – dimensional fuse networks*", Physical Review Letters 80 (325), 2.
[4] Ergun, S., 1952, *Fluid flow through packed columns*, Chemical Engineering Progress, vol.48, nr.2, 89-94.
[5] Oron, A.P. and Berkowitz, B. 1998, "*Flow in rock fractures: the local cubic law assumption reexamined*", Water Resources Reasearch 34 (11), 2811-2825.
[6] Comiti, J., Renaud, M., 1989, *A new model for determinating of flow regimes in various porous pressure drops measurements: application to beds packed with parallelipipedal particles*. Chem. Eng. Sci., 44, 1539-1545.
[7] Abbood, D., W., 2009, *An analytical model study for flow throught porous media*, 17th International Water Technology Conference, IWTC, Egypt.
[8] Aulisa, E., Bloshanskaya, L., Hoang, L., Ibragimov, A., 2009, *Analysis of generalized Forchheimer flows of compressible fluids in porous media*, Inst. for Math. and H. Appl., University of Minnesota, www.ima.uma.edu.
[9] xxx, 2009, *Cercetări asupra curgerilor turbulente în medii poroase permeabile rigide*, Grant 2298, Contract 589/2009. UTI.-CNCSIS.
[10] Florea, J., Panaitescu, V., 1979, *Mecanica Fluidelor*, Editura Didactică şi Pedagogică, Bucureşti.
[11] Guardo, A., et all., 2004, *CFD flow and heat transfersimulation in nonregular packing for fixed bed equipement design*, Ind. Eng. Chem. Res. Vol.43.
[12] Pedras, M.H.J., Lemons, M.J.S., 2001, *Macroscopic turbulence modeling for incompressible flow through undeformable porous media*, Int.J.Heat and mass transfer, vol. 44.
[13] Bartha, I., Marcoie, N., Toacă, D., Toma, D., Gabor, V., Molnar A., Lupuşoru A. – *The free level uniform post – Darcy filtration through a sphre – made homogenous medium*, Environmental Engineering and Management Journal, ISSN 1582-9596;
[14] Bartha, I., Marcoie, N., 2010, *Post Darcy filtration though rigid, permeable media and real situations in engineering practice*, Analele Univ."Ovidius" Constanța, Anul XII 2010, ISSN 1584-5990.
[15] Bartha, I., Marcoie, N., Toma, D., Gabor, V., Toacă, D., 2010, *Research of filtration through uniform geometry permeable material-glass spheres*, Analele Univ."Ovidius" Constanța, Anul XII (2010), ISSN 1584-5990.
[16] Herrman, H., and Roux, S., 1990, *Statistical models for the fracture of disordered media*, North – Holland.

Ovidius University Annals Series: Civil Engineering, Issue14, October 2012

EFFECTS OF OLT RIVER REGULATION ON THE CHANNEL MORPHOLOGY

Ioan Ilaş, Josif Bartha

Abstract – **This paper presents the morphological changes of the new, regularized Olt River channel upstream Tuşnad. Based on surveys, the channel deformations are quantified during operation, especially on depth without bed reinforcing.**

Hydraulic parameters changing are taking place in relation to the longitudinal slope and roughness modifications.

Upstream erosions and downstream silting are influencing the natural flow network stability, intakes operation, drainage arrangements operation from the dikes protected flood plane. The ground water table and the surroundings environmental conditions are influenced.

The need to complete transversal flow bed reinforcements and channel sides' protection is underlined.

Keywords – **Environmental effects, morphological change, new channel bed, river regulation.**

1. INTRODUCTION

The Olt River regulation and embanking, between Madaras and Tusnad within Ciuc basin and the drainage of the embanked flood plain within Ciuc basin began their operation in 1985, based on studies and designs completed since 1901 [1,5,6].

The embankments of the floodplain are interrupting the water bodies connectivity between the channel and the floodplain. Surface runoff by drainage systems or canals parallel to dikes are collected and convoyed to the river. The outlets to the emissary by one way check valves are control (to prevent floorings the embanked area).

2. BASIC DATA

The relief of Ciuc basin, on the analyzed water course, is located at 640 m up 780 m in altitude; is bordered by the Harghita (1800 m), Hasmas (1792 m) and Ciuc (1499 m) mountains.

The basin downstream by the natural apron from Tusnad Bai (made of hard rocks) is limited, the apron elevation being 637 m.

The relief is varied, and features a steppe-like configuration towards the Olt River Valley: mountains, pre-alpine hills, terraces and floodplain. The floodplain includes the meandered, drained sand banks, and swampy intermediary zones on which the main river's tributaries are split.

The climate is a mountain-type, sheltered one, typical for enclosed depressions, featuring annual average temperatures between 6 and 8°C, with variations on a range of 75°C (-35…30°C). The average yearly rainfall in

Manuscript received June 25, 2012. This paper is part of PhD thesis, Ioan Ilas, tutor Josif Bartha.

Ioan Ilaş PhD Student is with "Gheorghe Asachi" Technical University of Iasi, Faculty of Hydrotechnical Engineering, Geodesy and Environmental Engineering, 65 Prof. dr. docent Dimitrie Mangeron Street, 700050, Iasi, Romania (corresponding author to provide phone: +40232 270804; e-mail: ilas.ioan@yahoo.com).

Josif Bartha is with "Gheorghe Asachi" Technical University of Iasi, Faculty of Hydrotechnical Engineering, Geodesy and Environmental Engineering, 65 Prof. dr. docent Dimitrie Mangeron Street, 700050, Iasi, Romania (e-mail: i_bartha@yahoo.com).

ISSN-1584-5990

the depression is 602 mm, ranging between 580 and 800 mm, depending on altitude. The annual potential evaporation reaches 564 mm. Thus, the annual water balance represents an excess of 37 mm.

From a geological standpoint the floodplain consists of sandy clay, mud, gravel and peat. The peat layer has a thickness between from 1,55 and 1,75 m and it is covered by thin soil (0,25 m). The underground includes more or less permeable geological strata (gravels, sands, loams or clays).

Soils formed in depression bioclimatic conditions are clayish alluvial soils and alluvial soils with ground water table at small depth of different types.

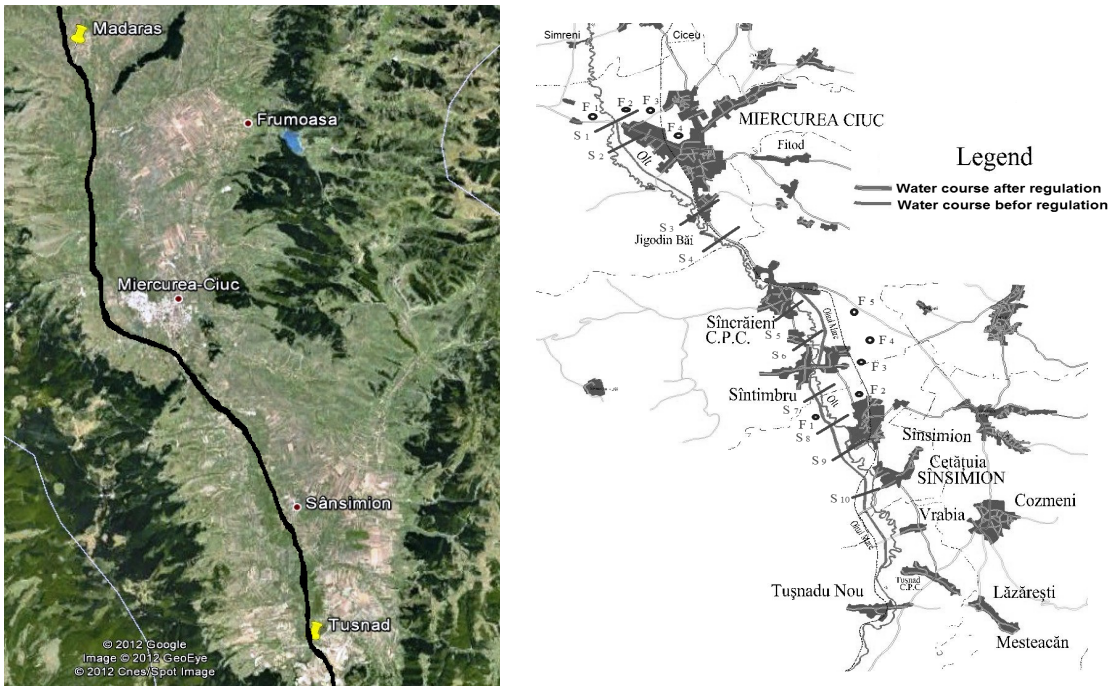

Fig. 1. The Olt River course before and after regulation, between Madaras and Tusnad

Hydrological, the Olt River, on its regulated sector, receives several tributaries, such as: Madars, Racu, Var, Fitod, Fisag, Tusnad and Mitaci. The river network average density is 2,2 km/km^2.

Olt River hydrological flow rates, with different computed probabilities, are listed in **Table 1**.

Table 1. Olt River characteristic flows

River	Section	Q_m (m^3/s)	Q_{max} (m^3/s) for various probabilities						
			0,1%	0,5%	1%	2%	3%	5%	10%
Olt	Downstream the V.Mădăraş confluence	2,45	280	205	170	147	120	105	85
Olt	Sâncrăieni station	4,76	290	210	180	140	120	105	90
Olt	Tuşnad Băi	6,79	605	440	360	305	255	205	160

Average annual flow variation is shown in **Fig. 2**.

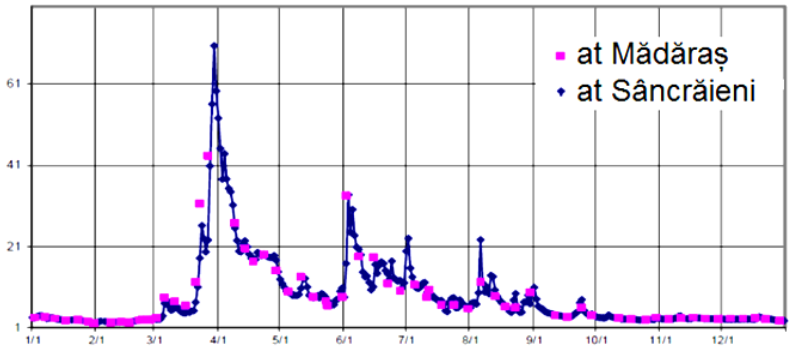

Fig. 2. Olt River: Average flow rate hydrograph on

Hydro-geologically, the Olt River flood plane is characterized by a layer of ground water (having a thickness of 0,4….1,4 m and a filtration coefficient of 1,5….16 x 10^{-5} m/s), and a pressurized layers of groundwater of different thicknesses and having a filtration coefficient between 2,7 x 10^{-4} and 6,1 x 10^{-4} m/s. The two layers are in connection in the area of tributaries valleys.

3. THE REGULATION OF OLT RIVER WITHIN THE CIUC DEPRESSION

The regulation works consist of: new river bed completed between Miercurea Ciuc and Tusnad (**Fig. 1**, sections S1…..S10), correction and consolidation of the channel, and river embankments. Tributaries beds within the built up areas have been rectified, being provided with concrete or rock control walls and embankments for protection against back water.

The new bed's cross section is different within and outside the built up areas (**Fig 3** and **Table 2**), the important sectors being sideways protected (**Fig. 4**).

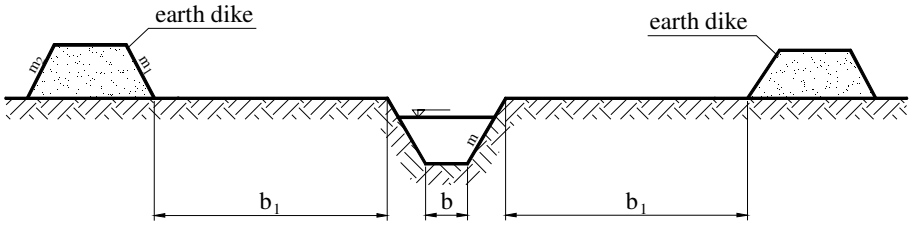

Fig. 3. Olt River: Regulated cross section

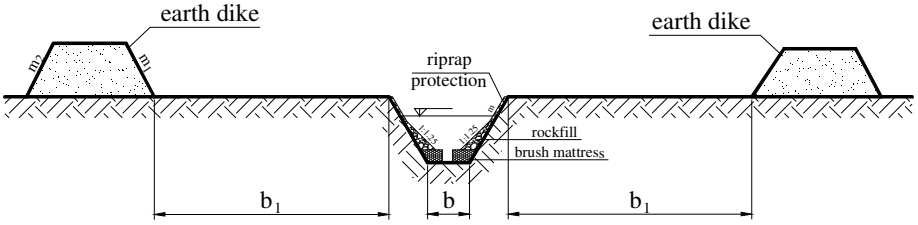

Fig. 4. Olt River: Regulated and consolidated section

Table 2. Characteristic construction elements on the Olt River

Localization	New river channel	b (m)	b_1 (m)	c (m)	m	m_1	m_2	L (m)
inside localities	consolidated	10…12	50	4	2	3	2	240
	non-consolidated	10….12	50	4	2	3	2	2770
		20	3	4	2	3	2	330
outside localities	non-consolidated	10…20	≥ 50	4	2	3	2	17.800
	nature rectified	-	≥ 50	4		3	2	880

The bank protection consist of brush mattress (45 cm thickness, 3m width), a filling of rock with a thickness of 1,5 m (30 cm over the average water level), made up of natural rocks having a slug mass between 150 and 500 kg for each rock piece.

The riverbed bank is protected with a 30 cm thickness riprap layer placed on a 15 cm thick ballast bed (**Fig. 4**) [2, 6].

The tributaries' channels inside localities have regulation works on a length of 750 m. The channel depth is variable, but overall may convey the average discharge with a minimum 30 cm safety depth.

The earth banks have a trapezoidal shape (**Fig. 3** and **Fig. 4**, respectively **Table 2**) and the total length within Ciuc depression reaches 78 km (21,45 km on the studied sector).

For all the Olt River constructions the next calculation probabilities have been considered:

- inside localities – design value: 5 %, checking value: 1%
- outside: 10%, respectively 3%.

The Olt River regulation between Miercurea Ciuc and Tusnad (section S1…S10) has been shortened by 34 % its total length. The total river length has decreased from 32,48 km down to 21,44 km due to the route of the new channel.

The new channel longitudinal slop nearby to Miercurea Ciuc is 1,24 %, than, to Sansimion 0,8%, and downstream to Tusnad 0,6 % (**Fig. 5**).

The new channel roughness is estimated for an n = 0,03 (roughness coefficient).

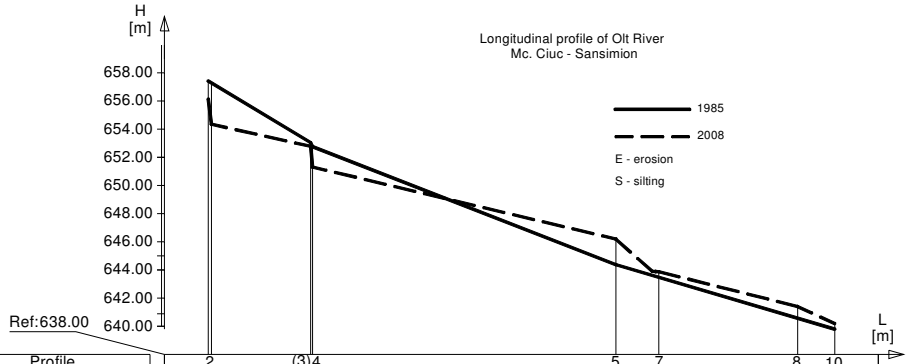

Profile		2	(3)	4			5	7		8	10
Distance [m]	partiale		3395		10450		1470		4750		1270
	cumulate	105		3500			13950	15420		20170	21440
Bed level (CF) [m]	1985	657.30		653.05			644.39	643.51		640.66	639.90
	2008	654.36	(652.79)	651.32			646.20	643.88		641.41	640.11
Slope [‰]	1985		1.24		0.8		0.6	0.6		0.6	
	2008		0.50		0.5		1.6	0.5		1.0	
Channel evolution	Δh	- 2.94		- 1.41			+ 1.21	+ 0.34		+ 0.75	+ 0.21
		E		E			S	S		S	S

Fig. 5. Olt River: longitudinal profile on the analyzed sector (Miercurea Ciuc –Sansimion)

4. THE BEHAVIOR OF RIVER REGULATION AND EMBANKMENT BETWEEN 1985-2008

The consequences of that shortening generated by the new Olt channel and the roughness decreasing have been and increasing of the general longitudinal slope and of the average velocity. A new river channel with shore protections, close to the intersection with communications (roods railway, etc) has been provided. No bottom conservation construction elements have been designed nor completed, in spite of fact that two intakes on the sector were in operation.

After floods the bottom erosion upstream, silting downstream and shore erosions, deformations were registered. The operation of an industrial water intake within S3 section, due to channel bed erosion in 1986, led to the need of a concrete threshold construction (**Fig. 6**). The threshold's elevation corresponds to the necessary intake level. The same, in the same way, a cross section with bank protection has been provided, by means of rock fillings and riprap mattresses.

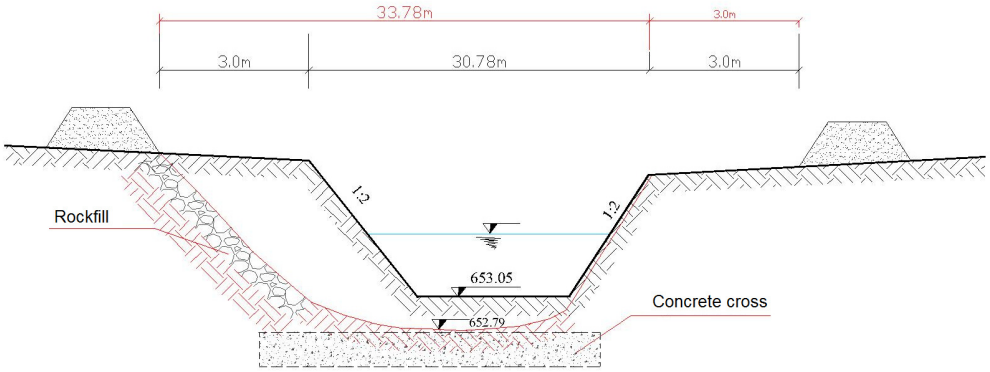

Fig. 6. Concrete transversal threshold within S3

On the double trapezoidal cross section of the embanked new channel strong erosions upstream (**Fig. 7**), shore erosion and bottom silting (**Fig. 8**) downstream took place. Limit of bed erosion and silting is nearby Sâncraieni location, between sections S4 and S5.

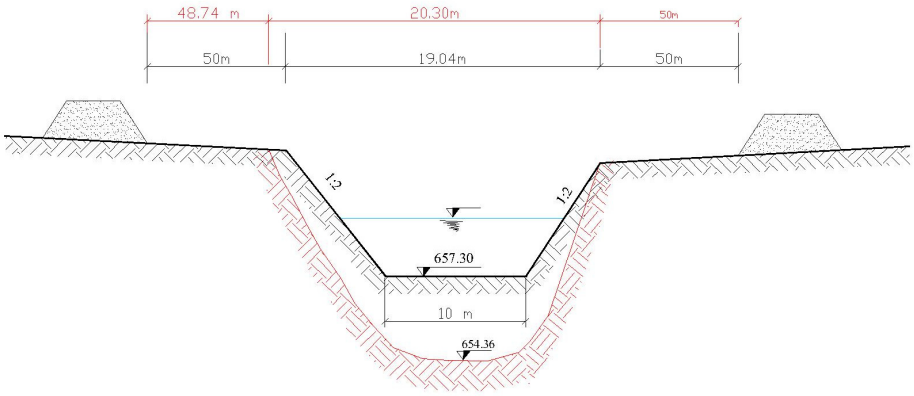

Fig. 7. Channel bed erosion upstream (S2)

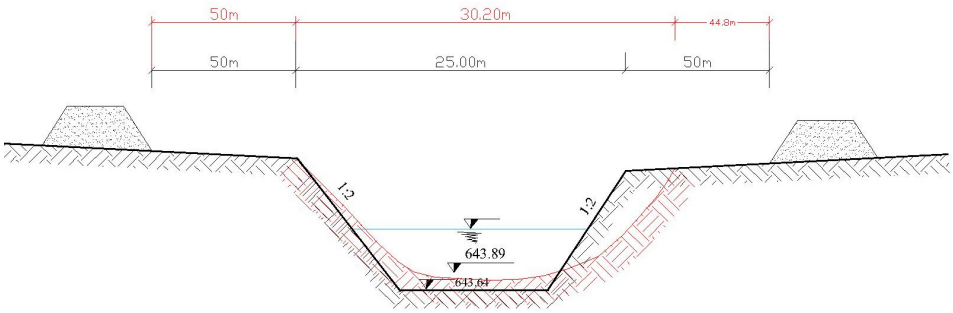

Fig. 8. Bed silting and sides erosions downstream (S6)

The morphological changing of the Olt River new channel along the interval 1985…2008 correspond to values shown in **Table 3** and **Fig. 5**.

Table 3. Characteristics of completed transversal sections (1985) and deformed ones (2008)

Section	Bottom level		Δh	Distance	i	b	b_1
S	CF (1985)	CF (2008)	(m)	(m)	‰	(m)	(m)
1	657,43	656,11	-1,29	0+000	1,25	10	10
2	657,30	654,36	-2,94	0+105	1,25	10	10
3	653,05	652,79	-0,26	3+500	1,25	10	3
4	652,76	651,32	-1,41	3+570	4,15	10	10
5	644,39	646,20	1,21	13+950	0,6	10	10
6	643,64	643,89	0,25	15+200	0,6	20	50
7	643,51	643,88	0,37	15+420	0,6	20	50
8	640,66	641,41	0,75	20+170	0,6	20	50
9	640,33	640,92	0,39	20+720	0,6	10	10
10	639,90	640,11	0,21	21+440	0,6	10	10

The upstream bed erosion took place along the channel's first 3570 m, the maximum deepening of the bottom being of 2,94 m; on the other hand, the downstream silting has led to a rising of channel bed by 1,21 m.

In 2011, downstream Sâncraieni, between sections S5…..S7, due de-silting actions, 60.000 m^3 of alluviums have been removed.

5. THE EROSION OF THE RIVER'S NEW CHANNEL: CAUSES, EFFECTS AND CONSEQUENCES

Due to radical regulation and embankment of the Olt River within Ciuc depression the new channel's section gained a double trapezoidal shape, its length being considerable reduced (34%), the upstream sector longitudinal slope increased up to 1,25 %, being reduced on downstream to 0,6 ‰.

These items, combined with roughness decreasing (regular contact surface of water and bed, large curves) led to a velocity increasing and, without channel bottom and sides consolidation, to river bed erosion (upstream) and bottom silting and sides erosion (downstream).

This phenomenon is normal and can be explained by the dynamics of the channel morphology that leads an instability of the bed [3, 4, 7].

Expressing the current potential power on unit length

$$P = \gamma Q \frac{\Delta h}{L} = \gamma QI \quad \text{(w/m)} \tag{1}$$

or the specific potential power (on unit surface):

$$P_s = \frac{P}{B} = \frac{\gamma Q I}{B} \quad \text{(w/m)} \qquad (2)$$

where: Q – the volume flow rate that fills the considered cross section;
Δh - water level difference on length L;
I – channel longitudinal slope;
B – channel width at the free water surface;
γ - the unit weight of the liquid,

the morphology dynamic tendency can be defined.

The limit of specific potential power of the river for anthrop interventions is Ps = 35 w/m^2.

Below this limit value the river bed is stable, but over it the river dynamics have the tendency to return to its initial characteristics. For Ps > 100 w/m^2 this tendency is more important.

The calculation of the Olt River specific potential power, for a river bed real profile, and for the maximum flow that the profile is able to convey are given in **Table 4**.

Table 4. Olt River specific potential power al Miercurea Ciuc

Channel	**h (m)**	**A (m^2)**	**P (m)**	**B (m)**	**I (‰)**	**Q (m^3/s)**	**Ps (w/m)**
River bed	3,1	66,38	27,78	25,45	1,25	132,5	67,2
At banks capacity	4,0	99,83	43,15	40,34	1,25	206,0	62,5

Without consolidation of the bed and sides, the new channel suffers important erosion (tendency to restore the initial slope and shape in plane). The new channel can be maintained only by thresholds and shore protection. Channel bed deformations imposed the building of a threshold and sides consolidation at the water intake zone, near sector S3. The eroded bed's slope tendency is to return to the initial one (≈ 5 ‰). Even between thresholds the slope has the tendency to return to the initial one but these can maintains the projected slope.

Erosion of the upstream sector bed has led to a decreasing of water level. These have major effect on the erosion base level on tributaries. The Olt River and its tributaries are providing the natural drainage of the zone (flood plain). Considering this, the decreasing of water level in rivers has the same influence on groundwater tables. So, the drainage systems built in a floodplain from Miercurea Ciuc to Sâncraieni lost their drainage role (bottom of the drainage channels being over the decreased groundwater table). These channels are collecting surface runoffs only and evacuate them into the emissary. These drainage channels are insufficiently equipped with level controllers, water being discharged too quickly and dry the peat layer on their depth.

Because of decrease the groundwater level (due to erosion on the river bed), and due to excessive operation of drainage canals, the peat layer is dried. Biochemical anaerobic processes turn themselves into aerobic ones, when flammable gases are released (methane), this leading to auto-ignition. The peat layer when burn smoldering is generating polluting gases, and lead to an air pollution of the zone **Photo 1** [9, 10].

Photo 1. Peat burning at Ciceu in 2011

6. CONCLUSIONS

The regulation of Olt river within the Ciuc depression, without a consolidation of the channel (bottom and sides), lead to an increasing of river slope and a decreasing of roughness, higher velocities and, as a consequence, to bed erosion (especially at bottom).

The erosion processes are presents upstream the river; downstream, due to silting, the river has a trend to return to the initial slope. These morphological processes are influencing the level of the erosion base of tributaries, and of the level's hydrograph, phenomena that finally are increasing the flooding danger. The river's shape instability requires consolidation of the channel for ensuring its maintenance (thresholds, stone riprap, rock fill gabions, etc).

The distance between the thresholds is of major importance in stabilizing the river.

7. REFERENCES

[1] ANAR, ABA, Olt, 2004, *Planul de management al bazinului hidrografic Olt*, Bucureşti, www.rowater.ro
[2] Băloiu, V., 1980, *Amenajarea bazinelor hidrografice şi a cursurilor de apă*, Ed. Ceres, Bucuresti.
[3] Brooks, A., 1988, *Rivers channelization. Perspectives for environmental management*, Ed. Wiley Interscience, ISBN 0471919799.
[4] Diaconu, S., 1999, *Cursuri de apă. Amenajare, impact reabilitare*, Ed. H.G.A., Bucureşti.
[5] ISCH, 1964, *Studii de hidrologie. Monografia hidrologică a bazinului hidrografic ale râului Olt*, vol. X, Bucureşti.
[6] ISPIF, 1974, *PE- Regularizarea, îndiguirea şi desecarea zonei Oltului Superior în depresiunea Racu-Miercurea Ciuc –Tuşnad, jud. Harghita, Sibiu*.
[7] Ichim, I. şi colaboratori, 1989, *Morfologia şi dinamica albiilor râurilor*, Editura Tehnică, Bucureşti.
[8] Van de Ven, G.P., 1993, *Man made lowlands. Hystory of water management and land reclamation in the Netherlands*, Uitqeverij Matrijs, Utrecht.
[9] Page, S.E., et all, 2002, *The amount of carbon released from peat and forest fires in Indonesia during 1997*, Nature 420.
[10] Rein, G., Cleaver, N., Ashton, C., Pironi, P., Torero, J.L, 2008, *The severity of smouldering Peat Fires and Damage to the Forest Soil*, Catena 74(3); 304-309.

Two-phase Flow over Stepped and Smooth Spillways: Numerical and Physical Models

Duangrudee Kositgittiwong, Chaiyuth Chinnarasri, and Pierre Y. Julien

***Abstract* –Numerical modeling of stepped spillways is very complicated and challenging because of the high roughness and velocity recirculation regions. Two types of multiphase flow models are used: a mixture multiphase flow model (MMF) and a volume of fluid multiphase flow model (VOF). In both models, the realizable k-ε model is chosen to simulate turbulence. The computational results are compared with large-scale experimental data from Colorado State University. The spillway was 1.22m wide and consisted of smooth, 25, and 50 horizontal steps. The discharge was varied from 0.20 to 3.28 m^3/s. The data series obtained for model comparison include; velocity profiles, energy dissipation, and characteristics of flow. Both models can satisfactorily simulate the flow pattern and the recirculation regions. The velocity profiles are more accurately simulated using the VOF model.**

***Keywords* – Smooth spillway, Stepped spillway, Numerical model, Physical model.**

1. INTRODUCTION

In recent years, there has been an increase in the rate of surplus or flood waters which cause high flow into the reservoirs. Due to the increase of water flow, the storage capacity may be exceeded. The dam spillways must be designed to release surplus or flood water and to avoid exceeding reservoir capacity. Gonzalez and Chanson [1] mentioned higher design flows that affect the insufficiency of the existing spillway capacity. A spillway is kind of hydraulic structure that is provided at storage and detention dams to release water that cannot be safely stored in the dam [2]. To be safe, the spillway must be capable of passing high flow without jeopardizing the dam. A stepped spillway is an important kind of spillway having profile made up of steps. It dissipates much more energy than other types of spillways when water is flowing over the spillway profile. According to Chanson [3], stepped spillways have been used for at least 1500 years. Historically, very active experimental research has been done on the air-water flow over stepped spillways, such as flow patterns, inception of air entrainment, air concentration, velocity field, pressure field and energy dissipation [4]. The engineers have normally investigated the flow through laboratory experiments on scaled down models of spillways. The complexity of the flow structure which includes complicated boundary conditions, the curved free surface, and the unknown scale effects has caused uncertainties in transposing the experimental results to prototype scales. With the development of computational fluid dynamics (CFD) and high-performance computers, complex multiphase flows can be simulated numerically and with validation the results can be trusted to be reliable.

Manuscript received August 15, 2012. This work was supported by the Thailand Research Fund/Royal Golden Jubilee PhD Grant (TRF/RGJ) under grant number PHD/0225/2548 and BRG5280001 and the National Research University Project of Thailand's office of the Higher Education Commission.

D. Kositgittiwong is with Water Resources Engineering & Management Research Center (WAREE), Department of Civil Engineering, King Mongkut's University of Technology Thonburi, Bangkok 10140, Thailand. (e-mail: duangrudee.k@gmail.com)

C. Chinnarasri is with Water Resources Engineering & Management Research Center (WAREE), Department of Civil Engineering, King Mongkut's University of Technology Thonburi, Bangkok 10140, Thailand. (phone: +662-470-9136-7; fax: +662-427-9063; e-mail: chaiyuth.chi@kmutt.ac.th).

P. Julien is with Department of Civil and Environmental Engineering, Colorado State University, Colorado 80523, USA. (e-mail: pierre@engr.colostate.edu).

ISSN-1584-5990

Given reduced time demand and lower cost of the numerical method than physical experiments, simulation of the stepped spillway overflow has a significant advantage.

The two well established and widely used computational methods are the finite difference and finite element methods. Tabbara et al. [2] used the finite element method to predict stepped flows at the small scale of experiments. In the upper part of the flume as well as in the bottom part steps were introduced along the chute such that the envelope of their tips followed the smooth spillway chute profile. Although the results of this study are encouraging, physical or laboratory measurements are still crucial for providing reference data. Benmamar et al. [5] developed a numerical model for two-dimensional boundary layer flow over a stepped channel with steep slope, which was based on the implicit finite difference scheme. The finite volume method, which has been extensively used to model a wide range of fluid-flow problems, was originally developed as a special finite difference formulation. Qian et al. [4] used a MMF model to simulate flows over a stepped spillway. The turbulence models those were investigated are realizable k-ε model, SST k-ω model, v^2-f model and LES model. There were 40 steps with the step height of 0.05 m. The study region comprised the 6^{th} to 12^{th} steps from the crest. The realizable k-ε model show the best agreement in simulating flow over stepped spillways. Dong [6] studied numerical simulation of skimming flow over mild stepped channel. The channel consisted of 40 steps with the ramp angle, θ of 10^o and 20^o. All air boundaries were defined as pressure boundaries with zero pressure specified. Smooth channel flow was also simulated to compare the hydraulic characteristics of the stepped channel flow with the smooth one. Chen [7] used the k - ε turbulence model to simulate the complex turbulence overflow. Their first five steps were varied while the size of the rest were 0.06 m high and 0.045 m long. The study indicated that the turbulence numerical simulation is an efficient and useful method for the complex stepped spillway overflow.

Most of the previous studies focused on the small scale stepped spillways and tested discharge. Since 1966, the possible scale effects for steep spillways had been already mentioned [8]. Due to the viscosity and surface tension play an important role in highly turbulent air-water flow, so, only Froude similitude is not enough to study flow in stepped spillway without the scale effects. For the true similarity, the Froude similitude can be used when the step height >2 cm, Reynolds number $>10^5$ and Weber number ≥100 [9, 10, 11]. Therefore, large scale of stepped spillway is studied for both experiments and numerical model. Also due to less time demand and lower cost of the numerical method than that of experiments, this study will be emphasized on numerical model to attest that numerical model can be used compared with large scale experiments. The flow pattern and flow characteristics, flow profiles along the spillway, velocity profiles, and air concentration profiles, were collected from the experiments which consist of nappe flow and skimming flow. The VOF and MMF were used as a multiphase flow model to compare the better one using with large scale experiments.

2. NUMERICAL MODEL

The stepped spillway was modeled as shown in Fig. 1. For each case studied, there are 230,565 quadrilateral cells with 232,109 nodes created. Quadrilateral meshes with 0.1×0.1 m^2 are used. The boundary conditions in this study are no-slip wall, outlet as a pressure outlet type, free surface as a pressure inlet type, air inlet and water inlet as a velocity inlet type. The inlet water velocity is set as uniform at the inlet. Then water flows into the tank before approaching the spillway. The segregated solver was used because it is multiphase flow with 2 materials, water and air, each with different velocity. The VOF and/or MMF models were used to deal with the multiphase fluids.

2.1 The volume of fluid model (VOF)

The VOF model, which was completely reported by Hirt and Nichols [12], is based on a concept of a fractional volume and the fact that the phases are not interpenetrating. The fields for all variables and properties are shared by the phases and represent volume-averaged values, as long as the volume fraction of each of the phases is known at each location. Thus the variables and properties in any given cell are either purely representative of one of the phases, or representative of a mixture of the phases, depending upon the volume

fraction values. The standard interpolation schemes are used to obtain the face fluxes when a cell is completely filled with one phase while the geometric reconstruction scheme is used when the cell is near the interface between two phases. In each control volume, it must be filled with either a single fluid phase or a combination of phases while the volume fractions of all phases sum to unity. The same set of governing equations describing momentum and mass in a single-phase flow is solved throughout the domain, and the resulting velocity field is shared among the phases. The conservation equations, (1) and (2), are dependent on the volume fractions of all phases through the properties of density, ρ and dynamic viscosity, μ. The velocity in x_i and x_j directions are defined by u_i and u_j, respectively. The pressure, P, time, t, turbulent dynamic viscosity, μ_t, are also defined in these equations.

$$\frac{\partial \rho}{\partial t}+\frac{\partial \rho u_i}{\partial x_i}=0 \tag{1}$$

$$\frac{\partial \rho u_i}{\partial t}+\frac{\partial \rho u_i u_j}{\partial x_j}=-\frac{\partial P}{\partial x_i}+\frac{\partial}{\partial x_j}(\mu+\mu_t)\left(\frac{\partial u_i}{\partial x_j}+\frac{\partial u_j}{\partial x_i}\right) \tag{2}$$

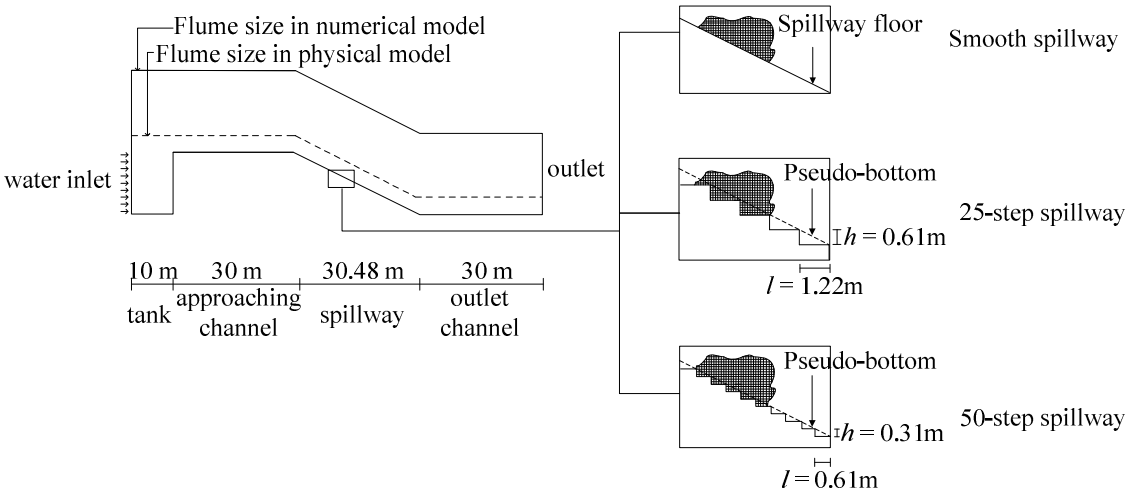

Fig. 1. Schematic diagram of the stepped spillway

2.2 The mixture multiphase flow model (MMF)

The MMF is a simplified multiphase model that can be used where the phases move at different velocities, but assume local equilibrium over short spatial length scales. The mixture model can model *n* phases by the conservetion equations for the mixture and the volume fraction equation for the secondary phases, as well as algebraic expressions for the relative velocities. The continuity equation for the mixture, (3), is defined by velocity of mixture, $\vec{v}_m=\frac{\sum_{k=1}^{n}\alpha_k\rho_k\vec{v}_k}{\rho_m}$, and density of mixture, $\rho_m=\sum_{k=1}^{n}\alpha_k\rho_k$. The fraction, density, and velocity of each phase can be defined by α_k, ρ_k, and $\vec{v}_k$, respectively.

$$\frac{\partial}{\partial t}(\rho_m)+\nabla\cdot(\rho_m\vec{v}_m)=0 \tag{3}$$

The momentum equation for the mixture, (4), can be obtained by summing the individual momentum equations for all phases. The dynamic viscosity, $\mu_m = \sum_{k=1}^{n} \alpha_k \mu_k$, and the velocity difference between each phase and mixture, $\vec{v}_{dr,k} = \vec{v}_k - \vec{v}_m$, are also defined.

$$\frac{\partial}{\partial t}(\rho_m \vec{v}_m) + \nabla \cdot (\rho_m \vec{v}_m \vec{v}_m) = -\nabla P + \nabla \cdot \left[\mu_m \left(\nabla \vec{v}_m + \nabla \vec{v}_m^T\right)\right] + \rho_m \vec{g} + \nabla \cdot \left(\sum_{k=1}^{n} \alpha_k \rho_k \vec{v}_{dr,k} \vec{v}_{dr,k}\right) \quad (4)$$

The differences between the models are the manner in which they handle phase interpenetration and the phase velocities. With these two differences, the initial boundary condition must be different. The air velocity in mixture model should be set at zero and then reduced to homogeneous multiphase model while the air velocity in VOF model should be the same as water velocity. Flow over different kinds of spillways produce different patterns and have different effects.

For operating conditions, the specified operating density, 1.225 kg/m^3, was used with gravitational acceleration, -9.81 m/s^2, and operating pressure 101,325 Pa. The boundary conditions were set by using water velocity at water inlet. The Realizable k-ε model [13], which is a relatively recent development from the standard k-ε model, was used to simulate turbulence. The modeled transport equations for turbulent kinetic energy, k, and turbulent dissipation rate, ε, in the realizable k-ε model are (5) and (6), respectively. The generation of k due to the fluid shear, $G_k = \mu_t S^2$, generation of k due to buoyancy, G_b, effect of compressibility on turbulence, Y_M ,source terms of kinetic energy, S_k, $C_1 = \max\left[0.43, \frac{\eta}{\eta+5}\right]$, $\eta = S\frac{k}{\varepsilon}$, $S = \sqrt{2S_{ij}S_{ij}}$, source terms of dissipation rate, S_ε, C_2 = 1.9, kinematic viscosity, ν, $C_{1\varepsilon}$ = 1.44, relation of flow velocity in x_i and x_j -direction, $C_{3\varepsilon} = \tanh\left|\frac{v}{u}\right|$ are defined in both equations.

$$\frac{\partial}{\partial t}(\rho k) + \frac{\partial}{\partial x_j}(\rho k u_j) = \frac{\partial}{\partial x_j}\left[\left(\mu + \frac{\mu_t}{\sigma_k}\right)\frac{\partial k}{\partial x_j}\right] + G_k + G_b - \rho\varepsilon - Y_M + S_k \quad (5)$$

$$\frac{\partial}{\partial t}(\rho \varepsilon) + \frac{\partial}{\partial x_j}(\rho \varepsilon u_j) = \frac{\partial}{\partial x_j}\left[\left(\mu + \frac{\mu_t}{\sigma_\varepsilon}\right)\frac{\partial \varepsilon}{\partial x_j}\right] + \rho C_1 S_\varepsilon - \rho C_2 \frac{\varepsilon^2}{k + \sqrt{\upsilon\varepsilon}} + C_{1\varepsilon}\frac{\varepsilon}{k} C_{3\varepsilon} G_b + S_\varepsilon \quad (6)$$

3. PHYSICAL MODEL

The experiments were obtained using an outdoor testing facility located at Colorado State University Engineering Research Center tested by Ward [14]. The facility permits large scale experiments so the water was supplied from nearby Horsetooth Reservoir. The concrete chute is approximately 34.14 m long, 1.22 m wide, and 1.52 m deep on a 2:1 (horizontal: vertical) slope and has a total height of 15.24 m. Plexiglas windows with the size of 1.22 m by 1.22 m were installed at five locations in the dividing wall to provide observation of flow.

The spillways can be divided into 3 groups; smooth, 25 and 50 steps. The 25-step spillway height, h, is 0.61 m and length, l, is 1.22 m. The data on the 4th, 8th, 12th, 16th, and 20th steps were measured, perpendicular to the pseudo-bottom. The 50-step spillway height, h, is 0.31 m and length, l, is 0.61 m. The data on the 7th, 15th, 23th, 31th, and 39th steps were measured, perpendicular to the pseudo-bottom. The Characteristics of flow over spillways are shown in Table 1.

Air concentration and velocity instrumentation were mounted on a point gage and carriage system. All profiles were taken along the centerline of the flume. The lowest points were taken at approximately 0.015 m from the tip of the step. The highest points were taken where both instruments measured data that was near the dry-air readings and visually appeared almost out of the flow. Videotape recording and photographs were used to collect the flow pattern at the overtopping crest and along the spillway. Flow condition in this study may be described as high-velocity, turbulent, two-phase flow. The probe is sturdy and provides a means of continuous back flushing to ensure a single density fluid within the Pitot tube. Velocity from the back-flushing Pitot tube is determined by the difference in pressures at the kinetic and static ports while continuously back flushing to prevent air bubbles from entering the instrument. Therefore, a balance between ensuring that air does not enter the Pitot tube and the sensitivity of the pressure difference must be found.

Table 1. Characteristics of flow over spillways

Parameters	Smooth spillway				25-step spillway					50-step spillway				
	$S_{0.57}$	$S_{1.13}$	$S_{1.70}$	$S_{2.27}$	$T_{0.57}$	$T_{1.13}$	$T_{1.70}$	$T_{2.27}$	$T_{3.28}$	$F_{0.20}$	$F_{0.60}$	$F_{1.16}$	$F_{1.70}$	$F_{2.27}$
Discharge (m^3/s)	0.57	1.13	1.70	2.27	0.57	1.13	1.70	2.27	3.28	0.20	0.60	1.16	1.70	2.27
Critical depth (m)	0.28	0.45	0.58	0.71	0.28	0.45	0.58	0.71	0.91	0.14	0.29	0.45	0.58	0.71
y_c/h	-	-	-	-	0.46	0.73	0.96	1.16	1.48	0.46	0.96	1.48	1.91	2.32
Flow regime	-	-	-	-	NA	NA	SK	SK	SK	NA	SK	SK	SK	SK

Remarks: NA is Nappe flow, SK is Skimming flow

4. RESULTS AND SIGNIFICANCES

4.1 Flow characteristics on step

For the flow regime, Chinnarasri and Wongwises [15] proposed the minimum critical flow depth required for the onset of skimming flow on horizontal and inclined steps for $0.10 \le \frac{h}{l} \le 1.73$, with θ = angle of the upward inclined step in degrees, is

$$\frac{y_c}{h} = (0.844 + 0.003\theta)\left(\frac{h}{l}\right)^{-0.153+0.004\theta} \tag{7}$$

The maximum critical flow depth for the nappe flow regime is

$$\frac{y_c}{h} = 0.927 - 0.005\theta - 0.388\left(\frac{h}{l}\right) \tag{8}$$

For the present study, at 0.57 m^3/s and $\frac{y_c}{h} = 0.46$, nappe flow existed with ponded water in the interior of the step beneath a cascading free jet. At 1.13 m^3/s, with $\frac{y_c}{h} = 0.73$, partial impact of the flow near the end of step and incomplete filling of the step cavity suggest a partial nappe flow regime. The condition of skimming flow was first observed at 0.37 m^3/s or greater. Therefore, the flow regime at discharges of 2.83 and 3.28 m^3/s, which $\frac{y_c}{h} = 1.34$ and 1.48, respectively, were skimming flow. The complete submergence of the steps with water flowing down the slope as a coherent stream cushioned by recirculating vortices in the interior of the step was

found. However, the general flow conditions were extremely turbulent along the entire spillway with erratic flow patterns and significant splash occurring at all flow rates.

The flow direction, and location of the recirculating vortices on the step from the simulation both from VOF and MMF models are similar. There are two zones; lower and upper zones, along the spillway. Closing to the step is lower zone with the recirculating vortices rotates clockwise and is located in the triangular zone of the step corner. The upper zone is far from the step and drops of water flow through the air. The results for the VOF model calculations can separate the air from the water flow so the connected surface between air and water can be seen clearly and the flow direction of water flow can be shown.

4.2 Velocity profiles

For the velocity profiles tend to have the same shape beginning with velocity gradually increasing from the bed until a maximum velocity gradient is reached. At some point in the upper region of the depth, an immediate change is observed where the velocity abruptly increases or decreases. Velocity profiles similar to this shape have been observed in several studies of stepped spillway flow Flow conditions in the upper region consisted of a highly irregular, wavy surface above which large particles of water ejected from the main flow. It was hypothesized that shear stress develops from increased resistance on these particles due to atmospheric drag and the change in momentum and the return of particles back to the main flow results in a loss of velocity.

For both nappe flow and skimming flow, the VOF model shows better agreement with measurements compared to the MMF model. The velocity profiles for the discharges of 0.57 m^3/s, nappe flow, and 3.28 m^3/s, and skimming flow on the 16th step are shown in the Fig. 2.

A comparison of the velocity results from the numerical model and experiments shows that with a nappe flow regime, the maximum error in their values mainly amount to 30% in the zone upper when 0.10 m from the floor bed of the spillway. For a skimming flow regime lower than 0.20m, the error is quite high as well as the one from nappe flow while the maximum error is not more than 27% in the upper zone. Given the grid size of 0.1×0.1 m^2 for the numerical model with the finite volume method, the maximum error is from the point that is located on the center of the cell, at 0.05 m. The results of the lower zone, therefore, are interpolated from the boundary of the cell. With this reason, the error from the floor to the depth 0.20 m is quite high.

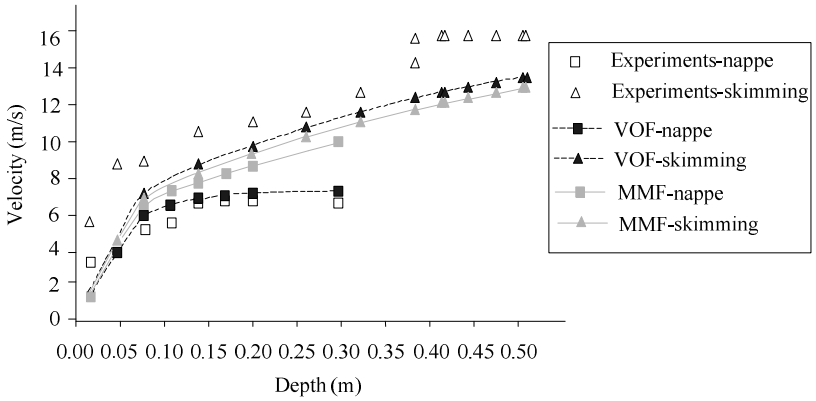

Fig. 2. Velocity profiles on the 16th step of 25-step spillway

4.3 Energy dissipation

The energy dissipation can be observed and calculated from the energy between the inlet section at the approach channel of spillway, E_0, and any section downstream, E_i. From many previous studies, the energy dissipation, $\frac{E_L}{E_0}$, is one of the dimensionless parameter which is widely used. The energy loss, E_L, is the difference between energy at the inlet section, E_0, and energy at any section, E_i. It can be written as $E_L = E_0 - E_i$.

To consider on the inlet discharge on stepped and smooth spillways, Fig. 3. shows the energy dissipation at the last station for both step and smooth spillways. The last observed station for smooth spillway is 25.76 m apart from the inlet and the 20th and 39th step for 25 and 50-step spillway, respectively. The relative length, which is the ratio between the distances from inlet to station over the spillway length, for all of those stations is 0.75. It is shown that for the same spillway, the energy dissipation decreases when the discharge, q, increases. The energy dissipation for the smooth spillway is rapidly decreased with increasing of discharge while the one for stepped spillway is gradually decreased. It can be stated that the stepped spillway is better used for higher design discharge than the smooth one because more energy can be dissipated due to the macro roughness of the steps.

Consideration on the certain discharge, the results indicate that a great amount of energy dissipation is occurred in a stepped spillway. It is also shown that for a given height, the energy dissipation increases when the number of steps increases. The results can be compared with the study from Rad and Teimouri [16] and the same trend is found as shown in Fig. 4. The spillway slope [16] was 26.6°, the number of steps was 32, and the Reynolds number was 10^5. The trend of results by Rad and Teimouri (2010) which $0.04 \le \frac{y_c}{ih} \le 0.13$ fits very well with the results from the present study which $0.02 \le \frac{y_c}{ih} \le 0.60$. Because each step acts as a macro roughness, the more steps can cause the thickness of turbulent boundary layer and more flow resistance and also significantly causes more energy dissipation. However, with high roughness, Chanson [3] reported the skimming flow will become fully developed and the stepped spillway behaves like a smooth spillway.

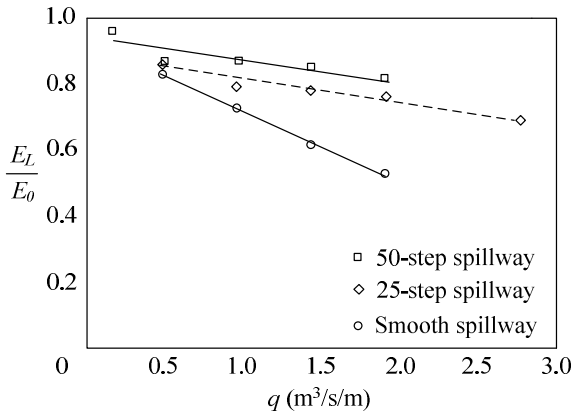

Fig. 3. Energy dissipation near the outlet

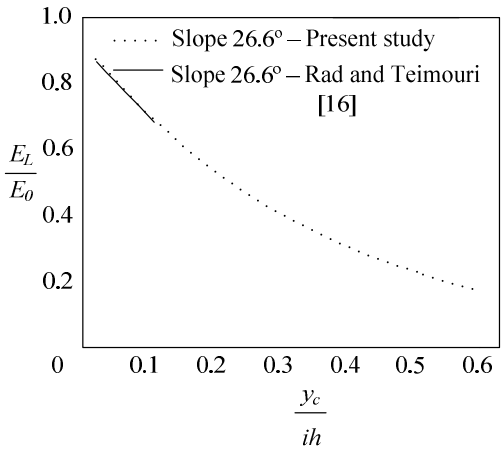

Fig. 4. Comparison of energy dissipation with previous studies

5. CONCLUSIONS

A numerical model using different multiphase flow models, VOF and MMF model, is used to study and compare the flow over a stepped spillway. The data from large-scale experiments are used to calibrate and verify the model. The grid size of quadrilateral meshes of 0.1×0.1 m^2 were used in the numerical model. For nappe flow, there is only an air pocket which is not clearly seen from the model. According to the simulation results for skimming flow, it is obvious that there is a recirculating vortex in the corner of the step, which is called lower zone, verified by the measurements. The upper zone is a wavy water surface in which air is trapped in the surface. The point of inception can be found in MMF model but without recirculating vortices shown on the step.

For the velocity profiles, they tend to have the same shape beginning with velocity gradually increasing from the bed until a maximum velocity gradient is reached. For both nappe flow and skimming flow, the VOF model shows better agreement compared to the MMF model. The maximum error in their values was 30% in the zone greater than 0.10 m from the floor bed of the spillway. For a skimming flow regime, the maximum error is not more than 27% in the upper zone. The energy dissipation from stepped spillways is compared with the smooth spillway. It is also compared with the previous studies and the same trend was found.

6. ACKNOWLEDGMENTS

The authors thank Professors James F Ruff and Robert N Meroney from Colorado State University for their supporting data, facilities and recommendations.

7. REFERENCES

[1] Gonzalez, C.A. and Chanson, H. 2006. Air entrainment and energy dissipation on embankment spillways. Proceedings of the International Symposium on Hydraulic Structures, IAHR Symposium, 12-13 October, Ciudad Guayana, Venezuela.

[2] Tabbara, M., Chatila, J. and Awwad, R. 2005. Computational simulation of flow over stepped spillways. Computers and Structures, Vol.83, pp.2215–2224.

[3] Chanson, H. 1994. Hydraulics of skimming flows over stepped channels and spillways. Journal of Hydraulic Research, Vol. 32, No.3, pp.445-460.

[4] Qian Z.D., Hu, X.Q., Huai, W.X. and Amador, A. 2009. Numerical simulation and analysis of water flow over stepped spillways. Science in China Series E:Technological Sciences, Vol.52, No.7. pp.1958-1965.

[5] Benmamar, S., Kettab, A. and Thirriot, C. 2003. Numerical simulation of turbulent flow upstream of the inception point in a stepped channel. Proceedings of 30th IAHR Congress, 24-29 August, Thessaloniki, Greece.

[6] Dong, Z.Y. and Lee, J.H. 2006. Numerical simulation of skimming flow over mild stepped channel. Journal of Hydrodynamics Series B, Vol.18, No.3, pp.367-371.

[7] Chen, Q., Dai, G. and Liu, H. 2002. Volume of fluid model for turbulence numerical simulation of stepped spillway overflow. Journal of Hydraulic Engineering, Vol.128, No.7, pp.683-688.

[8] Henderson, F.M. 1966. Open channel flow, Macmillan, New York.

[9] Boes, R. and Hager, W.H., 2003. Two-phase characteristics of stepped spillways. Journal of Hydraulic Engineering, Vol.129, No.9, pp.661-670.

[10] Gonzalez, C.A. and Chanson, H., 2004. Scale Effects in Moderate Slope Stepped Spillways. Experimental Studies in Air-Water Flows. In: Hubert Chanson and John Macintosh, 8th National Conference on Hydraulics in Water Engineering, 13-16 July, Australia.

[11] Chanson, H. and Gonzalez, C.A., 2005. Physical Modelling and Scale Effects of Air-Water Flows on Stepped Spillways. Journal of Zhejiang University, Vol.6A, No.3, pp.243-250.

[12] Hirt, C.W. and Nichols, B.D., 1981. Volume of Fluid (VOF) Method for the Dynamics of Free Boundaries. Journal of Computational Physics, Vol.39, No.201, pp.201-225.

[13] Shih, T.H., Liou, W.W., Shabbir, A., Yang, Z. and Zhu, J., 1995. A new k-ε eddy viscosity model for high Reynolds number turbulent flows. Computers and Fluids, Vol.24, No.3, pp.227-238.

[14] Ward, J.P., 2002. Hydraulic design of stepped spillways, Dissertation for the degree of doctor philosophy, Colorado State University, 245pages.

[15] Chinnarasri, C. & Wongwises, S. 2004. Flow regimes and energy loss on chutes with upward inclined steps. Canadian Journal of Civil Engineering, Vol.31, No.5, pp.870–879.

[16] Rad, I.N. and Teimouri, M., 2010. An investigation of flow energy dissipation in simple stepped spillways by numerical model. European Journal of Scientific Research , Vol.47, No.4, pp.544-553.

Flow Modeling with Free Level in the Polycentric Channels

Luca M. Mihail, Tamasanu Fabian, Luca M. Alexandru Lucian

***Abstract* – The paper presents the modeling of free level flow phenomena in the polycentric riverbeds sections. The classical section of hydrotechnical galleries is modified in exploitation through phenomena of hydrodynamic erosion. The water movement in the gallery is formed of a succession of non-uniform movements gradually varied and rapidly varied, which differently influence the functional state and the hydrodynamic stability. The model answers the hydraulic requirements imposed to the adductions of the type of hydrotechnical galleries with free flow regime and affected by the phenomena of hydrodynamic erosion. The calculation model adopted considers a flow section formed of lines and circular curves. For the polycentric section specific to the case study analyzed, we determined the calculation relations of the hydraulic parameters. The mathematic model presented above was implemented in the computer program MATLAB Sect_Poli_Centr_Masurat.m. For determining the hydraulic parameters in the modified flow sections, we drew up two calculation programs in MATLAB for the uniform movement and the non-uniform movement.**

***Keywords* – flow modeling, gallery, hydrodynamic erosion, polycentric riverbeds.**

1. INTRODUCTION

An important place within a hydrotechnical system is represented by the adduction pipes. The flow in adductions can be characterized by free level under the pressure, or in certain situations in a mixed manner. The modification of design parameters and of the hydrodynamic regime in the adductions for water is developed in a continuous destructive process or variable in time. The multiple actions determine the modification of the constructive and functional parameters of the adduction, diminish the mechanic resistances, disturb the stability and decrease the safety in the construction exploitation. Most of the times, the remedy of destructive effects involves expensive works and which are executed in extremely difficult conditions [3, 8].

To analyze these phenomena to theoretical and experimental study conducted on a supply system adduction of Iasi. The analysis was thorough the central section consist of a hydrotechnical concrete gallery [5].

The theoretical and experimental researches were carried out on the second pipe section of the head race Timişeşti - Iaşi. The pipe section is made up of a hydrotechnical gallery with the role of under-crossing of Strunga Hill. The gallery takes the rate of flows transported gravitationally by three pipes: two pipes PREMO Dn 1000 supplied from Timişeşti source; the third pipe Dn 600 from Verşeni source [9].

The total flow taken from the gallery is transferred in pipe section III under the adduction pressure (Dn 2000, steel, PREMO). The pipe section III is connected to the compensation reservoir of Iaşi city [9]. The hydrotechnical structure was built directly excavating the bedrock of the Strunga hill, excepting the extreme areas. Strunga hill is made up of shale and limestone. The structure of the gallery is made of reinforced monolith built-up concrete. There is a row of prefabricated blocks at the rock contact. To the interior on the arch bricks

Luca Mihail is with Technical University "Gh. Asachi" Iasi, Bd. D. Mangeron nr. 63-65, 700587-Iasi, Romania (corresponding author to provide phone: +40-744 709809; fax: +40-232-223111; e-mail: mluca2004@yahoo.com).

Tamasanu Fabian is with Technical University "Gh. Asachi" Iasi, Bd. D. Mangeron nr. 63-65, 700587-Iasi, Romania (e-mail: tamasanufabian@yahoo.com).

Luca Alexandru Lucian is with Technical University "Gh. Asachi" Iasi, Bd. D. Mangeron nr. 63-65, 700587-Iasi, Romania (e-mail: lucalucian@gmail.com).

ISSN-1584-5990

there is a lining of monolith reinforced concrete that was to be covered with jetcrete. The internal diameter is of 2.00 m and external diameter, 3.00 m (Fig. 1).

The gallery supply is achieved through a loading chamber, with the rectangular shape section and the depth of 6.00 m. The gallery empties downhill into a cable chute where the pipe section III is connected. In the downhill cable chute, a weir is mounted for putting pressure in the gallery. The gallery length is of 1324 m, and the medium downgrade has the value of 1.14 ‰. According to the longitudinal execution profile, on the first half of the length, the foundation mat downgrade is of 1.0 ‰. On the last gallery length, the foundation mat downgrade is of 1.28 ‰ [3, 9].

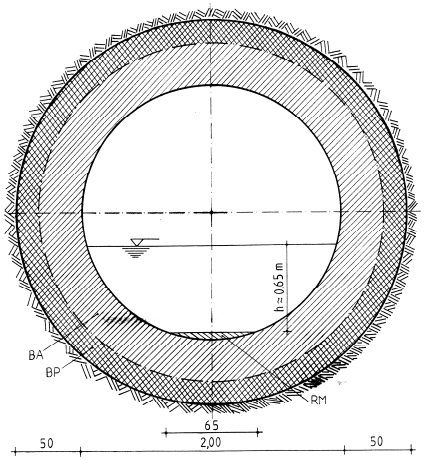

Fig. 1. Flow section of the Strunga gallery

Fig. 2. View of the flow section of the Strunga hydrotechnical gallery

The gallery carries the gravitationally transported discharge through two water pipes (PREMO Dn = 1,000 mm) was supplied by the Timişeşti water source and transfers the discharge to the underpressure transportation pipe (steel, Dn = 800 mm), which is connected to the balancing reservoirs of Iasi. The supply of the gallery is accomplished through a loading chamber, with a rectangular cross-section and a depth of 6.00 m.

2. THE CALCULATION MODEL

The calculation model was conceived for the characterization of the free-level flow in structurally modified sections in the exploitation process. The model answers the hydraulic requirements imposed to the adductions of the type of hydrotechnical galleries with free flow regime and affected by the phenomena of hydrodynamic erosion [3, 5, and 9].

The technologies for the galleries construction and the effects of the hydrodynamic erosion model the free-level flow section in a certain form. In some situations, there are also corrosion phenomena determined by the transport of the alluvium material and some chemical characteristics of water.

In some cases, a significant modification of the geometrical shape of the free-level flow section has resulted. The hydraulic, mechanical, chemical phenomena etc., acting together, have determined a new shape of the flow section. Knowing the evolution in time of the flow section imposes the determination of the hydraulic parameters with direct influences on the geometrical dimensions. Among these parameters, we notice speed, the load loss, the cavitations coefficient etc.

For modeling polycentric movement uneven whites saw a computer program. The program was developed in MATLAB and was named MGVAT1-Str. Modeling longitudinal movement in the bed profile polycentric steps was achieved by [9]:

- modeling of the state of motion by determining the critical depth, slope and Froude number;
- modeling of the gradually non-uniform motion on the gallery sections according to initial condition and contour;
- modeling rapidly varying non-uniform motion on the section to enter the gallery according to initial condition and contour.

The calculation model is based on the observations and measurements achieved in the flow section of pipe section 2 that ensures the head race Timişeşti –Iaşi, line II. The flow section is modified due to the technological considerations regarding the gallery construction and as a result of the water hydrodynamic action during about 42 years of exploitation [8].

The virtual circular section given through the design is replaced in the inferior part by a polycentric section. The calculation model considered the Strunga hydrotechnical gallery. The calculation model has taken into account the following modifications of the flow section (Fig. 1, Fig. 2):

- the inferior part is achieved in a flat shape out of technological considerations;
- the wall in the flow area is modified differentially regarding length through the hydrodynamic erosion;
- the hydrodynamic erosion, the abrasion, the chemical corrosion, in some cases the cavitations have determined modifications of the roughness per perimeter.

The section of the calculation model is formed of lines and circular curves.

The erosion areas per perimeter can be approximated with circular curves of a certain radius. In the first stage, we determined the hydraulic parameters specific to the modified flow section (Fig. 3).

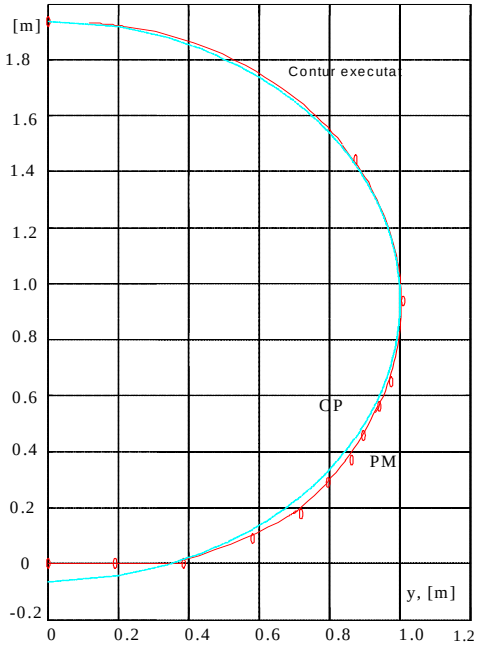

Fig. 3. Strunga hydrotechnical gallery: CP/blue – designed contour; PM/red - executed contour.

The flow section perimeter (initially circular) was approximated with portions through $N_A = (N_M - 1)/2$ line segments or circular curves (NM – number of measuring points, NA – number of segments). In the case analyzed, we admitted 6 circular curves and the flat foundation mat.

Geometric parameters of the section flow are dependent on water depth:

$0 < h \le (z_{i+1} - z_{C0})$, i = 1,…,$N_A$.

The geometrical parameters considered are: the free-level width of the liquid, $B_i(h)$;

- wet perimeter, $P_i(h)$;
- area of transversal section, $A_i(h)$;
- the ordinate of the centre of gravity of the section, $z_{Gi}(h)$.

The support circles are given by the equation:

$$(y-b_i)^2+(z-a_i)^2-R_i^2=0,(i=2,\dots,N_A) \tag{1}$$

The expression of geometrical parameters for the calculation model is the following:

- width at the liquid free-level,

$$B_i(h)=2\cdot\left[b_i+\sqrt{R_i^2-(h-a_i)^2},(i=2,\cdots,N_A)\right]; \tag{2}$$

- wet perimeter,

$$\begin{cases} P_i(h)=\{P_i(z_{M0})=2\cdot B_{C0}, for\rightarrow i=1 \\ P_{i-1}(z_{i-1})+2\cdot R_i\left|arccos|t_i(h)|-arcsin\dfrac{y_{i-1}-b_i}{R_i}\right|, \\ for\rightarrow(i=2,\cdots,N_A) \end{cases} \tag{3}$$

where:

$$t_i(h)=\frac{h-a_i}{R_i}\text{, for i = 2,...,}N_a \tag{4}$$

- area of the transversal section,

$$A_i(h)=\begin{cases} A_i(z_{M0})=0, for\rightarrow i=1 \\ A_{i-1}(z_i)+2\cdot[F_i(h)-F_i(z_{i-1})], \\ for\rightarrow(i=2,\cdots,N_A) \end{cases} \tag{5}$$

where:

$$F_i(z)=b_i\cdot z+\frac{1}{2}\cdot R_i^2\cdot\begin{bmatrix} t_i(z)\cdot\sqrt{1-t_i^2(z)}+ \\ +arcsin(t_i(z)) \end{bmatrix}, \tag{6}$$

$$for\rightarrow(i=2,\cdots,N_A)$$

- the ordinate of the centre of gravity,

$$z_{Gi}(h)=\frac{I_{zGi}(h)}{A_i(h)}, \tag{7}$$

where:

$$I_{z_{Gi}}(h)=\begin{cases} I_{z_{Gi}}(z_{M0})=0,\ for \rightarrow i=1 \\ I_{z_{Gi}}(z_{i-1})+2\cdot\left[G_i(h)-G_i(z_{i-1})\right], \\ for \rightarrow (i=2,\cdots,N_A) \end{cases} \tag{8}$$

with:

$$G_i(z)=\frac{1}{2}\cdot b_i\cdot z^2+\frac{1}{2}\cdot R_i^2\cdot \left\{ a_i\cdot\left[t_i(z)\cdot\sqrt{1-t_i^2(z)}+arcsin(t_i(z))\right]- \frac{2}{3}\cdot R_i\cdot\left[\sqrt{1-t_i^2(z)}\right]^3 \right\} \tag{9}$$

$$for \rightarrow (i=2,\cdots,N_A)$$

With the relations above we determined the hydraulic parameters of the modified flow section: the hydraulic radius R_h, the speed module W, the rate of flow module, K, the hydrostatic force appropriate to the active section, F_h.

The mathematic model presented above was implemented in the computer program MATLAB Sect_Poli_Centr_Masurat.m [9]. The program achieves the following operations based on some data known through measurements made in the field:

1. The shape of the channel section (included in the yOz, with Oz – vertical symmetry axis) is determined through the precision airborne survey of the coordinates (y_i, z_i) for $N_M=2\cdot N_A+1$ points.

2. Determining the equations for N_A circular curves or line segments that describe the flow section.

3. Determining the geometric and hydraulic parameters B, A, P, R_h, z_G, W and K for a transversal flow section made up of N_A circular curves or line segments connected , appropriate to the depth h imposed.

The program Sect_Poli_Centr_Masurat.m was run for the input data according to the case study “Strunga hydrotechnical gallery”. The flow section is defined by a line and five circular curves [9].

3. EXPERIMENTAL RESULTS

Researches carried out to the interior of the flowing section showed significant changes in the channel roughness of the cut-off trench with influences on the roughness perimeter distribution pattern [3, 9]. The free flow running led to the hydrodynamic erosion of the apron. The differentiated roughness led the formation of four different areas. The cut-off trench of the gallery was carved under the action of the water current forming a cavity in the concrete and macro roughness in the hydraulic phenomenon. Also on the inferior third part of the perimeter one can note the decreasing effects of the erosion that continuously carves the roughness of the wall in the area of water contact.

The studies made within the flow section emphasized important modification in the channel roughness, with influences on the manner of distribution of the perimeter of the roughness. The free-level flow determined a foundation mat conditioning through the hydrodynamic erosion phenomenon. The roughness differentiated in an obvious manner on the perimeter, forming four characteristic dimensional areas [5].

The gallery hearth was modelled under the action of the water flow, forming some cavities in the concrete mass, respectively a macro-roughness in the hydraulic phenomenon. In addition, on the inferior third of the perimeter we notice, in decreasing manner, the effects of the erosion phenomena, which continuously model the wall roughness in the area of water contact [9].

Modeling motion was made for a range of flow rates Q = 0.60…1.60 m^3/s. The checking of hydraulic parameters emphasized a modification of the transported rate of flow and of the speed.

The water movement in the gallery is formed of a succession of non-uniform movements gradually varied and rapidly varied, which differently influence the functional state and the hydrodynamic stability (Fig. 4).

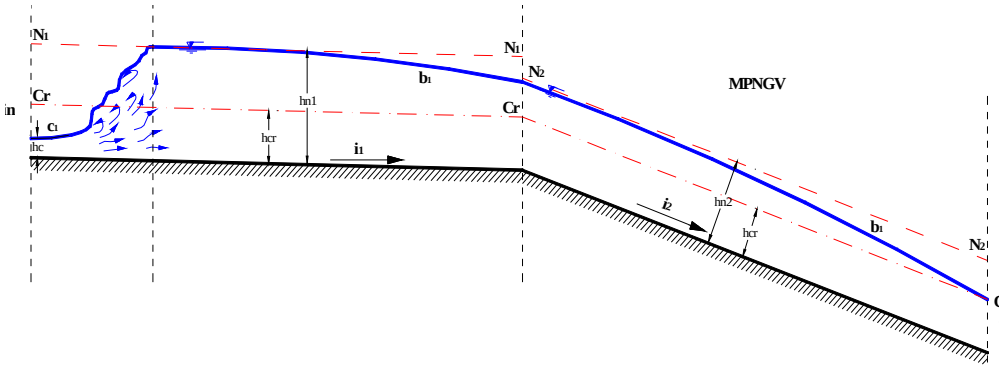

Fig.. 4. The water movement in the gallery Strunga hydrotechnical gallery.

For calculating the non-uniform movement, we created the computer program MGVAT1_Strunga.m in the MATLAB. Numerical simulation results polycentric motion in the bed was presented tabular and graphic for each section and flow calculation (Fig. 5).

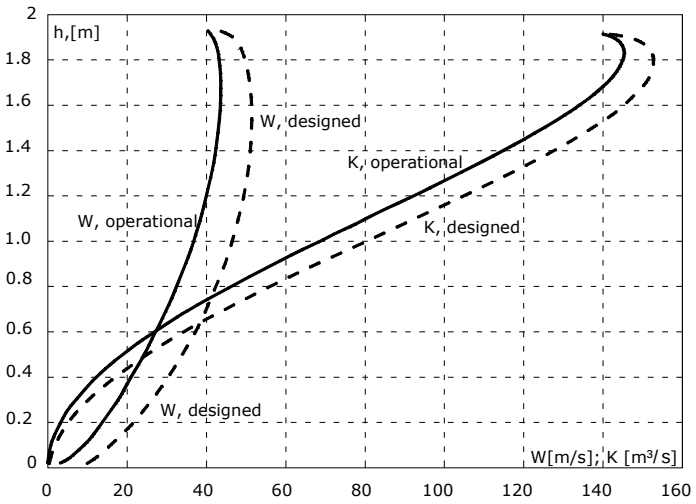

Fig.. 5. Strunga hydrotechnical gallery - designed and effective characteristics

On the input section of the gallery to form a curved free surface c_1 (the supercritical state of motion, Fig. 6).

The downstream section of the gallery forms a curve b1 (subcritical state of motion, Fig. 7) where the gate is lowered. Because of the non-compliance of geometrical parameters and the execution technology stipulated in the project for Strunga gallery (the current situation is presented in Fig. 1), the following result in the current stage of exploitation of the analyzed pipe section:

- at the same depth of water in the gallery, the water speed is diminished with up to 19%;
- accordingly, the rate of flow is diminished with up to 12.5%;
- the increase of the gallery rate of flow must be achieved through works of the flow section rehabilitation.

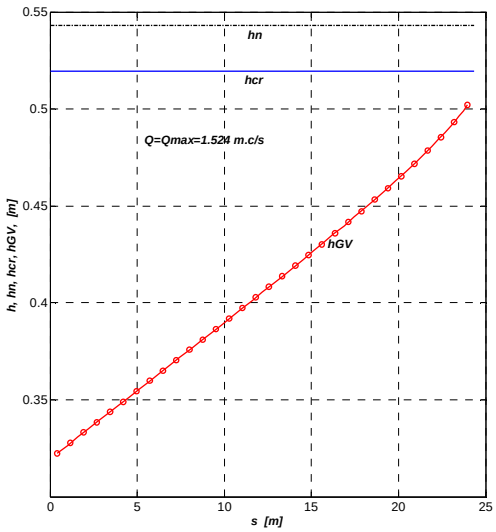

Fig. 6. Curved free surface c_1 on the input section Strunga hydrotechnical gallery (Q = 1.52 m^3/s).

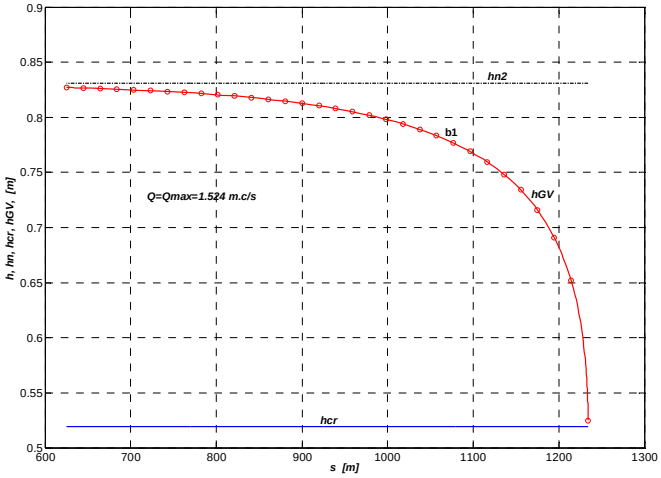

Fig 6. Curved free surface b_1 on the downstream section Strunga hydrotechnical gallery (Q = 1.52 m^3/s).

The most unfavourable situation from the hydraulic point of view is registered on the first pipe section of the gallery (about 60…110 m). according to the investigations in the gallery, and the data obtained through simulation, it results that on a distance of 15…95 m after the entrance in the gallery, the water current evolves in a supercritical state of movement, this fact is proven by the state of the flow section, where we register a hydrodynamic continuous and significant erosion, with a intense transport of material of different dimensions.

At the same time the degradation in the apron area can lead to the apparition of the cavitation phenomenon on the first 10…30 m of the input section. This phenomenon, combined with dynamic erosion, can accelerate the process of degradation of the gallery's apron in this area, a situation that was also emphasized at the time of the visualization of the flow sections.

Research in this field has proved the existence of a continuous exchange of water between the gallery and the underground, through an infiltration - ex-filtration process. The quality of water in the rock massif (mineral water of a sulphurous nature) also determines chemical erosion upon the execution materials of the gallery.

The speeds registered in this area have values of 4.90…9.20 m/s in the entry section, according to the value of the control depth. In the final section of the supercritical movement area, the speeds reach values of 1.70…1.90 m/s. Thenceforth, the supercritical movement goes through a hydraulic bounce into an under-critical movement, and the bounce position is marked at different distances through the phenomenon of sedimentation of the alluvial material.

The next stage will increase operating flow rate. This will affect the hydraulic regime parameters.

Hydraulic manifold structure must be restored to safe operation. The rehabilitation works will flow path hydraulic regime stability [7, 9].

4. CONCLUSIONS

The interpretation of data obtained allows the exposal of the following general conclusions:

-The gallery flow section presents a hydrodynamic erosion phenomenon differentiated according to length, more intensified on the entry pipe section and less active on the central and final pipe sections.

-The flow into the gallery is formed of a section of gradually varied and rapidly varied non-uniform movements, which differently influence the functional state and the hydrodynamic stability.

-For determining the hydraulic parameters in the modified flow sections, we drew up two calculation programs in MATLAB for the uniform movement and the non-uniform movement.

-The results regarding the modeling of the water movement in the gallery for the modified section indicates different values of the speed and the rate of flow compared to the designed values.

-Adopting some rehabilitation measures must take into account the current state of the flow section and the modified value of the hydraulic parameters.

5. REFERENCES

[1] Carlier M., Hydraulique générale et appliqueé, Editure Eyrolles, Paris, 1972.

[2] Luca M., Hobjilă V., 1996, Consideraţii privind parametrii hidraulici de exploatare ai galeriilor hidrotehnice cu curgere liberă,. **Rev.** Hidrotehnica, vol. 41, Nr. 8, 1996

[3] Luca M., Hobjila V., Considerations on hydraulic running parameters of hydrotechnical free flow culvert. Proc. The XXVIII IAHR Congress, Graz, Austria, 1999.

[4] Luca M., Hobjilă V. Complemente privind proiectarea şi expertizarea unor tipuri de construcţii hidrotehnice Edit. CERMI, Iaşi, 2000.

[5] Luca M., Hobjila V., Cotiusca D., The hydraulic and mechanic analysis of the Strunga gallery of the Timisesti-Iasi aqueduct after 27 years running, Bulet. Inst. Polit. Iasi, tom XLVII (LI) fasc. 1-4, Iasi, 2001.

[6] Luca, M., Tămăşanu F., Luca, Al., L., 2010, The modeling of flow phenomena in the polycentric river beds, Scien. Bulet. of the "Politehnica" Univ. Timişoara, tom 55 (69), Fasc. 1, 2, Hidrotehnica, Timisoara, Romania, 2010.

[7] Luca Al., L., Tămăşanu, F**.**, Alexandrescu S., The rehabilitation of the water adductions unndercrossing constructions, Proc. The "Innovations in the field of water supply, sanitation and water quality, 1st Danube - Black Sea Regional Young Water Professionals Conference, Bucuresti, Romania, 2011.

[8] Pâslăraşu I., Consideraţii privind conductele lungi de aducţiune ale apei potabile. Rev Hidrotehnica, vol. 34, nr. 7, Bucureşti, 1989.

[9] Tămăşanu F. Contribuţii la optimizarea hidraulică şi funcţională a aducţiunilor de apă. Teză de doctorat. Universitatea Tehnică „Gheorghe Asachi" din Iaşi, 2012.

[10] Zayed T., Al-Barqawi H., "Condition Rating Model for Underground Infrastructure sustainable Water Mains", Journal of performance of constructed facilities, American Society of Civil Engineers ,2006

RESEARCH OF FILTRATION THROUGH SORTED SAND

Daniel Toacă, Josif Bartha, Agnès Montillet, Nour-Eddine Sabiri

Abstract – **Experimental results of fluid flow through homogeneous permeable media – sorted sand of diameter 0.392 mm, 0.699 mm, 0.974 mm and 1.820 mm – the paper presents.**

Experiments for hydraulic gradients corresponding to Darcy's law up to 7,5 (post Darcy's movement) has been undertaken.

Using a capillary tube model of filtration, parameters of the movement has been determined: porosity, pores diameter, tortuosity, Forchheimer type quadratic relationship of hydraulic gradient, the dynamic and static specific area and friction factor law in function of pore diameter Reynolds number.

Keywords – **Newtonian fluid, post Darcy's filtration, pore diameter, sand filtration.**

1. INTRODUCTION

The velocity of filtration through permeable medium, beginning with a certain limit may overpass the Darcy's linear filtration law.

For higher values of Reynolds number then Re > 1, the filtration is described by nonlinear laws, proposed by Forchheimer [1], in different forms, as:

- power relationship,

$$\frac{\Delta p}{L} = \alpha \cdot V_0^{\beta} \tag{1}$$

- or polynomials of 2nd or 3rd order,

$$\frac{\Delta p}{L} = a \cdot V_0 + b \cdot V_0^2 \tag{2}$$

$$\frac{\Delta p}{L} = a \cdot V_0 + b \cdot V_0^2 + c \cdot V_0^3 \tag{3}$$

These laws are widely commented until today [2, 3, 4, 5, 6]. Post Darcy's filtration has many technical applications, as it follows: in the hydraulic of permeable bed rivers [7], in medicine [8], flows within permeable hydraulic structures [9], movement over permeable walls [10], fluid raw material extraction [11], dispersing polluting substances within built areas, oxygen and carbon dioxide exchanges in vegetation zones, forest fires propagation [12], in the drain and well filters, packed bed reactors computation [13], etc.

Manuscript received June 15, 2012. This paper was supported by the project PERFORM-ERA "Postdoctoral Performance for Integration in the European Research Area" (ID-57649), financed by the European Social Fund and the Romanian Government.

Daniel Toacă is with "Gheorghe Asachi" Technical University of Iasi, Faculty of Hydrotechnical Engineering, Geodesy and Environmental Engineering, 65 Prof. dr. docent Dimitrie Mangeron Street, 700050, Iasi, Romania, (corresponding author to provide phone: +40232 270804; e-mail: daniel.toaca@yahoo.com).

Josif Bartha is with "Gheorghe Asachi" Technical University of Iasi, Faculty of Hydrotechnical Engineering, Geodesy and Environmental Engineering, 65 Prof. dr. docent Dimitrie Mangeron Street, 700050, Iasi, Romania (e-mail: i_bartha@yahoo.com).

Agnès Montillet is with IUT de Saint-Nazaire – Université de Nantes, 58 Rue Michel Ange, 44600, Saint-Nazaire, France, (e-mail: agnes.montillet@univ-nantes.fr).

Nour-Eddine Sabiri is with IUT de Saint-Nazaire – Université de Nantes, 58 Rue Michel Ange, 44600, Saint-Nazaire, France, (e-mail: nour-eddine.sabiri@univ-nantes.fr).

2. CAPILLARY TUB MODEL OF FILTRATION

Capillary tubes model of the permeable media considers that bed void is formed as a set of cylindrical small diameter equivalent curved tubes within which the loss of head occurs like in circular pipes, having equivalent roughness equal to the fictive tubes diameter (**Fig. 1**) [1, 3, 4, 13, 14, 15].

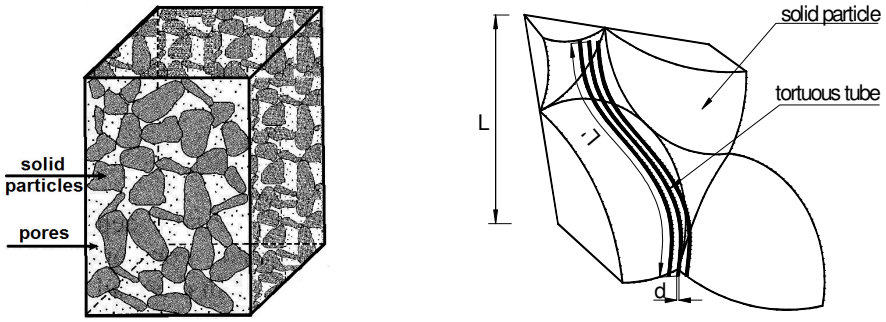

Fig. 1. Scheme of the capillary tub model of permeable medium [3, 16, 17]

The parameters of filtration on micro scale: real velocity - V, tortuosity - τ, the measure of fictive diameter of pores - d and the friction factor λ through macro scale experimental measurements are obtained. The macro scale pressure gradient - $\Delta p / L$, in function the superficial velocity V_0 on infiltrometer, together porosity - n is measured.

Considering the pressure drop due to viscous friction (after Poiseuille relationship) and due to the inertia through the tubes of the model, that are working in the rough pipe zone ($k_e = d$), relationship (2) can be brought to the form [4, 15]:

$$\frac{\Delta p}{LV_0} = 2 \cdot \tau^2 \mu A_d \frac{(1-n)^2}{n^3} + 0.0968 \cdot \tau^3 \rho A_d \frac{1-n}{n^3} V_0 = N + M \cdot V_0 \tag{4}$$

where $\Delta p / L$ is the hydraulic gradient, V_0 – the superficial velocity, τ – tortuosity, μ – the dynamic viscosity, A_d – the specific dynamic area, n – porosity and ρ – the liquid density.

The walls' effects on results have to be corrected [4].

In the neighborhood the infiltrometer wall the roughness of the tubes of the model is considered $k_e = d / 2$, then resulting the corrected factors of equation (4):

$$N^* = 2\tau^2 \mu A_d \frac{(1-n)^2}{n^3} \left[1 + \frac{4}{A_d D (1-n)} \right]^2 \tag{5}$$

$$M^* = \left\{ 0.0413 \left[1 - \left(1 - \frac{d_p}{D} \right)^2 \right] + 0.0968 \left(1 - \frac{d_p}{D} \right)^2 \tau^3 \; A_d \; \rho \frac{1-n}{n^3} \right\} \tag{6}$$

where D is the infiltrometer's diameter. For acceptable accuracy results, $D / d_p > 10$ condition has to be satisfied [4].

After computation parameters A_d and τ, using equations (5) and (6), the diameter d of fictive tubes, the friction factor λ and the microscopic Reynolds number will be determined:

$$d = \frac{4n}{A_d (1-n)} \tag{7}$$

$$4f = \lambda = \frac{\Delta p}{L} \frac{n^3}{2\rho\tau^3 (1-n) A_d V_0^2} \tag{8}$$

$$Re_{pore} = \frac{\rho V_0 d}{\mu} \frac{\tau}{n} \tag{9}$$

3. EXPERIMENTAL EQUIPMENT

The experimental equipment contains a vertical cylindrical infiltrometer, with upstream and downstream fixing permeable walls **Fig. 2.**, **Photo 1 and 2** [2, 16, 17].

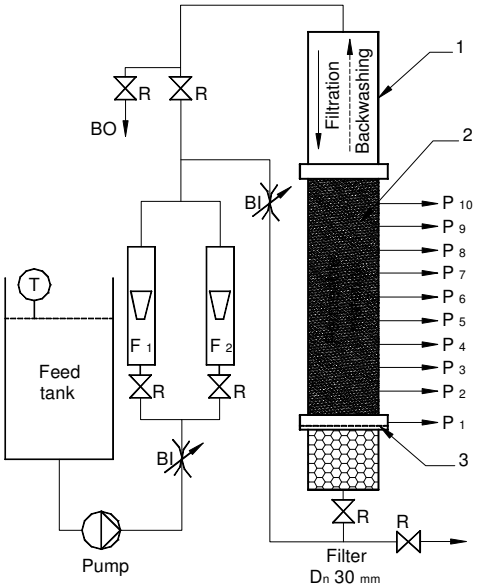

1- Plexiglass Filter Dn 30 mm; 2 – Permeable material; 3 - Sieve; $P_1 \ldots P_{10}$ – Pressure plugs; BO – Output backwashing; BI – Entry backwashing; R – valves; F_1, F_2 – Flowmeters; T – Temperature sensor.

Fig. 2. Vertical infiltrometer under pressure

Photo 1. General view of the equipment Plexiglass Filter Dn 30 mm

Photo 2. General view of the equipment with pressure plugs

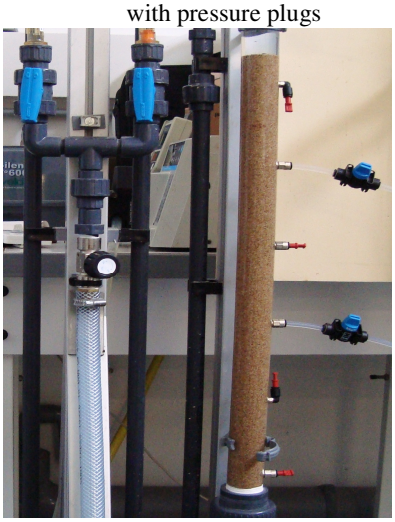

The sand is contained in a plexiglass column (inner diameter of 30 mm) and the pressure measurements were carried out, using differential pressure sensors DeltaBar (ENDRESS and HAUSER), on different sections 10 cm in length ([P1-P2]; [P2-P3].....[P9-P10]). The pressure sensors can perform measurements on nominal measuring range from 0 to respectively 25, 100 and 500 mbar with an accuracy of 0.1% from the top of the scale.

4. SAND CHARACTERISATION

Silica sand with different size distributions was used as filter medium, its chemical composition is given in **Table 1.** Measurement techniques for characterization of particle shape have developed with time in many application areas, in basic research and for industrial purposes. Sieving is a classical method for measuring grain-size distributions. However, the method is not suitable for the fine fractions.

Table 1. Chemical composition of the sand used

SiO_2	Al_2O_3	CaO	MgO	Fe_2O_3	Na_2O	K_2O	SO_3
87%	6.61%	0.11%	0.07%	0.25%	1.10%	3.51%	0.03%

In this study, sand was first sifted, and image analysis was used to measure various grain dimensions such as the mean diameter. For each type of sand, hundreds of particles were observed and images were recorded by a CCD camera. The image obtained is processed using commercial image analysis software (OPTIMAS 6-Bioscan). The number of particles studied is rather important to represent the whole sample, the criterion chosen to estimate this number is based on the calculation of the standard deviation which must be stabilized.

Grading parameters are reported in **Table 2** and **Photo 3**. In our calculation, the equivalent mean diameter of the grain is defined as the geometrical diameter of a sphere that has the same surface as the particle.

Table 2. Geometric characteristics of sand obtained by image analysis

Sand	$d_{g\ min}$ (mm)	$d_{g\ max}$ (mm)	$d_{g\ mean}$ (mm)	Number of measurements
1	0.038	0.589	0.392	39
2	0.129	1.238	0.699	39
3	0.066	1.405	0.974	39
4	0.350	3.020	1.820	39

Circularity values were calculated from 2D sand images. The circularity is defined as the ratio of the area perimeter length (P) squared divided by the surface area (A) (i.e., $C = P^2 / A$). This is a dimensionless number with a minimum value of four pi (12.57) achieved only for circular boundaries (the value is 16 for square boundaries and 20.78 for equilateral triangular boundaries). Circularity values of sand grains are ranged from 14 to 21 with a mean value close to 16. Thus, sand particles used in this study are non-spherical with a pseudo-cubic shape.

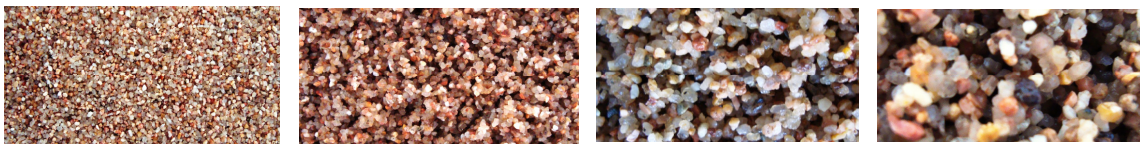

$d_{g\ mean}$ 0.392 mm $d_{g\ mean}$ 0.699 mm $d_{g\ mean}$ 0.974 mm $d_{g\ mean}$ 1.820 mm

Photo 3. Sand used in experiments

5. RESULTS AND SIGNIFICANCES

Loss of head measurements in a function the superficial velocity, expressed in relative hydraulic gradient - $\Delta P / LV_0 = f(V_0)$ are presented in **Fig. 3 - 6.**

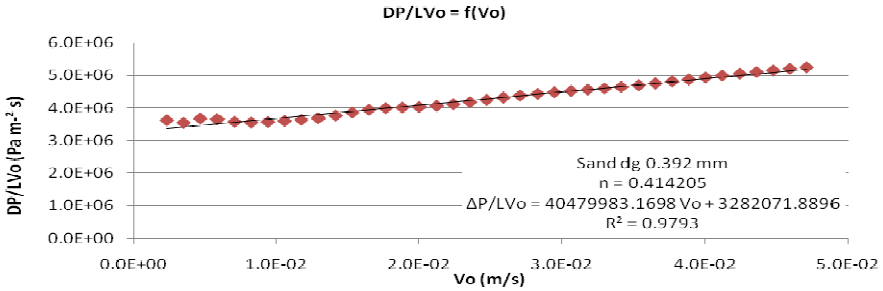

Fig. 3. Experimental relative hydraulic gradient for d_g = 0.392 mm

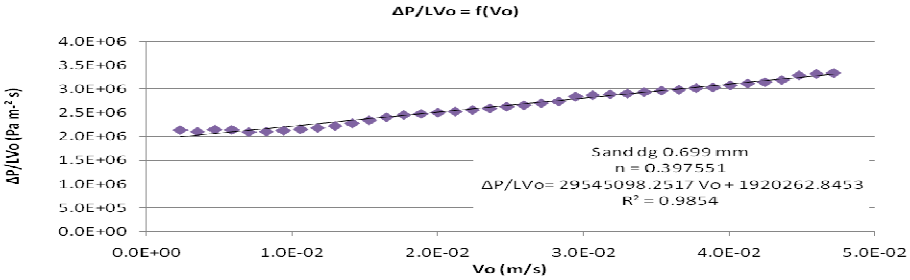

Fig. 4. Experimental relative hydraulic gradient for d_g = 0.699 mm

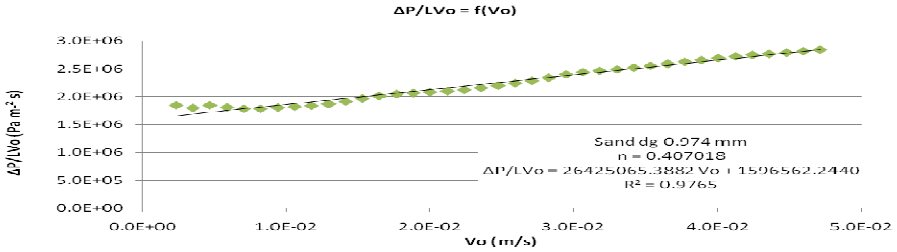

Fig. 5. Experimental relative hydraulic gradient for d_g = 0.974 mm

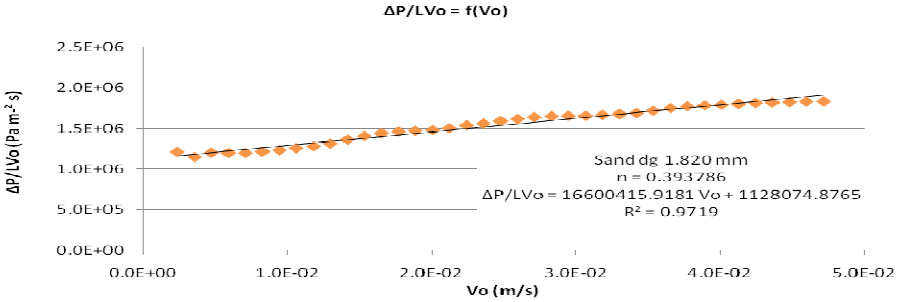

Fig. 6. Experimental relative hydraulic gradient for d_g = 1.820 mm

The hydraulic gradient ΔP/L for the experimented permeable material with respect superficial velocity Vo corresponds to **Fig. 7.**

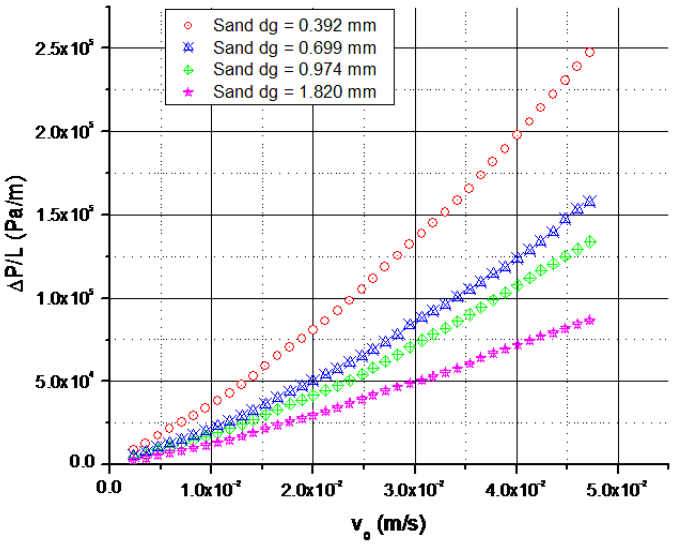

Fig. 7. Hydraulic gradient in the superficial velocity function for sand

Other computed hydraulic characteristics refer: M and N parameters of (4), M^* (5) and N^* (6),computed for $\Delta h = \Delta p / \gamma$ with determinating coefficient R, specific static and dynamic surfaces A_s, A_d, tortuosity τ, diameter of fictive tubes d, (7), mean velocity in the pore v, pores Reynolds number Re_{pore}, (9), and friction factor f, (8). Experimental conditions and part of determined hydraulic characteristics are presented in **Table 3**, without wall effect and **Table 4**, with wall effect.

Table 3. Filtration parameters through homogenous sand without wall effect

dg (mm)	M x 10^{-7} (SI)	N x 10^{-6} (SI)	n	θ (^{o}C)	τ	A_d (m^{-1})	A_s (m^{-1})	d_{pore} x 10^{3} (m)
0.392	4.048	3.282	0.414	21.6	1.664	11006	15306	0.257
0.699	2.954	1.920	0.398	21.6	1.576	8125	8584	0.325
0.974	2.643	1.597	0.407	21.7	1.589	7736	6160	0.355
1.820	1.660	1.128	0.394	21.6	1.340	7177	3297	0.362

Table 4. Filtration parameters through homogenous sand with wall effect

dg (mm)	M^* x 10^{-7} (SI)	N^* x 10^{-6} (SI)	n	θ (^{o}C)	τ	A_d (m^{-1})	A_s (m^{-1})	d_{pore} x 10^{3} (m)
0.392	4.055	3.501	0.414	21.6	1.668	11112	15306	0.254
0.699	2.959	2.047	0.398	21.6	1.595	8071	8584	0.327
0.974	2.647	1.702	0.407	21.7	1.618	7621	6160	0.360
1.820	1.663	1.001	0.394	21.6	1.457	5999	3297	0.433

Friction factor, f (8), in a pore Reynolds number function, Re_{pore}, (9) for all experimental diameters **Table 2** is draw in **Fig. 8.**

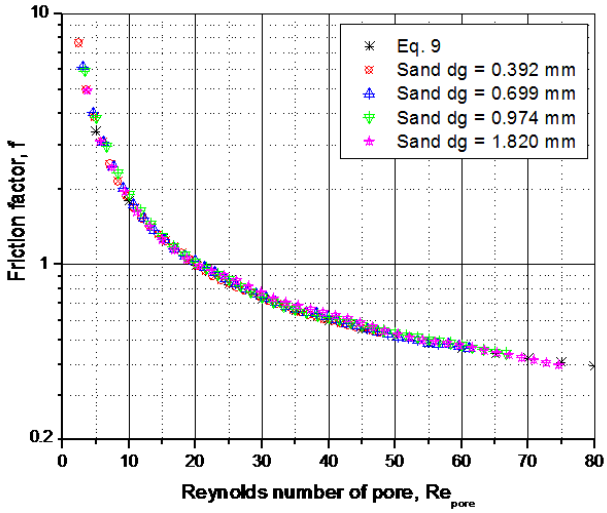

Fig. 8. Pore friction versus pore Reynolds number

6. CONCLUSIONS

In certain situations it has been seen that flowing of liquids through porous media occurs within the post-Darcy domain. The real filtration phenomena are approximately satisfied by the thin tubes geometrical model and are able to solve engineering problems. In the case of post-Darcy flows, besides head losses due to viscosity, certain inertial losses also occur, losses that must be taken into equation for hydraulic calculations.

The proportion in which viscous and inertial losses contribute to the total pressure losses can be determined from equations (4), (5) and (6), in function of the Reynolds number computed for the fictive tube diameter d and for the velocity of fluid within them, v. The term $64/Re_{pore}$ within equation (8) is the viscosity's contribution, and λ is the inertial contribution to the total head losses.

The filtration can be considered a Darcy type filtration for $Re_{pore} \leq 0.89$, when inertial losses are reaching about 1% of total losses. The domain of weak inertia corresponds to Reynolds numbers $0.89 \leq Re_{pore} \leq 4.3$, at upper limit the inertial losses reaching up to 5% of total losses. Calculations, in this domain too, can be performed with the Darcy equation. The domain of high inertia (the Forchheimer domain) occurs for $4.3 < Re_{pore} \leq 180$, when inertial energy losses are reaching (5 - 69) % of total losses. These three domains, together, belong to a laminary flow regime. The domain for the transition regime extends for $180 < Re_{pore} < 900$, the proportion of inertial losses reaching (69 - 92) %. Starting at a Re_{pore}=350 - 450 local turbulences within pores already start to occur. A turbulent filtration regime is defined for $Re_{pore} > 900$.

APPENDIX

a – coefficient, $m^{-1} \cdot s^1$;
b – coefficient, $m^{-2} \cdot s^2$;
c – coefficient, $m^{-3} \cdot s^3$;
d_g – gravel diameter, m;
d_{pore} – pore tub equivalent diameter, m;
k_e – equivalent roughness, m;
n – porosity, dimensionless;
A_d, A_s –dynamic and static specific area, m^{-1};
Re_{pore}– pore diameter Reynold's number, dimensionless;
f – friction factor, dimensionless;
Δp – pressure drop, Pa;
V – mean pore velocity, $m \cdot s^{-1}$;
V_0 – superficial velocity, $m \cdot s^{-1}$;
A – cross section area, m^2;
M, M^*– coefficient, $Pa \cdot s^2 \cdot m^{-3}$;
N, N^* – coefficient, $Pa \cdot s \cdot m^{-2}$;

Greek Letters

α – coefficient, $m^{-\beta} \cdot s^{\beta}$;
β – coefficient, dimensionless;
γ – unit weight, $N \cdot m^{-3}$;
λ – Darcy-Weisbach coefficient, dimensionless;
ν – kinematic viscosity, $m^2 \cdot s^{-1}$;
μ – dynamic viscosity, Pa·s;
ρ – density, $kg \cdot m^{-3}$;
τ – tortuosity, dimensionless;

7. ACKNOWLEDGMENTS

This paper was supported by the project PERFORM-ERA "Postdoctoral Performance for Integration in the European Research Area" (ID-57649), financed by the European Social Fund and the Romanian Government.

Experiment due to courtesy of IUT de Saint-Nazaire – Université de Nantes, GEPEA (Process Engineering for Environment and Food) Laboratory, has been realized during the study stage.

8. REFERENCES

[1] Comiti, J., Sabiri, N.E., and Montillet, A., 2000, "Experimental characterization of flow regimes in various porous media – III: Limit of Darcy's or creeping flow regime for Newtonian and purely viscous non-Newtonian fluids", Chem. Eng. Sci., vol. 55, pp. 3057-3061;
[2] Bartha, I., Marcoie, N., Toacă, D., Toma, D., Gabor, V., Molnar, A. G., and Lupuşoru, A., 2010, "Post-Darcy Filtration Through Rigid Permeable Media", Environmental Engineering and Management Journal, vol. 9, No. 12, pp. 1727-1734;
[3] Forchheimer, P., 1914, "Hydraulik. Druck und Verlag von B.G. Teubner", Leipzig und Berlin;
[4] Comiti, J., and Renaud, M., 1989, "A new model for determining mean structure parameters of fixed beds from pressure drop measurements: application to bed packed with parallelepipedal particles", Chem. Eng. Sci., vol. 44, No. 7, pp. 1539-1545;
[5] Firdaouss, M., Guermond, J.L., and Le Quéré, P., 1997, "Nonlinear corrections to Darcy's law at low Reynolds numbers", Journal of Fluid Mechanics, vol. 343, pp. 331-350;
[6] Balhoff, M., Mikelic, A., and Wheeler, M.F., 2009, "Polynomial filtration laws for low Reynolds number flows through porous media", Research report, The University of Texas at Austin;
[7] Klark, M., 2005, "Design of endoscopic 3D particle tracking velocimetry system and its application in flow measurements with a gravel layer", PhD Theses, Ruperto Carola University, Heidelberg, Germany;
[8] Feng, J., and Weinbaum, S., 2000, "Lubrification theory in highly compressible porous media: the mechanics of skiing, from red cells to humors", J. Fluid Mech., nr. 422, pp. 281-307;
[9] Martinet, Ph. G., 1998, "Flow and dogging mechanisms in porous media with applications to dams", PhD Thesis, Stockholm, Sweden;
[10] Dunn, L. S., 2001, "Wave setup in river entrens", PhD Thesis, Brisbane, Australia;
[11] Klow, T., 2000, "High velocity flow in fractures", PhD Thesis, Trondheim;
[12] Meroney, N. R., 2004, "Fires in porous media: Natural and urban canopies", Colorado State University, Fort Collins, USA;
[13] Seguin, D., Montillet, A., and Comiti, J., 1998, "Experimental characterization of flow regimes in various porous media – I: Limit of laminar flow regime", Chem. Eng. Sci., vol. 53, No. 21, pp. 3751-3761;
[14] Seguin, D., Montillet, A., Comiti, J., and Huet, F., 1998, "Experimental characterization of flow regimes in various porous media – II: Transition to turbulent regime", Chem. Eng. Sci., vol. 53, No. 22, pp. 3897-3909;
[15] Wahyudi, I., Montillet, A., and Khalifa, A.O.A., 2002, "Darcy and post-Darcy flows within different sands", Journal of Hydraulic Research, vol. 40, No.4, pp. 519-525;
[16] Bartha, I., Marcoie, N., Toma, D., Gabor, V., and Toacă D., 2010, "Research of filtration through uniform geometry permeable material-glass spheres", Annals of the University "Ovidius" Constanţa, Construction Series, XIII, pp. 165-172;
[17] Bartha, I., Marcoie, N., Toma, D., Gabor, V., and Toacă, D., 2010, "Research of filtration through sorted river gravel", Scientific Bulletin of the „Politehnica" University of Timisoara, Transactions on Hydrotechnics, Tomul 55(69), Fascicola 1, 2, pp. 71-76;

SECTION IV

INTEGRATED WATER MANAGEMENT

Thailand Flood 2011: Causes, Lessons Learned, and Future Conceptual Plan

Chaiyuth Chinnarasri

Abstract – **During July to November 2011, severe flooding was experienced over vast areas of northern and central Thailand in the Chao Phraya River basin, including Bangkok and its suburbs. The economic damage and number of people affected have been termed the worst disaster in Thailand. It was caused by the combination of excessive rainfall, poor reservoir operation, policy conflict, and wrong decision making by the governmental sectors. After the flood, the government setup a strategic committee to draft a conceptual plan for flood warning, prevention, flood fighting, and mitigation. However, the current implementation of the government policy does not make this clear to the public. In this paper, the causes and lessons learned are reviewed. The future conception plan is presented. The policy and water management of both normal and crisis situations are discussed to improve the implementation.**

Keywords – **Conceptual plan, lessons learned, severe flood, Thailand flood 2011.**

1. INTRODUCTION

Thailand is a Southeast Asian country located in the tropical zone within latitudes 5°30'N to 20°30'N and longitudes 97°E to 105°E. There are five regions, i.e. the north (mountainous), Central Plain (Chao Phraya River basin), Khorat plateau, Eastern uplands, and the Southern peninsula as shown in **Fig. 1**.

The Chao Phraya River basin is the largest and the most important for land and water resources development. It is located in the north and central regions of the country and occupies about 35% of the total area of Thailand. The annual rainfall in the basin ranges from 1,000 to 1,400 mm. The tropical climate is based on two major wind systems; the northeast and southwest monsoons. The northeast monsoon occurs in the dry cool period from November to February. The southwest monsoon occurs in the wet period from May to October. As well as monsoons, these areas are subjected to tropical storms, which mostly originate in the South China Sea. About 90% of the annual rainfall occurs during the wet period, causing heavy floods. The total volume of available runoff is estimated at 31,300 million cubic meters per year [1].

The Chao Phraya River basin consists of eight river basins including Ping, Wang, Yom, Nan, Chao Phraya, Sakae Krung, Pa Sak, and Tha Chin, covering an area of 158 thousand square kilometers. It can be characterized geographically into upper and lower basins. The upper basin is mountainous while the lower is floodplain and is well suited for rice cultivation. The average annual rainfall is 1,300 mm while the average annual runoff is 33,123 million m^3 [2]. The direction of flow is mostly from the north to the central plain and finally to the Gulf of Thailand. Two important multipurpose dams, the Bhumibol and Sirikit dams, are located in the upper basin. In the lower part of the river basin, flood protection systems such as dikes, polder systems, flood barriers, and

Manuscript received August 15, 2012. This work was supported by the National Research Council of Thailand.

C. Chinnarasri is with Water Resources Engineering & Management Research Center (WAREE), Department of Civil Engineering, King Mongkut's University of Technology Thonburi, 126, Bangmod, Thungkhru, Bangkok 10140, Thailand (phone: +662-470-9136; fax: +662-427-9063; e-mail: chaiyuth.chi@kmutt.ac.th).

ISSN-1584-5990

pumping stations are constructed to protect Bangkok (the capital of Thailand), which is located in the lower floodplain.

During July to November 2011, the Chao Phraya River basin suffered from severe flooding, which caused flash floods in many industrial estates in the suburbs of Bangkok. The damage from this flooding was estimated to be more than 10 times that of the previous flooding, especially in the industrial sector [3]. The objectives of this study are to analyze the collected available data to summarize the causes and the impact of the flood. The lessons learned from flood fighting and the future conceptual plans proposed by the government are reviewed. Some alternative recommendations are also suggested.

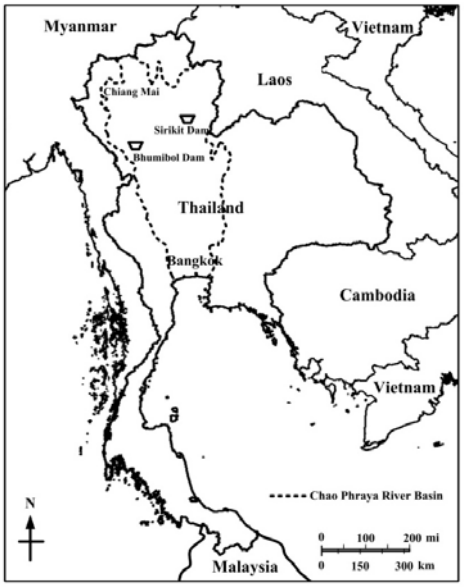

Fig. 1. Map of Thailand and Chao Phraya River basin

2. CAUSES AND LESSON LEARNED FROM THE2011 FLOOD

The causes of the 2011 floods came from three main sources: climate change, human intervention, and poor flood fighting management and operation. As concerns the role of climate, 5 tropical storms hit Thailand, which was more than the annual average of 3. These storms hit the northern and some parts of the central plains. They started from Haima on 25-26 June (came early than normal), Nock Ten on 31 July-1 August, Haitang on 27-28 September, Nesat on1-2 October, and Nalgae on 3-5 October 2011 (see **Fig. 2**).

Therefore the amount of rainfall in 2011 was higher than in the past. The unusual total amount of rainfall in northern Thailand was about 39% higher than the average rainfall in that area. A comparison of the amount of rainfall in the north between 2011 and other flood years is shown in **Fig. 3,** while the total amount of rainfall in central Thailand was about 22% higher than the average amount in that area. The excessive rainfall was attributed to the 5 tropical storms from the South China Sea hitting Thailand, compared to the 2-3 storm hits on average. The two big dams on the Ping and Nan river basins were filled to capacity within 2-3 months. The excessive water flowed from the north to the central plains and overflowed the river banks in Sukhothai province due to narrow blocks of Yom River. The combination of damage to hydraulic structures, irrigation gates, and flood barriers resulted in widespread flooding from the central floodplains down to the lower floodplain. When

the flood reached the river deltas, tidal fluctuation at the river mouth affected the drainage of the river flow into the Gulf of Thailand. This effect prolonged the period of flooding, especially in the coastal provinces, including Bangkok.

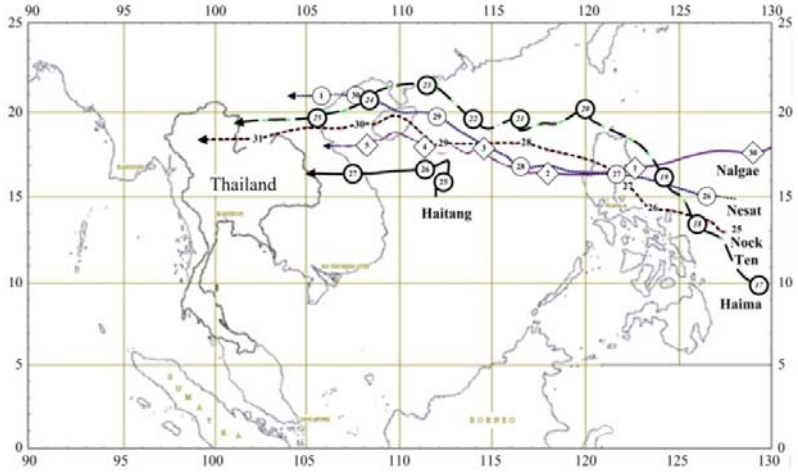

Fig. 2. The route of the tropical storms during late June to beginning of October, 2011

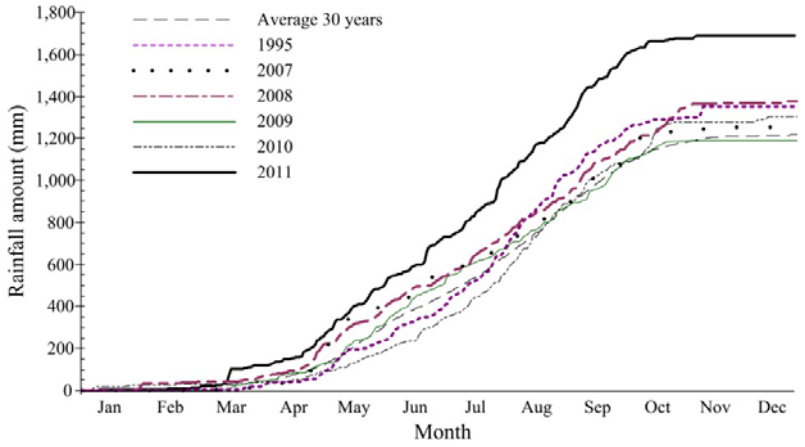

Fig. 3. Amount of rainfall in the northern part of Thailand for serious past floods

During the past three decades, human activities have changed the natural conditions due to the rapidly increasing population. Deforestation in the upper river basin has increased the flood peak and reduced the lag time between rainfall and runoff. Construction of roads without sufficient culverts has obstructed the passage of inland flood flows and increased flood water levels. The increased flood flow is a result of housing construction in floodway zones, public areas, and along river/canals, due to the lack of a master plan for land use zoning. Law enforcement could not be applied because the politicians did not want to lose votes. In addition, a large amount of wetlands have deteriorated and been trespassed upon by both the private and public sectors. About half of these wetlands have been turned into agricultural and settlement areas. The remaining available wetlands such as rivers, canals and hydraulic structures have reduced their flood flow or water control capacity. Due to the

unexpectedly high water levels, dozens of irrigation structures successively failed during the flood, resulting in flash floods in many places downstream of those structures.

The unusual amount of rainfall flowed into the reservoirs in northern Thailand, raising the level of the reservoir water in the big dams in the upper river basin in mid-September 2011. However, it was found that the reservoir operations were very poor. The water was still held in the reservoirs because the authorities didn't want to release much water downstream, where the paddy fields of the central floodplain had not yet been harvested. Unfortunately, when two storms hit the central plain in October (Nesat and Nalgae), people in the lower floodplain therefore suffered from the full amount of water released both from the upstream reservoirs and by the heavy rainfall from the storms. An example of the reservoir operation of the Bhumidol dam is shown in **Fig. 4**.

The last major cause of the 2011 flood was the poor flood fighting management and operation. There was an ineffective flood forecasting and warning system. The accuracy of weather forecasting is less than 65% for 7 day forecasting. The government announced incorrect information to people and the private sector, including the industrial sector, in the lower floodplain and delta. Therefore, people and the private sector were not sufficiently aware and had little time to protect themselves, setup flood barriers, or even evacuate before the flood reached them. This created a panic situation for people living in Bangkok and its vicinity. Nobody could answer the questions "will we be flooded?" or "how deep will the flood be?". It was ironic that even the ad hoc action centre setup by the government to take care of flood victims had to move its temporary base for rescue operations twice to as yet unflooded locations.

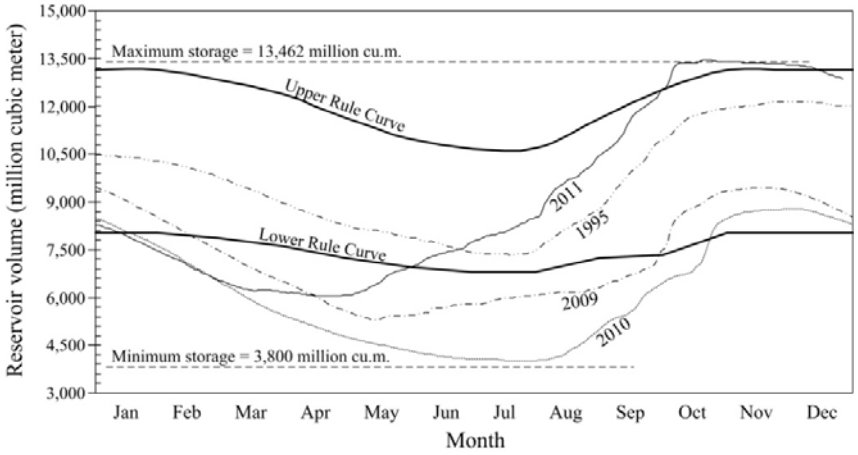

Fig. 4. Reservoir operation of Bhumibol dam

Over 800 factories in 7 industrial estates established in the flood plains and low-lying areas were affected. Labourers and workers were at risk because many factories were closed. Production of computer hard disk drives, automobiles, electrical circuits, and electrics for global export was interrupted for a few months. Japanese companies such as Toyota, Hitachi, and Honda, which have plants in Thailand were also affected. The production of a few hundred thousand cars was abandoned for some months. Some factories considered moving to other countries. The forecast of the country's economic growth was reduced from 4.1% to 2.6% by the Bank of Thailand [4]. The cost of the disaster has been estimated at more than US $ 45 billion [5].

The rainfall forecast announced was not accurate, the flood prediction system was incorrect and there was no real-time warning system, so the affected people were not aware of the situation and did not have time to prepare protection or evacution in time, resulting in panic in many areas. Some academic sectors have tried to predict flood conditions, but due to a lack of topographic data and flow conditions both upstream and downstream, the simulation results were found to have limited accuracy. However, surprisingly, a web-based

flood information system was introduced during the 2011 flood and area-based data was shared to give almost real-time flood information.

Some of the flood barriors were destroyed by the people living in areas outside the flood protection area in the hope that this would reduce the flood water level in their areas. There was also conflict between local administrative authorities wanting to protect just their own areas without considering wider problems. The Prime Minister, who failed to take action in her capacity as the single command authority. The flood fighting system was therefore unsystematically applied depending on each local administrative authority.

3. FUTURE CONCEPTUAL PLAN PROPOSED BY THE GOVERNMENT

The government of Thailand set up a Strategic Committee for Water Resources Management (SCWRM) to formulate a master plan for sustainable water resource management for both urgent and long term measures in order to ensure the continuity of the country's development even with future drought and flood [2]. The government of Thailand also set up two committees: the National Water Policy and Flood Committee (NWPFC) chaired by the Prime Minister and the Water and Flood Management Committee (WFMC), chaired by the Ministry of Science and Technology as shown in **Fig. 5**.

The duty of the NWPFC is to i) formulate policies for water management and guidelines on the water management action plan and ii) make recommendations to the cabinet on budgets, loan management, and all work relating to water management. The SCWRM provides advice and recommendations on short and long term measures for the NWPFC. The duty of the WFMC is to i) formulate a water management action plan, ii) develop, review, and approve work plans for related agencies, iii) formulate work guidelines for the authorities involved, and supervise relevant agents, and iv) exercise the authority it is given to order state agencies to comply with the work plans.

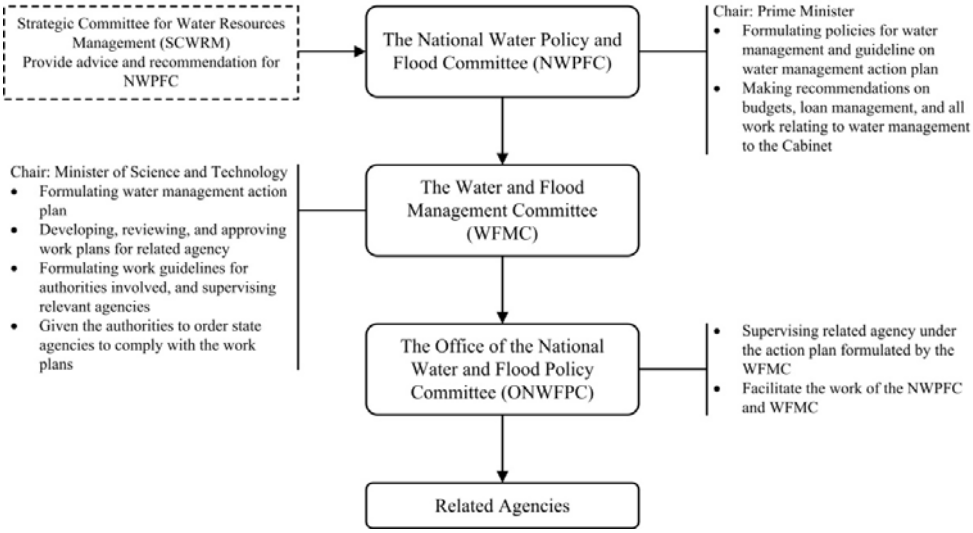

Fig. 5. Mechanism for flood relief, rehabilitation, and prevention

The WFMC has been drafting the terms of reference (ToR), which were adapted from the master plan on sustainable water resource management. The WFMC has a plan to select and hire a world-class flood prevention consortium and experts. In the conceptual action plan for integrated and sustainable flood mitigation in the Chao Phraya River Basin, the measures include structural and non-structural systems, with a total budget of US $ 9,700 million [6]. The action plan comprises 8 work plans, as shown in **Table 1.**

Table 1. The action plan in the Chao Phraya River Basin [6].

No.	Work plan	Aim	Project example
1	Restoration and conservation of forest and ecosystem	1. To restore watershed forests along the river basin where water is retained. 2. To develop additional water reservoirs according to the capacity of the areas. 3. To develop a land use plan that fits with its socio-geographical conditions.	1. Soil improvement and conservation in the upper river basin by reforestation and rehabilitation of forest areas in the river basin in Ping, Wang, Yom, Nan, Sakae Krung, Tha Chin, and Pa Sak. 2. Reservoir construction in Yom, Sakae Krung, Nan, and Pa Sak basins.
2	Management of major water reservoirs and formulation of water management	1. To improve the efficiency of the country's water management system and main dams. 2. To develop a water management plan for major water reservoirs in various scenarios. 3. To disseminate water-related information to public.	Formulation of a water management plan in major dams and water management in various scenarios, as well as dissemination of related information to the public.
3	Restoration and efficiency improvement of current and planned physical structures	1. To prevent and mitigate the impact of floods by renovating, improving and preparing existing buildings, physical structures and instruments to be ready for efficient use.	1. Construction of floodways or water channels, roads, and dams and improvement of water dikes, reservoirs, water drainage and water gateways in order to divert waters from Pa Sak and Chao Phraya Rivers to the east or west efficiently. 2. Land use zoning and land utilization including setting up an area protection system. 3. Improvement of the quality of water in the main water channels and the remaining dikes.
4	Information warehouse and forecasting and disaster warning system	1. To provide necessary information on water management. 2. To create an efficient disaster warning system. 3. To establish a united disaster warning entity.	1. Establishing the database system, forecasting system, and warning system. 2. Setting up the institution, rules and regulations and enhancing public participation.
5	Response in specific areas	1. To build the capacity to prevent and mitigate the impact of floods by developing systems of flood prevention and mitigation in important areas.	1. Develop a system of flood prevention and mitigation in important areas. 2. Set up a system of instrument and tool warehouses. 3. Negotiation with flood-affected communities. 4. Treatment of water polluted due to flooding.

Table 1. The action plan in the Chao Phraya River Basin [6] (contd).

No.	Work plan	Aim	Project example
6	Assigning water retention areas and recovery measures	1. To mitigate the impact of floods. 2. To support the water management plan in the flood plain, Bangkok, and its vicinity. 3. To provide proper and systematic assistance to victims in water retention areas.	Improving/ adapting irrigated agricultural areas into retention areas of around 3,200 km^2. comprising irrigated agricultural areas in flood plain areas so as to be able to grow a second rice crop.
7	Improving water management institutions	1. To set up an integrated water management organization as a permanent single command authority that can make fast decisions during a crisis with all related agencies involved.	1. Setting up the task force committee for action plan management during crisis periods. 2. Setting up permanent integrated water management organizations.
8	Creating understanding, acceptance, and participation in large-scale flood management from all stakeholders	To set up a water management organization in targeted areas with collaboration among partners.	Increasing public awareness of the progress in water management carried out by the public sector, as well as encouraging people's participation in water management.

4. DISCUSSION AND RECOMMENDATIONS

As mentioned in reference [7], anticipating, educating, and informing are the keys to reducing the deadly effects of such natural disasters. Unfortunately, such activities have not been given priority. However, the 2011 flood disaster showed a greater risk of vulnerability because the agencies could not accurately estimate the enormity and extended period of destruction from the flooding [8]. Given that it was the responsibility of the government, it clearly failed in its role of setting up an ad hoc action center to help flood victims during the 2011 flood. The structure of command was loose; there was a lack of specific procedure, a lack of remedies, and no legal support. A number of staff were appointed to take care of flood operations. However, many of them lacked knowledge and experience and were not qualified for the emergency mission.

The existing act on disaster prevention and mitigation (2007) could not be put into practice, even though the operational processes for dealing with a disaster to clearly and promptly fix the problem were defined in the act. The Prime Minister could be empowered by the act (2007), which put a system in place in order to reinforce her role as the single commander.

The current implementation of government policy does not make it clear to the public whether they will be saved from possible flooding in 2012. Will the government be able to deal with a disaster? The current implementation still lacks clarity in government policy. Which agency is responsible? Which part of the budget will be used for the operation?

The plan issued by the government must be clearly and widely understood at the national, provincial, and local levels, without any political distortion of data and information.

The technical terms and different standard units used proved difficult for the public to recognize and understand. Links are needed between local regions so that communications can be distributed evenly and quickly, providing news so that the people affected can prepare themselves for flood fighting, flood protection, and even evacuation via the transport logistics provided. Coordination and collaboration between the public and private sectors, including volunteers, were found to be very important during the flood event. The coordinator

may request financial support from the various organizations involved, and the government should therefore take action as the center of the mission. The roles and responsibilities of the agencies involved in water management in both normal and crisis situations must be clear. Duplication of agency responsibilities must be avoided.

There is a need to strengthen the community level to take care of themselves in a crisis situation, to be aware of their need to participate, and to assume responsibility for themselves, encouraging public awareness of the need to make sacrifices and work together to contribute to society.

Town and city planning was found to be out of date. Industrial estates, economic areas, and residential buildings were settled in the floodplains and flood-prone areas, and were blocking the flow of water. The traditional Thai lifestyle of living with water, such as by using stilts to raise buildings, was cast aside. It was a mistake to consider only short term benefit without a view to sustainable development. The use of land for building that might create a barrier to the water flow must be restricted. The continued development of towns or the establishment of factories in the wrong locations must not be allowed; otherwise, a mega flood will certainly occur again soon.

5. CONCLUSIONS

It was clearly seen that the 2011 flood disaster was not simply the result of heavy rainfall or poor reservoir management, but also resulted from the failure to prepare for disaster management and crisis operations. The government must revise the existing act on disaster prevention and mitigation (2007), which provides for the operational processes needed to deal with a disaster. The plan issued by the government must be clearly and widely understood at the national, provincial, and local levels, without any political distortion of data and information. Town and city planning should be revised to address land use, flood prone areas, wetland areas, and floodways, restricting the use of land for buildings that act as barriers to the flow of water. The continued development of towns or establishment of factories in the wrong locations must not be allowed and some may need to move out; otherwise, another mega flood will certainly occur again soon.

6. REFERENCES

[1] S. Hungspreug, W. Khao-uppatum, and S. Thanopanuwat, Flood management in Chao Phraya River Basin. Proceedings of the International Conference on The Chao Phraya Delta: Historical Development, Dynamics and Challenges of Thailand's Rice Bowl. F.Molle and T.Srijantr (eds). Kasetsart University, Bangkok, 12-15 December, 2000, pp.1-20.

[2] The Strategic Committee for Water Resources Management, Master plan on water resources management, Office of the Strategic Committee for Water Resources Management and Office of the National Economic and Social Development Board, Thailand, January 2012.

[3]The Ministry of Finance and The World Bank, Thailand flooding 2554 rapid assessment for resilient recovery and reconstruction planning, Technical Report, 18 January 2012.

[4] The Bank of Thailand, Mega flood 2011, Impact and recovery trend from entrepreneur survey. Economics and Monetary Matters, Technical Report, Thailand, December 2011.

[5] The World Bank, The World Bank supports Thailand's post-floods recovery effort. Available from: // http:// www.worldbank.or.th(accessed on 8 July 2012)

[6] The Water and Flood Management Committee, The conceptual plan for design and construction of the sustainable water resources system and flood prevention system in Thailand, The Ministry of Science and Technology and Bureau of Prime Minister, Thailand, July 2012.

[7] UNESCO, Natural disaster preparedness and education for sustainable development, Asia and Pacific Regional Bureau for Education, Bangkok, 2007.

[8] W. Uddin, Airborne LIDAR remote sensing and geospatial technology for flood disaster prevention and infrastructure planning, in Thailand's Post-Flood Seminar: Lessons learned from 2011 great flood disaster and future directions for flood prevention, Bangkok, 21 December 2011.

Attenuation of flood waves through a reservoir. Case Study in Fizeş watershed.

Pisculidis Gheorghe[1], Biali Gabriela[2]

***Abstract* – Through the attenuation of flood waves in these accumulations, both the direct and indirect damages are avoided. This paper also analyses the role of fishing in artificial reservoirs, thus managing the significant corroboration of the minimum fishing level for increasing the attenuation volumes. As a result of routing a flood wave through the Taga Mare storage, the computed outflow value is 25.69 m^3/s for an inflow of 31.3 m^3/s and achieving a value of the attenuation coefficient of 0.144.**

***Keywords* –flood wave, attenuation software, stock pond.**

1. INTRODUCTION

Accumulations represent the fastest and most efficacious way of flow rates regularization, regarding the water uses they comply with their requirements the best, and regarding the fight against the floods, accumulations present the advantage that they can control the flood flows from concentrated points [1].

Accumulations represent the works of water management which ensure the modification of the temporary regime of water flows by retaining a part of the inflow in certain periods and increasing the deflux in other periods. In this sense, we consider as accumulations: the set of artificial lakes and ponds created on the water courses, the non-permanent retentions for floods created both on the water course, the non-permanent retentions for the floods achieved both on the water courses and laterally (attenuation enclosures), the naturally created lakes so that the flow regime downhill and the alluviums retention works on the torrents can be managed, [3].

The accumulations from the meadow area have barrages of small heights and large lengths usually built from earth and present the advantage that they are near the populated centres and the irrigated lands.

But also the disadvantage that they require large barrage lengths and have great water losses through the evaporation and infiltrations; for attenuating the flood waves in the meadows of the large rivers people create accumulations through banking, called polders that have the shape of floodable enclosure compartments.

If we refer to the accumulations placed on the surface running waters, then we ascertain that they are water management establishments that create aggradations of levels and at the same time modify the distribution in time of the river flow rates where they are situated through the water volume that they retain [2].

Thus, within a hydrographical basin, the accumulations achieve two types of modifications of natural conditions and namely: the modification of the levels and the modification of the flow rate regime.

2. LOCALIZATION OF RESEARCHES

Later, the artificial lakes also appeared. In time, the number of lakes fluctuated and it was determined by optimal natural conditions (impermeable sub layer, permanent flow on the main valleys, small longitudinal

[1] Water Management System SGA, Cluj , Romania (gheorghe_pisculidis@yahoo.com)
[2] Technical University "Ghe. Asachi" of Iasi , Bd. D. Mangeron nr.65, 700050, Iasi, Romania (gbiali@yahoo.com)

ISSN-1584-5990

backfalls, relatively flat floodable meadows, optimal temperatures etc.), of religious considerations (ensuring the food – the fish – for the long posts), of economic needs (hemp melting plants, crushing mill, fishery).

Today, the majority of lakes are positioned along the rivers Fizes and Bent Brook.

Fizes River has a total length of 40 km. The ponds studied are situated on the main course in the Puini left affluent and Ghiolt right affluent, in the middle sector of the river. In this area, the valley is characterized through the minor bed dug in its own alluviums, the floodable large meadow with local contractions, very small longitudinal backfills, less significant tributaries (the most important is Sucioas).

The 3 ponds have different ages. Without a doubt, Țaga Mare is one of the oldest ponds from Transylvania Field.

In the Fizes catchment, 11 ponds are positioned on the main tributary systems (Catina, Taul Popii, Sf. Florian, Geaca1, Geaca2, Geaca3, Sucutard1, Sucutard2, Taga Mare, Taga Mica, Ghiolt), and a few lakes are on the affluents (Rosieni on the Ciortus valley, Nasal on the Sucioas, Santioana and Santejude on the Sic valley, Stiucii on the Bontului valley), (fig 1). The stock ponds from Fizes Valley have been executed on a hearth of lakes and existent ponds (Taul Popii, Geaca si Taga) between the years 1953 and 1985.

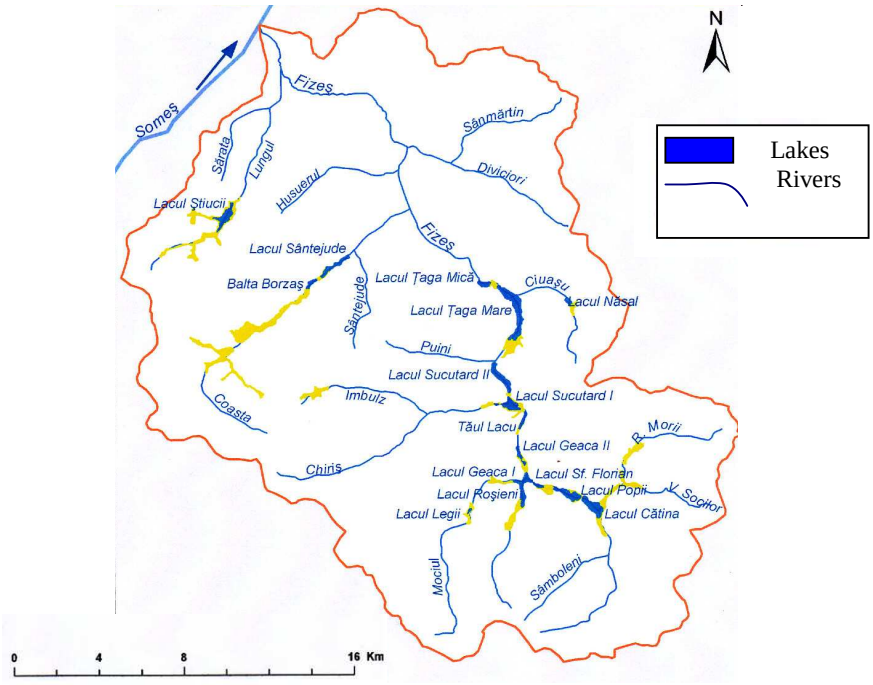

Fig. 1. Hydrographicaly network in basin of Fizeş (position of the acumulation lakes).

3. RESEARCH METHOD

For understanding the manner of attenuation of the flood waves in an accumulation, we must know the constructive composition and the functioning of the respective accumulation.

The attenuation of the flood waves in a given accumulation is influenced by the following elements:

The curve of the lake capacity V=f(Z);

The characteristics of the wasteways $q_G=f(Z)$, $q_D=f(Z)$;

The level of the water in accumulation at the moment of the outrush production.

The manoeuvres of the high waters wasteway regulating gate, if they expire.

Taking into account these elements, the attenuation calculations can be made taking into account different hypotheses of accumulations functioning. They can be hypotheses of functioning in a normal situation or functioning hypotheses in an accidental situation.

In the case of permanent accumulations:

- The lake is full at the maximum quota of the normal retention level and the wasteways function at the maximum capacity (normal hypothesis of functioning);

- The lake is full at a smaller quota than the maximum quota of the normal retention level as a result of the consume or an intentional pre-discharge; the wasteways function at the maximum capacity (the favourable functioning hypothesis)

- The lake is full at a larger quota than the maximum quota of the normal retention level because of a previous outrush or the erroneous exploitation; the wasteways function at the maximum capacity (the accidental functioning hypothesis) .

The frontal accumulations modify the hydrograph of the flood wave from the basic area.

The calculation hypotheses will be established taking into account the most difficult situations of accumulation functioning without exceeding the calculation probability and normal check. Their simulation in attenuation calculations is achieved by constructing the wasteways characteristics in accordance with the simulated hypothesis.

When passing through a frontal accumulation, a part of the volume of the flood wave is stocked in the accumulation lake, and a part is evacuated through the surface wasteways or through the bottom discharge. (figure 2)

If the volume of the flood wave is high and the level of water in the accumulation lake exceeds the quota of the high waters wasteway, then a part of the volume of the flood wave is evacuated through the high waters wasteway.

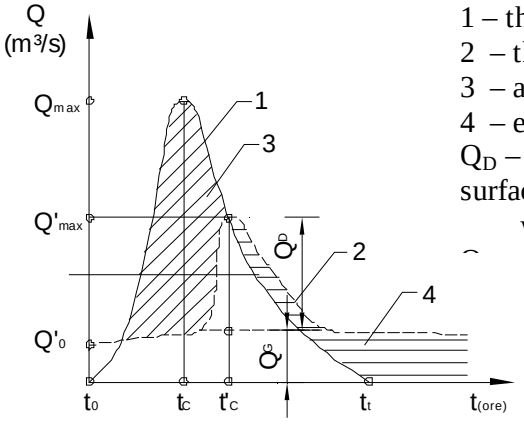

Fig. 3. The effect of frontal accumulation on the flood wave

When the level of water in the lake reaches the maximum quota, the maximum flow rate of effluent is achieved Q'_{max} and the maximum flow rate in natural regime Q_{max} (equation 1). The β attenuation degree is the ratio between the difference of the natural and effluent maximum flow rates Q_{max} - Q'_{max} and the natural maximum flow rate Q_{max} .

The water volume stocked in accumulation is integrally evacuated downhill ($W_{ac}=W'_{ev}$). The maximum flow rate is displaced in time to the natural one ($t_c>t_ç$), and the total duration of the outrush is much bigger than that of the natural outrush ($t_{t'}>t_t$).

The attenuation achieved in a frontal accumulation mainly depends on the volume of the flood wave in natural regime and less on the value of the maximum natural flow rate.

The passage of flood waves through Ţaga Mare accumulation (fig. 3) leads to their attenuation achieving in the downhill barrage sections much smaller attenuated levels and flow rates than the flood wave ones that lead to the diminishing in a great extent of the potential damages that could be produced in the lack of these works on the water courses. In addition, the existence of these accumulations leads to the much more reduced dimensioning of hydrotechnical works downhill because of the attenuations in the lakes. Through the attenuation of the flood waves in these accumulations both the direct and indirect damages are avoided: the direct damages representing the value of destructions of the damages of objectives affected and the value of expenses made with the intervention operations for defending the endangered areas, of evacuation and helping the population; the indirect damages given by the losses registered in the economy.

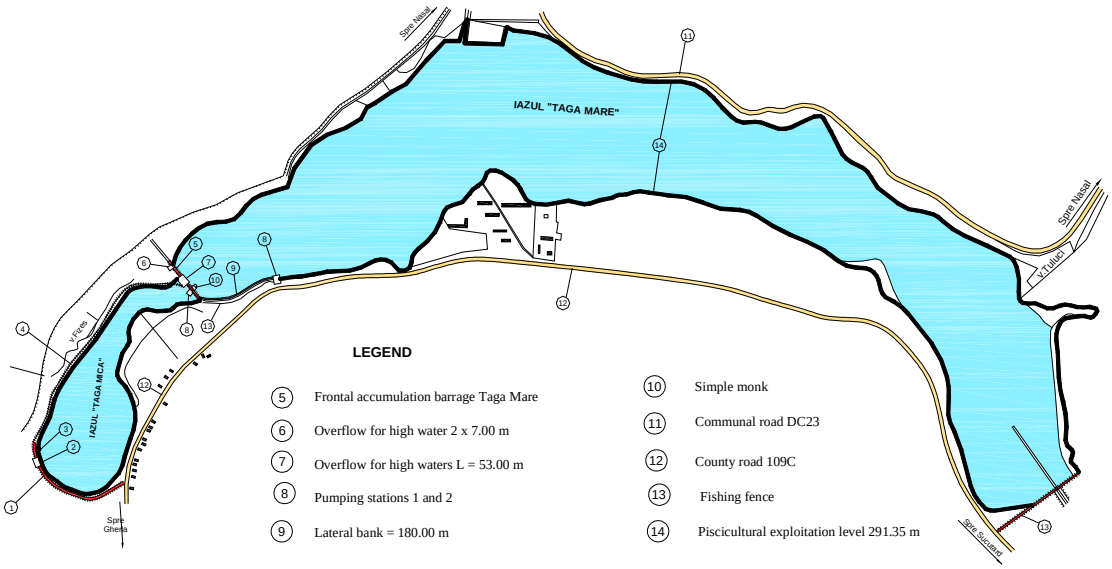

Fig. 3. Ţaga Mare accumulation, Fizes hydrographic basin

4. CALCULATION / SIMULATION PROGRAM. RESULTS OBTAINED.

The research method approached in the present thesis is the graphic-analytical methods of attempts. This is based on knowing the following elements: the hydrograph of the affluent flows in the calculation section $Q_a=f(t)$; the superior part of the lake's capacity curve and namely $W_{at}=f(h)$, taking into account that the lake is full until the overflow level (NNR) ; the rating flow $Q_d=f(h)$, built when we know the length of the overflow, giving values to "h" and calculating the "Q_d" ; the key of the bottom discharge $Q_g=f(h)$, built when we know the section of the bottom discharge and the depth of the weight centre of the section; from the last three curves, the curve $Q_{def}=f(W_{at})$ is built.

The calculation operations are presented in the following manner:

- the duration of the outrush is divided in time intervals "Δt" whose value is chosen according to the precision desired

- it is considered that the outrush finds the lake full until the crest of the overflow (NNR) and the bottom slide valve is closed (blocked), although the lake attenuation capacity is formed of the own attenuation overflow volume (W_{at})

- we aim at the construction of the hydrograph of effluent flow rates (the blue interrupted line), which, at the intersection with the affluent flow rates hydrograph gives us the value of Q_{dmax}, and the surface comprised between the 2 hydrographs represents exactly the searched W_{at} .

4.1. PRIMARY DATA OF PROGRAM ENTRY

F_{BH} = 283 km^2 –surface of the reception basin
k = 0,28 m^3/s – transformation coefficient of the rain intensity
α = 0,40 – the global reduction coefficient
$I_{60.1\%}$= 115 mm/hour –the maximum hour intensity of the rain with the exceeding probability 1 %
n = 0,50 – reduction coefficient
$p_{calculation}$ = 5 % ; $p_{verification}$ = 1 %
$Q_{1\%}$ = 216,293 m^3/s
Q_m = 2,83 m^3/s

We will continue to present the results of the simulation with the program used in this application, software Mathcad 14.

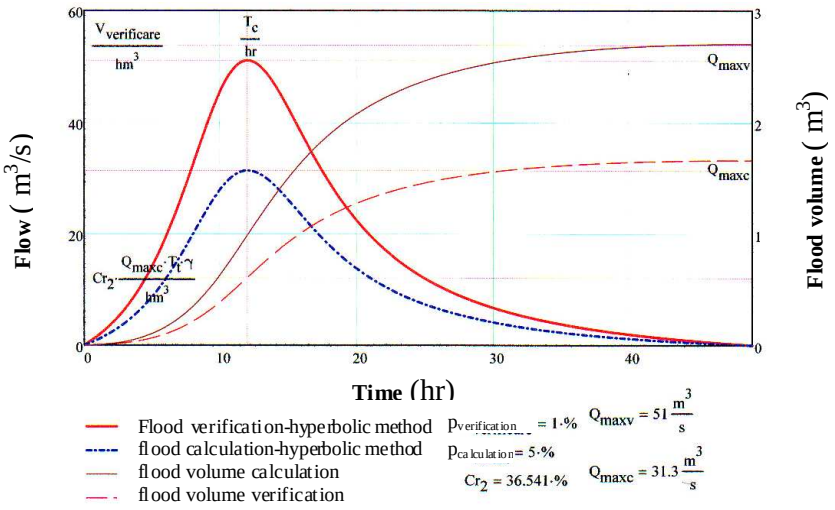

Fig. 4. The hydrographs and the volumes of outrushes for Taga Mare accumulation

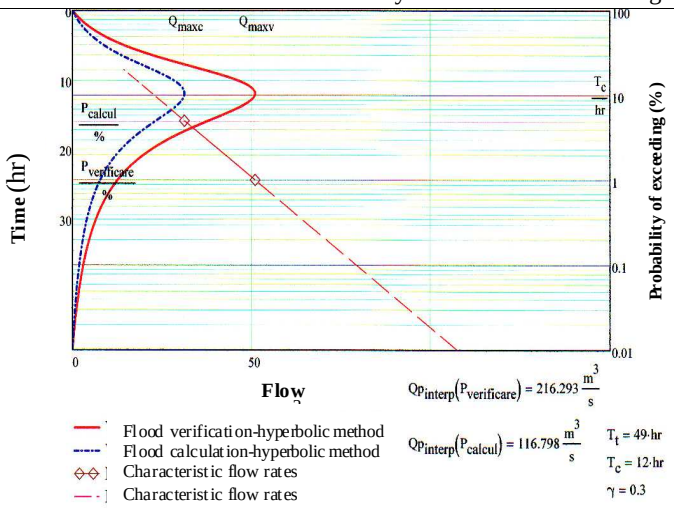

Fig. 5. The hydrographs of the outrushes and the flow rates characteristics for the Taga Mare accumulation

4.2. CALCULATION OF FLOOD WAVES

$$Cotalin_{lac}(vx) := linterp\left(\frac{Vol_{lac}}{hm^3}, \frac{Cota_{lac}}{mdM}, \frac{vx}{hm^3}\right) m$$

$$Cotaps_{lac}(vx) := interp\left(pspline\left(\frac{Vol_{lac}}{hm^3}, \frac{Cota_{lac}}{mdM}\right), \frac{Vol_{lac}}{hm^3}, \frac{Cota_{lac}}{mdM}, \frac{vx}{hm^3}\right) m$$

$vx := 0hm^3, 0.0001hm^3 .. max(Vol_{lac})$

$Cota_{dev} = 282.55\,m$

$NNR = 282.64\,m$

$$Vollac(hx) := linterp\left(\frac{Cota_{lac}}{mdM}, \frac{Vol_{lac}}{hm^3}, \frac{hx}{mdM}\right) hm^3$$

$Cota_{coronament} = 284.87\,m$

$hx := min(Cota_{lac}), min(Cota_{lac}) + 0.1mdM .. max(Cota_{lac})$

$Cota_{golire} = 279.9\,m$

$V1x := 1000hm^3$

$Cota_{pregolire} := NNR$

Given

$Cotalin_{lac}(V1x) = Cota_{pregolire}$

$V1xc := Minerr(V1x)$

$V1xc = 2.31 \cdot hm^3$ $V1v_1 := V1xc - 0hm^3$ $V2v_1 := V1xc - 0hm^3$ $V3v_1 := V1xc - 0hm^3$

The interpolation is linear and the spline type parabolic of the accumulation characteristics $\{Cota_{lac} = f(Vol_{lac})\}$.

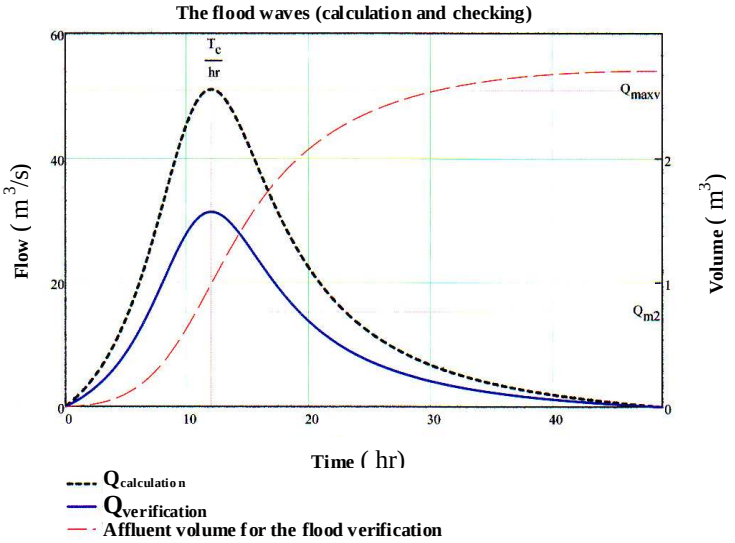

Fig. 6. The flood waves (of calculation and checking) for Taga Mare accumulation

4.3. THE ATTENUATION OF THE FLOOD WAVE IN THE LAKE

We will determine the aspect of effluent waves q(t) when we know the dimensions of the overflow, the variation of the volume in the lake according to the height and the hydrographs of the affluent flow rates.

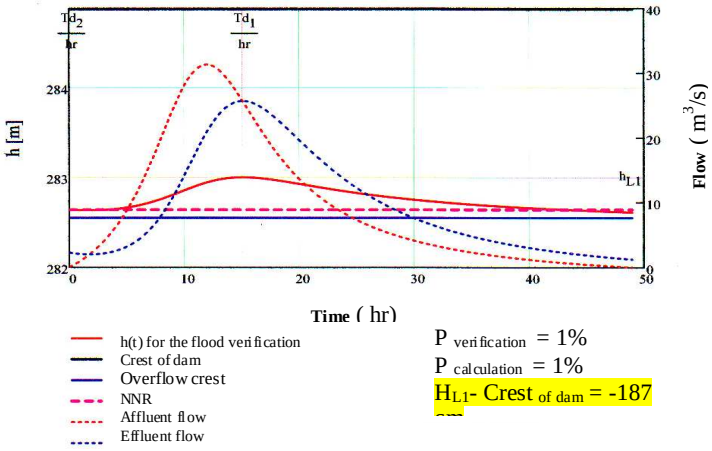

Fig. 7. The evolution of the water quota in Taga Mare lake

Based on the entry data, we draw up the graphs of the calculation outrushes as follows:
- we will analyze the attenuation effect for the calculation flow and the checking flow

(Q-q)dt = Sdh, which shows the difference between the effluent and affluent volumes in a time interval dt, causes an aggradations dh of the lake level.

The linear and parabolic spline type interpolations of the affluent flows follow.

5. CONCLUSIONS

Taga Mare storage, taken in the study, ensures through the barrier of the Fizes valley, the fastest and most efficient method of regularizing the outrush flow rates. In addition, it ensures a water glitter for the fishy activity. Through the exploitation according with the exploitation rules and having at the disposal an efficient information flow, pre-discharges of these accumulations can occur until the minimum fishy level, creating the possibility of achieving higher attenuation capacity and implicitly achieving a higher attenuation coefficient of the effluent flow rates from the accumulation.

This exploitation takes into account as well the possibility of using these accumulations, from accumulations with fishy role in accumulations used for sportive fishing, thus managing the significant corroboration of the minimum fishy exploitation level and implicitly increasing the attenuation volumes.

As a result of the transiting of the flood wave through Taga Mare storage, the effluent flow rate when ensuring the calculation have values of 25.69 m^3/s compared to the calculation affluent flow rate of 31.3 m^3/s, achieving an attenuation coefficient of 0.179.

In addition, the effluent flow rate in the case of insuring the checking is of 43.671 m^3/s compared to the affluent flow of 51 m^3/s, achieving a value of the attenuation coefficient of 0.144.

6. REFERENCES

[1] Bâla M., (1977), Baraje din din materiale locale, Editura Tehnica Bucuresti.
[2] Cretu Gh., (1976), Economia apelor, Editura Didactica si Pedagogica, Bucuresti.
[3] Giurma I. (2000), Sisteme de Gospodarire a apelor, Editura Cermi, Iasi.
[4] Hâncu S., s.a. (1971), Hidrologie agricola, Editura Ceres, Bucuresti
[5] Podani M., 1993, Apararea impotriva inundatiilor, Editura Tehnica Bucuresti.
[6] Popovici N.C. (1993), Regularizari si gospodarirea apelor, Institutul Politehnic Iasi.
[8] Serban P. s.a. (1989), Hidrologie dinamica, Editura Tehnica Bucuresti.
[9]. Sofronie C. (2000), Amenajari hidrotehnice in bazinul hidrografic Somes Tisa, Casa de Editura Gloria,Cluj.

Water Supply and Sewerage Security in the Time of Extreme Climatic Conditions

Štefan Stanko, Ivona Škultétyová, Ivana Mahríková, Karol Molnár

***Abstract* – The contribution of the paper focuses on the water supply and sewerage in the time of extreme situations, drought, floods, flooding and low temperatures. The paper describes the critical situation through the winter 2012 in Slovakia. The water supplies were frozen by temperature decreasing, mainly in the part of East Slovakia. Various problems were generated by this situation. The paper describes the solution concerning the early monitoring, the risk management and the emergency plans of water supply and sewerage in emergency conditions. Climate change as one of the indicators has a negative impact on water supply too.**

***Keywords* – Water supply, sewerage, extremes of nature, the risk, climate change**

1. INTRODUCTION

The climate change impacts us every day. We are also the witnesses of various local and global changes that affect many areas of daily life in short period. It is very significant on a long exposure time to the environment. We have spent huge amount of energy on elimination of the risk caused by a direct threat to human activity, whether accidental or deliberate caused. Many events held in the world, and dedicated to resolving this topic, were directed to eliminate risk, depending on the strategic objectives and ultimately the fear of terrorist attacks at all strategic levels.

Water, as a basic raw material for human life, together with the air create basic condition for the life. Environmental quality worsening can have fatal consequences. Not only water quality but also its lack can greatly affect the lives not only humans but also other organisms. In terms of endangering the lives of people by the lack and poor water quality, we are already convinced that natural factors may play a negative role on the places with relative safe water conditions before natural impacts.

In the winter of 2012, we have witnessed just such an effect of natural factors whose combination caused the stoppage of public water supply for two or more weeks in towns and villages in Eastern Slovakia.

This situation was caused by several factors - freezing of available water resources and distribution system. Surface impact of low freezing temperatures, more than 20 degrees Celsius below zero. In the case of long freezing time, more than one week, water resources frozen to a great depth. Water had no possibility to fill in the water supply system.

Manuscript received July 19, 2012. The Research Grant VEGA 1/1079/12 Vega 1/1143/11 held by the Department of Sanitary Engineering Faculty of Civil Engineering, Slovak University of Technology Bratislava has supported this paper.

Štefan Stanko, is with Slovak University of Technology Bratislava, Civil Engineering Faculty, Department of Sanitary & Environmental Engineering, Radlinského 11, 813 68 Bratislava, Slovak Republic stefan.stanko@stuba.sk

Ivona Škultétyová, is with Slovak University of Technology Bratislava, Civil Engineering Faculty, Department of Sanitary & Environmental Engineering, Radlinského 11, 813 68 Bratislava, Slovak Republic ivona.skultetyova@stuba.sk

Ivana Mahríkova, is with Slovak University of Technology Bratislava, Civil Engineering Faculty, Department of Sanitary & Environmental Engineering, Radlinského 11, 813 68 Bratislava, Slovak Republic ivana.mahrikova@stuba.sk

Karol Molnár, is with Slovak University of Technology Bratislava, Civil Engineering Faculty, Department of Sanitary & Environmental Engineering, Radlinského 11, 813 68 Bratislava, Slovak Republic karol.molnar@stuba.sk

ISSN-1584-5990

As a negative factor was defined the drought, which during the summer months in 2011 did not fill up the natural reservoirs of water resources in the amounts which would have been safe even for longer lasting frost. This serious situation impacted the municipalities in Slovakia for the first time, therefore nobody did expect and nobody was ready for such situation.

The distribution system itself, due to an insufficient coverage, frosted across, which was another negative factor. The very sensitive places became regular measurement shafts, which were not adequately insulated against prolonged time of frost. In the very cold sites the temperature reached 30 degrees Celsius below zero. The operational company, tried to solve the situation, but without success. The final solution was made after strong and long lasting frost fall back.

Population could spend a few days without water without major problems. Experts estimated that the problem would be solved after a few days of frost subsidence. Two weeks of water absence in the water supply system caused unmanageable problems of everyday life. The authorities with experts decided that the municipality reservoir tank should be filled in with water from other resources.

The problem was with the freeze of the water in the truck tanks. There were no warming tanks. Only firework trucks had the suitable tanks, but water quality in these tanks did not reach the quality of drinking water. Despite the poor water quality, people were allowed to use the water for at least basic toiletries - toilet, wash.[1]

If we want to prevent disaster, respectively negative effects due to the action of natural factors, we need to define it. It won't be in our power to manage solution during the available time. The operational time is relatively short, and always the conditions are more or less extreme.

It is necessary to define the process by which we can overcome any extreme conditions. We have to define the emergency plan and we have to define the alternative solutions with acceptable level.

2. DEFINITION OF NATURAL EXTREMES

Extreme conditions may bring in the various problems concerning water supply, water quality worsening, its scarcity, the impact on infrastructure. Among the basic natural negative effects we can include: drought, floods, flooding, prolonged heat, changes in rainfall, hurricanes, increased solar activity. Other factors can include forest fires caused by human or natural influences, water temperature, tornadoes, strong winds, snow storms, hail, storm activity accompanied by excessive lightning.[5]

2.1 DROUGHT

Drought is caused by various factors which have a significant impact on water scarcity and this is the one of the factors, which consequently causes adverse effects. Prolonged droughts have resulted in drying up water sources. The lack of rainfall cycle activity causes droughts which changes the country. It causes the extremes, which we know and which expands the desert. We are aware that the drought, which occurs as a result of natural change also affected the development of entire civilizations. It led to complete changes of cultures and way of life over time.[5]

Fig. 1 represents the factors affecting the formation of drought and subsequent water scarcity due to natural factors - weather, due to agricultural activities in relation to hydrological drought. All of these factors ultimately affect the economy, having a negative social impact, and finally changing the environment. The principle in the figure goes from the problem, which is defined as the change of climatic conditions, which are undoubtedly present, and in view of our perception are going much faster than we could anticipate.

In the study of climate change should be noted, that the average annual temperature increase affects the change in weather. Global warming is controversial among scientists. There is the question of who is responsible for this situation which leads to changes that result in extreme weather events, negative impact on the affected landscape that may negative affect on water management. Local warming effect occurs in the large cities following their overheating caused by very low albedo. This situation is caused by the dark surfaces such as concrete, asphalt and others surfaces without green areas. This phenomenon we call the UHI effect - Ultra Heat

Island Effect. This effect changes the local weather in the cities due to adverse surface albedo. It necessarily causes not only the extreme heat in the cities, but also extreme storms. Storms have a very negative impact on urban drainage, the drainage system and can cause excessive damage.

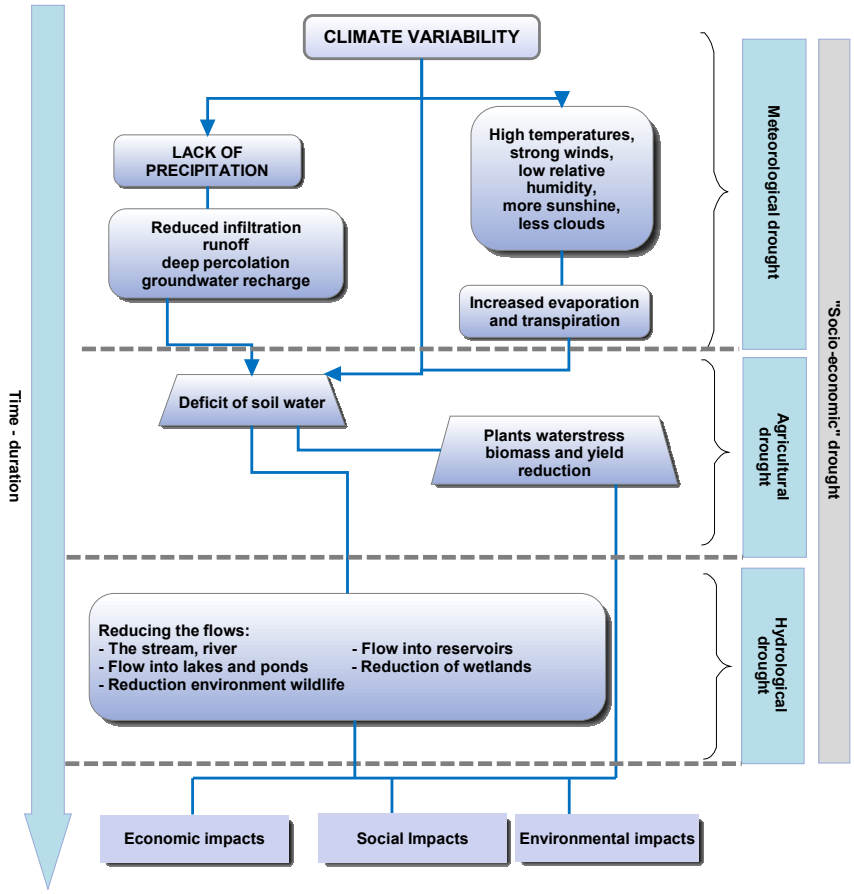

Fig. 1: Relations between meteorological, agricultural, hydrological and socio-economic impacts of drought resp. of water scarcity. [2]

2.2 FLOODS AND FRESHETS

Floods and freshets have other significant impact on the environment. We know their influence from history. Years 1997 and 2002 were very wet years. The floods impact was intensive in Czech and Slovak republic. Floods and freshets have occurred in the summer, before relatively dry months, nightmares in areas that have previously not known flooding for previous decades (Slovakia's cities Modra, Pezinok). What is difference between flood and freshet? The difference is based in their creation. Flood is caused by water rise up above the shore. Freshet can be caused by other factors, e.g.: strong summer storms, melting snow, etc. Floods and freshets had been occurring in the history of mankind since ancient history. Documentation on their forces, causes and impacts has been made only from 19th century, from the same time as meteorological data recording. The occurrence of earlier floods is noticed only in chronicles and similar documents.

2.3 SEWERS THREATS

Drainage system, respectively wastewater diversion system, may be represented by combined or separated sewer system. It can be attacked during the extreme events. Sewer system could have negative back effect on the environment by polluting up during floods. One of the factors that threaten this system is its flooding during the floods, at the time of extreme storms and contamination of the surface area by the waste water pollution. Removal of damages due to contamination by flooding must be done in a short time. There are threats of epidemics due to surface contamination.[3]

2.4 IMPACT ON RIVER AND LAKE

Heavy rain causes the high runoff from the catchment and can have erosive influence and can float huge amounts of contaminants to the lakes and rivers. It may have significant impact not only on the cities, but in the summer months in recreation areas can causes contamination with pathogenic microorganisms by erosive soil. It could have negative impact in fish reproduction and enormous negative impact on the health of humans, fish and animals that come in contact with the water. [5]

3. RISK AND FACTORS AFFECTING THE RISK

In relation to the extreme, especially natural influences, it is necessary to realize the risk in the consequences of floods. Risk is a combination of the probability (frequency) of a particular state and its adverse consequences. The risk has always at least two components: frequency and consequences. The risk R we can calculate by the formula (1) [8].

$$R = P \times C \tag{1}$$

where

P – probability, C – consequence

Risk assessment is used to assess the degree and probability of human health and environmental harm, for example - pollution or habitat loss.

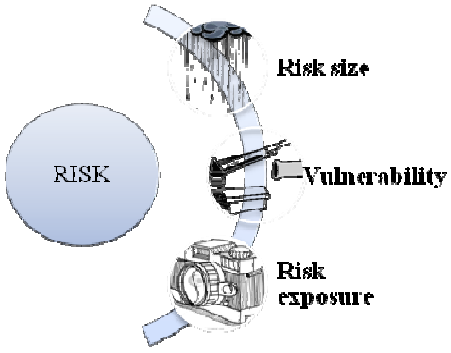

Fig. 2: Risks aspects

3.1 THE RISK AND ADVERSE EFFECTS ELIMINATION

Risk is an essential part of all change activities. We can't exactly define risk processes. These are always more or less stochastic events. If we want to manage a risk, it is necessary to define risk management. Managing risk is an essential business requirement across the process and utility sectors. If the goal of risk management in the water utility sector is to assure safe drinking water, we need to consider what is safe. To demand an absolute standard it would guarantee that nothing could be considered safe. We can only reduce the level of risk. We used the risk management scheme for risk management implementation (Fig. 3). We can never be sure with nothing.

This is true in general. If we accept the risk as plain fact, we have the possibility of reduction by various influences of behaviour in the system. If we want to reduce the risk, avoid it or eliminate it, we must at least meet the basic principles of behaviour.[7]

It should be rational in decision-making; clearly resolve uncertainties; to seek logical, sustainable and determined solving problems; to have the best available information; to take into account human and environmental factors; to respond for changes in the system; be able of the continual improvement.

Risk management is relatively very well developed in the water sector, thanks to research projects of universities. The example of WaterRisk project clearly defines by what it is in this process, defines the backgrounds of problem. The goal is a reliable and safe water supply for population. Fig. 2 represents the risk aspects.

This process can also be defined by the following steps:

- **Exposure assessment** - exposure to risk - describes the population or ecosystem exposed to stress, the magnitude, duration and spatial extent of exposure.
- **Hazard identification** - identification of adverse effects (e.g., cancer, short-term illness) that may occur as a result of environmental exposure – stress
- **Dose - response - evaluation** - determining the effectiveness or toxicity stressors.
- **Risk characterization** - based on data collected in the first three steps one can describe and estimate the impact of human or environmental exposure to a stressor.[4]

3.2 THE PHASES OF THE CYCLE DISASTER PROCESSES

We can split the disaster process into four basic activities (Fig. 3):

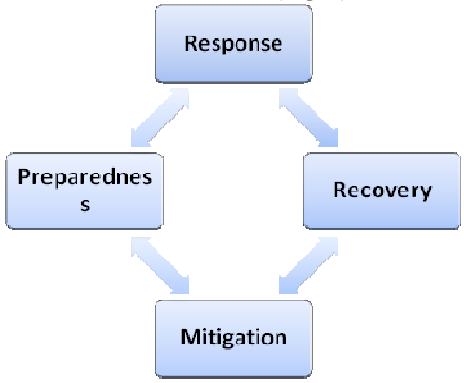

Fig. 3: Disaster phases

Mitigation phase - reduces negative impacts of natural disasters, environmental degradation and technological hazards. Adverse consequences of risk are often not completely to prevent, the extent or severity can be significantly reduced by various strategies and activities.

Preparedness Phase - This phase is taken to minimize losses and other damages through the organization, rapid and effective operation of the rescue and recovery. Activities focused on the readiness to focus on minimizing the damage caused by natural disasters, strengthening disaster response operations and training organizations and individualizes the ability to respond. Also includes planning, organizing, training, collaboration with other organizations and agencies related resources inventory, test plan.

Phase of response – The aim is to save lives and health of residents, alleviate suffering and reduce economic losses. The main tool is the implementation of plans that were prepared before the event.

Recovery phase – this focuses on restoring essential services and start repairing the physical, social and economic losses from damage such as health, communications equipment and utility systems. Recovery phase also includes efforts to reduce disaster risk factors.

3.3 EMERGENCY PLAN

Emergency plan is a very important part of the operation of water works - the water supply, sewerage and wastewater treatment. It establishes the procedure to be adopted in case of threat to the health, life and property of population in relation to a possible disaster, respectively unwanted technical condition of water supply and sewerage.[7]

The emergency plan serves as a tool to ensure the basic needs of acute functionality of the system, the possibility of alternative sources of crisis that may arise due to natural forces or human activity. It have to contain the instructions how to proceed in emergency situations and offers clear solutions in adverse conditions without undue delay time, which is often a very significant negative factor in critical situations.

4. CONCLUSION

Collection of information on specific events and their comparison with available information from the world and a comprehensive evaluation learns us, how to behave in extreme situations and to overcome them, how to eliminate them. The modern computer simulations of natural disasters in extreme conditions can greatly assist us in protection of health and asset of citizens, to rescue the country that is often largely affected due to floods, by heat and wind.

Not least, the impact of continuing anthropogenic activity that uses large-scale technical resources and energy could have a significant impact on the change in the country, environment and the effects of various consequences. For example, the often debated issue of climate change, which, depending on the scientific advice, is very often assigned in a large scale to anthropogenic impacts.

5. ACKNOWLEDGMENTS

The Research Grant VEGA 1/1143/11, and VEGA 1/1079/12 held by the Department of Sanitary Engineering Faculty of Civil Engineering, Slovak University of Technology Bratislava has supported this paper.

6. REFERENCES

[1] Act No. 364/2004 Slovak republic. About water, as amended (Water Act) (2004)

[2] Sinisi, L., Aertgeerts, R.: *Guidance on Water Supply and Sanitation In Extreme Weather Events*, WHO, (2010)

[3] Hlavínek, P.: *Perspectives of Decentralized Waste water treatment of rural areas*. In: Proceedings of ARW, Advanced Water Supply and Wastewater Treatment: a Road to Safer Society and Environment, Published by Springer, Netherland, p. 75-87 (2011)

[4] Hrudeya, S.E, Hrudeya, E.J, Pollard, S.J.T.: *Risk management for assuring safe drinking water*, Environment International, Elsevier, Volume 32, Issue 8, December 2006, p.948–957, (2006)

[5] Stanford, B.: *Extreme Weather Impacts on the Water Sector,* Water Environment Solutions, Horizons (2012)

[6] EPA: *Condition Assessment Technologies for Water Transmission and Distribution Systems*, EPA/600/R-12/017 www.epa.gov/nrmrl, Office of Research and Development National Risk Management Research Laboratory - Water Supply and Water Resources Division, (2012)

[7] Tom De Veer: *Water supply in disasters and emergencies*, SamSamWater Foundation, Westzijderveld 101R, 1507 AA Zaandam, The Netherlands (2012)

[8] Waterrisk -www.WaterRisk.cz, official website of the project 2B06039 – 2006-2010, (2010)

HYGIENIC INSPECTION – THE LAST STEP OF WASTE WATER´S SLUDGE TREATMENT

Štefan Stanko, Ivana Mahríková, Ivona Škultétyová, Kristína Galbová, Michal Holubec

Abstract – **Hygienic inspection is the last step of sludge treatment before its reuse. Sewage sludge is a waste product, which comes into being in the process of wastewater treatment and so underlies under Waste Low. Sludge often consists of toxic chemical matters, which we can be classified as a dangerous waste. Hygienic inspection is the technological process of sludge treatment, which is used in the case, when the sludge properties don't fulfil the request of valid European legislation for next sludge reuse in agriculture, or other fields of treatment. This paper describes present methods of hygienic inspection used in Slovakia and neighbouring countries.**

Keywords – **sewage sludge disposal and treatment, hygienic inspection, methods, reuse.**

1. INTRODUCTION

Sewage sludge definition is: it is a disposal from urban wastewater treatment. We define it as a disperse system, which consists of suspended, colloid matters. The main part creates suspended matters with characteristics concentration 5-50 g./1. The sludge consistence may vary from liquid till greasy. Sludge contains 1 - 2% of waste water volume and 50-80% of primary pollutants. The sludge as waste product from various steps of wastewater treatment is no stabile; it is the reason of the next sludge treatment, before its use as a lateral stuff.

2. SEWAGE SLUDGE CHARACTERISTICS

One of the most important sludge characteristics is hygienic aspect. Sewage sludge is a waste product, which comes into being in the process of wastewater treatment and so underlies under Waste Low. This act regards all stuff, from products that have at least one dangerous property to dangerous waste. The producer of this waste has to dispose the sludge as a dangerous waste. Lot of sludge produced on the WWTP has one dangerous characteristic. It is infective. Infectivity is caused by pathogen bacteria. Their amount depends on geographic, climatic and demographic factors. The main source of pathogen bacteria is the excrement of ill people or animals. Majority of these bacteria is the disposed by the treating process, but without a perfect sludge hygienic inspection, a small amount may still remain in the sludge. By the use of sludge in agriculture these

Manuscript received 19th July 2012. The Research Grant VEGA 1/1079/12 Vega 1/1143/11 held by the Department of Sanitary Engineering Faculty of Civil Engineering, Slovak University of Technology Bratislava has supported this paper.

Štefan Stanko, is with Slovak University of Technology Bratislava, Civil Engineering Faculty, Department of Sanitary & Environmental Engineering, Radlinského 11, 813 68 Bratislava, Slovak Republic stefan.stanko@stuba.sk

Ivana Mahrikova, is with Slovak University of Technology Bratislava, Civil Engineering Faculty, Department of Sanitary & Environmental Engineering, Radlinského 11, 813 68 Bratislava, Slovak Republic ivana.mahrikova@stuba.sk

ISSN-1584-5990

pathogenic germs threaten the healthy of living organisms. Among the pathogenic organisms which occur in the waste waters there are:

- viruses;
- germs as a Salmonella, Escherichia coli;
- protozoas;
- lateral worms.

Sludge often contains toxic chemical matters, which we can classify as dangerous waste. There are some organic matters and heavy metals. The source of heavy metals refers to Cadmium, Chrome, Copper, Mercury, Lead and Zinc. We can find these matters into the industrial wastewaters from the metal and leader industry, from the wet and dry deposition.

3. SEWAGE SLUDGE PRODUCTION AND MANAGEMENT

In the context of increasing requirements for wastewater treatment - the implementation of Council Directive 91/271 EEC on Urban Waste Water, the increase of sludge production by about 20-40% is to be expected in the near future. It is mainly the addition of sludge from small sewage treatment plants without significant involvement of industrial waste water, so a certain degree of contamination of sludge can be expected, which corresponds to the requirements of the process, limiting its application to the soil. [3]. Overview of sludge production from urban wastewater treatment in the time period of 2001 – 2010, as shown in Figure 1.

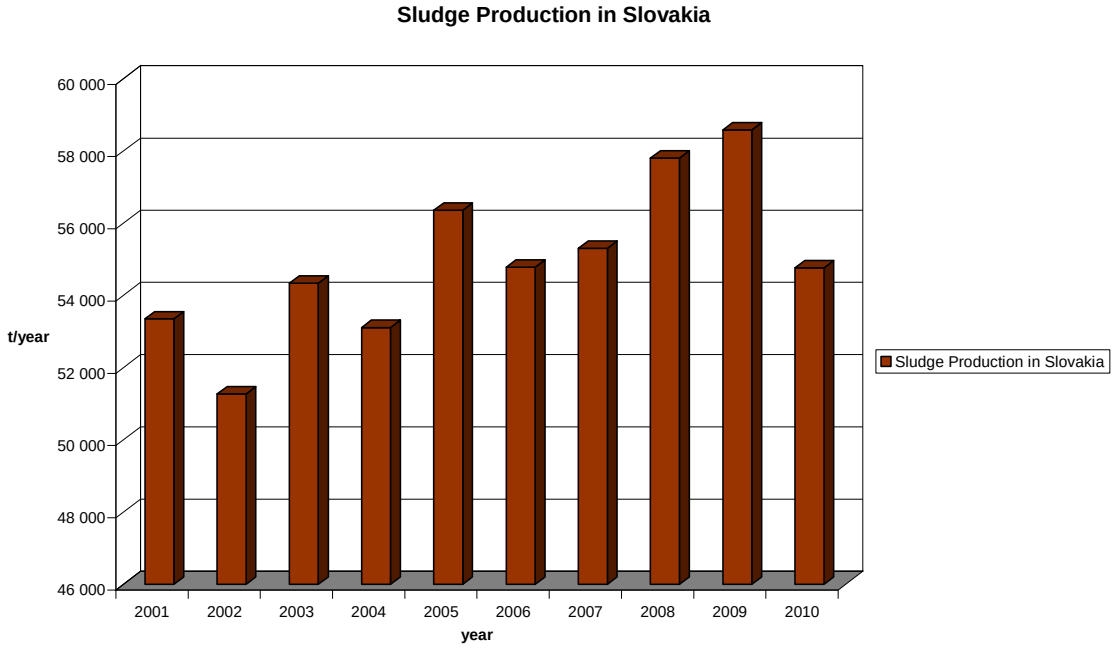

Figure 1: Sewage sludge production in Slovakia

Today in Slovakia, there are two valid Acts refering to the sewage sludge management. Act no. 231/2000 Coll., on the Waste and Act no. 188/2000 Coll. on application of waste water sludge on soil.
There are the methods of controlled application of sludge on soil:

- Direct application of sludge on soil, according to the Act no.188/2003 Coll. on application of waste water sludge on soil.
- Application according to the Act no. 136/2000 Coll. in wording of Act no.555/2004 Coll. on fertilizers, for example, as compost or soil-growing medium. In this case the product is subjected to certification.

4. METHODES OF SEWAGE SLUDGE DISPOSAL AND HYGIENIC INSPECTION

The most used process of sewage sludge disposal in Slovakia is application into the soil. The controlled application must be done according to the valid legislation (Act no.188/2003 Coll. and Act no. 136/2000 Coll.). Hygienic inspection is the technological process of sludge treatment, which is used in the case, when the sludge properties do not fulfil the request of valid Slovak legislation. The hygienic and sanitary properties of the sludge are improved by hygienic inspection. We can use for it various methods such as pasteurisation, aerobic thermophilic stabilisation, chemical methods- using CaO, gamma radiation or irradiation and incineration.

4.1 Pasteurisation

Pasteurisation is the process of sludge heating during relative short time at a temperature of 70°C. The process of pasteurisation was established in Switzerland. The goal of it is elimination of germs and viruses especially of salmonella. Pasteurisation can't replace process of sludge stabilisation. It has to be combined with some other process of stabilisation. The process of pasteurisation is highly effective by killing various types of viruses especially on entherogerms and salmonella. It is no effective by thermo tolerant types of life forms as a certain types of viruses and spores.

4.2 Irradiation

There are only marginal experiences of irradiation of sewage sludge in the Europe. By the irradiation, salmonella and entherogerms are mostly reduced. By the operational point of view, it is interesting that the irradiated sludge has better dewatering properties than a no irradiated sludge.

4.3 Aerobic thermophilic stabilisation

Aerobic thermophilic stabilisation was developed for the sewage sludge stabilisation. High level of aeration reinitiates the biological processes with such intensity, that the warmth generated by the process keeps the needed temperatures for the disinfection. We know two concepts of aerobic thermophilic stabilisation:

- aeration by pure oxygen
- aeration by air oxygen

By using pure oxygen, the reached average temperatures are about 60-80°C. The disinfection effect will be comparable with the pasteurisation and we can reach also better results than by pasteurisation. When the process is supplied with oxygen from the air, the reached temperature is 40-60°C. In this temperature interval the process of disinfection is reduced and a longer time for deactivation of pathogens is needed. To find the optimal relation between aeration and temperature is not easy.

4.4 Composting

Composting is a process, which depends on aerobic reduction of organic matter by thermophilic germs. Sludge is mixed with filling mass, that serves to the increase of porosity for better aeration, to the reduction of content of humidity and to the improvement of relationship between C:N. There are often combined all three

functions in one product. For example: straw, wood peel or household waste. There can be used also no degradable material, as plastic. There were developed many types of composting processes, so it is really difficult to define average data for requested disinfection effect. Generally we can speak about two basic processes:

- Composting in composting lagoon
- Composting in bioreactor

By composting in composting lagoon the sewage sludge is in a role of filling mass. For requested sanitary effect it is necessary to achieve the critical temperature for requested time. For elimination of salmonella, in summer period, the critical time is established at 6-7 weeks.

4.5 Lime treatment

Lime is often added into the sewage sludge before dewatering. That causes an increase of pH level, which can reache a value from 9-13 in dependency of lime supply and sludge characteristics. Vegetative germ cells (coliform germs or salmonella) are fast reduced to nothing by value of pH from 9 to 10. According to Strauch and Berg, pH level has to be higher than 11,5 for reaching of requested efficiency. By these pH values will be destroyed the most of viruses. Destruction of the viruses is not effected directly by pH effect, but by unlocking of free ammonia by pH level around 12. Complete destruction can be reached by adding of quicklime into the dewatered sludge. At this moment the temperature increases up to 70-80 °C and all pathogens die very fast. The destruction factor is temperature.

4.6 Incineration

Incineration is one of the most effective processes of sewage sludge treatment and sanitation. By the still growing amount of sludge it is a perspective solution for sludge disposal. But the process of sewage sludge incineration is not easy to realise in really conditions. The dewatered sludge contents about 75% of water. The complication is also the high value of heavy metals in sludge. It can cause creation of vapours by higher incineration temperatures. Fluid layer is one of the perspective methods of sewage sludge incineration. The fluid layer creates thermal homogeneous environment, which is reach in oxygen with strong abrasive influence on the sludge elements.

The thermal degradation has a lot of advantages. At first it is a volume reduction, about 87%. The ash from the incinerated sludge is inorganic and it is mostly sterile matter. So we can use it in building industry. The heavy metals are strong bounded on sorbate and so they are not washed up. The gas emissions are deep under allowed limits. Also the process of thermal degradation is friendly to the environment. By the treatment on WWTP we can skip the sludge treatment from the technology of waste water treatment and replace it with thermal sludge degradation.

The financial cost of the sludge processing, however, the overall economic balance significantly affects the treatment of waste waters, which represents more than half of the total cost of waste water treatment. The production of the sewage sludge, cannot be avoided, but innovative technologies can reduce the amount of sludge or energy use. The significant step in sludge treatment is sludge reuse. One of the possibilities is slow thermal decomposition of sludge, which is able to use maximum of its energy potential. The sludge is not perceived as a waste, but as the raw material, which is energy – valuable product. It is possible to produce high quality energy products from the sewage sludge, namely gas, liquid and solid fuels, which can be used directly on WWTP or can be sold to the other areas of our life. On the Figure 2 are illustrated the most used sludge disposal methods in Slovakia.

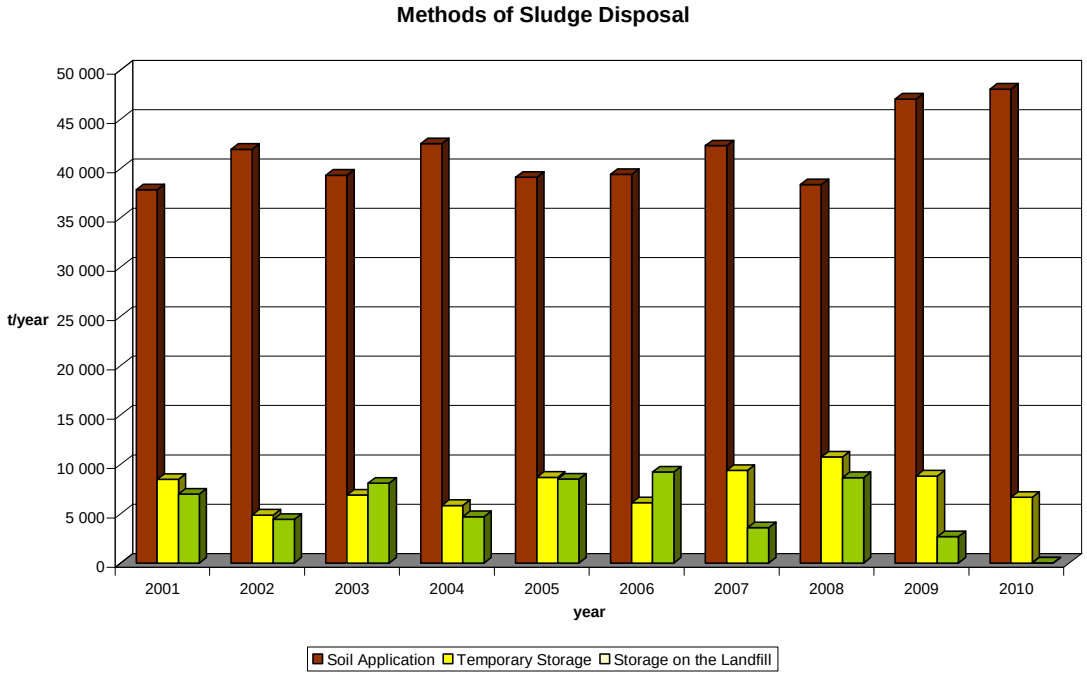

Figure 2: Methods of Sludge Disposal in Slovakia

5. CONCLUSIONS

Wastewater treatment involves the generation of large volumes of sludge and other waste whose management in an economical and environmental acceptable way has become a matter of increasing importance during the last few years. While the technologies and processes to reduce sludge generation are being widely studied, contributions relative to economic aspects are much more limited. However, when WWTPs operators face the implementation of these technologies, not only technical aspects must be considered but also the influence on environment has to be regarded. Technical solution, economical aspect and environment care are the three highlights, which have to be in balance. As we can see, that is possible to use various methods for sludge disposal. But our goal is to choose the best alternative from the technical, environmental and last, but not least economical point of view. Each WWTP has its own sludge treatment and also specific condition for sewage sludge disposal and hygienic inspection. We have to find the optimal solution for the people and for the environment.

6. ACKNOWLEDGMENTS

The Research Grant VEGA 1/1079/12 Vega 1/1143/11 held by the Department of Sanitary Engineering Faculty of Civil Engineering, Slovak University of Technology Bratislava has supported this paper..

7. REFERENCES

[1] MAHRÍKOVÁ, I.: Operation of Sludge Tanks in Small and Mid-Sized Waste Water Treatment Plants. In: Proceedings of ARW, Advanced Water Supply and Wastewater Treatment: a Road to Safer Society and Environment, Published by Springer, Netherland 2011, pp. 163-171

[2] MAHRÍKOVÁ I.: Doktorandská práca Optimalizácia prevádzky kalojemov ma malých a stredných komunálnych ČOV, Bratislava 2009

[3] RAJCZYKOVÁ, E. A Kol.: Základné princípy odvádzania a čistenia odpadových vôd, Bratislava, 2001

[4] Situačná správa zneškodňovaní komunálnych odpadových vôd a čistiarenských kalov V Slovenskej republike, Ministerstvo životného prostredia SR, 2008, Bratislava

[5] Správa o stave vodného hospodárstva v Slovenskej republike v roku 2008, Ministerstvo životného prostredia SR, Bratislava

[6] ŠUMNÁ J., DRAHOVSKAÁ D., KOZÁKOVÁ, K.: K stratégii nakladania s kalmi z čistiarní odpadových vôd. Zborník z konferencie Kaly a odpady 2008, s.25-28

[7] STANKO, ŠTEFAN - KRIŠ, JOZEF - ŠKULTÉTYOVÁ, IVONA: Environmental impact of waste-water reuse. In: 31st International Geographical Congress: Resumes/Tunis, 12.-15.8.2008, pp. 378-379

[8] HLAVÍINEkK P.: Perspectives of Decentrazed Waste water treatment of rural areas. In: Proceedings of ARW, Advanced Water Supply and Wastewater Treatment: a Road to Safer Society and Environment, Published by Springer, Netherland 2011, pp. 75-87

[9] Senante Molinos, M.: Techno-economical efficiency, cost modelling and economic valuation of environmental benefits from waste after treatment, Doctoral thesis, Valencia 2011

Water Management Of The Macedonian Watersheds In The Age Of Climate Change

Marija Vukelic-Shutoska

Abstract **- Water resources management planning in Macedonia is based on the principles of water management, territorial basis, professional and scientific data on water resources and on other socio-economic plans. The water management plan is a crucial document that defines the strategy of water use, water protection and flood protection in watersheds on the national territory. The watershed is the fundamental and natural unit in water protection and water use in Macedonia. Observation and interpretation of landscape features can help to understand the functioning of watershed ecosystems. Climate change affects all forms of land use and the key question is how to bring the water and agricultural sectors in watersheds closer together in terms of policy making, in the development of institutional mechanisms, capacity development and field projects as well as in terms of economic development. This paper describes the origins and development of organized water management of watersheds in Macedonia in the age of climate change.**

Keywords **- Climate Change, Water management, Water Resources, Watersheds.**

1. INTRODUCTION

The Republic of Macedonia is landlocked country in the central part of the Balkan Peninsula positioned between 40°50' and 42°20' North Latitude, and between 20°27'30" and 23°05' East Longitude.

With its status of the country in transition, the Republic of Macedonia receives multilateral technical and financial assistance in the areas of environment, agriculture, forestry, water management, but also in some others areas. This could indirectly help in the capacity building for implementation of the three global conventions and in overcoming the constraints for implementation of the national priorities in the three thematic areas - biodiversity, climate change and land degradation. In the area of national policy the most important is to build the capacity to plan and prioritize. Water administering and management includes planning of long term development of water resources. This comprise long term water policy measures taken by the society, management of water consumption and water saving in all forms, legal protection of water resources and the environment, etc. [7]. With the growth of the water crisis, the responsibilities of the government agencies in conducting of the water management policy become greater and more operational, and planning becomes more long-term and more complex. The sequence of activities in the process of general planning in water management may be presented as follows:

1. Defining objectives, criteria and standards, i.e. Planning needs
2. Determining requirements: quantification of requirements in relation to other plans
3. Determining resources: required and available resources
4. Defining standards of evaluation and selection of scenarios

Manuscript received June 20, 2012.

Marija Vukelic-Shutoska is with Faculty of Agricultural Sciences and Food, Ss. Cyril and Methodius University in Skopje, Blvd. Aleksandar Makedonski bb, 1000 Skopje, Republic of Macedonia, marija.vukelic-shutoska@t-home.mk

ISSN-1584-5990

5. Institutional framework for planning requirements.

Watersheds are the familiar landscapes created by mountain ranges as they slope down to valleys, with creeks and torrents flowing downstream. Also known as drainage areas or river basins, watersheds are the zones from which rain or melting snow drains downhill into a river, lake, dam, estuary, wetland, sea or ocean [19].

The climate and the climate changes have an impact on all segments in the country - society, ecosystems, national economy in various sectors (agriculture, forestry) and human health. The possible negative impacts have been identified and the adaptation measures in the most vulnerable sectors: agriculture, forestry and land-use change, water resources, biodiversity and human health, have been proposed. Climate change, especially global warming will cause negative effects on the soil production, causing degradation, desertification, and soil erosion. The adaptation measures have to be undertaken on both the farm and national levels. As adaptation measures, long-term activities have been proposed, such as: establishing scientific infrastructure, training the experts, collection of data and establishment of database.

Water resources are also very much influenced by climate change. According to the hydrological analysis it can be concluded that the most vulnerable regions in Macedonia are the Eastern and South-eastern parts, while the most vulnerable water economy sectors are water supply and irrigation. The proposed adaptation measures in various segments include modernization of the hydro-meteorological network, establishment of data monitoring, reconstruction and rehabilitation of existing structures and water economy systems and integrated water resources management.

The Ministry of Environment and Physical Planning is the institution responsible for coordination of the climate change related activities. The National Climate Change Committee as an inter-ministerial body is entitled to observe and coordinate the implementation of UN Framework Convention on Climate Change. Besides the two universities in Skopje and Bitola, few new universities, faculties and educational institutions have been established recently.

In the water resources sector there's an array of adaptation measures. The monitoring of required meteorological, and especially hydrological, parameters is far from satisfactory. It is necessary to undertake the following priority activities: modernization of the network and establishment of data monitoring of hydro-meteorological and water quality parameters with modern and usable database. In the water supply sector, dual supply systems for potable and non-potable water and water losses reduction, while in the irrigation sector, the proposed measures comprise: covering-lining of canals, introduction of drip, micro-spray, and other low water consumption irrigation systems, night-time irrigation and systems management. Climate change and change in climate variability pose serious risks to the environment and to life itself. All people and all sectors are likely to be affected. Parties to the United Nations Framework Convention on Climate Change – almost all countries in the world – have recognized the need to take action in climate change adaptation and mitigation [4].

A top country priority is the integration into the EU structures, with an ultimate goal being full EU membership. In this context, the sound knowledge of the EU sector policies is of utmost importance, since every valuable national policy intending to contribute to the realization of the EU integration targets, has its own strategic determinations to base upon, or at least, to make them compatible with the European ones.

The climate change area, the subject of this article, will occupy the topmost position in the EU policy in the next few years, being clearly presented in the sixth Environmental Action Plan of the EU Commission.

2. DESCRIPTION OF THE WATERSHEDS IN MACEDONIA

The Republic of Macedonia is bordering Bulgaria to the East, Serbia and Kosovo to the North, Albania to the West, and Greece to the South. Total surface area of the country is 25.713 km^2. The country lies between East-West direction of 210 km and South-North of 160 km with a border line of 850 km. The country ranges from an elevation 50 m above sea level around Gevgelija in alluvial lowland of the Vardar River in the South to the high mountainous area in the West and North-West where the peaks range from 2.200 m to 2.700 m. The

country consists of 19.1% plain area and 80.9% hilly area. Valleys and plains intersect the mountainous relief structures. The most distinct valleys are those extending along the Vardar River.

2.1 Topography

The Republic of Macedonia has a very complex geology and developed relief which ultimately leads to a great variation of soil types. Mountains represent the large relief forms covering approximately two thirds of the territory of the country. Principally they are part of the old Rhodope group in the Eastern part and young Dinaric group in the Western part of the country. Eastern mountains are in general lower than 2.000 meters. The Dinaric are a much higher mountain range at over 2.500 meters. In between these groups of mountains are the Vardar zone along both banks of the Vardar River and the Pelagonija horst anticline in the central part of the country.

Karstic relief is specific for Macedonia mostly represented with Paleozoic, Mesozoic, Palaeogenic and Neogenic limestone, found mostly in the central and western part of the country. The relief includes surface karstic forms of depressions, crevices, fissures and karstic plains as well as underground forms including 164 caves and 12 pits and sinkholes.

2.2 Climate

Due to specific natural and geographic characteristics, there are two main types of climate in Macedonia: modified Mediterranean and moderate continental. Thus, two prominent seasons occur: cold, wet winters and dry, hot summers interlinked with transitional spring and autumn. In addition to these, in the high mountainous areas there is also a mountainous climate characterized by short, cool summers and considerably cold and moderately wet winters, where precipitation is mainly in the form of snow. The average annual temperature is 11.3°C. The average precipitation of the Republic is 683.7 mm/year. Based on measurements and observations of the basic climatological parameters, several rather homogeneous climatic regions and sub-regions are defined in Macedonia: Sub-Mediterranean, Moderate Continental/Sub-Mediterranean, Hot Continental, Cold Continental, Sub-Forest-Continental-Mountainous, Forest-Continental Mountainous, Subalpine Mountainous and Alpine Mountainous.

2.3 Water resources

Surface waters are the most important part of the ecosystems in the country. They are mostly spread in the space and are the closest to the area of human activities. Due to the geographic location of the Republic of Macedonia, major part (84%) of the surface waters is domestic. The quantity of surface waters mainly depends on precipitation and snowmelting. Due to topographic, geological and morphological characteristics of the relief the runoff is running into the hydrographic network-rivers, streams and lakes. The karst areas (in the central and western part of the country) are the exception, where the water retains longer in the ground and recharge running waters of the river network.

Fig. 1. Rivers and Lakes in the Republic of Macedonia
Source: www.macedoniatravel.com, 2010

A river basin corresponds to the complex system of watersheds and sub-watersheds crossed by a major river and its tributaries while flowing from the source to the mouth [19]. The hydrographic territory of the Republic of Macedonia is divided into four watersheds: Vardar, Strumica, Crn Drim and Juzna Morava.

Vardar watershed is the largest and covers an area of 20.546 km^2 or 79.9% of the total territory of the country and gravitates towards Aegean Sea. The River Vardar is the longest and largest river in Macedonia. It has a length of 301.6 km with an average elevation at 793 m, from 2.748 m at Titov Vrv down to 44 m at Gevgelija. The spring of the river is in Shara massif near the village of Vrutok (Gostivar) at 683 m above the sea level. The average annual volume of discharged water at the border with Greece is accounted for approximately 4.56 x 109 m^3/year. Due to hydrographic characteristics of the Vardar watershed it is divided into Upper (above Skopje), Central (between Skopje and Veles), and Lower part (between Veles and Gevgelija).

Strumica watershed is in the South-eastern part of the country. It covers an area of 1.520 km^2 or 5.9 % of the total territory of the Republic of Macedonia. Strumica river is a tributary of Struma River in Bulgaria and flows into the Aegean Sea. Average annual volume of discharged water is approximately 132 x 106 m^3/year. This watershed is the poorest with water resources.

Crn Drim watershed is in the Western part of the country. Crn Drim watershed covers the watersheds of Prespa Lake and Ohrid Lake and the watershed of Crn Drim with its tributaries on the territory of the Republic of Macedonia to the Macedonian – Albanian border. Crn Drim watershed covers an area of 3.355 km^2 or 13% of the total territory of the country and gravitates towards Adriatic Sea. The river Crn Drim has a length of 44.5 km in the country. Average annual volume of discharged water is approximately 1.64 x 109 m^3/year.

Juzna Morava watershed is in the Northern part of the country. It is the smallest one with an area of 44 km^2 or 0.2% of the total territory of the country. Juzna Morava river flows into the Black Sea. This watershed has no significant impact on the availability of the water resources in the country. River Morava spring is in Macedonia and it belongs to the Danube watershed.

Water discharging in Macedonia is performed through the following rivers: Vardar at Gevgelija, Crn Drim at Debar and Strumica at Novo Selo. Watershed areas of the major and minor river basins are presented in Fig. 2 and Table 1.

Fig. 2. Watersheds in the Republic of Macedonia

Table. 1.

	River / Lake	Watershed area (km^2)	Watershed area (%)
1	**Major River Basins**		
	Vardar	6.813	26,5
	Treska	2.068	8,0
	Pchinja	2.373	9,2
	Bregalnica	4.307	16,8
	Crna	4.985	19,4
	Subtotal: 1	**20.546**	**79,9**
2	Crn Drim	3.355	13,0
3	Strumica	1.520	5,9
	Subtotal: 1 to 3	**25.421**	**98,8**
4	**Minor River Basins**		
	Dojran Lake	120	0,5
	Cironska & Lebnica	128	0,5
	Juzna Morava	44	0,2
	Subtotal: 4	**292**	**1,2**
	Total: 1 to 4	**25.713**	**100**

Source: Integrated Water resources Development and Management Master Plan in the Republic of Macedonia, Nippon Koei Co., Ltd. KRI International Corporation, Japan International Cooperation Agency – JICA, (1999)

The water potential of the watersheds depends on the precipitation regime. The average precipitation sum in Vardar watershed is 700 mm; in Strumica watershed is 790 mm and in Crn Drim watershed is 980 mm.

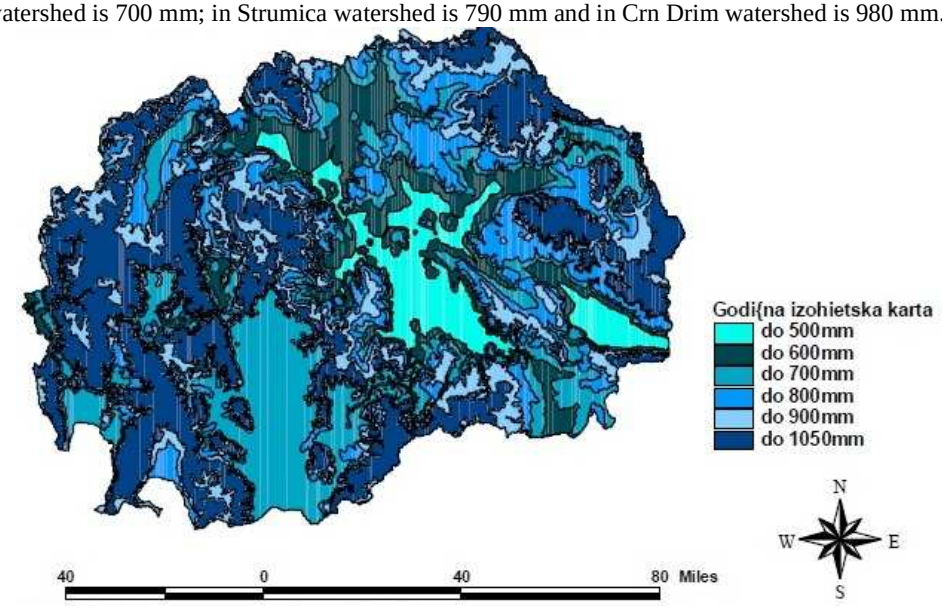

Fig. 3. Annual Isohietic Map of Macedonia

Source: National Action Plan to Combat Desertification and Land Degradation in Macedonia-draft, Ministry of Environment and Physical Planning/ UNDP, 2006

Maximum precipitation sums of 1.400 mm are registered in the Western part and the minimum precipitation sums of 380 mm are registered in the Eastern part of the country.

There are three natural lakes in Macedonia - Ohrid, Prespa and Dojran Lake. They also have great significance for the hydrographic characteristics of Macedonia. All of them are shared with the neighboring countries.

Ohrid and Prespa lakes are naturally connected by underground karsts channel and their waters flow through the Crn Drim watershed.

The total volume of Ohrid Lake is 50.683,3 x 109 m^3, the water surface covers an area of 348.8 km^2 (Macedonian part is with 229.9 km^2), with maximum depth of 285 m. We share Ohrid Lake with the neighboring Albania.

Lake Prespa is the second largest natural tectonic lake in the Republic of Macedonia. The total area of Prespa Lake is 274 km^2 (Macedonian part is 176.8 km^2) and has maximum depth of 52.4 m. It is recognized for its rich natural and cultural heritage. Two natural parks, Galicica and Pelister and the strictly protected wetland area Ezerani are within its watershed. Besides the natural beauty, the lake is an important resource for the economies of the three countries that share it - Macedonia, Greece and Albania. In the last two decades, the surface water level of the lake has dropped for more than 6 meters, endangering thereby both the fragile wetland environment and the economies in the region. The watershed of Lake Prespa does not have a surface outflow. The lake drains through karstic massif of Mountain Galicica to 150 meters lower Ohrid Lake.

The smallest natural lake is Dojran Lake. It is located in the South-eastern part of the country at an average altitude of 148 m. The watershed and the lake water surface are shared by Macedonia and Greece. Total watershed area of the lake is 271.8 km^2 out of which 92.1 km^2 or 32% belongs to Macedonia. Water surface area of the lake at normal elevation (147.34 m) is 42,2 km^2 out of which 27.1 km^2 or 63,6% belongs to Macedonia. Major surface inflows in the lake are from the Greek part of the watershed. Dojran Lake doesn't have surface outflows.

Groundwater is a generally renewable resource. However, the natural supply of groundwater is limited in time and space. One of the most important issues in water resources research is the management of groundwater systems in order to avoid or minimize bad effects on the environment and to maximize economic benefits [21].

The total water potential of the Republic of Macedonia in an average year amounts to 7.8 million m^3, out of which 5.6 million m^3 from the Vardar river valley, the Crn Drim river with 2.2 x 10^9 m^3. So far, irrigation systems have been constructed for 126.617 ha, out of which 99.918 ha in the Vardar catchment area; 18.432 ha in Strumica catchment area and 8.267 ha in Crn Drim catchment area [22].

The hydro-amelioration systems (HMS) in Macedonia, depending on the way waters are used for irrigation (running waters, reservoirs, lakes and groundwater) represent technical, technological and economic entity. The existing potential of HMS covers 173.000 ha, and they consist of: 16 irrigation systems encompassing 133.000 ha by catching 731.5 x 10^6 m^3 of water from reservoirs, 42 irrigation systems covering about 20.000 ha, pumping water from natural water courses, reservoirs and lakes, and 48 irrigation systems covering about 20.000 ha, where the water is taken from the natural water courses by gravitation.

Considering the limited possibilities of the natural sources and the underground waters, the water supply of the population and the industry in future can be resolved by water catchment from groundwater and reservoirs. With the future development of the water supply, it is planned to satisfy the needs of the population and the industry.

From energetic aspects, the construction of the hydro-electric power plants along the Vardar river valley within the period 2000-2015 represents a basis for long-term development of the electric power system of the Republic. To that effect, 12 hydro-electric power plants are planned to be constructed along the Vardar river course, from Skopje to the border on Greece, 200 km length. It is envisaged that two hydro-electric power plants will be constructed on each of the tributaries-Treska and Crna Reka. In total, 16 hydro-electric power plants with a total installed power of aggregates of about 1.000 MW and annual production of 2.2 x 10^9 KWh.

3. IMPACT OF CLIMATE CHANGE ON WATER RESOURCES IN THE WATERSHEDS

According the climatic classifications of the territory of Republic of Macedonia we can distinguish the following more homogeneous termical-climatic regions and sub-regions [5]: Region with sub-Mediterranean climate (50-500 m); Region with moderate-continental-sub-Mediterranean climate (to 600 m); With hot continental climate (600-900 m); With cold continental climate (900-1.100 m); Region with sub-forest-continental-mountainous climate (1.100-1.300 m); With forest-continental mountainous climate (1.300-1.650 m); Region with sub-alpine mountainous climate (1.650-2.250 m) and Region with alpine mountainous climate (h>2.250 m).

About 76% of the territory indicate signs of aridity or semi-aridity [20]. With the global climate changes it is realistic to expect that this percentage will increase. This leads to desertification, decrease of their forestation, loss of bio-diversity and increase of the erosive processes. According the data from the map of erosion, about 38% of whole territory is affected by middle and intensive erosion processes. Erosion is mostly treated in the water economy. From time to time, they cause huge damages with their destructive power by precipitating drifts and degradation of the urban and agricultural land.

Republic of Macedonia has ratified the United Nation Framework Convention on Climate Change on 4th December 1997. As a Party to the Convention, there is an obligation to prepare a regular National communication on climate change.

The first National communication on climate change was prepared in 2003, according to the guidelines set by the Conference of the Parties for the countries not included in the Annex I of the Convention.

From March 2005 until March 2008 the Second National communication on climate change has been elaborated, where the part which is dedicated to climate observations and research comprises:

- Basic characteristics and factors influencing the climate in the Republic of Macedonia,
- Analysis and interpretation of the long term climatological data for the periods 1961-1990 and 1971-2000 and their comparation.

Both National communications also comprise elaboration of different scenarios for the changes of the main climatic elements such as air temperature and precipitation in the 21st Century.

The expected change of the air temperature in the 21st Century in Macedonia is much higher than the expected change of the global temperature. In general, almost no change in precipitation is expected for the winter season on the area of Macedonia, but it is expected quite a strong decrease in the summer precipitation.

The local projections of climate change indicate that different climatic regions of Macedonia will respond slightly different to the large scale climate changes. The continental climate region in the South-western part of Macedonia, close to Ohrid and Prespa Lakes, seems to have the weakest response to the large scale climate change in a sense of absolute temperature and precipitation changes and the North-western part under the prevailing mountain/Alpine climate impact seems to have the strongest response.

Obtained differences show the need for further investigations and application of various methods and tools for critical review of present results and definition of the future climate change on the territory of the Republic of Macedonia [2].

Watershed ecosystems are relatively stable and solid. Throughout history, there are very few instances of watershed collapse due to human activities. However, starting in the 20th century, unsustainable development has often threatened the ecology of watersheds in many parts of the world.

In many cases, local population growth (resulting from better health status and education) has played a primary role in this process. To support the lives of ever-increasing numbers of people, upland forests have been cleared and turned into agricultural or grazing land. Large-scale timbering and fuel wood collection have contributed to watershed degradation. Loss of forest cover has increased upstream erosion and downstream sedimentation. Because of these changes, many watersheds are losing their capacity to regulate runoff. Subsequently, upland soil has become more arid, and nearby lowland areas more exposed to seasonal flooding. Landslide threats have also increased.

Freshwater available on Earth has a global volume of about 35 million km^3. However, 99,6 % of this water is stored in glaciers or underground. The remaining 0.4% corresponds to the atmosphere water, surface water and the soil moisture [3].

In humid areas, the proportion of water generated in the mountains can comprise as much as 60% of the total freshwater available in the watershed, while in the arid and semi-arid areas, the proportion is much higher – up to 95% [14].

At the moment, 45 countries with over 750 million people, face a situation of water stress, which means that the renewable water resources per person are less than 1.700 m^3/year. In 2025, this will concern 54 countries and more than 2.8 billion people [3].

Global climate change is contributing to watershed degradation. Because of global warming, glaciers and perennial snow are melting more quickly, thus reducing this important freshwater reserve and altering down-slope flows. Changes in the vegetation that are connected with changes in the temperature and water availability can be observed. Areas that were once fertile have become barren and unproductive.

In order to analyze the climate change impact on the watersheds, the data from the monitoring of the water quality of the river Vardar at the sampling points in Skopje and Demir Kapija are processed. The data were provided by the Administration of Hydrometeorology in the process of preparation of the 2nd Communication on Climate and Climate Changes and Adaptation in the Republic of Macedonia. The decision to analyze river Vardar at these sampling points is made upon the conclusion that the Central and the South part of the country belong to sensitive regions and upon already poor water quality at both sampling points mainly due to discharge of untreated urban waste water [6]. The data obtained from these two sampling points is rather reliable.

Climate change can affect the water quality aspect in three manners: a) reduced hydrological resources may leave less dilution flow in the river, leading to degraded water quality or increased investments in wastewater treatment, b) higher temperatures reduce dissolved oxygen content in water bodies and c) in response to climate change, water uses, especially those for agriculture, may increase the concentration of pollution being released to the rivers [10]. Alltogether, they pose a serious treat to the water quality.

The River Vardar during the hot periods (late spring, summer and early autumn) has low discharges, which means that the water temperatures are increasing with the decrease of the discharges. The temperature is very important ecological factor and every increase means treat to the aquatic balance and aquatic species. In the climate change conditions, reduced discharges with increased water temperatures would have negative impact on the aquatic environment. From the economic aspect, deteriorated water quality in the climate change conditions increases the costs for treatment of the wastewater.

Prespa Lake forms a transboundary water body shared by Albania, Greece and Macedonia. Being the largest international water body on the Balkans, Prespa Lake is very important for the region. Close co-operation between the countries sharing the lake is a prerequisite for sustainable management of water resources in the region and it is neccessary to ensure support from the international community for their sustainable management. Human activity in the Prespa Lake watershed covers fishery, tourism, industry, agriculture, forestry and urbanisation. All of them cause disruptive or polluting consequences for the Prespa Lake. From the past to the present date, the handling of water resources in the Prespa Lake watershed was and it is still mostly driven by the actual day-to-day needs and technical possibilities of each of the parties and countries. At the moment, only general objectives and goals for the management of the Prespa water resources have been defined and agreed upon by the three countries. Consequently it might be concluded that the water resources are being exploited rather than managed [18]. Management of transboundary waters is a complex issue, which has to overcome many challenges in order to achieve its environmental objectives.

Establishment of a reliable water balance of Lake Prespa is a necessity for sound planning and management decisions. It is required to study the elements of the water balance of the watershed. There are scarce hydrological and meteorological data available. The output of the balancing model has been checked with historical data of the lake surface water level and the outflow at the karstic springs in Lake Ohrid.

Possible changes in the temperature and precipitation regime and the seasonal distribution may have significant impacts on the elements of the overall water balance of the lake. These future development scenarios

have been applied to predict possible consequences of the climate change and increased water use in the watershed.

These days global warming has more and more attendance in all part of living. Global warming has very big influence in appearances of drought and drought periods. According global warming scenarios, drought and drought periods will happen more often in the Republic of Macedonia

4. INTEGRATED WATER RESOURCES MANAGEMENT IN WATERSHEDS

The Global Water Partnership (GWP) [8], defines integrated water resources management as a process that "promotes co-ordinated development and management of water, land and related resources, in order to maximise the resultant economic and social welfare in an equitable manner without compromising the sustainability of the vital ecosystems". At the river or lake watershed and aquifer level, Integrated Water Resources Management (IWRM) can be defined as a process that enables the co-ordinated management of water, land and related resources within the limits of a basin in such manner to optimise and equitably share the resulting socioeconomic well-being without compromising the long-term health of vital ecosystems. The IWRM approach at the national level does not conflict with the IWRM approach at the watershed level. In fact, they are complementary. A comprehensive national framework for IWRM is essential for both national and transboundary watershed management.

Within the limits of a watershed, it is not an easy task to integrate land uses and water management. The reason is that land management, which covers planning, forestry, industry, agriculture and the environment, is usually governed by policies not connected to water policy and is managed by many different parts of the administration.

The accurate planning of water resources systems is a complex interdisciplinary problem which involves complicated environmental, ecological and economical aspects.

Watershed degradation can be prevented and degraded watersheds restored by appropriate watershed management. Modern watershed management was born during the 20th century as a technical practice, largely based on major hydraulic engineering and forestry interventions. However, the experience has shown that technical measures alone are not enough to address watershed problems. Although water and runoff are the main focus of watershed management, most experts nowadays agree that relevant programmes need to be embedded in broader sustainable development processes.

One of the key issues in developing long-term watershed management strategic plans is to assess risks, such as those posed by floods, droughts or other natural disasters and to devise measures to alleviate these risks. For example, it is becoming increasingly important to plan for the risks posed by changes in climate.

The mechanisms for cooperation exist and agreement on the nature of the problems has been reached. It will be nonetheless important that many individual actions are taken together which will in total add up to a cleaner and healthier rivers and lakes in watersheds.

The future of the watersheds in the Republic of Macedonia will be dependent upon the solutions to the challenges that exist. Those challenges are many and varied:

- Achieving agricultural development that protects the waters,
- Adopting industrial strategies that prevent pollutant releases,
- Providing flood control that maintains and improves the hydromorphology of rivers and responds to the challenges of climate change,
- Ensuring energy needs and transportation that does not undermine the naturalness of rivers and lakes.

We have not had significant success in efforts to achieve cooperative management, but these efforts will be tested in the future by the challenges mentioned above. It is the responsibility of each and every one of us, people in Macedonia and elsewhere in the transboundary watersheds, to ensure our actions and activities benefit the maintenance and sustainability of the ecosystems that supports us.

Watersheds that cover more than one country – transboundary watersheds – present particular challenges for managers. Historically, transboundary watersheds have encouraged regional cooperation but, as resources dwindle and demands grow, the potential for conflict over shared waters also grows. To offset this, some basins

are using a shared vision approach that incorporates many of the principles of the Integrated Water Resources Management approach. For example, the use of participatory processes to consider basin issues in the overall development context of all the riparian states in the basin [1].

The Shared Vision Program also builds stakeholders' capacity to participate in managing natural resources across boundaries, share benefits and improve water efficiency in agriculture for example, all of which are consistent with IWRM principles.

Natural resources bring risks. One is that too many people become locked in low-skill intensive natural-resource-based industries, including agriculture, and thus fail through no fault of their own to advance their own or their children's education and earning power. Another risk is that the authorities and other inhabitants of resource-rich countries become over confident and therefore tend to underrate or overlook the need for good economic policies as well as for good education. In other words, nations that believe that natural capital is their most important asset may develop a false sense of security and become negligent about the accumulation of human capital. Indeed, resource-rich nations can live well of their natural resources over extended periods, even with poor economic policies and a weak commitment to education. Nations without natural resources have a smaller margin for error and are less likely to make this mistake [9].

5. CONCLUSIONS

Global climate studies examining the larger geographical areas of the East Mediterranean and the Middle East predict that, along with an expected increase of the air temperature by 1-3°C, rainfall will replace snow in winter, annual precipitation will show a significant decrease, the annual flow of rivers will decrease, evaporation losses will increase, the water levels of reservoirs will fall, flood damage will increase because of the rapid melting of the mountain snow, and the rapid depletion of this natural reservoir will mean that it will not be able to feed water sources for longer periods [13].

According to the Report on Climate Change Scenarios for Macedonia, Review of Methodology and Results [12], expected changes of the air temperature for the time horizon 2010, as provided by the meteorological station in Bitola, are more intensive in the summer periods than in winter ones. Changes in the rains are not expected during winter months or such changes would be minor. Decrease in the rains is recorded in all other seasons.

If measures are not taken to counter these adverse effects of climate change on the watersheds, the country will face serious problems of water security and consequently food security.

Watershed management could be a weak point in water sector in the country. Watershed managers may wonder where to start with an integrated approach, who to target and at what level. A simple and effective way to find out where to target action initially is to identify entry levels:

1. Local level (sub-basin plan, local aquifer management plan, local water allocation plan in water user districts, local government plan).
2. Implementation level (basin or provincial scale management plan).
3. Policy level (national and international processes for developing water policies, treaties, and laws).

Strategic planning of watersheds in Macedonia should involve setting long-term goals for water management in a watershed:

- Develop water footprints under different climate change scenarios,
- Develop procedures to rapidly update water management strategies and plans with the latest hydrological data and changes in water use, and present these as water footprint scenarios,
- Use risk assessment to evaluate water resources management options under different climate change scenarios,
- Have a clear view of the actual situation of water resources in the watersheds,
- Link the watershed strategy to broader development goals, and national and regional development planning processes,
- Allocate human and financial resources to the strategic planning process,

- Define the boundaries of the watershed (river watersheds or sub-watersheds, aquifers, lake watersheds,

national or transboundary).

- Analyses of priority issues,
- Water allocation and water quality objectives,
- Benefit shares.

The strategic plan needs to be flexible enough to adjust to the new information and changing circumstances as they emerge.

Environmental dimensions of water developing projects must be evaluated seriously, water management based on water supply should be changed with water management based on water demand.

6. REFERENCES

[1]. Global Water Partnership and International Network of Basin Organizations, A Handbook for Integrated Water Resources Management in Basins, 2009, Printed by Elanders, Sweden, ISBN:978-91-85321-72-8.

[2]. S. Alcinova Monevska, P. Ristevski, V. Pavlovska, S. Snezana Todorovska, Projection of Temperature and Precipitation Changes in the XXI Century on the Territory of Republic of Macedonia, BALWOIS 2010, Ohrid, Republic of Macedonia.

[3]. Aquastat online data base, www.fao.org/ag/aquastat, FAO, Rome, 2007.

[4]. National Forest Programme, Climate Change for Forest Policy-Makers, An approach for integrating climate change into national forest programmes in support of sustainable forest management, Facility nurturing the process, FAO, 2011.

[5]. O. Cukaliev, K. Donevska, I. Blinkov, D. Mukaetov, P. Ristevski, N. Aleksovska, Capacity Self-Assessment within the Thematic Area of land Degradation and Desertification, Draft Report 2003, Self-Assessment of Country Capacity Needs for Global Environment Management, Skopje.

[6]. K. Donevska, S. Dodeva, Climate Change Impact on Surface Water Quality in the Republic of Macedonia, BALWOIS 2008, Ohrid, Republic of Macedonia.

[7]. D. Geresh, Integrated water management (in Croatian), Gradjevinar, 47 (1995)7, pp. 391-396.

[8]. GWP TAC, Background Paper No. 4. Integrated Water Resources Management. Global Water Partnership, 2000, Stockholm, Sweden.

[9]. T. Gylfason, Natural Resources, Education and Economic Development, Institute of Economic Studies, Working Paper Series, 2000, W00:10, For the 15th Annual Congress of the European Economic Association, Bolzano

[10]. IPCC Technical Guidelines for Assessing Climate Change Impact and Adaptations, Handbook on Methods for Climate Change Impact Assessment and Adaptation Strategies, 1998

[11]. Integrated Water resources Development and Management Master Plan in the Republic of Macedonia, 1999, Nippon Koei Co., Ltd. KRI International Corporation, Japan International Cooperation Agency – JICA.

[12]. B. Klemen, Report on Climate Change Scenarios for Macedonia, Review of Methodology and Results, 2006

[13]. P.G. Mengu, S. Sensoy, E. Akkuzu, Effects of Global Climate Change on Agriculture and Water Resources, BALWOIS 2008, Ohrid, Republic of Macedonia.

[14]. Mountains of the world. Water towers for the 21st century, Mountain Agenda, University of Bern, Bern, Switzerland, 1998.

[15]. Report on Climate Change Scenarios for Macedonia, Review of Methodology and Results, 2006.

[16]. Report on Second Communication on Climate and Climate Changes and Adaptation in the Republic of Macedonia, Section: Vulnerability Assessment and Adaptation for Water Resources Sector

[17]. Review of the First Communication on Climate and Climate Changes and Adaptation in the Republic of Macedonia, Section: Hydrology and Water Resources, Ministry of Environment and Physical Planning/ UNDP, 2004.
[18]. Z. Vukelic, K. Donevska, M. Vukelic-Sutoska, M. Murati, Possibilities for Waste Management in the Prespa region, International Symposium Sustainable Development of Prespa Region, Proceedings 2000, Otesevo – Macedonia, pp. 336-343.
[19]. Why invest in watershed management?, FAO, 2009.
[20]. M. Vukelic-Sutoska, Problems in research and complex use of water resources in semi-arid areas, Doctoral thesis, 2002, University of Zagreb, Faculty of Civil Engineering in Zagreb, Croatia.
[21]. Z. Vukelic, M. Vukelic, Influence of Nitrate and Pesticide on Groundwater, International Conference Agriculture and Water Economy, Proceedings 1994, Bizovacke Toplice (Croatia), pp. 105-110, 2010.
[22]. Expert Report on Water Resources Management, 2010.
[23]. National Action Plan to Combat Desertification and Land Degradation in Macedonia-draft, Ministry of Environment and Physical Planning/ UNDP, Republic of Macedonia, 2006.
[24]. https://www.macedoniatravel.com/index.php?option=com_content&view=article&id=201&Itemid=181&lang=en, 2010.

SECTION V

SURFACE AND GROUNDWATER HYDROLOGY

Soil Clay Fraction Impact on Coefficient of Linear Extensibility

M. Gomboš, A. Tall

Clay minerals are the main cause of soil volume changes due to their behaviour during saturation with water and drying. Volume changes influence on soil water regime in unsaturated zone of a soil profile, transporting processes in soil and they are often to be accounted for the damages to engineering constructions and buildings. From that reason it is important that volume changes characteristics be explored. One of them is the coefficient of linear extensibility which quantifies the shrink-swell soil potential. The aim of this paper is to analyze clay minerals impact on the value of coefficient of linear extensibility. The analysis is based on the measurements of soil particle-size and soil volume changes during drying. It has shown significant clay minerals influence on the soil potential for volume changes. The presented results have been obtained in the Slovak Republic on the East-Slovakian Lowland.

***Keywords*– volume changes, coefficient of linear extensibility (COLE), particle size distribution**

1. INTRODUCTION

Clay minerals are able to absorb water and incorporate it to its microstructure. During this processes (water absorption or loss), volume changes occur in clay particles. High content of clay particles in soils can cause their volume changes provided there are simultaneous moisture changes. When saturated with water, heavy soils tend to swell up and, on the contrary, when dried, they shrink.

Volume changes intensity depends on the amount and type of clay minerals forming the soil, that is to say, elements which are soil structural elements. As a result, there is a wide range of volume changes occurring during their interaction with water. Clay minerals, such as kaolinite, are relatively inactive and of lower swelling potential. Illites are slightly expansive and montmorillonite clays are highly expansive. As for other soil types, volume changes occurring during drying depend on the clay fraction ratio contained in the soil texture. Volume changes in the clay-loam soils during their drying or water absorption are a three-dimensional process. Generally speaking, this process is not homogeneous in all the three directions. It depends on porous environment homogeneity and on isotropy of the soil shrinking properties. Under the field conditions, volume changes in the vertical line are represented by vertical movement of soil surface. In horizontal line, these volume changes are manifested by crack formation.

The characteristics described above influence on transporting processes in the soil aeration zone, on water regime in the soil profiles [1], [2] and [3], and they often have negative impact on engineering constructions. In the areas with a heavy presence of clay soils it is hence important to be aware of the characteristics of volume changes- coefficient of linear extensibility (COLE) being one of them. COLE is used to quantify the potential for volume changes and it plays a vital role in assessing soil volume changes impact on hydrological processes in soil.

The aim of the paper is to analyse the impact of clay minerals on soil potential for volume changes with regard to clay content in soil. The results were obtained in the Slovak Republic on the East-Slovakian Lowland (ESL).

MilanGomboš is with Institute of Hydrology Slovac Academy of Scientes, Hollého 42, 071 01 Michalovce, Slovakia (corresponding author to provide phone: 00421-056-6425147; fax: 00421-056-6425147; e-mail: gombos@uh.savba.sk).

Andrej Tall is with Institute of Hydrology Slovac Academy of Scientes, Hollého 42, 071 01 Michalovce, Slovakia (e-mail: tall@uh.savba.sk).

ISSN-1584-5990

2. EXPERIMENT DESCRIPTION

Coefficient of linear extensibility (COLE) [4] is a parameter that quantifies soil shrink-swell potential. It is defined as follows:

$$COLE = \left(\frac{V_{wet}}{V_{dry}} \right)^{\frac{1}{3}} - 1 \quad \textbf{(1)}$$

where

V_{wet} is volume of wet soil sample,
V_{dry} is volume of dried soil sample.

COLE values are further used to classify soil horizons with regard to shrink-swell soil potential to soils with low, medium, high and very high potential, **Table 1**.

Table 1. Soil classification by COLE and shrink-swell potential (Parker - Amos - Kaster, 1977)

Shrink – swell potential	**COLE [-]**
Low	< 0.03
Medium	0.03 – 0.06
High	0.06 – 0.09
Very high	> 0.09

V_{wet} and V_{dry}, where "wet" and "dry" are relatively vague terms what allows for subjective interpretation of them, need to be exactly defined as for the minimal moisture and dryness level that is sufficient for the soil sample to be considered "wet" or "dry". It is especially important when COLE values measured in different places around the world are compared. In the US classification system [5], V_{wet} is defined as the volume of a soil sample with moisture potential 333cm of pressure head and V_{dry} as the volume of a soil sample with moisture level obtained by maximal drying of the soil profile under natural conditions. These levels should consider climatic conditions of the area where the samples are taken and analysed. However, more often than not samples dried in laboratory are used. In a Dutch study [6] V_{wet} was defined as the volume of a soil sample saturated with water and V_{dry} as the volume of a soil profile with the moisture level representing pressure head – 16 000cm. Under ESL conditions, V_{wet} was defined as the volume of saturated soil sample and V_{dry} as the volume of a laboratory-dried soil sample. This is the quickest and simplest way because retention curve does not have to be used here which is of great help as its measurement in clay soils is extremely time-demanding.

The work method is based on analysing the dependence between COLE values found in compacted soil samples of a particular volume and texture. Altogether, 146 samples of 14 profiles taken from 52 different layers and 9 areas, were analysed. Position and characteristics of the areas are listed in Table 2.

After sampling, the samples were saturated with water until reaching level of saturated soil moisture content and then their volume was weighed. The samples were gradually dried at the temperature of 30°C until the point their weight differentials were approaching measurement error. Then the temperature was raised to 105°C and they were dried up. The value of the sample volume measured after being dried is V_{dry}.

Particle size analysis was performed by the pipette method with regard to five particle-size fractions. In the first fraction (Fr.I), percentage of particles from the interval $\langle 0{,}000; 0{,}001\ mm \rangle$ was determined, in the second (Fr.II) = $\langle 0{,}001; 0{,}01\ mm \rangle$, in the third (Fr.III) = $\langle 0{,}01; 0{,}05\ mm \rangle$, fourth (Fr.IV) = $\langle 0{,}05; 0{,}25\ mm \rangle$ and fifth (Fr.V) = $\langle 0{,}25, 2{,}00\ mm \rangle$. The particles contained in the particular fractions are colloidal clay (Fr.I), physical clay to very fine dust (Fr.II), dust (Fr.III) very fine sand (Fr.IV) and medium sand to coarse sand (Fr.V). For the identification of soil types the textural classification to clay$\langle 0{,}000; 0{,}001\ mm \rangle$, silt $\langle 0{,}001 - 0{,}05\ mm \rangle$, and sand $\langle 0{,}05 - 2{,}0\ mm \rangle$ is usually used. With regard to texture, soil types are classified by soil textural triangles. In this paper USDA textural triangle is used [5]. Apart from this, cumulative contents of particles "< 0,002 mm",

Table 2. Location of analysed areas and sampling

lokality	number of profiles	depth profiles	počet vrstiev	number of layers	location		altitude [m]
					ϕ	λ	
Michalovce	1	0,8	8	24	48°44´17,38´´	21°56´37,04´´	107
Senné	2	0,8	16	48	48°39´48,19´´	22°02´53,90´´	97
Vysoká	1	0,6	6	18	48°36´47,48´´	22°06´54,23´´	104
Somotor	2	0,8	9	26	48°23´10,40´´	21°48´14,20´´	95
Milhostov	4	0,2	4	12	48°40´11,08´´	21°44'18,02"	100
Pribeník	1	0,8	3	6	48°23´41,30´´	21°59´32,80´´	98
Veľký Kamenec	1	0,8	2	4	48°21´02,90´´	21°48´52,60´´	96
Veľký Horeš	1	0,8	3	6	48°22´32,40´´	21°53´54,40´´	95
Zatín	1	0,8	1	2	48°28´43,50´´	21°54´55,10´´	99

"< 0,004 mm", "< 0,005 mm", "<0,01 mm", "< 0,05 mm", "< 0,25 mm" were calculated for all soil samples. All results of the analyses were used to quantify the physical clay impact on COLE values.

In the analysis of the particle-size structure impact on COLE values were used statistical tool, particularly, the methods of correlation and regression analysis. The analyses evaluated the correlation relations between COLE and different particle-size fractions.

The following was identified upon the results of the analyses: the impact of particle-size analysis on COLE, textural fraction influencing COLE most, clay minerals impact on COLE. Moreover, equation for determining COLE value from soil texture was proposed. The results are compared to the results by other authors from different parts of the world.

3. RESULTS AND SIGNIFICANCES

In **Fig.1** (USDA textural triangle), soil types of the analysed soil samples are identified. It shows that clay soils predominate in the taken soil samples. The soils marked in **Fig.1** are typical of ESL. **Fig.2** shows the results of correlation analysis of the dependence between COLE and selected particle-size intervals. The values clearly show that COLE is influenced the most by the content of colloidal clay, i.e. particles from the interval $\langle 0{,}000; < 0{,}001\ mm \rangle$. The value of correlation dependence (**Fig.2**) is 0.939, which is high degree of dependence.

The results of the correlation analysis of relations between cumulative contents of textural fractions and COLE, stated above, are shown in **Fig.3**. As in the previous case, the analysis confirmed the importance of colloidal clay as for COLE values. The course of empiric correlation dependence shows that cumulative accrual of coarser fractions to fine sand (< 0.25mm) gradually lower the tightness of correlation relation to 0.555. It means that the more silt and sand fraction soil has, the smaller is COLE value. On the contrary, the more clay soil has, the tighter is the correlation relation.

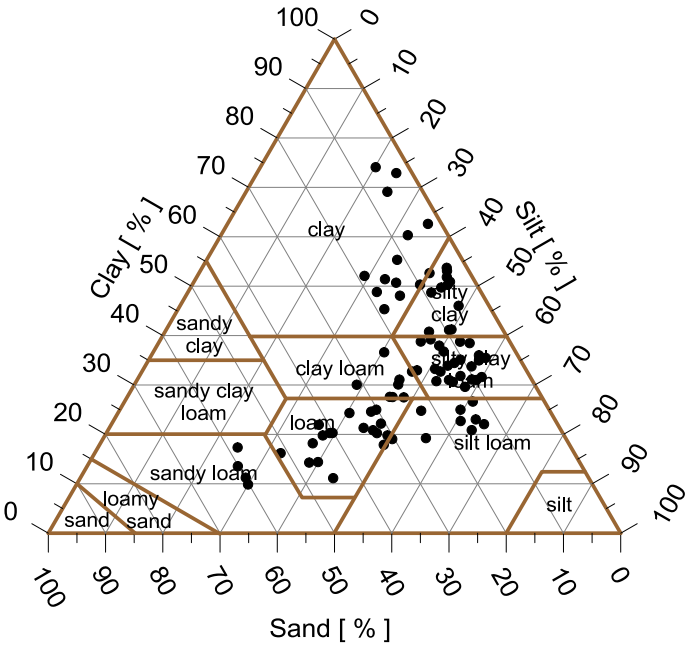

Fig. 1. Identification of the particular soil types in the analysed soil profiles by means of USDA textural triangle.

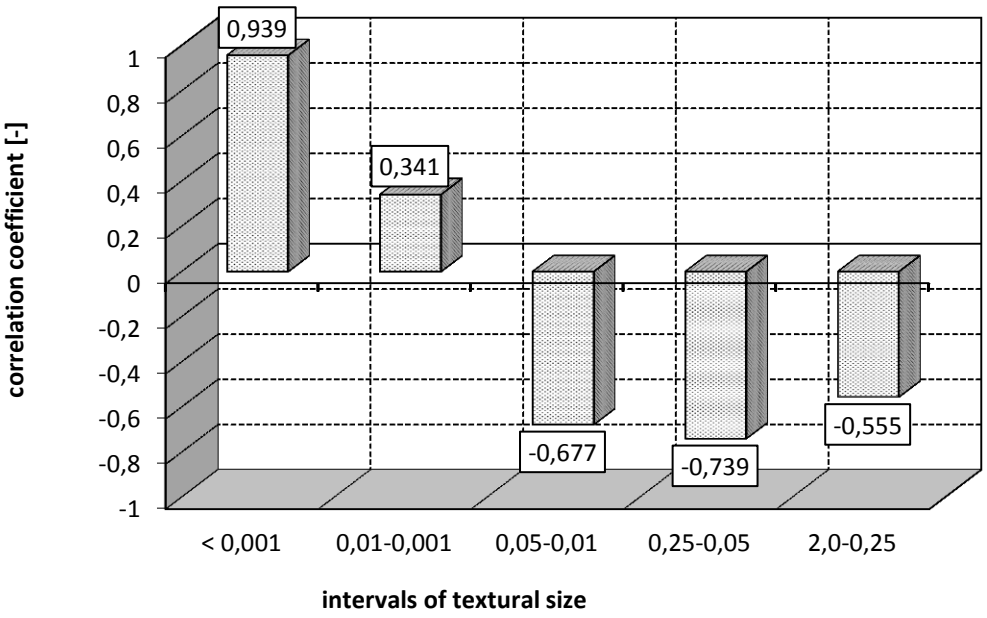

Fig. 2. Degree of correlation dependence between COLE and textural fractions.

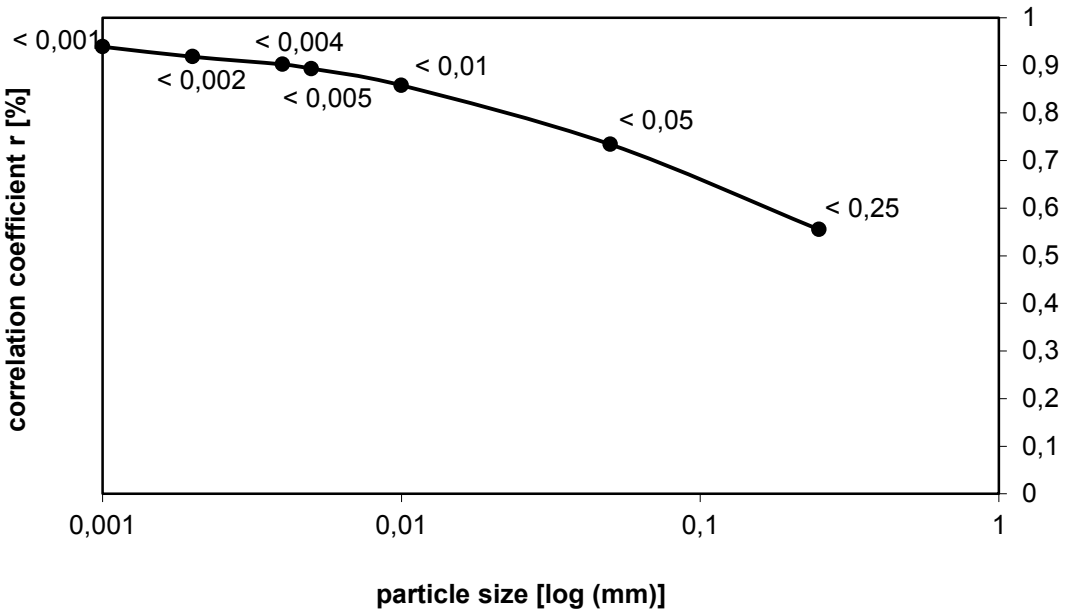

Fig. 3. The course of correlation dependence between COLE and cumulative textural fractions.

Fig.4 is a graphical representation of the dependence between COLE values and the content of clay particles ((< 0.002 mm) and **Fig. 4b** shows the dependence between COLE values and the content of Fration I. (fine clay < 0,001 mm). Degree of correlation dependence is very high (r = 0.937 and 0.939). In either case it is almost the same, r = 0.94. Clay content in soil is commonly used for identifying soil types with regard to classification triangles. Consequently, it is better to estimate COLE on the basis of clay content in soil, using the equation below:

$$COLE = 0{,}2967 \times (contents\ clay\ [\%]) - 4{,}6632 \quad [\%] \qquad \textbf{(2)}$$

This equation (2) can be adjusted and verified to suit the needs of the analysed area by further measurements.

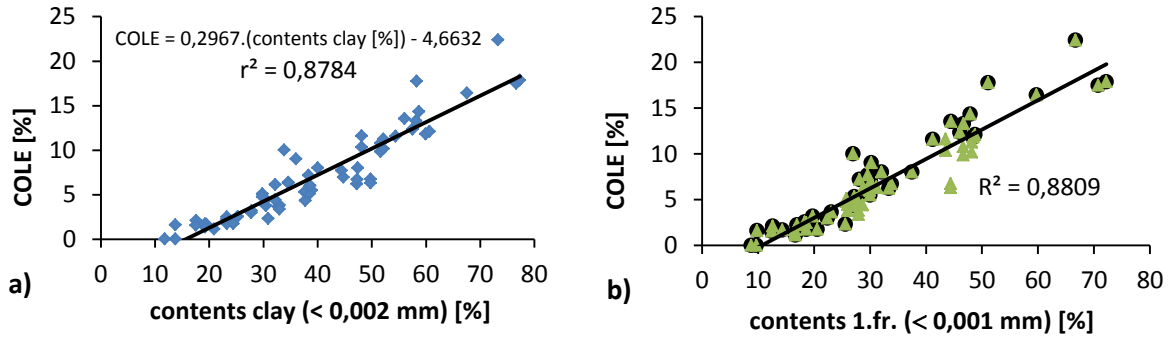

Fig. 4. Graphical representation of linear dependence between COLE and clay particles content (< 0,002 mm), **Fig. 4a**, and Fraction 1 (colloidal clay < 0,001mm), **Fig.4b**, in ESL soils.

COLE dependence on clay minerals content measured in ESL was compared to the results obtained in the Netherlands and USA [6], [7] and [8]. In their calculations, the authors used clay fraction containing particles of < 0,002 mm. The comparison is represented in **Fig.5.** It is obvious that the line representing ESL data is more inclined than the other lines, which is probably assigned to great spatial variability of mineralogical structure of clay minerals, particularly illites and montmorillonites.

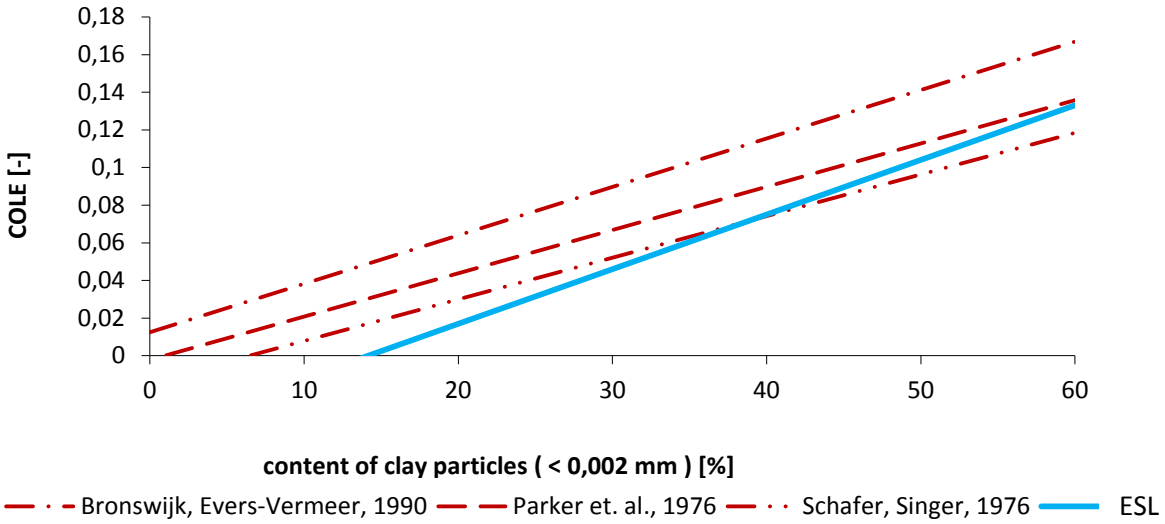

Fig.5. Comparison of dependence between COLE and clay minerals content in ESL and the dependencies measured in heavy soils of the Netherlands and USA.

Tab.3 shows contents of clay particles in soil samples classified according to **Tab.1.** The higher the shrinking potential, the higher is the percentage of clay fraction contained in samples. This observation is represented in **Fig.6.**

Table 3. Clay fraction content in soil samples of different shrink-swell potential

shrink - swell potential	number of samples		content of particles (clay) < 0,002 mm v [%]			content of particles (fine clay) < 0,001 mm v [%]		
	absolute	%	average	min	max	average	min	max
low	16	25,81	20,70	11,79	30,86	16,14	8,78	25,56
medium	14	22,58	33,61	27,77	38,90	26,63	19,77	29,96
high	13	20,97	42,02	32,19	49,75	33,42	28,07	44,41
very high	19	30,65	57,68	33,80	77,33	49,86	26,93	72,22

Fig.6 graphically shows the percentage of clay fraction with particle size < 0,002 mm in soil samples of different shrink-swell potential. The average values of clay content increase by 2.8-times. Variation range (max. – min.) of clay fraction also increases. Very high COLE values were documented at 57% clay particles content. Maximal values of clay content in soil samples reach up to 77%.

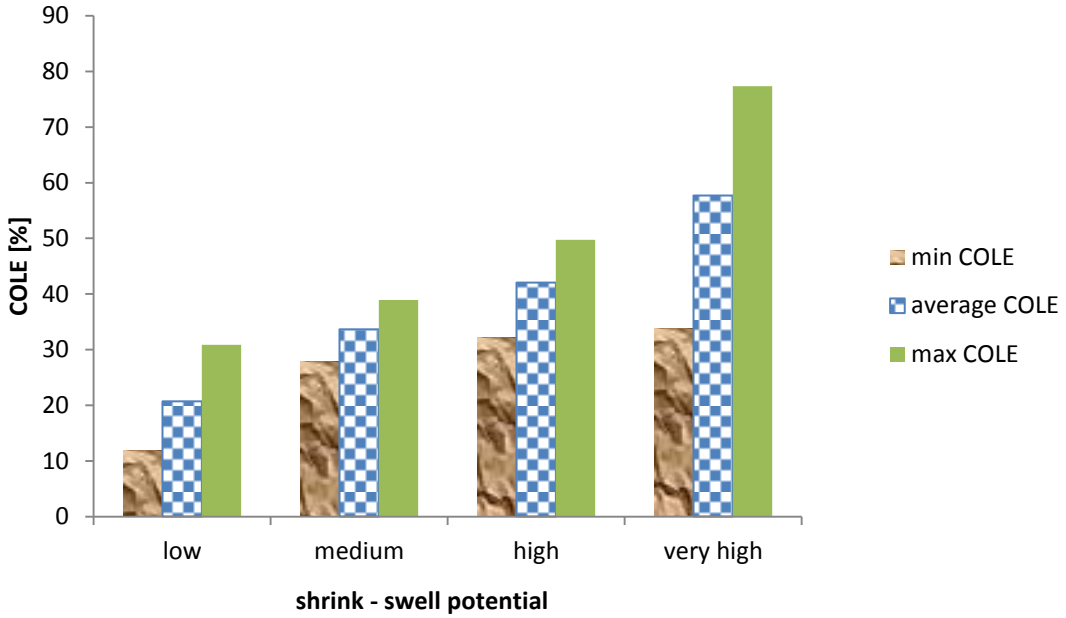

Fig.6. Percentages of clay fraction with particle size of < 0,002 mm in soil samples with different shrink-swell potential.

4. CONCLUSIONS

The aim of this paper is to present the results of the analysis of clay fraction impact on coefficient of linear extensibility (COLE) of soils. COLE is used to quantify the ability of soil to change volume and it serves as source data for the calculation of shrink-swell potential of one or two-layer soil profiles.

The analysis was based on the results of the measurements of soil texture and volume changes in soil samples of definite volume, sampled in selected localities on ESL**, Tab.2**.

The analysis shows that COLE values in soil are influenced by clay particles content, i.e. particles < 0,002 mm. Degree of correlation dependence is 0.94. With regard to significant correlation dependence and for the purposes of the specific ESL conditions, empirical equation for assessing COLE from clay particles content was proposed (2). This equation can be used to efficiently gain the data on heavy soils shrink-swell potential. The data can serve for classification of ESL soils according to their potential for volume changes. It is one of the parameters necessary for optimization of lowland water regime considering the ongoing climatic changes.

5. ACKNOWLEDGMENTS

The authors would like to thank for the kind support of the project VEGA 2/0142/12 and project APVV-0139-10.

6. REFERENCES

[1]Štekauerová, V., Weather, Effects on Plants. In Encyklopedia of Agrophysics. - Springer Sci : Business Media B.V., 2011, s. 984-987. ISBN 978-90-481-35854.
[2]Štekauerová, V., Šútor, J., Nagy, V., Halasi-Kun, G. J.,Soil hydrophysical characteristics and their function in the soil water storage formation, dynamics and evaluation. In Pollution and Water Resources, Columbia University Seminar Proceedings : Environmental Protection of Central Europe and USA. vol. XL, 2010-2011. - Bratislava ; Pécs : Institute of Hydrology SAS : Hungarian Academy of Sciences, 2011, s. 296-318. ISBN 978-80-89139-24-8.
[3] Šoltész, A, Květon, R, Baroková, D, Vércseová E., Hydrologichydraulicassessment of internal water drainage in lowland regions of Slovakia, NinthInternational Symposium on Water Management and Hydraulic Engineering, IXWMHI, pp 427-434, 2005, Austria.
[4] Grossman, R. B., Brasher, B. R., Franzmeier, D. P. et al., Linear extensibility as calculated from natural-clod bulk density measurements. In: Soil Science Society of America Proceedings. 1968, č. 32, s. 570-573.
[5] Soil taxonomy: a basic system for soil classification for making and interpreting soil surveys. Agric. 1975. Handbook 436. In: Soil Survey Staff. Washington : US Department of Agriculture. 1975, 754 s.
[6] Bronswijk, J. J. B. – Evers-Vermeer, J. J. 1990. Shrinkage of Dutch clay soil aggregates. In: Netherlands Journal of Agricultural Science. 1990, č. 38, s. 175-194.
[7] Schafer, W. M. – Singer, M. J., Influence of physical and mineralogical properties on swelling of soils in Yolo County, California. In: Soil Science Society of America Journal. 1976, č. 40, s. 557-562.
[8]Parker, J. C. – Amos, D. F. – Kaster, D. L. 1977. An evaluation of several methods of estimating soil volume change. In: Soil Science Society of America Journal. 1977, č. 41, s. 1059-1064.

Groundwater participation in evaporation from the root zone of soil profiles of different texture

M. Gomboš, D. Pavelková, B. Kandra

***Abstract*–Lower boundary of unsaturated soil zone is formed by groundwater level. At this level, water from unsaturated soil zone flows to groundwater and vice versa, groundwater penetrates unsaturated zone. By capillary rise, groundwater can supply water storage in root zone and thus influence on actual evaporation in this soil layer. Degree to which this occurs depends on given soil texture and the groundwater level position with regard to position of lower root zone boundary.**

The paper does not quantify the impact of soil texture on the involvement of groundwater in evaporation process. The results were obtained by numerical experiment on GLOBAL model. The measurements used for model verification and numerical simulation were gained in ESL (East-Slovakian Lowland).

***Keywords*– groundwater level, particle size distribution, actual evapotranspiration**

1. INTRODUCTION

From the systemic point of view, hydrological cycle is a complex system composed of different interrelated elements. It comprises atmosphere-plant cover- unsaturated zone- groundwater. This structure implies further issues to be investigated, including the research and quantification of interaction processes between the individual subsystems of hydrological cycle.

Generally, unsaturated zone is a three-phase system limited by soil surface upwards and groundwater level downwards. Unsaturated zone and surrounding sub-systems are linked by interaction processes. The intensity of such processes depends on hydro-physical soil properties, i.e. every soil type reacts differently to the changes of meteorological elements. Similarly to unsaturated zone, groundwater forms part of the system *atmosphere – plant cover – unsaturated zone – groundwater*. In the calculations of soil water regime, groundwater level is considered as the lower boundary condition. Unsaturated zone lower boundary is dynamic and on account of the interaction with groundwater it changes in time and space. At the boundary, water flows from unsaturated zone to groundwater and vice versa. Groundwater hence flows by capillary rise to unsaturated zone and provides water supply to water storage in the root zone, influencing on the actual evapotranspiration occurring in this layer. This is particularly evident in the periods of soil drought [1], [2], [3] and [4].

Water supply to root zone from the groundwater level causes groundwater level to drop. When groundwater level drops under certain critical level, water transfer stops between groundwater level and root zone. Root zone moisture conditions depend wholly on precipitation and evaporation [5].

MilanGomboš is with Institute of Hydrology Slovac Academy of Scientes, Hollého 42, 071 01 Michalovce, Slovakia (corresponding author to provide phone: 00421-056-6425147; fax: 00421-056-6425147; e-mail: gombos@uh.savba.sk).

Dana Pavelková is with Institute of Hydrology Slovac Academy of Scientes, Hollého 42, 071 01 Michalovce, Slovakia (e-mail: pavelkova@uh.savba.sk).

BranislavKandra is with Institute of Hydrology Slovac Academy of Scientes, Hollého 42, 071 01 Michalovce, Slovakia (e-mail: kandra@uh.savba.sk).

ISSN-1584-5990

The aim of the paper is to quantify the impact of texture on the degree of groundwater impact on water evaporation from the root zone of a soil profile. Evaporation from different soil types was analysed with regard to modelled positions of average groundwater level during the vegetation period.

2. EXPERIMENT DESCRIPTION

Soil water regime, its elements and interaction with groundwater can be determined in two ways: by monitoring or calculation.

The former is an extremely time and financially demanding and very extensive process. In addition to this, soil water storage monitoring in unsaturated zone is very rarely applied under natural conditions in Slovakia. The monitoring method is being launched just nowadays.

The latter, quantification of soil water regime and the development of its elements, is performed by means of numerical simulation on mathematical models. The problem of this method is the necessity of a wide range of reliable input data. On the other hand, the method enables to obtain time series, usually with one-day time interval, of soil moisture in the analysed soil profile horizons. Daily water flow development can be calculated at the boundary between aeration soil zone and groundwater level, or at a lower boundary of aeration zone, determined otherwise. Numerical simulation facilitates the experiments that would be expensive, time-demanding or unfeasible in reality. Moreover, this method is harmless to environment and enables the change in time criterion. From the reasons stated above, numerical experimental method was used and it was performed by means of numerical simulation on GLOBAL [6], [7] mathematical model.

The model was verified by means of the results obtained in soil moisture monitoring (2007). Verification was performed in the southern part of ESL in Somotor area (48°23´10,40´´; 21°48´14,20´´). For the purposes of the verification, courses of soil water storage up to depth of 0.80m were calculated for the vegetation periods in 2007. These are compared to the measured values. For better illustration, daily sums of actual and potential evapotranspiration were calculated.

Numerical simulation was realised for the hydrometeorological conditions and for GWL in 2001 vegetation periods. Precipitation conditions (345mm) are approaching long-term average precipitation monitored during normal period of 1961 – 1990 (348mm). The calculations were performed in four soil types selected with regard to USDA textural triangle [8] – sand, silt, loam and clay soils. Their hydraulic functions were determined by calculation software RETC [9], [10]. Numerical experiment was performed as follows. Groundwater level in 2001 vegetation period was gradually moved to two positions. In its first position, average GWL value was at the lower boundary of the root zone, and in the second position it corresponded to the critical depth value. The root zone is an area where majority of plant roots are located. ESL root zone, covered with field plants, was determined up to 1m depth. GWL influence on evaporation is greatest here. If GWL permanently passes through the root zone, air regime in soil and plant biological activity is disturbed. As calculation critical depth was determined 3.73m under soil surface [11]. Daily sums of actual evapotranspiration were calculated for both GWL positions during vegetation period - ET_a^r at GWL at lower boundary of root zone and ET_a^{cr} at GWL critical position. Maximal volume of groundwater, which was consumed for the evaporation $ET_{a\,max}^{GW}$, can be calculated as follows:

$$ET_{a\,max}^{GW} = ET_a^r - ET_a^{cr} \qquad (1)$$

This value was analysed in the particular soil types. In case actual evapotranspiration at real level is calculated and is used instead of ET_a^r in the equation (1), then the equation (1) expresses actual percentage of groundwater at actual evapotranspiration value. The course of ET_a^r, ET_a^{cr} and their accumulation value for the whole vegetation period were analysed. For the individual soil types, the dependence $ET_a = f(GWL)$,

where GWL is GWL during 2001 vegetation period moved in vertical line of a soil profile to different calculation levels, was analysed.

3. RESULTS AND SIGNIFICANCES

Fig.1 illustrates the measured and numerically simulated development of water storage in a soil profile to the depth of 0.80m. The scheme indicates that the model is very precise in quantifying the size and trends of the measured values. Apart from this area, it was verified and used successfully for simulating water regime in other areas in Slovakia [12] and ESL [13], [14]. This implies the model is precise enough for the proposed numerical experiment.

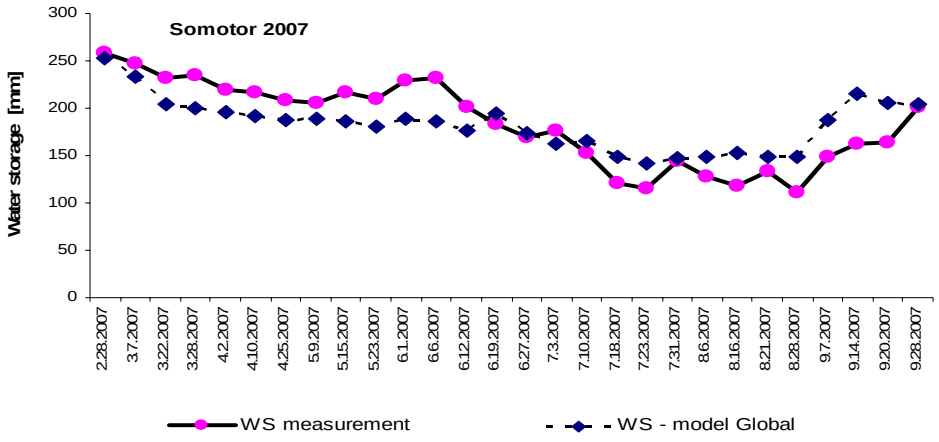

Fig. 1. Developments of the monitored and calculated water storage in a soil profile to the depth 0.80m in Somotor area during 2007 vegetation period.

Fig.2 represents daily sums of precipitation, actual (ET_a) and potential (ET_0) evapotranspiration and their 7-day moving average in Somotor area, during 2007 vegetation period. It is obvious that almost during the whole vegetation period ET_a value was lower than ET_0 value. This fact testifies lack of water in the root zone of a soil profile. The soil profile was under drought conditions, what started to change in early September. At that time, precipitation replenished soil water storage and ET_a reached ET_0 value.

Further on, four soil types of different texture were selected. Their classification is illustrated in USDA textural triangle in **Fig.3** and their texture, retention curve parameter and saturated hydraulic conductivity are listed in **Table 1**. The results of numerical experiment are shown in **Fig. 4, 5, 6 and 7**. Moreover, developments of daily sums of ETa at critical average GWL and at average GWL at the level of lower root zone boundary – 1m below soil surface – are mentioned there. Daily values of actual evapotranspiration are processed also in the form of 7-day moving average. For the purpose of comparison, precipitation is shown there too.

Fig.4 – 7 show the differences between ET_{a1} and ET_{a2} in the analysed soil types and thus also the differences in ET^{GW}_{aMax}. In loamy and clay soil there are two identifiable periods – May and August – during which water supply for the root zone came mostly from groundwater. These are the periods when precipitation was least. In sand and clay soils water supply coming from groundwater is less usual. The overall value of

ET^{GW}_{annual} during the whole vegetation period in 2001 was 292mm for sand soils, 175mm for clay soils, 312mm for loamy soils and 257mm for silt. Consequently, at the optimal GWL position, the percentage of groundwater participating in evaporation is up to 70% in sand soils, 54% in clay soils, 60% in loamy soils and 45% in silt. These results can be useful in the design of irrigation system with GWL control.

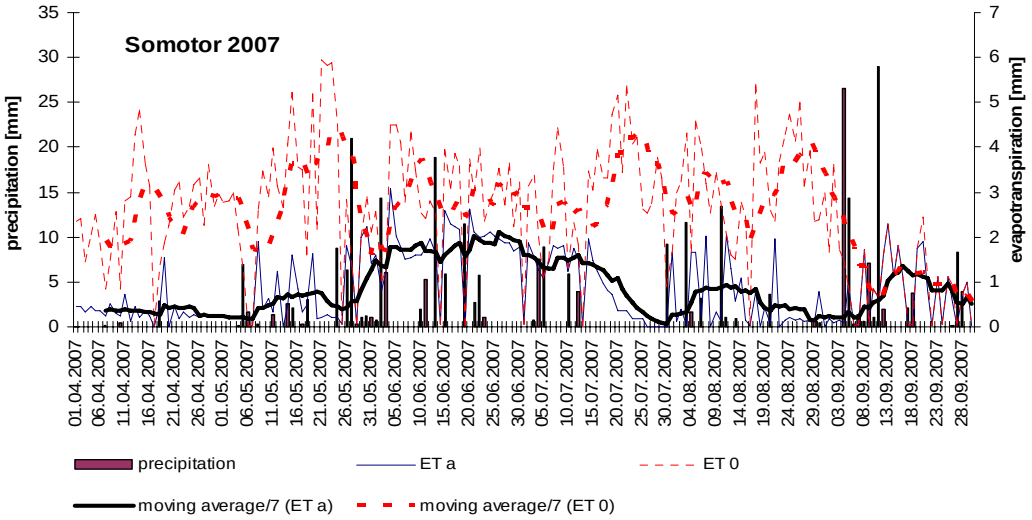

Fig. 2. Daily sum of precipitation, actual evapotranspiration (ET_a), potential evapotranspiration (ET_0) and their 7-day moving average in Somotor area, during 2007 vegetation period.

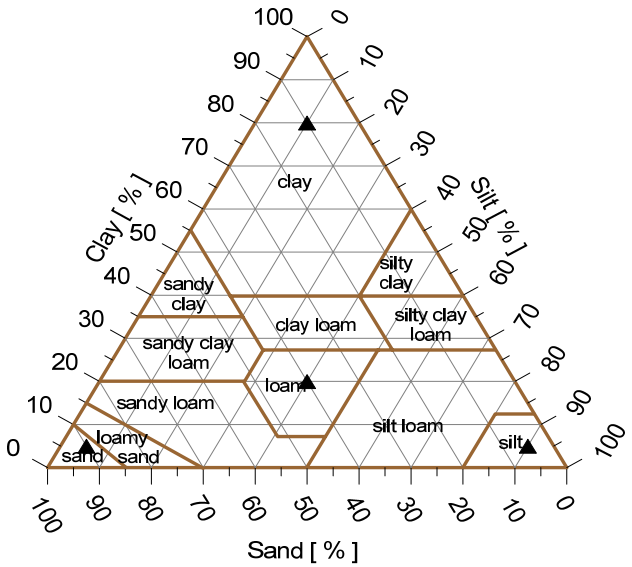

Fig. 3. Classification of soils analysed during numerical experiment according to USDA textural triangle.

Table 1. Hydro-physical soil characteristics.

soils	clay	silt	sand	alfa	n	theta s	theta r	Ks
	[%]	[%]	[%]	[-]	[-]	[mm]	[mm]	[cm.day^{-1}]
sand	5	5	90	0,0332	2,5032	0,38	0,05	322
clay	80	10	10	0,0202	1,1562	0,50	0,10	17
loam	20	40	40	0,0097	1,4966	0,41	0,06	10
silt	5	90	5	0,0083	1,6488	0,52	0,05	41

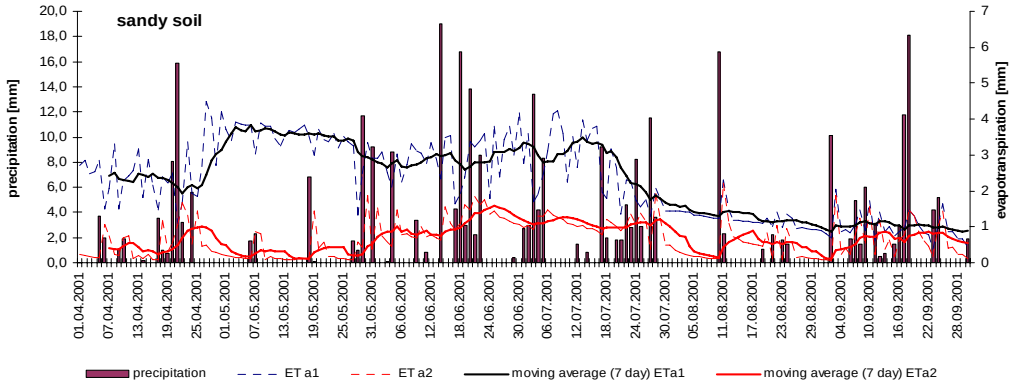

Fig. 4. Development of daily sums of precipitation and actual evapotranspiration at average GWL level of 1.00m under the surface (ET_{a1}) and 3.73m under the surface (ET_{a2}) in sand soil.

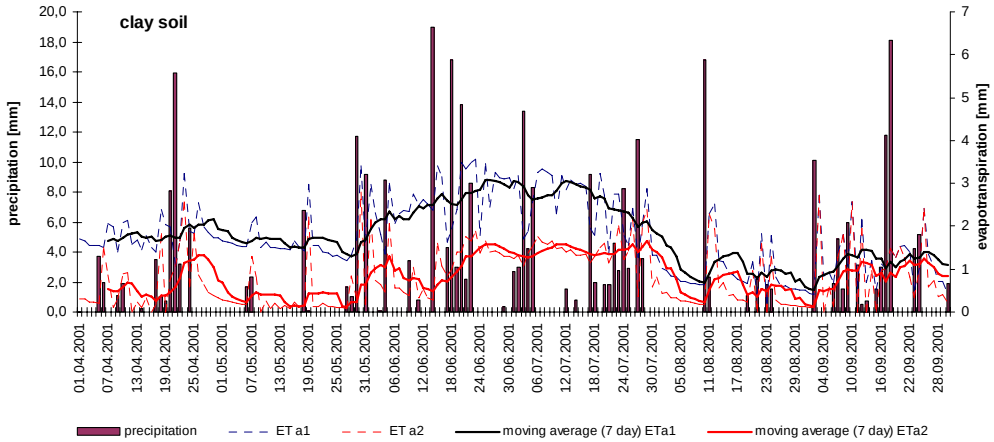

Fig. 5. Development of daily sums of precipitation and actual evapotranspiration at the average GWL of 1.00m under the surface (ET_{a1}) and 3.73m under the surface (ET_{a2}) in clay soil.

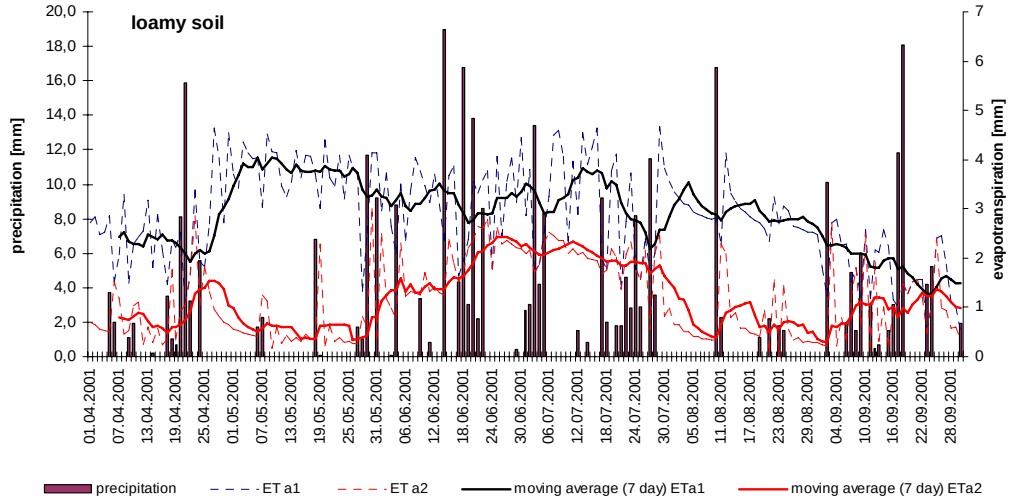

Fig. 6. Development of daily sums of precipitation and actual evapotranspiration at average GWL level (ET_{a1}) and 3.73m under the surface (ET_{a2}) in loamy soil.

Fig. 7 shows the dependence $ET_a = f(GWL)$ with regard to analysed soil types. It is obvious that the course of the dependence $ET_a = f(GWL)$ is different in all soil types. The critical GWL depth in silt and loamy soils was not reached. GWL potential for its participation in evaporation is even greater than evidenced. In order to refine the calculations, lower boundary will need to be re-defined in calculation profile. Hydrophysical characteristics impact on evaporation processes and soil water storage is the subject of IH SAS tasks.

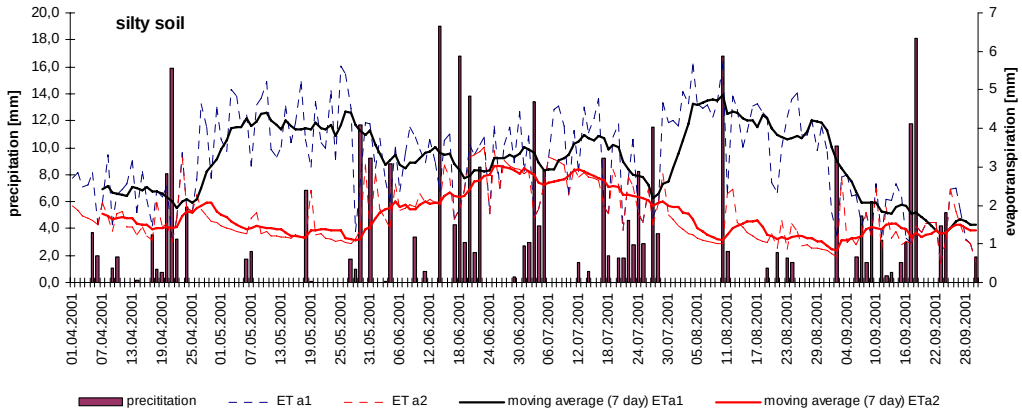

Fig. 7. Development of daily sums of precipitation and actual evapotranspiration at average GWL level of 1.00m under the surface (ET_{a1}) and 3.73m under the surface (ET_{a2}) in silt.

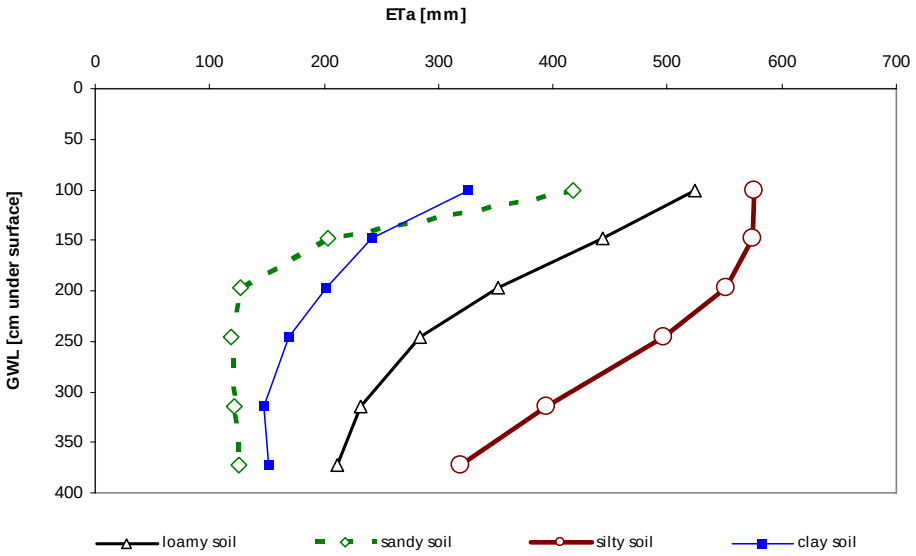

Fig. 7. Dependence $ET_a = f(GWL)$ for the analysed soil types.

4. CONCLUSIONS

This paper presents the results of the research in which the participation of groundwater in actual evapotranspiration was quantified for soils with different texture. For this purpose, numerical simulation method was used. Input hydro-physical characteristics data and average GWL values were changed. GWL variability data during vegetation period and hydro-meteorological conditions were taken from 2001. Sandy soils, clay soils, silt and loamy soils were analysed. Texture and hydro-physical characteristics were proven to have a significant impact on the groundwater participation in evaporation. It was shown that groundwater can participate 40% – 70% in overall evaporation.

The issue described in the present paper is still the subject of research in IH SAS. The results show that groundwater level control can be efficiently used for irrigation purposes.

5. ACKNOWLEDGMENTS

The authors would like to thank for the kind support of the project VEGA 2/0142/12, project APVV-0139-10 and project APVV-0163-11.

6. REFERENCES

[1] Štekauerová, V., Weather, Effects on Plants. In Encyklopedia of Agrophysics. - Springer Sci : Business Media B.V., 2011, s. 984-987. ISBN 978-90-481-35854.

[2] Štekauerová, V., Šútor, J., Nagy, V., Halasi-Kun, G. J., Soil hydrophysical characteristics and their function in the soil water storage formation, dynamics and evaluation. In Pollution and Water Resources, Columbia University Seminar Proceedings : Environmental Protection of Central Europe and USA. vol. XL, 2010-2011. -

Bratislava ; Pécs : Institute of Hydrology SAS : Hungarian Academy of Sciences, 2011, s. 296-318. ISBN 978-80-89139-24-8.
[3] Šoltész, A, Květon, R, Baroková, D, Vércseová E., Hydrologic hydraulic assessment of internal water drainage in lowland regions of Slovakia, Ninth International Symposium on Water Management and Hydraulic Engineering, IX WMHI, pp 427-434, 2005, Austria.
[4] Šoltész, A. - Baroková, D.: 2004. Analysis, prognosis and control of groundwater level regime based on means of numerical modelling. In: Global Warming and other Central European Issues in Environmental Protection: Pollution and Water Resources, Columbia University Press, Vol.XXXV, Columbia, pp.334-347, ISBN 80-89139-06-X
[5] Novák, V., Vyparovanie vody v prírode a metódy jeho určovania. Bratislava: Veda, 1995. 253 s. ISBN 80-224-0409-8., (In Slovak).
[6] MAJERČÁK, Juraj - NOVÁK, Viliam. GLOBAL a numerical model for water movement in the soil root zone. Bratislava : Institute of Hydrology, 1994. 75 s.
[7] Majerčák, J., Novák, V., GLOBAL, one-dimensional variable saturated flow model, including root water uptake, evapotranspiration structure, corn yield, interception of precipitations and winter regime calculation. Bratislava : Institute of Hydrology, 1994. 75 s.
[8] Soil Survey Division Staff. 1993. Soil survey manual : USDA Handb. 18. Washington, DC. : U.S. Gov. Print Office.
[9] http://imel.mel.ar.wroc.pl/retc.pdf
[10] Rodný, M., Igaz, T., Tóthová, I., Šurda, P., Horák, J. Determination of the retention curve points using the artifical neural network. In Journal of International Scientific Publications: Ecology & Safety, 2010, vol. 4, no. 1, p. 177-185.
[11] Gomboš, M., Pavelková, D., The Impact of Groundwater Level Position on the Actual Evapotranspiration in Heavy Soils in Eastern-Slovakian Lowland, In OVIDIUS UNIVERSITY ANNALS CONSTANTZA - Civil Engineering, 2011, vol. XIII., issue 13, pp. 65-71. ISSN 1584-5990.
[12] Igaz, D., Bárek, V., Halaj, P., Takáč, J., Čimo, J., A comparison of measured soil moisture with simulated results obtained by selected models for Danubian lowland. In Cereal Research Communications. ISSN 0133-3720, vol. 36, no. 1, 2008, pp. 1619-1622
[13] Balkovic, J. - Orfanus, T. - Skalsky, R., Potential water storage capacity of the root zone of cultural phytocoenoses in the Zahorska Nizina lowland - A quantification of soil accumulation function. In EKOLOGIA-BRATISLAVA. ISSN 1335-342X, 2004, vol. 23, no. 4, p. 393-407.
[14] Mati, R., Kotorová, D., Gomboš, M., Kandra, B., Development of evapotranspiration and water supply of clay-loamy soil on the East Slovak Lowland. In Agricultural and Water Management, 2011, vol. 98, issue 7, p. 1133-1140. (1.782 - IF2010). (2011 - Current Contents). ISSN 0378-3774.

Ovidius University Annals Series: Civil Engineering, Issue14, October 2012

Nutrient-phytoplankton-zooplankton interaction in Siutghiol Lake

Ichinur Omer, Razvan Mateescu and Gina Muntiu

***Abstract* – One of the most serious problems affecting water quality in lakes is eutrophication. The main cause of eutrophication is the increase of nutrients, nitrogen and phosphorus concentration. This work presents the influence of various factors such as nutrients, phytoplankton and zooplankton on Siutghiol Lake eutrophication.**

***Keywords* – nutrients, phytoplankton, zooplankton, Siutghiol Lake.**

1. INTRODUCTION

Siutghiol Lake (Fig. 1) has an area of 19 km ² and is situated at an altitude of 1.5 m, with average depth <3 m and silica substrate. The lake has lagoon origin and was formed on Jurassic and Cretaceous limestone. It is located in Mamaia and it is extensively used in industry, fishing, irrigation and for sport recreation.

Fig. 1. Location of Siutghiol Lake

Manuscript received September, 2012.

Ichinur Omer is with Ovidius University of Constanta, 124, Mamaia Blvd., 900356-Constanta, Romania (corresponding author to provide phone: +40-241-545091; fax: +40-241-545093; e-mail: ichinur.omer@univ-ovidius.ro; ichinur.mirzali@yahoo.com).

Razvan Mateescu is with National Institute for Marine Research and Development "Grigore Antipa", 300, Mamaia Blvd., 900356-Constanta, Romania.

Gina Muntiu graduated master degree at Ovidius University of Constanta, Faculty of Civil Engineering.

ISSN-1584-5990

Siutghiol Lake is fed by underground sources. By a connecting canal, Siutghiol Lake supplies Tasaul Lake with freshwater and through Tannery Lake it flows to the Black Sea. Catchment area is 92 km ² and consists of Mamaia - Village, Cogealia, Career, Caragea, Cişmelei Valleys and the most important Black Valley (18.9 km²). Except for the last valley which is permanent and brings at the lake about 8 l/s, the others have intermittent flow regime.

In terms of water balance, Siutghiol Lake presents special characteristics, representing an important source of water to feed the population, for the industrial objectives and tourism. Although it has a very small catchment area relative to the surface of lake, the water balance is still surplus in natural conditions. Main morphometric characteristics are presented in Table 1.

Table 1. Morphometric characteristics of Siutghiol Lake

Average level (H med) (cm)	Shoreline length (l) (km)	Length (L)		Width (B)	
		straight (km)	median (km)	maximum (km)	average (km)
216	30	7,5	8,5	4,2	2,5

Elongation factor $\beta = \frac{L}{Bmed}$	depth (h)		Coefficient of specific depth $\alpha = \frac{hm}{hmax}$	Average slope of the bottom tg α
	maximum (m)	average (m)		
3,0	17,05	4,65	0,31	0.0092

Due to the rich underground intake, the water mineralization varies within very narrow limits, while the hydro - chemical type turns very slightly/easily from sodium bicarbonate into chlorinated sodium or magnesium bicarbonate. The large amount of magnesium of lake reflects the share of groundwater in the ionic balance. As for the physic - chemical parameters of Siutghiol Lake, they are presented in Table 2.

Table 2. Physic-chemical parameters of water in Siutghiol Lake (2010)

Pellucidness (SiO2 degree)	Water temperature (°C)	Dissolved oxygen (mg/l)	Alkalinity (mval/l)	Conductivity (µS/m)
0.69	16.79	10.24	6.08	2429.75

In Siutghiol Lake the phytoplankton consists mainly of green algae (Chlorophyceae, Scenedesmus quadricauda, Planctonema lauterbornii, Tetrahedron caudatum), diatoms (Bacillariophyceae, Cyclotella meneghiniana, Nitzsche acicularis, Amphora ovalis, Cymbella ventricosa, Diatomite vulgare), cyanobacteria (Cyanobacteria: Microcystis aeruginosa, Oscillatoria limnetica, Lingbya limnetica, Aphanizomenon flos-aque, Merismopedia glauca).

Most of algae from the listed groups float in the water and only a relatively small number of species have a limited capacity for locomotion by cilia or flagella using. The zooplankton consists of species of protozoa, rotifers and copepods. Among the major groups that make up zoo benthos macro invertebrates we mention: worms, mainly species annelid (Nais variabilis, Nais elinguis, Stylaria lacustris), insects larvae (Chironomus plumosus, Cricotopus triannulatus, Parachironomus arcuatus), gastropods (Dreissena polymorpha, Hypanis colored Theodoxus pallasii) and crustaceans (Paramysis lacustris, Asellus aquaticus). An important component of Lake biocenosis is the aquatic macrophytes - higher plants (Angiosperms) and lower plants - algae (macro algae).

These plants have an important role in the balance of oxygen and nutrients (belonging to the group of primary producers), the damping waves and erosion mitigation banks. Some species have the ability to filter certain chemical constituents in water and also represent the developing place for various bird species, insect larvae and fish larvae.

Due to the tourism and economic development of Mamaia zone, some vegetation of the lake was removed, this work having a negative effect on the ecological balance of the lake. Since Siutghiol Lake is a protection site, there are areas with such vegetation protected by law where the human intervention is limited.

Taking into account the values of eutrophication indicators, Lake Siutghiol can fall in hypertrophic type and in IV quality class, corresponding to an appropriate environmental weakness status (according to Order 161/2006).

The values for the eutrophication degree of the lake can only be worrying because overgrowth of algae (unicellular) allows development of other organisms (zoo benthos, fish larvae) only up to a certain point, becoming with time an inhibiting factor of its growth and development. Deprived of food and light (which cannot penetrate the deeper layers of the water due to algae table format display surface) macrophytes algae cannot grow. By their death, the benthos accumulates a large amount of debris; forming organic mass. In this organic mass an intense microbial activity takes place, with negative consequences for the numerous invertebrate groups which disappear. By/with their disappearance, it is reduced the amount of food needed to develop fish larvae which together with environmental altered conditions of the ecosystem (high toxicity resulting from intense microbial activity appear: H2S, free ions of Fe, Mg, Al and gas bubbles) led to their death and thus to a decreasing fish populations.

2. MATHEMATICAL MODEL

The equations describing the interaction of the food chain are specific to predator - prey type relationships; the system development of each partner is influenced by the abundance / absence of the other [10].

The balance equations for the three considered parameters are:

$$\frac{dP}{dt} = a_{pa}\left(1-\varepsilon\right)\cdot C_{za}\cdot Z\cdot A + a_{pc}\cdot k_{dz_0}\cdot Z - a_{pa}\cdot k_{\max}\cdot\frac{P}{k_{sp}+P}\cdot A \quad (1)$$

$$\frac{dA}{dt} = k_{\max}\cdot\frac{P}{k_{sp}+P}\cdot A - C_{za}\cdot Z\cdot A \quad (2)$$

$$\frac{dZ}{dt} = (a_{ca}\cdot\varepsilon\cdot C_{za})\cdot Z\cdot A - k_{dz}\cdot Z\cdot \quad (3)$$

where: A is the biomass of phytoplankton chlorophyll expressed in mass per unit volume of water, Z - zooplankton biomass expressed as the mass of organic carbon per unit volume of water, P - phosphorus concentration (mgP/m³)., a_{ca} - carbon - chlorophyll ratio in phytoplankton $\left(\frac{gC}{mgChla}\right)$, c_{za} - algal consumption speed by zooplankton $\left(\frac{m^3}{gC\cdot zi}\right)$, a_{pa} - phosphorus – chlorophyll relation $\left(\frac{mgP}{mgChla}\right)$, ε - efficiency factor (equal to 0.7), k_{dz} - extinction coefficient velocity (the breath, excretion and death) for

zooplankton $\left(\frac{1}{zi}\right)$, k_{ca} - net algal growth rate calculated by the relation $k_{ca} = k_{\max} \cdot \frac{P}{k_{SP} + P}$ with the maximum value $k_{\max}$ and k_{SP} - semi – saturation constant $\left(\frac{\mu gP}{l}\right)$ [10].

The already mentioned description is strictly based on the direct link between the three parameters and their interaction. In fact, algal growth rate is also influenced by temperature, light intensity and the possible presence of nitrogen [10].

3. RESULTS AND SIGNIFICANCES

For modeling, we introduced the following data:

$$A_0 = 1{,}5\,\frac{mgChla}{m^3};\quad Z_0 = 40\,\frac{mgC}{m^3};\quad P_0 = 11.6\,\frac{mgP}{m^3};\quad a_{ca} = 40\,\frac{mgC}{mg\ Chla};\quad a_{pa} = 1\,\frac{mgP}{mg\ Chla};$$

$$a_{pc} = \frac{a_{pa}}{a_{ca}} = 0.025\,\frac{mgP}{mgC};\quad C_{za} = 0.002\,\frac{m^3}{mgC \cdot zi};\quad k_{sp} = 2{,}5\,\frac{mgP}{m^3}$$

To solve the above system of equations (1-3) we use 4th order Runge - Kutta and account relationships which are to be found in NutrFitoZoopl program - the procedure RK4sist3.

The software (NutrFitoZoopl) used in the mathematical model simulation is written in Java. Java application framework was performed using NetBeans IDE platform which is also an integrated development environment for Java.

The chosen integration step is Δt= 1 day. The reading files are working by NetBeans IDE platform (Fig. 2) and the results are obtained also through it.

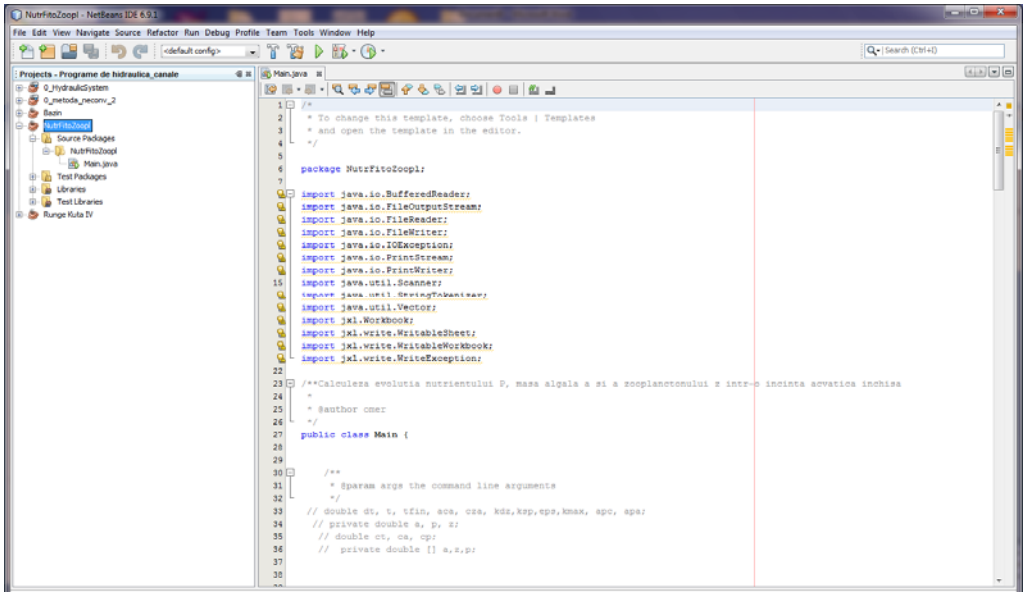

Fig. 2. NutrFitoZoopl software runs by NetBeans IDE platform

To compare them, the integration results for phytoplankton and phosphorus are transformed into equivalent carbon units using the relationship:

$$C_a = A \cdot a_{ca} \tag{4}$$

$$C_p = \frac{P}{a_{pc}} \tag{5}$$

In addition, at each step Δt the sum of these three constituents is calculated to highlight conservation of mass in the aquatic system.

The variations of these three parameters in time are shown in Figure 3.

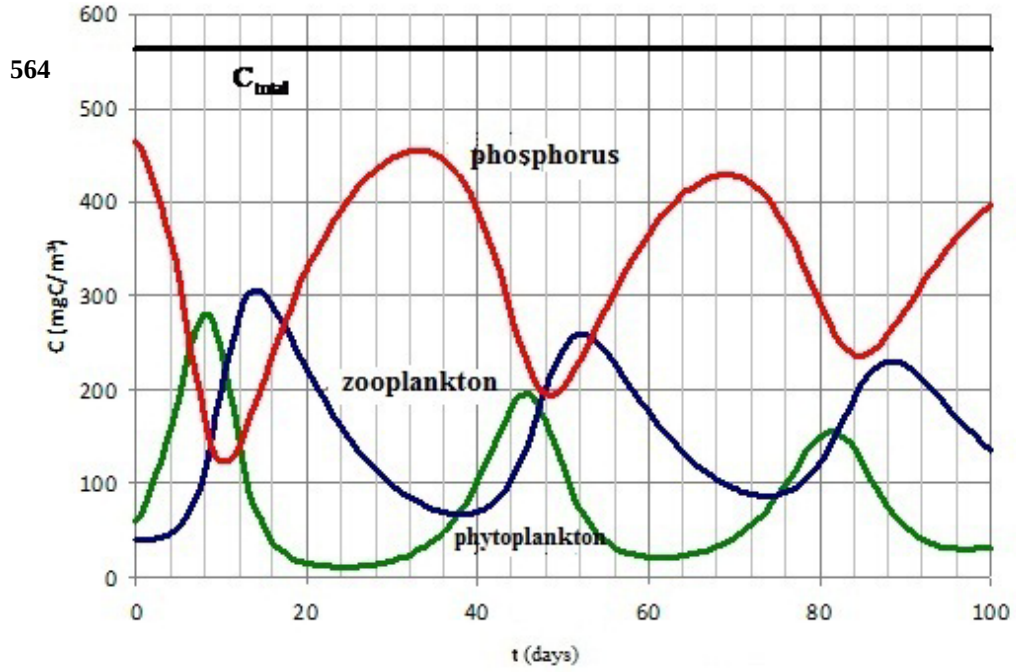

Fig.3. Variations of the food chain components in time for Siutghiol Lake

The chart above shows that the zooplankton reaches the concentrations of 306 mg/m^3 in about 14 days while the phytoplankton maximum of 280 mg/m^3 is reached in 8 days, and so the maximum concentration of zooplankton is reached 6 days later after the maximum phytoplankton concentration is reached. The maximum of phosphorus concentration (455 mg/m^3) is reached in 33 days. The total concentration is 564 mg C/m^3.

A high concentration of nutrients in water causes the algal biomass development, including zooplankton biomass (by algal consumption), and a decrease in nutrient concentrations determines a decrease of the phytoplankton biomass, with negative effects on zooplankton, which in turn has a smaller food amount.

Lack of food causes the death of zooplankton which by decomposition processes returns into the circuit of nutrients, a further increase of the nutrients concentration resulting.

4. CONCLUSIONS

Based on these results we conclude that the interaction of plankton biomass and nutrients to Lake Siutghiol fall into a "natural" regime. Siutghiol Lake is now strongly manmade, but the insufficiently treated water discharges, tourism and specific waste pollution activities are factors that can disturb this delicate balance, including eutrophication.

5. ACKNOWLEDGMENTS

The Authors thank to Dobrogea Litoral Water Basin Administration for the measured data from 2009 and 2010 concerning morphometric characteristics and physic-chemical parameters of water in Siutghiol Lake.

5. REFERENCES

[1]. Breier, A., *Lacurile de pe litoralul românesc al Mării Negre. Studiul hidrografic*. Editura Academiei Republicii Socialiste România, Bucureşti, 1976.
[2]. Brezeanu, Gh., Ionică, D., Parapală, L., Cioboiu, Ol., *Functioning mecanism of biocenotic stuctures from wetland residual cleaning systems*. Environ. & Prog., Ed. EFES Cluj – Napoca, 2007.
[3]. Brezeanu, Gh., Cioboiu, O., *The ecological development of the Iron Gate I reservoir*. Lymnological reports 36, 50 years IAD – 30 years AC– IAD, Viena, Austria, 2008.
[4]. Brezeanu, Gh., Cioboiu, Ol., Ardelean, A., *Ecologie acvatică*. Editura "Vasile Goldiş" Unversity Press, Arad, 2011
[5]. Chapra, S.C., *Surface water quality modeling*. McGraw-Hill, New York, 1996.
[6]. Hammmer, M.J., Mackinchan, K.A., *Hydrology and quality of water resources*. J. Wiely, New York, 1981.
[7]. Jorgensen, S.E., *Application of ecological modelling in environmental management*. Part A, Elsevier, Amsterdam, 1983.
[8]. O'Neill, P., *Fundamentals of ecology*. Chapman-Hall, London, 1993.
[9]. Papadopol, M., *Hidrobiologie (Limonologie biologică).* Universitatea din Bucureşti, Facultatea de Biologie, Bucureşti, 1978
[10]. Popa, R., *Modelarea calității apei din râuri.* Editura *H*G*A, Bucureşti, 1998.
[11]. Stănciulescu, FL., et. al.,. *Modele de simulare a unor ecosisteme din delta Dunării*. ICCI, 1983.
[12]. Surugiu, V., *Ecologie marină-Îndrumar de lucrări practice*. Editura Universității „Alexandru Ioan Cuza", Iaşi, 2007.

Urban vulnerability and risk management: A multifractal analysis for Mexico City

Sergio Puente-Aguilar, Jorge Javier Castro and Alin Andrei Cârsteanu

***Abstract* – The impact of a natural disaster on a human community is conceivably related to the size of the respective community. However, the highly intricate relationships between mitigation organization, demographic factors, media impact, architectural characteristics, urban traffic networks, as well as social and cultural perception aspects (such as civic solidarity or generalized panic) make this relationship non-trivial. In this work, we analyse the existence of a possibly multi-exponent power-law function describing compound vulnerability in Mexico City.**

***Keywords* – risk, vulnerability, urbanisation, multifractality**

1. INTRODUCTION

Common sense has it, that the larger a city gets, the worse become its traffic jams. The explanation is simple: under the hypotheses of constant population density and constant traffic network density, average distances one has to drive every day increase with the size of the city, and consequently, so does traffic density. This simple paradigm shows us how non-linear effects of nowadays' city growth affect our daily lives. It is also relevant to the analysis presented herein, since jammed traffic is a major problem in effective mitigation of natural disasters, affecting both evacuation efforts and the timely arrival of help for the victims (see e.g. *Christians* [2005] for the case of hurricane Katrina). However, the complexity of all factors involved in the vulnerability of a human community to natural disasters makes it virtually impossible to apply such heuristic arguments in order to deduce a functional expression for the vulnerability factor.

The various components of urban life are governed, taken separately, by their intrinsic scaling laws. While each aspect of vulnerability, such as mitigation organization, demographic factors, media impact, architectural characteristics, urban traffic networks, as well as social and cultural perception factors [*Puente-Aguilar*, 2004], when considered independently of the others, seems to cause increasing vulnerability with community size, when considered in interaction with all others however, becomes part of a self-organized system. Such a system generally has a non-linear behaviour (which also implies that it doesn't behave like a linear combination of its components), and it has been shown that self-organized systems tend towards a critical state, in whose neighbourhood they have a power-law behaviour with scale [see e.g. *Bak*, 1996]. The functional and dysfunctional relationships established between the components of urban life by metropolitan interaction result in a global behaviour, whose asymptotic scaling is examined in the present work for the role it plays in the

Manuscript received October 15, 2012. The authors gratefully acknowledge the organization of the 1st General Assembly of the European Geosciences Union. Jorge Castro and Alin Cârsteanu acknowledge funding of this research from SEMARNAT-CONACyT Grant C01-0306/2002.

Sergio Puente-Aguilar: Colegio de México - CEDUA, Mexico City, Mexico (e-mail: spuente@colmex.mx)

Jorge J. Castro: Cinvestav del IPN - Physics Department, Mexico City, Mexico (e-mail: jjcastro@fis.cinvestav.mx)

Alin A. Cârsteanu: Escuela Superior de Física y Matemáticas, IPN - Mathematics Department, Mexico City, Mexico (corresponding author, phone: +52-55-5729-6000x55011).

ISSN-1584-5990

response of the metropolis to extreme events. The present work focuses on the unique real-life laboratory that is the megalopolis of Mexico City, Mexico, attempting a validation of the power-law behaviour of vulnerability to natural disasters, as well as the estimation of its scaling exponent spectrum.

2. FORMALISM AND DATA

The multifractal analysis formalism [see e.g. Frisch and Parisi, 1985; Schertzer and Lovejoy, 1987] is concerned with the scaling behaviour of a measure R, defined on the Borel subsets of $\mathbf{R}^n$:

$$\tau(q)=-\log_{\lambda}\Sigma_k\}|R(\Delta t_k)|^q \qquad (1)$$

where $R(\Delta t)|=\int_{\Delta t} dR$. The existence of scaling in the measure R is defined as the r.h.s. of equation (1) being constant with scale λ. Whenever scaling exists, it is called *monofractal* whenever $d\tau/dq$ is constant with q, and is called *multifractal* otherwise. The estimation of $\tau(q)$ can be performed by linear regression of the natural logarithm of the sum in equation (1) against the logarithm of scale, for different values of q.

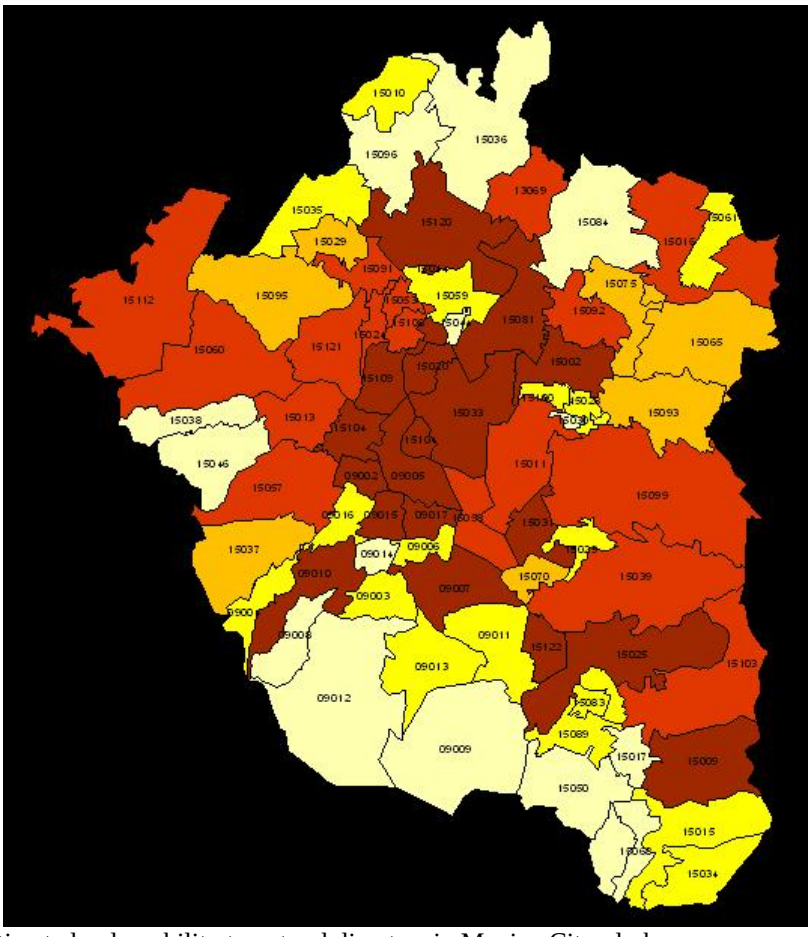

Fig. 1. Estimated vulnerability to natural disasters in Mexico City: darker areas represent higher vulnerability, on a linear colour scale.

Vulnerability data for Mexico City have been evaluated on a neighborhood-by-neighborhood basis, based on past events (notably the 1985 earthquake), updated to the current state of the infrastructure (**Fig. 1**). Aggregation to different scales has been performed pixel-by-pixel, on square-shaped subsets of the city area, applying the estimator for (1) in $\mathbf{R}^2$.

3. RESULTS AND CONCLUSIONS

The estimation of the scaling exponent spectrum for Mexico City vulnerability to natural disasters is presented in **Fig. 2**.

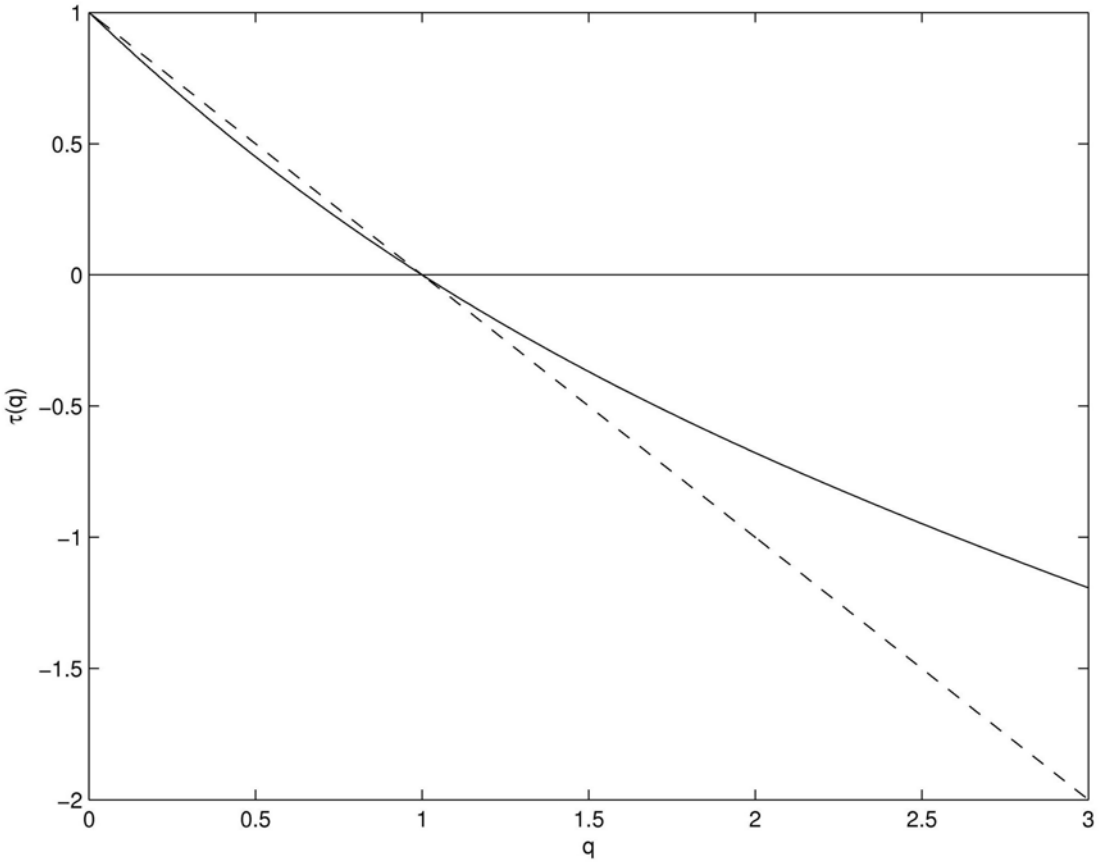

Fig. 1. Estimation of the $\tau(q)$ scaling exponent spectrum for vulnerability to natural disasters in Mexico City, showing a remarkable degree of multifractality.

A remarkable degree of multifractality can be observed in the figure. We can therefore conclude that the complex nature and spatial distribution of compound vulnerability gives rise to a multifractal measure on the city surface. The importance of such an exponent spectrum for scale-related decision-making (at the scale of neighborhoods, townships, districts, and finally the whole city) in Mexico City relies in its arguably being the

most populous community in the world at this time, and correspondingly difficult to administrate. The results presented herein allow for quantitative re-scaling of mitigation measures between administrative entities.

4. REFERENCES

[1] Bak, P. How nature works: The science of self-organized criticality, Springer, 1996.
[2] Christians, K. *Let the blame games begin*. 2005, AMFM Newsletter, 2(2), p.1.
[3] Frisch, U., and G. Parisi (1985). On the singularity structure of fully developed turbulence, in *Turbulence and Predictability in Geophysical Fluid Dynamics and Climate Dynamics*, eds.M. Ghil, R. Benzi, and G. Parisi, Elsevier, 1985.
[4] Puente-Aguilar, S. *Urban vulnerability and sustainable development: Culture of prevention and risk management*. 2004, Geophys.\ Res.\ Abstr., 6, p.07685.
[5] Schertzer, D., and S. Lovejoy. Physical modeling and analysis of rain and clouds by anisotropic scaling multiplicative processes. 1987, Geophys. Res. D, 92(8), p.9693.

Ovidius University Annals Series: Civil Engineering, Issue14, October 2012

Wetlands Restoration in the Senné Area

Andrej Šoltész, Dana Baroková, and Lea Čubanová

***Abstract* – Senné Area is located in the East Slovak Lowlands and protected bird reserve is placed there, as well. Therefore some improvements are planned in this area, because after the year 1970 periodic floods were stopped due to agricultural requirements. Two possibilities of the original wetlands restoration were examined – flooding by the surface water as well as groundwater level increase. For the numerical simulations HEC RAS and TRIWACO models were used.**

***Keywords* – Flooding, Groundwater Simulation, Open Channel Modelling, Restoration, Wetland.**

1. INTRODUCTION

Senianska wetland area is as a part of the central East Slovak Lowlands situated on the left bank side of the Čierna voda River above its junction with the Laborec River. It is a wide terrain depression on which many water management measures have been realised for drainage purposes [1], [2], [3]. The main aim is to consider the restoration possibility of wetland systems and for improving soil water regime in this area. Such measures have ecological importance for different fauna and flora. Senianske Ponds Nature Reserve was founded in 1955 to protect birdlife and unique water plants. It is also an international wetland site registered under Ramsaar Convention and a part of EU wide network of protected NATURA 2000 areas [4].

From previous concluded these partial tasks for the technical solution of the sufficient amount of water inflow to the area of interest which will cause the change of the soil moisture profile from dry to waterlogged (up to the local wetlands) [5]:

- reconnaissance of the actual existed conditions of the streams, channels and drains – morphology and hydrology,
- verification of the channel system function and analysis of the proposal possibilities for the water dotation to the area of interest,
- design of the technical solutions for changing of the channel system purposes from the draining to doping,
- mathematical model processing of the steady non-uniform flow for the Záchytný channel and for the channel system,
- water level and discharge regime examination (proofing) for various discharge scenarios in the channel system, discharge scenarios are determined by hydrology of the Záchytný channel, by inflows of the channels created the system in the area of interest and by the required outflow into the Senianske ponds,

Manuscript received July 15, 2012.

This work was supported by the Grant agency VEGA under contract No. 1/1011/12 and by the Slovak Research and Development Agency under the contract No. APVV-20-003705.

Prof. Ing. Andrej Šoltész, PhD. is with the Slovak University of Technology, Faculty of Civil Engineering, Department of Hydraulic Engineering, Radlinského nr. 11, 81368-Bratislava, Slovakia (phone: +421-2-59274320; e-mail: andrej.soltesz@stuba.sk).

Ing. Dana Baroková, PhD. is with the Slovak University of Technology, Faculty of Civil Engineering, Department of Hydraulic Engineering, Radlinského nr. 11, 81368-Bratislava, Slovakia (e-mail: dana.barokova@stuba.sk).

Ing. Lea Čubanová, PhD. is with the Slovak University of Technology, Faculty of Civil Engineering, Department of Hydraulic Engineering, Radlinského nr. 11, 81368-Bratislava, Slovakia (e-mail: lea.cubanova@stuba.sk).

ISSN-1584-5990

- verification of the function and capacity of the objects (weirs, culverts) on the channel system and design of the required technical measures on the existed weirs,
- recommendations for the technical design realisation and channel system operation,
- mathematical modelling of the surface water level impact on groundwater level regime.

2. EXPERIMENTAL MATERIALS AND EQUIPMENT

Generally, two possibilities for restoration of the described problem have been existed – flooding and groundwater level increase. Therefore the solution was divided into two parts – water level regime modelling in open channel systems and groundwater level simulations [5].

For the water supply to the mentioned area the existing channel system has been used which original function was to prevent inflow of surface waters from the Vihorlat Mountains to the area, it means, it was used as a drainage system [5].

Channel system in the area of interest (Fig. 1.) is created by nine main artificially built channels and by many smaller secondary and tertiary channels which fulfil the drainage function. These artificially built channels are partly non-prismatic.

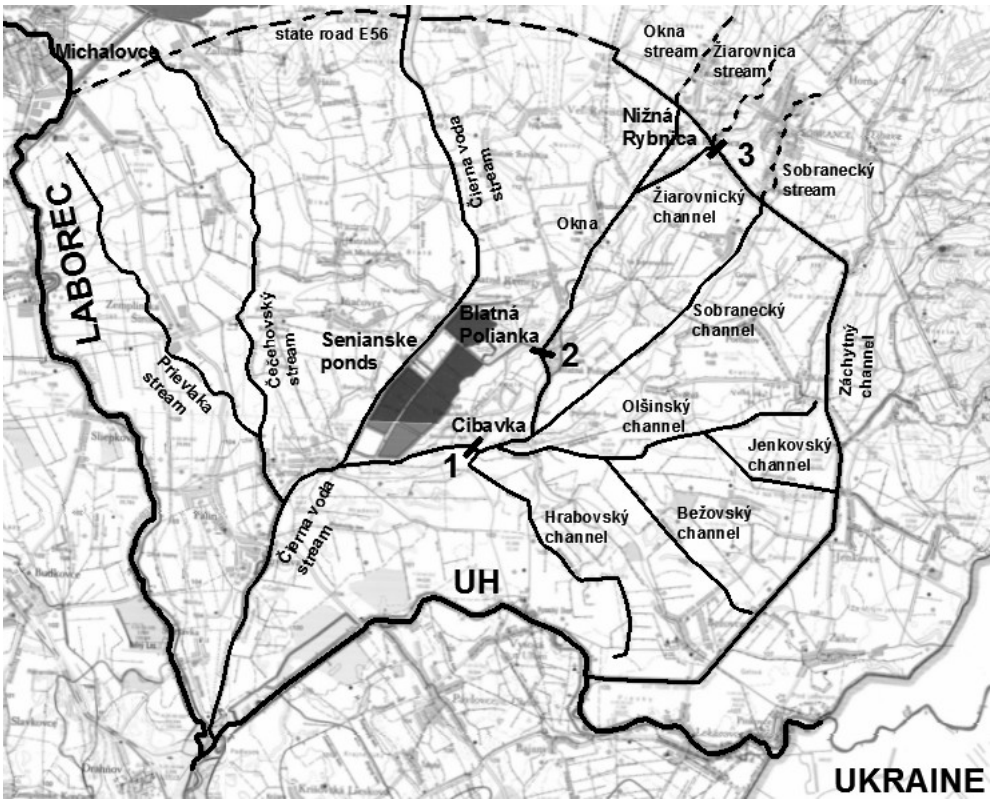

Fig. 1. Area of interest map (situation of the gates (1, 2, 3) on the Cibavka, Okna and Záchytný channels)

Surface waters were solved on the channel systems, which consist of these main drainage channels [6]:

- Cibavka – length L = 1.8 km, longitudinal slope i_o = 0.2 ‰, cross section width b = 1.2 m, bank slope 1:2, maximum capacity Q = 4.4 – 6.86 $m^3.s^{-1}$,
- Hrabovský – L = 8 km, i_o = 0.47 ‰, b = 1.2 m, slope 1:2, Q = 2.04 – 3.83 $m^3.s^{-1}$,
- Olšinský – L = 8.1 km, i_o = 0.4 – 0.78 ‰, b = 1.2 – 2 m, slope 1:2, Q = 2,42 - 4,63 $m^3.s^{-1}$,

- Bežovský – L = 7.3 km, i_o = 0.84 ‰, b = 1.2 m, slope 1:2, Q = 1.3 - 4 $m^3.s^{-1}$,
- Jenkovský – L = 3.8 km, i_o = 0.6 - 1 ‰, b = 1 m, slope 1:2.5,
- Sobranecký – L = 8.3 km, i_o = 0.78 – 1.2 ‰, b = 1.2 – 2 m, slope 1:2, Q = 1.58 $m^3.s^{-1}$,
- Žiarovnický – L = 2.2 km, i_o = 2.3 – 1.46 ‰, b = 1.1 m, slope 1:2, Q = 0.7 $m^3.s^{-1}$,
- Okna – L = 9.4 km, i_o = 0.5 – 2.37 ‰, b = 1.5 – 10.5 m, slope 1:2, Q = 2.5 – 4.64 $m^3.s^{-1}$,
- Záchytný – L = 5.9 km, i_o = 0.2 – 2.4 ‰, simple and compound trapezoid.

Groundwater was solved for the described area using TRIWACO software. The boundaries of the region were created by Latorica and Uh Rivers, Záchytný channel and state road E56 (Fig. 1., Fig. 2.). Hydrogeological and geological data were processed from the archival reports of the Geofond ŠGÚDŠ [7], [3]. These data were very important as an input for the groundwater model of the area of interest.

Hydrogeology of the solved area is very strongly influenced by the surface streams (the most important river is the Laborec River) and by Vihorlat and Popričné mountains. The most extended soil in the area is clay and also other sediments which are very heavy and not appropriate for the groundwater flow. More permeable soils (sand, sand with gravel) reach only small thicknesses and in many cases their permeability is degraded by the soil and loam. According to the pumping tests hydraulic conductivity value is from $2.52x10^{-6}$ $m.s^{-1}$ up to $3.5x10^{-5}$ $m.s^{-1}$, sporadically 10^{-4} $m.s^{-1}$, in dependence on the soil kind. From the previous it is possible to evaluate this area from the geological viewpoint as impervious porous media. Another area with occurrence of the good permeable sand-gravel sediments is situated in the south-east part of the area of interest. The thickness of the sand-gravel or sand layers is 3.0 – 9.0 m. The groundwater level seems tense and it is fixed 2.5 – 4.5 m under the terrain. Hydraulic conductivity of the permeable materials is from the value $5.65x10^{-4}$ $m.s^{-1}$ to $5.23x10^{-5}$ $m.s^{-1}$. Less valuable layers are permeable materials in the area of the Bankovce and Čertov, their conductivity is from $8.6x10^{-5}$ $m.s^{-1}$ to $1.47x10^{-6}$ $m.s^{-1}$. From the geological viewpoint Senné depression consists of heavy soils characterized by a low permeability.

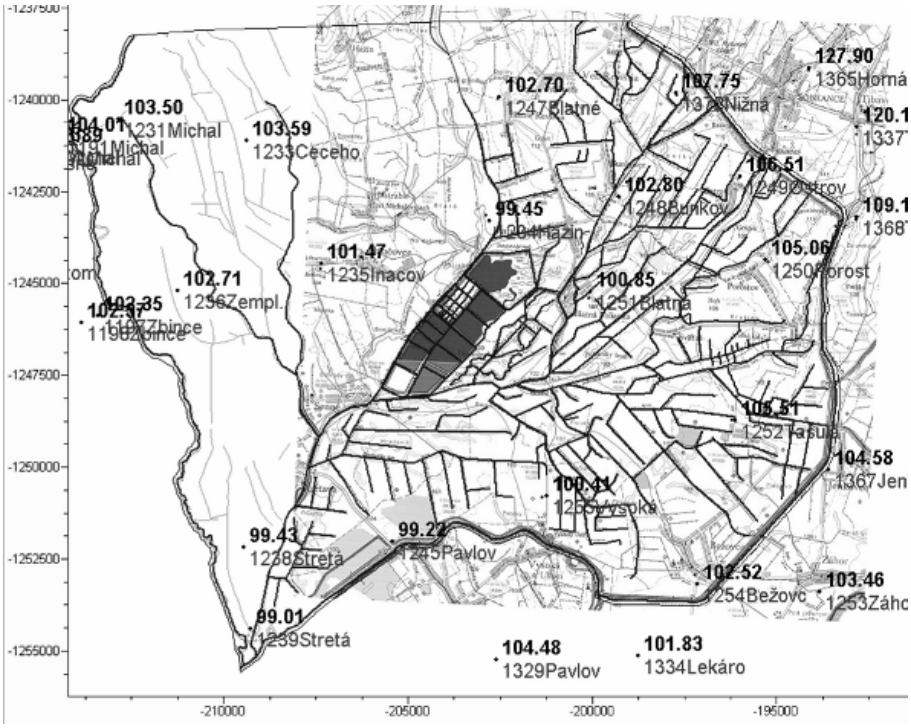

Fig. 2. Filtration area boundary (thin line), situation of Slovak Hydro-meteorological Institute (SHMI) boreholes with mean groundwater level elevation, location of the main and lateral channels

3. RESULTS AND SIGNIFICANCES

For the surface water level simulations, firstly the geometric data have been prepared for all mentioned channels and afterwards a discharge analysis in the channel system for the m-daily discharges has been performed. Inflows come from the Okna, Žiarovnica and Sobranecký stream and this sum of discharges were diverted into the Okna, Žiarovnický and Sobranecký channel through the culverts on the Záchytný channel. These streams have to secure fixed inflow to the neighbouring ponds [5]. Because of the complexity of the problem two mathematical models were prepared by using the HEC-RAS software (Záchytný channel separately and then the rest of the channel system) for 5 various hydrological scenarios for the steady non-uniform flow. The design is considering water level increase on the weir on the Cibavka channel (from the 99.7 m a. s. l. to 101.1 m a. s. l.) [6]. Created back-water will cause water fulfilling of lateral channels, whereas it is expected water overflow in some parts of the surrounding terrain (Fig. 3.).

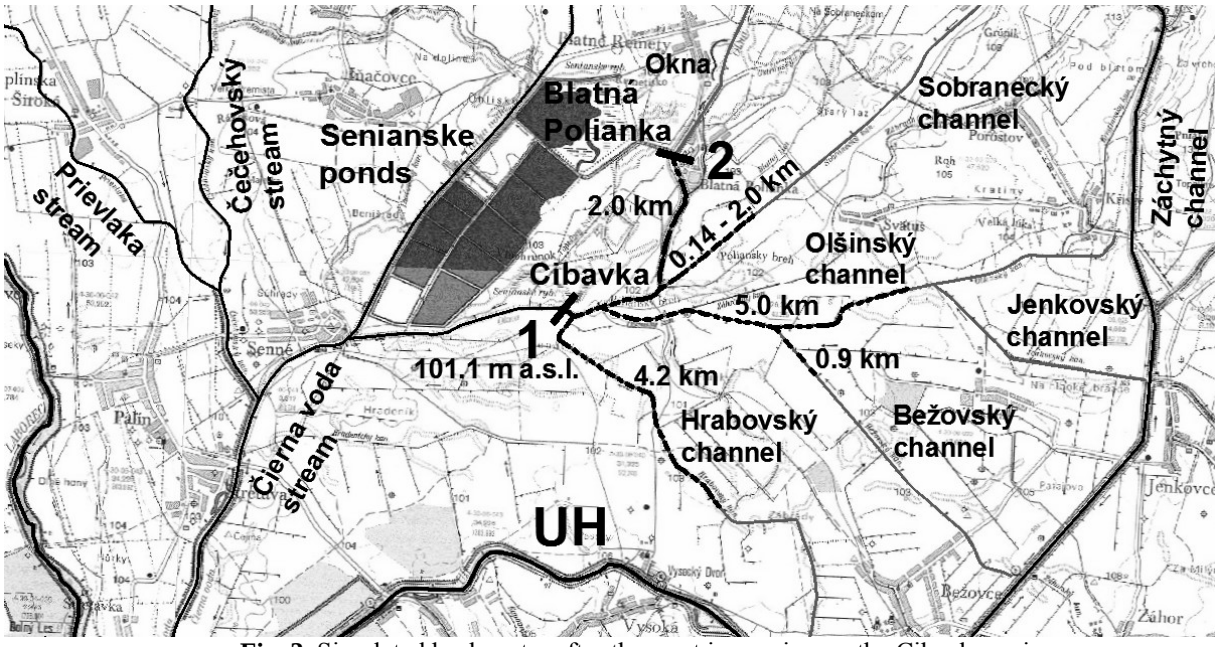

Fig. 3. Simulated back water after the crest increasing on the Cibavka weir

From the simulated surface water level regimes resulted that the back-water radius is independent on the discharge scenario and it is most dependent on the water level at the Cibavka weir which is possible to control by the weir crest [5].

Recommendation for the realization of the proposed design is that it is possible to supply the area of interest with adequate amount of water realising only small technical encroachment on the existed channel system (Fig. 3.) to secure wetland restoration. The function of the system can vary from the drainage to the water supply (in the sense of the surface runoff). Conditions for the water supply into the soil profile in the area of interest will be created.

From the viewpoint of the groundwater modelling, solved area – surroundings of the planned back-water on the Cibavka weir (No. 1 in the Fig. 1.), is situated nearly in the middle of the modelled area and in the sufficient distance from the edge of the filtration area. It is possible to assess that the value of the boundary condition at the edge of the filtration area will not influence the results in the solved area [2].

Dirichlet boundary condition was set on the whole boundary of filtration area. After entering of the filtration area boundary and stream location (Fig. 2.) the final element network in TRIWACO program [8], [9] was performed. Network was refined in the surroundings of the Cibavka weir which will cause the back-water.

Size of bigger elements was 100 m and smaller 50 m. Parameter testing (calibration, verification) of the model was done on base of hydrogeological analysis of the solved area. Water levels in the streams were entered into to the groundwater model on the basis of the described surface water level regimes from the HEC-RAS model, as well. [5].

Solved area is a region with the minimum total annual precipitation in Slovakia, less than 600 mm/year. For the groundwater level regime analysis the observation of GWL in 51 boreholes of the SHMI from the whole Laborec River basin were used. From these boreholes were just 17 used for the model calibration because they are placed directly in the modelled area (Fig. 2.).

Considering realization of the planned controlling measures it means a long-time water level increase (about 1.33 m) on the Cibavka weir and average discharge in channel system; groundwater level regimes were simulated for steady as well as unsteady conditions.

From the groundwater level simulations concluded that steady state (at unconverted conditions) is occurring for a relatively long time. The unsteady state simulation results (Fig. 4) showed that the groundwater level is changing very slowly by influence of back-water created on the Cibavka weir. After 1 year from the realization of planned water level increase in channels (caused by back-water on the Cibavka weir) groundwater level is increasing in the range of about 250 m (Fig. 5).

4. CONCLUSIONS

Area of interest could be from hydrologic and hydraulic point of view restored. The problem of realization of proposed measures is funding and disagreement of the land owners. In case of realizing such measures in the future for restoring wetlands in Senné area it can be realized only by over-toping of channel banks, it means to flood the field by surface water. In heavy soils it is really not realistic to realize the soil water logging by increasing the groundwater level.

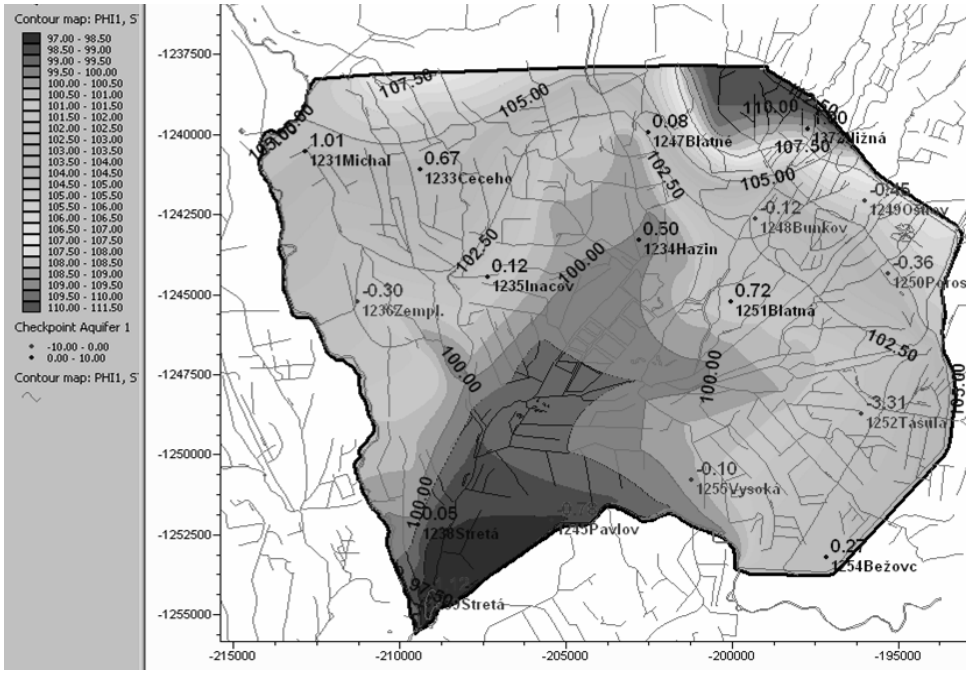

Fig. 4. Course of groundwater table contour lines for steady state with differences description at model calibration – result after model calibration

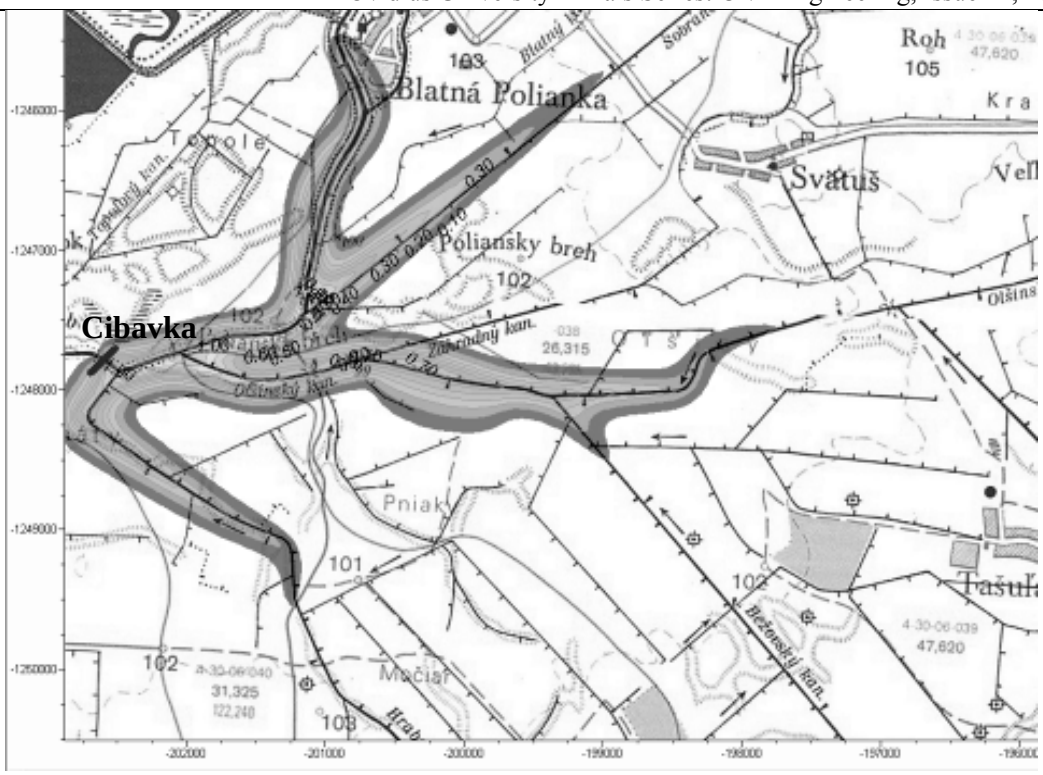

Fig. 5. The piezometric head increase after 1 year – radius of groundwater level backwater is max. 250 m

5. REFERENCES

[1] Bella, V. et al. Water management measures in the East Slovak Lowlands. Alfa Bratislava, 1971, 58 p. (In Slovak)
[2] Šoltész, A., Baroková, D., Čubanová, L., Kamenský, J., Gomboš, T. Possibility of restoration of wetlands In Senné depression. Acta hydrologica Slovaca, 10 (2), 2009, pp. 231-244. (In Slovak)
[3] Gomboš, M., Tall, A., Kandra, B. Creation of soil cracks as an indicator of soil drought. Cereal Research Communications. 37 (supplementum), 2009, pp. 367-370.
[4] Šoltész, A., Kamenský, J., Čubanová, L., Baroková, D. Hydraulic analysis of water supply for soil water regime improvement in Senné region: Partial report of the UNDP project "Integration of principles and practices of ecological management into landscape and water management in the East Slovak Lowlands". STU in Bratislava, 2009, 44 p. (In Slovak)
[5] Čubanová, L., Kamenský, J. Senné - analysis of planed measures on the surface water regime. In: People, buildings and environment. Brno, 2009, CERM, pp. 63-66.
[6] Šoltész, A., Baroková, D. Geological characterisation of the Senné region: Partial report of the UNDP project "Integration of principles and practices of ecological management into landscape and water management in the East Slovak Lowlands". STU in Bratislava, 2009, 34 p. (In Slovak)
[7] Royal Haskoning. TRIWACO Simulation Package for Groundwater. Version 3.0 internal release RH, Rotterdam: Royal Haskoning - division Water, 2002.
[8] Zaadnoordijk, W.J. Simulating piecewise-linear surface water and ground water interactions with MODFLOW. Ground Water, 47 (5), 2009, pp. 723-726
[9] Šlezingr, M., Foltýnová, L., Šulc, V. The design procedure for pre-grown stabilization reinforced grass carpet. Acta Universitatis Agriculturae et Silviculturae Mendelianae Brunensis. 59 (6), 2011, pp. 355-358.

Preparation of Papers for The Scientific Annals of Ovidius University of Constanta, Series of Civil Engineering

First A. Author, Second B. Author, and Third C. Author

***Abstract* – (no more than 10 lines) These instructions give you guidelines for preparing papers for WATER 2010. Use this document as a template if you are using Microsoft Word 6.0 or later. Otherwise, use this document as an instruction set. The electronic file of your paper will be formatted further at WATER 2010. We accept papers in the following formats: .doc, .docx and .pdf. Do not delete the blank line immediately above the abstract; it sets the footnote at the bottom of this page. Do not insert page numbers. Define abbreviations and acronyms in the abstract.**

***Keywords* – About four key words or phrases in alphabetical order, separated by commas.**

1. INTRODUCTION

An author may submit maximum two papers. Each paper should have an even number of pages and a maximum of 8 pages.

The paper size should be A4 with the margins top: 4.4 cm, bottom: 4.4 cm, left: 2.5 cm, and right: 2.5 cm. The article will be written on a single column, using the font Times New Roman. Please use the following table for Font and Paragraph styles:

	Case	Font size	Font style	Alignment	Line spacing	Spacing before text	Left indent first line
Title	Title case	16	Bold	Centred	Single	8 pt	-
Authors	Sentence case	10	Roman	Centred	Single	-	-
Abstract	Sentence case	10	Bold	Justified	Single	-	0.8 cm
Keywords	Sentence case	10	Bold	Justified	Single		0.8 cm
Section titles	Uppercase, small caps	10	Bold	Centred	Single	8 pt	-
Captions and legends	Sentence case	10	Regular	Centred	Single	-	-
Body text	Sentence case	10	Regular	Justified	Single	-	0.8 cm
Footnote (only on the 1st page)	Sentence case	8	Regular	Justified	Single	-	0.8 cm

Manuscript received February 15, 2010. (Write the date on which you submitted your paper for review.) Avoid writing long formulas with subscripts in the title; short formulas are fine. Full names of authors are preferred in the author field, but are not required. Put a space between authors' initials. This work was supported in part by the Romanian Government under Grant nr. 1222/2010 (sponsor and financial support acknowledgment go here).

F. A. Author is with Ovidius University of Constanta, Bd. Mamaia nr. 124, 900356-Constanta, Romania (corresponding author to provide phone: +40-241-619040; fax: +40-241-618372; e-mail: author@univ-ovidius.ro).

S. B. Author is with the University of Architecture, Civil Engineering and Geodesy, 1, Hristo Smirnensky Boulevard, 1046-Sofia, Bulgaria (e-mail: author@uacg.bg).

T. C. Author is with Ovidius University of Constanta, Bd. Mamaia nr. 124, 900356-Constanta, Romania (e-mail: author@univ-ovidius.ro).

Reference	Sentence case	10	Regular	Justified	Single	-	-

For Microsoft Word users, Highlight a section that you want to designate with a certain style, then select the appropriate name on the style menu. The style will adjust your fonts and line spacing. **Do not change the font sizes or line spacing to squeeze more text into a limited number of pages.** Use italics for emphasis; do not underline.

Before the abstract and after the keywords a horizontal line should be drawn.

A paper usually contains five sections: (1) introduction, (2) description of the theoretical model or method / description of the experiment, experimental materials and equipments, (3) results and their significance, (4) conclusions and (5) references. Synthesis papers are an exception from this recommendation.

2. EXPERIMENT DESCRIPTION

Tables and figures should be inserted in the text, preferably where they are referred to. Each of them must have a reference number and a title (tables) or a caption (figures). Place figure captions below the figures and table titles above the tables. If your figure has two parts, include the labels "(a)" and "(b)" as part of the artwork. Please verify that the figures and tables you mention in the text actually exist. **Do not put borders around the outside of your figures.** Tables and figures are separated from the above/under text by a single spaced line.

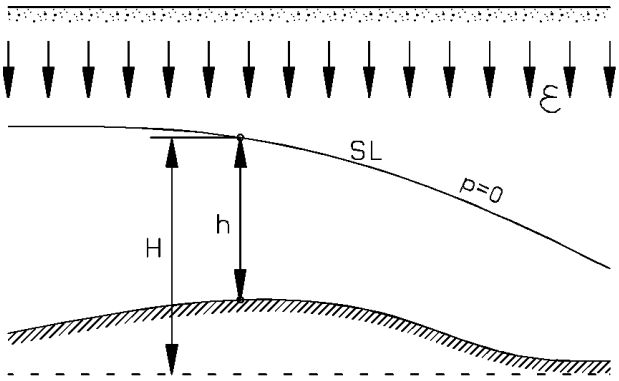

Fig. 1. Unsteady infiltration scheme (example)

Taking into account that the proceedings will be printed in black and white, coloured illustrations must have a proper contrast.

Tables and figures that exceed the width of the page may be rotated to the left, at 90^{o}.

Tables and figures should be cited as follows: **Table 1, Fig. 1.**

The abbreviation **Fig. 1** is not allowed at the beginning of a statement. In this case it should be written **Figure 1.**

Table. 1. Underground water level variation in time (example).

Year	**x (m)**	**Month in the irrigation season:**					
		IV	**V**	**VI**	**VII**	**VIII**	**IX**
1	26	0,03	0,17	0,29	0,47	0,63	0,67
5	26	0,12	0,62	1,00	1,63	2,13	2,21
10	26	0,29	0,97	1,56	2,54	3,33	3,43
1	620	0,02	0,11	0,17	0,28	0,36	0,38
5	620	0,09	0,46	0,73	1,19	1,56	1,61
10	620	0,16	0,78	1,25	2,03	2,66	2,74

3. RESULTS AND SIGNIFICANCES

Define abbreviations and acronyms the first time they are used in the text, even after they have already been defined in the abstract. Abbreviations such as SI, ac, and dc do not have to be defined. Abbreviations that incorporate periods should not have spaces: write "U.O.C.," not "U. O. C." Do not use abbreviations in the title unless they are unavoidable (for example, "DSA 2009" in the title of this article).

If you are using *Word,* use the Microsoft Equation Editor. Equations should be separated from the text by a single spaced line.

Equations should be numbered with Arabic numerals within brackets, aligned to the right on the last line of the equation (default tab stops at 15 cm), as in the following examples:

$$\varepsilon(k) = \varepsilon_o - 2t_o \cos(ka) \tag{1}$$

and also,

$$c_\alpha = \left(\frac{E_w}{\rho_w}\right) \cdot \left[\left(1 - \frac{\gamma_\alpha \cdot R \cdot T}{p}\right) \cdot \left(1 + \frac{\gamma_\alpha \cdot R \cdot T}{p^2} \cdot E_w + \frac{E_w}{E_c} \cdot \frac{D}{e}\right)\right] \tag{2}$$

Be sure that the symbols in your equation have been defined before the equation appears or immediately following. Italicize symbols (*T* might refer to temperature, but T is the unit tesla). Refer to "(1)," not "Eq. (1)" or "equation (1)," except at the beginning of a sentence: "Equation (1) is ... ."

4. CONCLUSIONS

References should be written at the end of the paper, after the text. When the text ends at the bottom of a page, references should be written on a new page.

Number citations consecutively in square brackets [1]. The sentence punctuation follows the brackets [2]. Multiple references [2], [3] are each numbered with separate brackets [1]–[3]. When citing a section in a book, please give the relevant page numbers [2]. In sentences, refer simply to the reference number, as in [3]. Do not use "Ref. [3]" or "reference [3]" except at the beginning of a sentence: "Reference [3] shows ... ."

Please do not use footnotes (except for the footnote on the first page). When necessary, a Notes section can be added at the end of the document.

Please note that the references at the end of this document are in the preferred referencing style. Give all authors' names; do not use "*et al*." unless there are six authors or more. Use a space after authors' initials. Papers that have not been published should be cited as "unpublished" [4]. Papers that have been submitted for publication should be cited as "submitted for publication" [5]. Papers that have been accepted for publication, but not yet specified for an issue should be cited as "to be published" [6]. Please give affiliations and addresses for private communications [7].

Capitalize only the first word in a paper title, except for proper nouns and element symbols. For papers published in translation journals, please give the English citation first, followed by the original foreign-language citation [8].

APPENDIX

Appendixes, if needed, appear before the acknowledgment.

5. ACKNOWLEDGMENTS

This section is optional. Use the singular heading even if you have many acknowledgments. Avoid expressions such as “One of us (S.B.A.) would like to thank ... .” Instead, write “F. A. Author thanks ... .” **Sponsor and financial support acknowledgments are placed in the unnumbered footnote on the first page**.

6. REFERENCES

[1] Boieru P., *Asupra unor rezultate privind curgerea bifazică apă-aer în conducte*. 1972, Hidrotehnica Nr.1, vol. XVIII, pag 23-29.
[2] Wylie E.B. Free air in liquid transient flow. Third International Conference on Pressure Surges. BHRA Fluid Engineering, Conterburz, England.
[3] H. Poor, An Introduction to Signal Detection and Estimation. New York: Springer-Verlag, 1985, ch. 4.
[4] B. Smith, “An approach to graphs of linear forms (Unpublished work style),” unpublished.
[5] E. H. Miller, “A note on reflector arrays (Periodical style—Accepted for publication),” IEEE Trans. Antennas Propagat., to be published.
[6] J. Wang, “Fundamentals of erbium-doped fiber amplifiers arrays (Periodical style—Submitted for publication),” IEEE J. Quantum Electron., submitted for publication.
[7] C. J. Kaufman, Rocky Mountain Research Lab., Boulder, CO, private communication, May 1995.
[8] Y. Yorozu, M. Hirano, K. Oka, and Y. Tagawa, “Electron spectroscopy studies on magneto-optical media and plastic substrate interfaces(Translation Journals style),” IEEE Transl. J. Magn.Jpn., vol. 2, Aug. 1987, pp. 740–741 [Dig. 9th Annu. Conf. Magnetics Japan, 1982, p. 301].
[9] J. Jones. (1991, May 10). Networks (2nd ed.) [Online]. Available: http://www.atm.com

OUR SPONSORS

S.C. ABC VAL

CELCO

ECO TERRA PROIECT

S.C. CIVICON INTER S.R.L.

S.C. GEOTECH DOBROGEA S.R.L.

R.A.T.C. CONSTANTA

ISSN-1584-5990